University of Alberta

Application of Dewatering Technologies in Production of Robust Non-Segregating Tailings

by

Reza Moussavi Nik

A thesis submitted to the Faculty of Graduate Studies and Research
in partial fulfillment of the requirements for the degree of

Doctor of Philosophy
in
Geotechnical Engineering

Department of Civil and Environmental Engineering

©Reza Moussavi Nik
Fall 2013
Edmonton, Alberta

Permission is hereby granted to the University of Alberta Libraries to reproduce single copies of this thesis and to lend or sell such copies for private, scholarly or scientific research purposes only. Where the thesis is converted to, or otherwise made available in digital form, the University of Alberta will advise potential users of the thesis of these terms.

The author reserves all other publication and other rights in association with the copyright in the thesis and, except as herein before provided, neither the thesis nor any substantial portion thereof may be printed or otherwise reproduced in any material form whatsoever without the author's prior written permission.

To my dear parents and my lovely wife,

who have always supported me with love and encouragement.

Abstract

One of the current technologies used by the oil sands industry to reduce the volume of fluid fine tailings and create a dry landscape is production of CT (Composite Tailings) and NST (Non-Segregating Tailings). CT and NST are engineered tailings streams obtained by recombination of fines (MFT or TT) and coarse tailings (sand) plus a chemical amendment. If produced on-spec, the main advantage of CT/NST would be its improved dewatering behavior and rapid release of relatively clear water during the hindered settling and self-weight consolidation, while a majority of the fine particles are entrapped within the matrix of its coarser fraction (sand).

Production of a robust CT/NST at a commercial scale has been a challenge for the industry. While CT/NST has been expected to be non-segregating when discharged, partial segregation and release and re-suspension of the fines has been observed following deposition. To produce a robust CT/NST and reduce its susceptibility to segregation, the yield stress of the carrier fluid (i.e. fines + water) must be enhanced. This can be achieved by increasing the solids content of CT/NST.

The present research reviewed the different methods of solid-liquid separation and experimentally investigated the possible application of some of these methods for improving the quality of CT/NST. A major part of this research was focused on dewatering of MFT and using it as a component for making CT/NST. A batch filtering centrifuge was utilized to dewater MFT samples received from three different operators and the major factors affecting the process of centrifugal filtration were investigated. The resultant dewatered MFT samples were mixed with a mixture of sand and pond water to produce CT/NST with higher solids content. The depositional behaviour and robustness of the produced CT/NST samples were investigated using a flume apparatus. The flow profile and variations of solids content and SFR (Sand to Fines Ratio) were identified for each deposition test, also the yield stress of the CT/NST samples was evaluated using a strain-controlled viscometer and vane spindles. The results of this study indicate that using dewatered MFT promotes production of robust CT/NST streams achieved with lower dosage of chemical additives.

Acknowledgements

I would like to express my sincere gratitude to Dr. Dave Sego and Dr. Norbert Morgenstern for their attentive guidance, continual support and encouragement. It has been a true privilege and an invaluable experience to complete this research work under their supervision; I have learned a lot from them, far beyond the technical and scientific skills.

Special thanks are also extended to the other members of the geotechnical group, especially to Dr. Dave Chan, who in our first communications encouraged me to apply for admission to the University of Alberta, to Dr. Don Scott for the insightful discussions, and to Dr. Kevin Biggar and Dr. Rick Chalaturnyk for all the useful reference material distributed during the related courses. I also wish to thank Dr. Del Fredlund for the Unsaturated Soil Mechanics course he presented at the U of A; attending his class was a unique and valuable opportunity.

Completion of this research would not have been possible without the valuable assistance of the highly competent technicians at the geotechnical group; my sincere thanks go to Christine Hereygers and Stephen Gamble for their kind and timely support during my experiments at the U of A geotechnical laboratories and at OSTRF. Also I would like to thank Jela Burkus for helping me during my experiments at the geo-environmental laboratory.

The support of Gerhard Schmidt for providing the solid-liquid separation device and its accessories is highly appreciated. I also wish to thank Jonathan Matthews, Nigel Goldup and Geoff Halferdahl for their helpful inputs on separation technologies and composite tailings.

I must express my gratitude to Sally Petaske for her kind support during my studies at the U of A, also for her valuable care and concern for the well-being of every individual student in the geotechnical group. In addition, I wish to thank the support staff and graduate advisors of the Civil Engineering Department, especially Anne Jones, Lorraine Grahn, Arlene Figley and Hope Walls.

Several of my friends and student colleagues assisted me with the experiments at the OSTRF and U of A geotechnical laboratories; in particular I wish to thank Nicholas

Beier, Bret Shandro, Chenxi Zhang, Saidul Alam, Ehsan Abazari and Amarebh Sorta. I would like to acknowledge my friend Silawat Jeeravipoolvarn for his support and all the insightful discussions.

During my studies at the U of A, I was lucky to have many kind friends who supported me with care and companionship; in particular I wish to thank Babak Asghari, Farshid Noorbakhsh and Vahid Jalili for all the joyful times we had in Edmonton.

Finally, and most importantly, I owe my deepest gratitude to my dearest ones in life who have always supported me with love, patience and encouragement: my beloved parents, my lovely wife and my caring and kind siblings. This would have never been possible without their support.

The financial support received from the University of Alberta and the Oil Sands Tailings Research Facility (OSTRF) for this study is greatly appreciated.

Table of Contents

List of Tables

List of Figures

List of Acronyms

AFD	Atmospheric Fines Drying
AGG	Agricultural Grade Gypsum
APAM	Anionic Polyacrylamide
ASTM	American Society of Testing and Materials
BAW	Beach above water
BBW	Beach below water
BT	Beached Tailings
C/O	Cyclone Overflow
C/U	Cyclone Underflow
CFC	Coaggulant-Flocculant-Coaggulant (Sequence of chemical treatment)
CFD	Computational Fluid Dynamics
CFF	Cross Flow Filtration
CHWE	Clark Hot Water Extraction Process
CNRL	Canadian Natural Resources Ltd.
COT	Cyclone Overflow Tailings
C-P Cell	Compression-Permeability Cell
CSS	Cyclic Steam Stimulation
CST	Capillary Suction Time
CT	Composite/Consolidated Tailings
CUT	Cyclone Underflow Tailings
DHR	Diameter to Height Ratio
DI	De-ionized (water)
DRU	Diluent Recovery Unit
EDL	Electric Double Layer
ERCB	Energy Resources Conservation Board
ETF	External Tailings Facility
EUB	Energy and Utilities Board
F/(F+W)	Fines to (Fines + Water) ratio
FC	Fines Content

FCF	Flocculant-Coaggulant-Flocculant (Sequence of chemical treatment)
FFT	Fluid Fine Tailings
FTFC	Fine Tailings Fundamental Consortium
FTT	Froth Treatment Tailings
FVST	Field Vane Shear Test
ID	Internal Diameter
ILTT	In-Line Thickened Tailings
IPS	Inclined Plate Settler
LEE	Low Energy Extraction
LEFM	Linear Elastic Fracture Mechanics
LL	Liquid Limit
MFT	Mature Fine Tailings
MRM	Muskeg River Mine
NEB	National Energy Board
NST	Non-Segregating Tailings
OCWE	OSLO Cold Water Bitumen Extraction
OSLO	Other Six Lease Operators/Owners
OSTRF	Oil Sands Tailings Research Facility
PD	Positive Displacement (pump)
PG	Phosphogypsum
PL	Plastic Limit
PNK	Ponder, Nakamura & Kuroda theory
PSD	Particle Size Distribution
PSV	Primary Separation Vessel
RCF	Relative Centrifugal Force
RI	Robustness Index
RPM	Revolutions per minute
SAGD	Steam Assisted Gravity Drainage
SC	Solids Content
SFR	Sand to Fines Ratio
TFT	Thin Fine Tailings
TRO	Tailings Reduction Operations
TSRU	Tailings from Solvent Recovery Unit
TT	Thickened Tailings

TTD	Thickened Tailings Disposal
VAPEX	Vapor Extraction Process
VFD	Variable Frequency Drive
WEC	World Energy Council
WT	Whole Tailings

Chapter 1

Introduction

In most mining operations the process of mineral extraction is associated with production of large volumes of waste material including solids, effluents and air emissions. The solid waste products are either in the form of chunks of rock or overburden (dry waste) transported to dumps via truck, dragline or conveyor; or in the form of a solid-liquid mixture (wet waste) transported to the disposal area by slurry pipeline (Morgenstern and Scott, 1995). The present research deals with the wet waste streams (tailings) produced as a result of extraction of bitumen from the mineable oil sands deposits in northern Alberta, Canada.

The oil sands deposits are primarily composed of quartzose sand layers containing a high proportion of bitumen, along with lenses of overconsolidated clays and clay-shales. These coarse and fine grained layers are mined together and after removal of the larger blocks of clay, are crushed to form the feed for the extraction plant. The hot water extraction process used to recover bitumen from the surface mined ore combines the effect of chemical additives, high temperatures and mechanical energy to prepare the extractive slurry. This process results in successful recovery of bitumen, however it also causes extreme dispersion of the clay particles in the process water. The whole tailings stream resulting from extraction is a segregating mixture of sand, silt and clay sized particles in process affected water; therefore during hydraulic fill construction a considerable percentage of fines are released into the tailings pond. Depending on the chemicals used in the extraction process and mineralogy of the ore, it may take the fine tailings a few months to couple of years to reach a solids content of about 30% due to sedimentation. At this stage a stable suspension of fine particles in process affected water, known as Mature Fine Tailings or MFT[1], is formed. MFT exhibits extremely low

[1] The term “Fluid Fine Tailings (FFT)” recently used in the oil sands industry refers to all fluid tailings contained in a tailings pond, from thin fine tailings located closer to the pond surface to thicker fine tailings with significant percentage of sand located at deeper elevations close to the pond bottom. Definition of FFT includes MFT as well.

dewatering rate and strength gain, therefore its long term storage is required and dry land reclamation is inhibited (Morgenstern and Scott, 1995; Jeeravipoolvarn, 2010; Miller et al., 2011).

The conventional approach for management of MFT has been storing it in in-pit cells and out-of-pit tailings ponds. However, poor water release characteristics of this material requires large retention structures that cover a significant land footprint and must contain fluid tailings for decades or probably hundreds of years. The long-term storage of MFT also poses a major environmental liability. To date, the total volume of MFT accumulated in tailings containment structures of different oil sands operators exceeds 800 million m^3, covering a total surface area larger than 175 km^2 (Alberta Environment and Sustainable Resource Development, 2012).

1.1. Statement of the problem

In recent years the trends in tailings management has been to eliminate the ponds by dewatering the fine tailings and incorporating them into a solid deposit that is modified to a trafficable landform. Different technologies have been developed or are currently under study to create a dry landscape. One of these technologies developed two decades ago at the University of Alberta is production of CT (Composite/Consolidated Tailings) (Caughill, 1992; Caughill et al., 1993) or NST (Non-Segregating Tailings). This technology is the focus of the present research. CT and NST are engineered tailings streams obtained by recombination of fines (MFT or TT: Thickened Tailings) and coarse tailings (sand) plus a chemical amendment. When produced on-spec, the main advantage of CT/NST would be its improved dewatering behavior and rapid release of relatively clear water during the hindered settling and self-weight consolidation, while the majority of the fine particles are entrapped within the matrix of its coarser fraction.

Although commercial production of CT has commenced on c. 1996 (Boratynec et al. 1998; Matthews et al. 2002), making a particularly robust CT/NST has been a challenge for the industry. While this engineered waste stream is expected to be non-segregating when discharged, in practice partial segregation of the coarse and fine fractions is observed, resulting in release and re-suspension of the fines with the release water following deposition. The main reasons for this non-robust behavior of CT/NST in field operations can be listed as follows:

- In some oil sands operations integration of the CT/NST mixing plant with the bitumen extraction plant results in poor/limited control of the process of CT/NST production.
- The recipe for making CT/NST (i.e. the minimum solids content, fines to water ratio and the range of sand to fines ratios) is determined based on static segregation tests. These tests set the minimum criteria for obtaining a non-segregating deposit for static conditions. However, the CT/NST stream must be robust enough not to segregate during the dynamic and high energy discharge and depositional conditions. In other words, meeting the criteria set by static segregation tests is the necessary, but not the sufficient condition for having a robust non-segregating CT/NST.
- The proper tools to control the energy of the depositional environment (e.g. tremies, diffusers) have not been commonly used in CT/NST operations.
- When the designed CT/NST mixture barely satisfies the static segregation criteria, the fluctuations in the feed streams (i.e. variations in solids content of the cyclone under flow (sand) and clay content/solids content of the fine tailings (MFT or TT)) make the CT/NST susceptible to segregation during deposition.

Therefore, to enhance the robustness of CT/NST and reduce its susceptibility to segregation, it needs to be produced at solids contents higher than the minimum criteria set by static segregation tests. However, the solids content of the coarse and fine tailings streams used as the feed for CT/NST production are usually not high enough to promise production of a combined mixture with the desired robustness.

1.2. Objective and scope of the research

The main objective of this research was to investigate the possible approaches to producing CT/NST at high solids contents, possibly with lower dosages of chemical additives usually used in the oil sands industry. This objective was accomplished by executing the following steps:

- The solid-liquid separation methods common in the process industries dealing with particulate slurries were reviewed.
- Laboratory scale experiments were conducted to investigate the possible application of some of these separation methods for improving the quality of CT/NST. The solids content of CT/NST can be increased either by dewatering it as a mixture of coarse and fine fractions, or by dewatering one or both of these components prior to mixing them together.
- A major part of this research was focused on dewatering of MFT, and using the resultant dewatered material as a component for making high solids content CT/NST. For this purpose, a batch filtering centrifuge was utilized at the OSTRF plant and the different parameters affecting the quality of dewatered MFT and resultant filtrate were experimentally investigated.
- Using regular MFT and dewatered MFT obtained from filtering centrifuge tests, CT/NST samples were produced at a variety of conditions and their flow profile and robustness were compared by conducting flume deposition tests.

1.3. Organization of the thesis

This thesis is organized into 7 chapters. A brief description of the contents of each chapter is presented in the following section. Each chapter has a self-contained review of the pertinent literature to guide the reader.

Chapter 2 provides a review of:

- The characteristics of oil sands deposits in northern Alberta and the bitumen extraction process;
- The different types and composition of tailings generated/produced in oil sands operations and the wet and dry landscape methods of reclamation;
- A comprehensive review of the CT and NST technologies;
- Chemical/Mechanical methods of dewatering oil sands fine tailings including thickening, in-line thickening, centrifugation, filtration, centrifugal filtration, cross flow filtration and thin lift dewatering;
- Natural dewatering of oil sands tailings through desiccation and freeze-thaw phenomena;

- Clay-Water interactions and application of flocculation/coagulation in fine tailings management; and,
- Processes of sedimentation and consolidation and the theories describing each phenomenon.

Chapter 3 reviews of the theory of separation and method of operation for thickeners, inclined plate settlers, filters, solid bowl centrifuges, filtering centrifuges, and hydrocyclones. The theory of centrifugal filtration is presented in more detail, considering that in the present research this method was utilized for dewatering of MFT.

In Chapter 4 the laboratory tests conducted to explore dewatering CT/NST as a mixture, also dewatering MFT as its component are presented. These laboratory experiments include dewatering of CT/NST in vessels with inclined walls and on inclined plates, also bench top bottle centrifugation of MFT. A detailed review of the vane and slump test methods for measurement of the yield strength of mine tailings is also presented.

In Chapter 5 the test setup used for centrifugal filtration of MFT is described, also details of the filtering centrifuge tests conducted at different condition and analysis of their results are discussed.

Chapter 6 presents the procedure of making NST from filtered/centrifuged MFT and the flume deposition tests conducted to investigate the flow behaviour and robustness of the CT/NST samples. Based on the position of the samples taken along the flume tests on the ternary diagram, a quantitative method for evaluation of the CT/NST robustness (a Robustness Index) is suggested.

Chapter 7 summarizes the main observations and conclusions and provides some recommendations for future research.

Chapter 2

Literature Review

2.0. General

In this chapter the process of bitumen extraction in northern Alberta and generation of the fluid fine tailings as a byproduct of this process will be briefly reviewed. The common approaches followed so far for management of these tailings streams and their shortcomings will be summarized; and the possible alternative management methods pursued by academia and industry will be presented. Finally, a review of the different chemical/physical phenomena involved during and after deposition of a solid-liquid slurry will be provided.

2.1. Introduction

The Alberta oil sands refers to the vast deposits of extremely heavy crude oil found in sand and carbonate sedimentary formations in northern Alberta, Canada. This kind of crude oil is a semi-solid form of petroleum with very high viscosity and is known as "Bitumen" (NEB: National Energy Board, 2000; Wikipedia, 2012). Including the oil sands, Canada has the second largest petroleum reserves in the world. According to the 2010 Survey of Energy Resources published by the World Energy Council (WEC), natural bitumen deposits are reported in 23 countries, with major resources in three countries: Canada, Kazakhstan and Russia. About 70% of the discovered in-place bitumen volumes are located in Canada, in three main regions of Northern Alberta: Peace River, Athabasca and Cold Lake (Figure 2.1) (NEB, 2000; WEC, 2010). The combined area of these three regions is 140,800 km^2 (ERCB, 2011). These deposits have been grouped on the basis of geology, geography and bitumen content. The previously defined Wabasca Area (Morgenstern and Scott, 1995) has been reclassified by the EUB (Alberta Energy and Utilities Board) and is considered as part of the Athabasca Oil Sands Area (NEB, 2000).

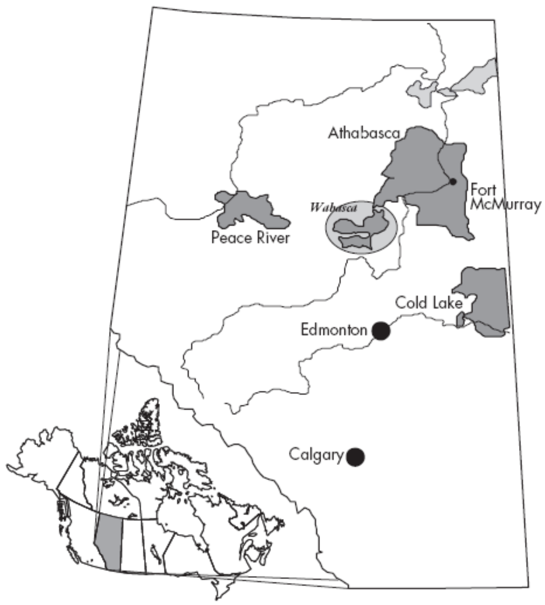

Figure 2.1. Oil sands deposits in northern Alberta (NEB, 2000).

The oil sands deposits are buried at varying depths beneath the earth's surface and are mostly covered by muskeg, sandstone, and shale, which together are known as "overburden" (Figure 2.2). Where thickness of this overlying formation is less than 75m, the oil sand deposits are surface mineable (ERCB, 2011). Among the three deposits, the Athabasca deposit has the largest areal extent with about 200 billion cubic meters of bitumen (initial volume in place), of which about 20 billion cubic meters is recoverable by surface mining techniques (ERCB, 2011). The Peace River and Cold Lake oil sands areas are too deep to be recovered by surface mining techniques and in-situ recovery methods like SAGD (Steam Assisted Gravity Drainage), CSS (Cyclic Steam Stimulation) and VAPEX (Vapor Extraction Process) are required for bitumen extraction. In the in-situ methods, steam, solvents or hot air is injected into the deep oil sand deposits to reduce the viscosity of bitumen and make it flow into extraction wells.

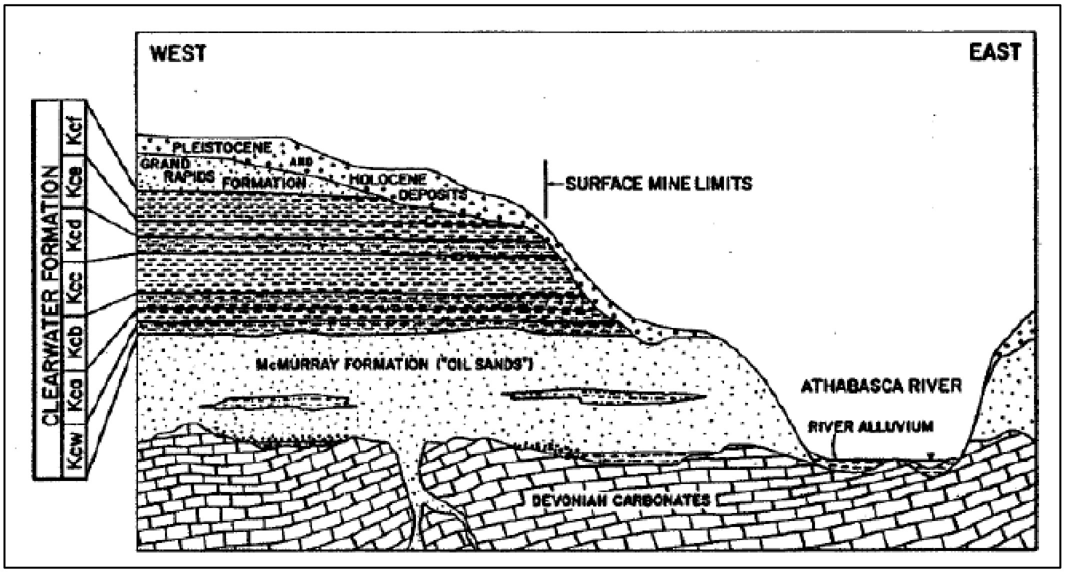

Figure 2.2 - Schematic cross-section of Athabasca deposit (after Dusseault and Morgenstern, 1978a)

The first major oil sands mining operations in the Athabasca region started in 1967 by Great Canadian Oil Sands Co. Ltd., a venture that later became Suncor, producing 7,150 m^3 (45,000 barrels) per day. In 1978 Syncrude Canada started its operation north of Fort McMurray with 17,300 m^3 (109,000 barrels) per day. In addition to Suncor and Syncrude, Shell Canada (Albian Sands) started its Muskeg River Mine operations in 2003 and Canadian Natural Resources Ltd. (CNRL) started its Horizon Oil Sands project in 2009. Currently (in 2011), industry extracts 236,700 m^3 (1.49 million barrels) of bitumen via mining each day and it is expected to rise to 429,000 m^3 (2.7 million barrels) per day by 2015 (ERCB, 2011).

2.2. Oil Sands Deposits Characteristics

A typical cross section of the geological formations adjacent to the Athabasca River is illustrated in Figure 2.2. The oil sands deposits are found within the McMurray formation. This formation underlies a heavily overconsolidated clay formation, called the Clearwater formation and overlies the Devonian formation, mainly limestone. The oil sands deposits are composed primarily of quartz sand, silt, clay, water and bitumen, along with minor amounts of other minerals, including titanium, zirconium, tourmaline and pyrite. Although there can be considerable variation, a typical composition of the oil sands deposits would be (NEB, 2000):

- 75 to 80 percent inorganic material, with this inorganic portion composed 90 percent of quartz sand;
- 3 to 5 percent water; and,
- 10 to 12 percent bitumen, with bitumen saturation varying between zero and 18 percent by weight.

Thin seams to thick beds of silty clay-shale are scattered through the oil sands, which play a major role in fines content of the tailings stream produced after extraction of the bitumen.

Figure 2.3 shows a schematic arrangement of the mineral grains and bitumen within the oil sand deposits. As illustrated, the sand particles are water-wet, i.e. a thin film of water known as connate[1] water separates the bitumen from the sand grains (Boratynec, 2003). Some fine clay particles may exist in this thin film of water (Chalaturnyk et al., 2002). The presence of connate water around the sand grains facilitates the bitumen recovery, since the bonding forces between the bitumen and water are weaker than those between the sand grains and the water (NEB, 2000).

In comparison to conventional crude oils, the bitumen contained within the oil sands has higher density and much higher viscosity. Table 2.1 (modified from NEB, 2000) provides a comparison of the density and viscosity for different types of crude oil. With a density varying from 970 to 1015 kg/m^3, and a viscosity typically greater than 50'000 centipoise at room temperature, bitumen is a thick, black, tar-like material that flows extremely slowly. Prior to transporting this material to refineries for processing, it is required to blend it with a diluent (also referred to as “condensate”) to meet pipeline specifications for density and viscosity (NEB, 2000).

[1] In the context of geology and sedimentology, the term “connate fluids” refers to the liquids that were trapped in the pores of sedimentary rocks as they were deposited. Largely composed of water, these liquids also contain many mineral components as ions in solution (Wikipedia, 2011).

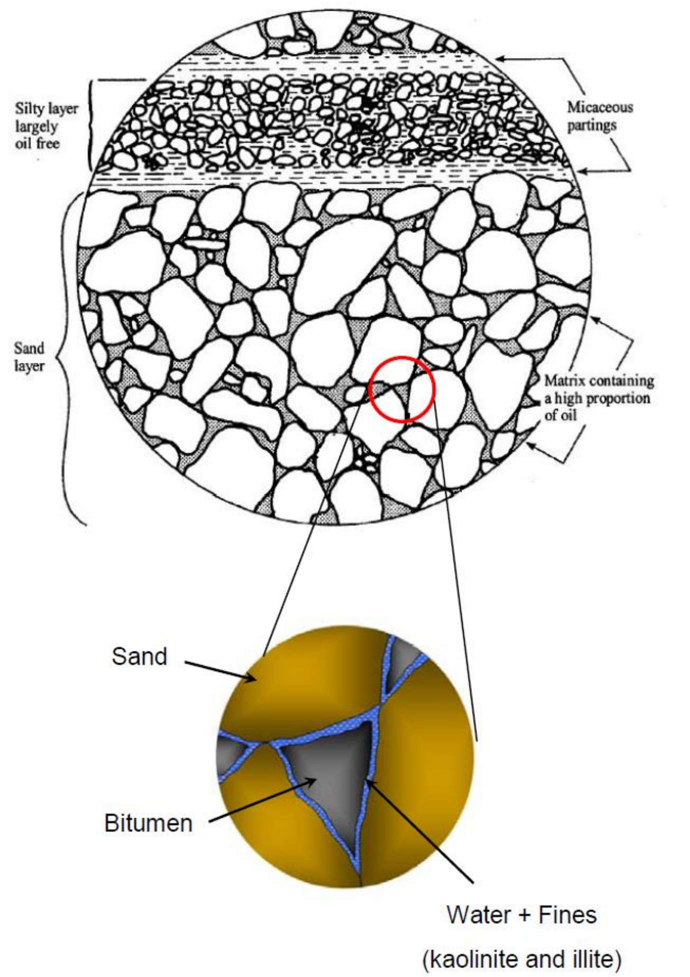

Figure 2.3. Water-wet arrangement of oil sands (modified from Dusseault and Morgenstern, 1978b)

Table 2.1 - Comparison of Crude Oil Characteristics (modified from NEB, 2000)

Crude Oil Sample	**Crude Type**	**Location**	**Density (kg/m3)**	**API Gravity (degrees)**	**Viscosity (cp @ 24^{o}C)**
Cardium	Light	Alberta	834	33	~4
Hibernia	Light	Newfoundland	828 - 896	30 – 40	~10
Sparky	Heavy	Alberta	959	14	2600 - 8900
Kern River	Heavy	California	964	13	2985
Athabasca	Bitumen	Alberta	970	11.6	17000 – 265000
Peace River	Bitumen	Alberta	1040	5.6	125000 - 155000

2.3. Mining of the Oil Sand Deposits

As mentioned in section 2.1, the oil sands deposits buried at depths shallower than 75 m are surface mineable. The initial stage prior to mining the deposits is to drain the water-laden muskeg layer that overlays much of the area. Then [during the winter] the surface vegetation, tree cover and muskeg layers are removed. The soil materials that are suitable for reclamation purposes are selectively excavated and stored. At the next stage, the overburden layer beneath the muskeg, which is composed of rock, clay, silt and sand, is removed to the in-pit cells (i.e. the previously mined-out areas). The oil sand deposits are exposed after removal of the overburden (NEB, 2000).

From mid 1960s to the late 1980s, giant bucket wheel excavators and huge draglines were used to excavate the oil sands in the Suncor and Syncrude operations. The excavated material was transported to the extraction and upgrading facilities by means of conveyor belts. During the 1990s, the oil sands industry converted to mining trucks and power shovels, as they became available in higher capacities. This method was considerably more flexible and less prone to interruption of service in comparison to massive and complex bucket-wheels and draglines.

Another significant change during the 1990s was converting from conveyor belts to hydrotransport technology. In this method the oil sands ore is introduced into a massive vessel called “Cyclofeeder” where it is crushed and mixed with hot water to form a slurry. This slurry is transported to the extraction plant through a pipeline. This method of transportation allows the mining to be carried out at much greater distances from the extraction plant. Another great benefit of this technology is that due to partial separation of the bitumen from the minerals during transportation, the operating temperatures in the first step of the extraction process can be reduced to less than 50^{o}C. (As will be explained in the next section, the required temperature in the conventional extraction process is about 80^{o}C). As a result, the energy consumption and the green house gas generation during the extraction process would be significantly lower (NEB, 2000, Syncrude website, 2011).

2.4. Bitumen Extraction Process

The basis of all the thermal extraction processes currently used in the oil sands industry is the Clark Hot Water Extraction (CHWE) process. This process was developed by Dr. Karl Clark of the University of Alberta in the 1920s, during his work with the Alberta Research Council (NEB, 2000).

In a CHWE plant, the oil sands ore undergoes three stages of conditioning, primary extraction and final extraction (Figure 2.4). During the conditioning stage, conveyors are used to move the oil sands ore from the base mine dump pocket towards large tumblers (Boratynec, 2003; NEB, 2000). Upon entrance of the ore into the large rotating tumbler, the hot water (80^{o}C to 85°C), steam and caustic soda (Sodium hydroxide: NaOH)[2] are added to it to make a slurry with a solids content of 70 – 85 wt%. Addition of NaOH increases the pH to 8.0 – 8.5 and reduces the surface and interfacial tensions which leads to disintegration of the oil sands ore structure and easier separation of the bitumen. Simultaneously, these conditions cause dispersion of the clay particles in the water, producing a tailings effluent with poor dewatering characteristics (Boratynec et al. 1998; Chalaturnyk et al. 2002). After the conditioning stage, the slurry from the tumblers is discharged onto vibrating screens to remove rocks and lumps of clay. The resultant stream is diluted and, through the hydrotransport line, enters the separation vessels for primary extraction (NEB, 2000). In the primary separation vessel (PSV), bitumen is recovered as a froth layer on top by means of flotation, and the coarser soil grains settle to the bottom and form a sediment layer. The remainder of the slurry, referred to as middlings, is composed of water, unrecovered bitumen and dispersed clay particles. Air

[2] In the Albian Sands extraction operations “Sodium Citrate” is utilized as a process aid (Mihiretu, 2009).

flotation is used for further separation of the bitumen from the fines in this part. After completion of the bitumen recovery, the fine and coarse mineral streams are combined and more water is added to form a pumpable whole tailings stream (Boratynec, 2003). In section 2.6 details of the tailings disposal is explained.

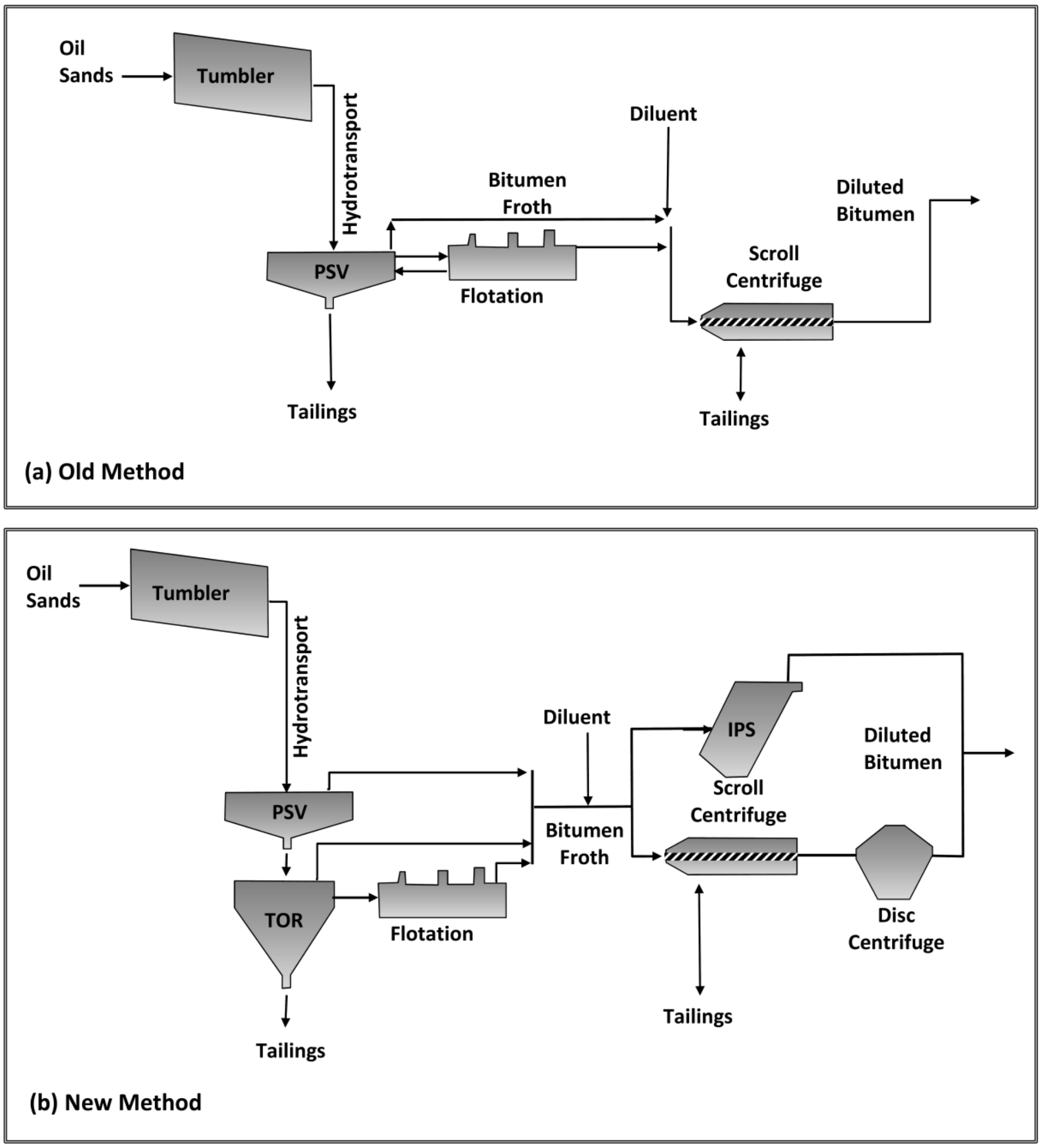

Figure 2.4. Bitumen extraction and froth treatment: (a) Old Method; (b) New Method (modified from NEB, 2000).

The bitumen froth recovered in the PSV is skimmed off and moved to a flotation unit, in which air-bitumen bubbles rise to the surface (NEB, 2000). The recovered bitumen froth consists of 60% bitumen, 30% water and 10% solids by weight (Gu et al, 2002). Prior to sending this froth to the upgrader, naphtha is added to it as a diluent/solvent and this mixture enters a high speed centrifuge to separate the solids and water. To provide more complete separation of the bitumen from solids and water, Suncor added inclined plate settlers (IPS) and disk centrifuges to the extraction process (Figure 2.4) (NEB, 2000).The bitumen cleaned from solids and water, is moved to the upgrading unit. The removed solids, water and residual solvent are added to the tailings stream (NEB, 2000). Because of the environmental impact of the residual solvent, the froth treatment tailings (FTT) are particularly important, however, they represent a relatively minor stream in terms of volume (Mikula et al., 2008).

It should be noted that Syncrude has developed a Diluent Recovery Unit (DRU) to recover naphtha from froth treatment tailings. Also in another innovation by Syncrude, called "Natural Froth Lubicity", water is used in the froth to create a lubricating sleeve. As a result, the froth can be transported through the pipeline without adding diluent (NEB, 2000).

2.5. Tailings Composition

The tailings stream resulting from the extraction process is referred to as the "Whole Tailings (WT)" and has an alkaline nature with a pH of 8.0 to 9.0. Its solids content varies from about 50wt% to 60%wt, consisting of residual bitumen (~1wt% of dry weight), sand particles (~82wt% of dry weight), dispersed fine grained material (~17wt% of dry weight), water and small amounts of soluble organic compounds (Chalaturnyk et al., 2002). The sand particles have a uniform size of ~150 μm. Depending on the variations of the plant feed, the fines content may vary from 8wt% to 25wt% (Caughill, 1992). It should be noted that the fines content in the oil sands related problems is determined according to sieve #325 (i.e. mineral particles smaller than 44 microns are considered fines). About 45wt% of the fines are clay sized (less than 2 microns) which predominantly consist of kaolinite (~65wt%) and illite (35wt%); with small traces of other clay minerals like chlorite, vermiculite and mixed layer clays of smectite (Scott et al., 1985; Omotoso and Mikula, 2004; Uhlik et al., 2008; Kaminsky et al., 2008). Due to its gap graded grain size distribution, the whole tailings stream has a segregating behavior when deposited.

2.6. Tailings Disposal

In the conventional method of tailings disposal, which was developed in the early years of oil sands mining and is still in common use today (Sobkowicz and Morgenstern, 2009), the whole tailings stream is hydraulically transported and discharged into surface (out-of-pit) or in-pit storage ponds. Upon discharge from pipeline into the pond, the tailings stream separates into a stable coarse sand deposit and a fluid fines pool (Figure 2.5). The sand that settles out of the waste stream is either used for construction of sand dykes in cells, or is discharged sub-aerially to form beaches. Some fine particles are trapped within the sand matrix of the beach and the rest are introduced into the tailings pond. Majority of the fines that enter the pond are clay sized (less than 2 microns) with the initial solids content of 6 – 10 wt% and are referred to as Thin Fine Tailings (TFT). After an induction period lasting up to several weeks the fines flocculate and over a period of few months settle to a solids content of ~20 wt%. Over the next couple of years the fine tailings layer consolidates very slowly and reaches to about 30 wt% solids content (i.e. 86 % of the volume is water). At this stage the slurry forms a stable structure which has a very slow dewatering rate and is called Mature Fine Tailings (MFT). Typically over 95% of MFT is fines with 30% to 50% clay content (Boratynec, 2003; Chalaturnyk et al., 2002; Kasperski, 1992). For very old MFT deposits that have gone through much longer periods of settlement, solids contents as high as 45% has been observed, although the sands content has also been higher (Sobkowicz and Morgenstern, 2009).

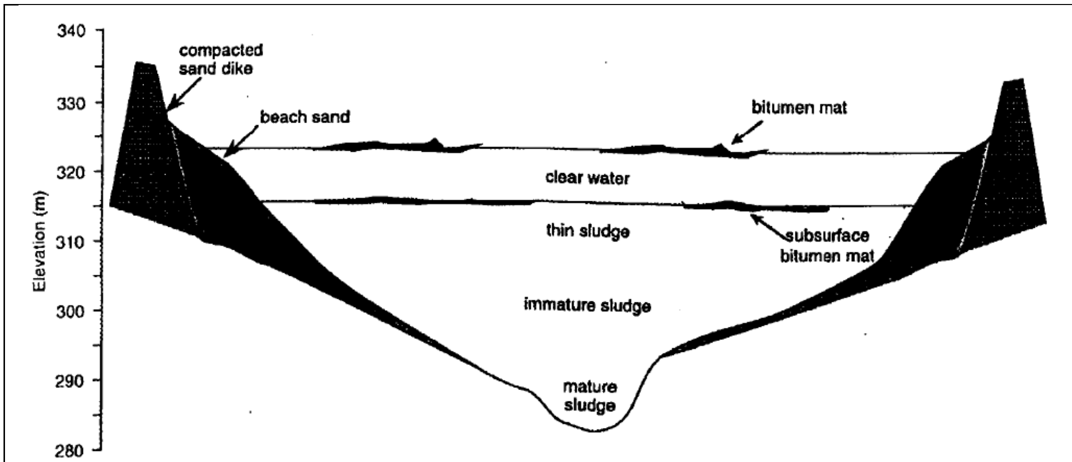

Figure 2.5. Schematic cross section of tailings pond (after Carrier et al., 1987; Dusseault et al., 1987; MacKinnon, 1989; Kasperski, 1992).

Poor water release characteristic of MFT has caused accumulation of large volumes of this toxic material in the tailings ponds. Figure 2.6 (modified from Houlihan et al., 2008) shows the increasing rate of MFT volume from 1968 to 2008 and the forecasted volume of MFT until 2060 based on operators submissions to the ERCB. According to this diagram if the companies involved in the oil sands industry continue using the same extraction and processing techniques, the MFT volume is forecasted to reach 1 billion m^3 in 2014 and 2 billion m^3 in 2034 (Houlihan et al., 2008). Accumulation of such large volumes of MFT raises multiple environmental and operational concerns (Kasperski, 1992; NEB, 2000):

- Long term maintenance of the retention structures: The tailings dams/dykes would have to last for long times (decades or probably hundreds of years) before the MFT is finally solidified. These structures need to be designed, constructed and monitored in a way that no erosion, breaching or foundation creep occurs during the service life of the tailings pond.
- Environmental liability: Fresh tailings water (process-affected water) resulted from bitumen extraction process is acutely toxic to aquatic organisms and mammals (Headley and McMartin, 2004). Monitoring programs are required for ground water and surface water to ensure that seepage of the toxic water from tailings ponds does not contaminate these sources of water.
- The tailings ponds may cover recoverable oil sands deposits within the mine lease boundaries. Extraction of the ores underlying these ponds would require transfer of large volumes of fluid tailings into alternate storage spaces (in-pit cells or new tailings ponds).

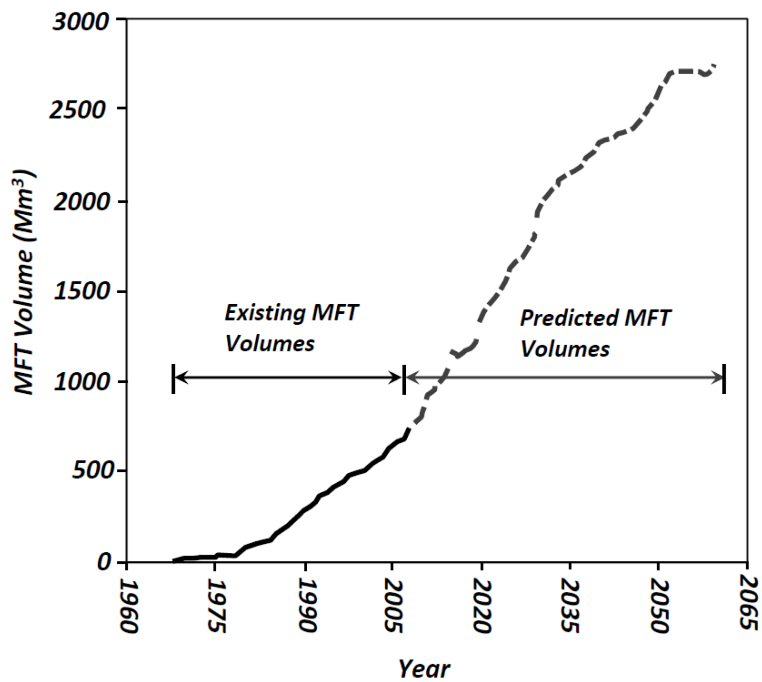

Figure 2.6. Trend of accumulation of MFT in tailings ponds from 1968 to 2008 and the forecasted volume of MFT based on operator submissions (modified from Houlihan and Mian, 2008)

In the more recent oil sands extraction operations (as in the Shell Albian Sands and CNRL Horizon operations) the whole tailings stream is first pumped through a hydrocyclone to separate the coarse and fine fractions, rather than being directly deposited into the tailings pond. The cyclone overflow (composed of fines, water and unrecovered bitumen) is introduced into a thickener for further dewatering. The cyclone underflow (mainly composed of sand) may either be used for construction of cells and dykes, or may be mixed with the thickened (dewatered) fine tailings from the thickener underflow to form Non-Segregating Tailings (Matthews, 2008; Chu et al., 2008; Beier et al., 2009). In section 2.8, the possible approaches for management and reclamation of the oil sands tailings will be discussed in more detail.

2.6.1. Reasons for slow consolidation rate of mature fine tails

Scott and Dusseault (1980) assumed that the high concentration of unrecovered bitumen leads to a hydraulic conductivity 0.1 to 0.01 that of equivalent material with no bitumen, and the low effective density of the solids is the reason for the slow consolidation rate of

MFT. As illustrated in Figure 2.7, Scott et al. (1985) hypothesized that the bitumen absorbed to the surface of clay particles creates a constricted tortuous path for drainage of water from the MFT. Other researchers have attributed the stable structure of the clay slurry to the asphaltic acids present in the bitumen, which become water soluble after addition of NaOH and act as surfactants (i.e. reduce the surface and interfacial tension of the water). Consequently, this causes dispersion of the clay particles. It has been shown that, especially at high solids concentrations, the double-layer repulsion of the clay particles acts as a stabilizing force (Kasperski, 1992; Chalaturnyk et al. 2002). Another assumption is that the bi-wetted clay particles of submicron dimensions (less than 0.2 micron), referred to as ultra-fines, are the reason for the formation of a stable gel-like structure, which contains up to 90 wt% water (Kasperski, 1992; Kotlyar et al. 1993; FTFC 1995; Chalaturnyk et al. 2002). Kasperski (1992) has provided a comprehensive review of the various theories for stability of the MFT structure.

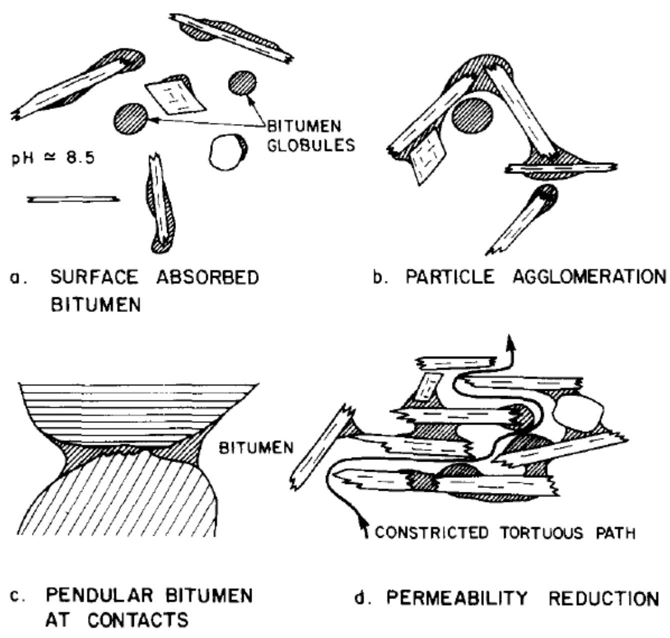

Figure 2.7. Effect of bitumen on particle settlement and permeability (adapted from Scott et al., 1985).

2.7. Types (Variety) of Oil Sands Tailings

As mentioned in section 2.6, the whole tailings stream may be deposited into the tailings pond without any post-extraction processing and classification (i.e. conventional disposal method), or it may be subjected to intentional classification (typically by hydrocyclones) prior to further processing and deposition. Based on this, the following tailings materials may need to be managed for disposal (Sobkowicz and Morgenstern, 2009):

Tailings materials produced from conventional deposition of the whole tailings:

- BT (Beached Tailings); is the coarse fraction of the whole tailings stream that settles out upon deposition and forms a beach. BT is further sub-divided into BAW (Beach Above Water) and BBW (Beach Below Water). BAW is referred to tailings deposited sub-aerially forming beach angles of 1% to 2%, and BBW is the tailings deposited sub-aqueously with beach angles of 2% to 4%. BT typically has a geotechnical fines content of up to ~20% (i.e. f/[f+s]).
- TFT (Thin Fine Tailings); is the dilute suspension of fines, with a solids content of 6% to 10%, which segregates from the coarse fraction of the whole tailings stream and runs into the tailings pond.
- MFT (Mature Fine Tailings); is the quasi-stable suspension of clay and silt particles with a very slow dewatering rate and a solids content of ~30%.
- FTT (Froth Treatment Tailings) and TSRU (Tailings Solvent Recovery Unit): As mentioned in section 2.4, FFT is referred to the solids, water and residual solvent removed from the bitumen froth prior to sending it to the upgrader. The tailings coming from a Solvent Recovery Unit are referred to as TSRU.

Tailings materials produced after classification of the whole tailings by hydrocyclones:

- C/U (CUT: Cyclone Underflow Tailings) and C/O (COT: Cyclone Overflow Tailings): Hydrocylones are used to classify the whole tailings stream to a coarse fraction (underflow) and a fines fraction (overflow). In comparison to the whole tailings stream, cyclone underflow has lower fines and water content with a solids content of ~70%. Cyclone overflow is a mainly composed of fines with a SFR (Sand to Fines Ratio) <1 and a solids content of ~8% to 10%.
- TT (Thickened Tailings): The fine tailings stream from cyclone overflow is mixed with a flocculating agent and then is introduced into a thickener/clarifier for further dewatering. The dewatered tailings stream obtained as thickener underflow is referred to as TT, which can have a solids content of ~50%.

- ILTT (In-Line Thickened Tailings): To enhance the settling behavior of the fine particles present in the cyclone overflow, this tailings stream is mixed "in-line" with some chemical additives and the resultant stream, now containing large aggregates formed by joining together of finer particles, is deposited into a settling pond/cell (Yuan and Shaw, 2007; Jeeravipoolvarn, 2010). The concept is very similar to production of TT.
- CT (Composite/Consolidated Tailings): CT is an engineered tailings stream obtained by mixing chemically treated MFT and sand from cyclone underflow (C/U) at a SFR of 3 to 5. The objective of chemical treatment is to produce a tailings stream with a non-segregating behavior. After deposition, CT is expected to settle, consolidate and develop some effective stress relatively quickly.
- NST (Non-Segregating Tailings): Similar to CT, NST is an engineered tailings stream but instead of using MFT, it is produced by mixing TT and sand from cyclone underflow.

In the following sections, CT and NST will be discussed in more detail as part of the dry land scape reclamation method.

2.8. Management and Reclamation of the Oil Sands Tailings

The traditional method for disposal of the mine tailings that are in the slurry form has been use of tailing ponds. Similarly in the oil sands operations the conventional approach has been to discharge the "segregating" whole tailings stream into in-pit cells or behind an out-of-pit dam structure (see section 2.6), resulting in tailings ponds that contain huge volumes of fluid fine tailings. This massive inventory of fluid tailings is referred to as "Legacy tailings" (Beier et al., 2009).

The most common method for reclamation of the tailings ponds has been the so called "wet landscape" technique. In this method the fluid fine tailings stored within the impoundment structures are capped with a layer of fresh water of sufficient depth. The purpose is to form an artificial lake and isolate the fine tailings from the surrounding environment. Field tests have shown that when isolated from the influx of fresh tailings, tailings pond water (i.e. process-affected water) naturally detoxifies with time through bioremediation and dilution (Kasperski, 1992; MacKinnon and Boerger, 1986). Creating wet landscapes, particularly when out-of-pit dam structures are utilized, will require costly monitoring and ongoing maintenance for decades following active mining.

In recent years the trends in tailings management has been to eliminate the ponds and instead create a "dry landscape". In the dry landscape technique, it is desired to dewater the fine tailings and/or incorporate them into a solid deposit which can create a trafficable landform. The final objective is to produce geotechnically stable landforms with self-sustaining, native vegetation cover, that are resistant to natural processes and are self-healing after natural erosion (MacKinnon and Boerger, 1986; Kasperski, 1992; Sobkowicz and Morgenstern, 2010).

The idea of eliminating the tailings ponds was first suggested and implemented by Dr. Eli Robinsky (1999) from the University of Toronto. In the late 60's he was requested to design a tailings pond for the Kidd Creek Mine project (zinc/copper extraction) in eastern Ontario. After being struck by the visible environmental damage that had occurred around some existing and abandoned tailings ponds, he thought of an innovative approach to tailings disposal: "*removing most of the process water from the tailings stream prior to its discharge*". Following this approach he invented the "*Thickened Tailings Disposal (TTD)*" system. The basic principles of this system are to thicken the tailings stream to create a heavy (i.e. high density) but pumpable slurry that would possess high viscosity or high internal friction. After releasing this slurry onto a surface, it would from a gentle self-supporting slope beneath the discharge point, requiring substantially smaller perimeter dam structures at the toe in comparison to the conventional approach (Robinsky, 1999). Invention of the TTD system was an important development for the minerals industry that can lead to significant environmental protection.

In the last two decades, the oil sands industry has been looking for tailings management approaches with the potential of creating a dry landscape. In general, two types of tailings streams have been developed:

- Tailings streams which have a relatively high water content upon deposition, but are amended or engineered in a way that can release a significant volume of water in a short time frame after deposition (e.g. CT or thin lifts of flocculated MFT); and,

- Tailings streams that are dewatered prior to their discharge and show higher yield resistance upon deposition [in comparison to the first type] (e.g. centrifuged or thickened tailings).

In the following sections, the tailings management strategies that have the potential of creating a dry landscape and have been considered in the oil sands industry, whether at a commercial scale or laboratory/plant scale, will be reviewed.

2.8.1. Composite/Consolidated Tailings (CT) and Non-Segregating Tailings (NST)

One of the current tailings management options used by the industry is production of CT and NST. As stated in section 2.7, CT and NST are engineered tailings streams obtained by recombination of fines (MFT or TT) and coarse tailings (sand) at sand to fine ratios of 3 to 5, plus a chemical amendment. In Suncor and Syncrude operations, CT is made by addition of gypsum to MFT and sand. In Shell Albian Sands operations, NST is produced by mixing TT (thickener underflow, already containing flocculants), sand and gypsum (Matthews, 2008). In the CNRL Horizon project, NST is made by addition of carbon dioxide (CO_2) to the mixture of TT and sand (Chu et al., 2008). Considering that the present research is focused on improving the quality of CT/NST, the rest of this sub-section will review the background, advantages and challenges of the current technology.

2.8.1.1. Background

Scott and Cymerman (1984) proposed that a non-segregating mixture of fine and coarse wet wastes would be a suitable blend for creating dry landscapes. By definition, a non-segregating mix is a deposit in which at least 90% of the fines are retained within the coarse fraction (Morgenstern and Scott, 1995).

MFT, mainly composed of clay and silt sized particles, usually needs a chemical amendment to achieve the viscosity/yield strength required for supporting sand particles (Mikula et al., 1998). Extensive research conducted at the University of Alberta showed that different organic flocculants and inorganic coagulants[3] may be used for treatment of the tailings to change their characteristic from a segregating slurry to a non-segregating one. Figure 2.8 shows the Slurry Properties Diagram. This ternary diagram was developed as a convenient tool for describing the properties and behavior of slurries composed of fine and coarse mineral matter (Scott and Cymerman, 1984; Morgenstern and Scott, 1995; Azam and Scott, 2005). According to this diagram, the segregation boundary is distinct and only a small change in solids concentration changes the tailings stream from a homogenous non-segregating slurry to a heterogeneous segregating one. The untreated oil sands tailings plot above the segregation boundary, and segregate due to their gap graded grain size distribution. As illustrated, addition of lime ($Ca(OH)_2$), phosphogypsum ($CaSo_4.2H_2O$), sulphuric acid, flyash ($CaSo_4$) and different combinations of these additives to MFT will enable it to support the sand particles, resulting in a non-segregating tailings stream[4] (Caughill et al. 1993; FTFC 1995; Morgenstern and Scott 1995). As a result, the segregation boundary for treated tailings is shifted towards lower solids contents. It should be noted that these segregation boundaries have been determined through use of static segregation tests.

Prior to commercial production of CT, extensive laboratory and field testing programs were conducted at Suncor and Syncrude testing facilities using tailings mixtures produced with a variety of chemical aids and at a range of sand to fines ratios. The objectives of these programs were to verify the possibility of producing non-segregating tailings under field conditions, also to study the depositional behavior, geotechnical characteristics (specifically consolidation properties in the lab versus the field) and potential environmental impacts of the CT mixes produced (Caughill et al., 1994; Liu et al., 1994; MacKinnon et al., 2001; Matthews at al., 2002).

During the summer and fall of 1993 a number of test cells and tanks were filled with Suncor tailings mixtures at an initial solids content of 51.8% to 54.7% and an initial fines content of 18.6 to 23.6%. Combinations of acid and lime/flyash were used as coagulant, and tailings mixtures were deposited at subaerial, subaqueous, and sub-MFT conditions.

[3] For definition of coagulants and flocculants see section 2.9.1.

[4] MacKinnon et al. (2001) provided a comprehensive review on the different chemicals available for production of CT and their effect on the release water properties.

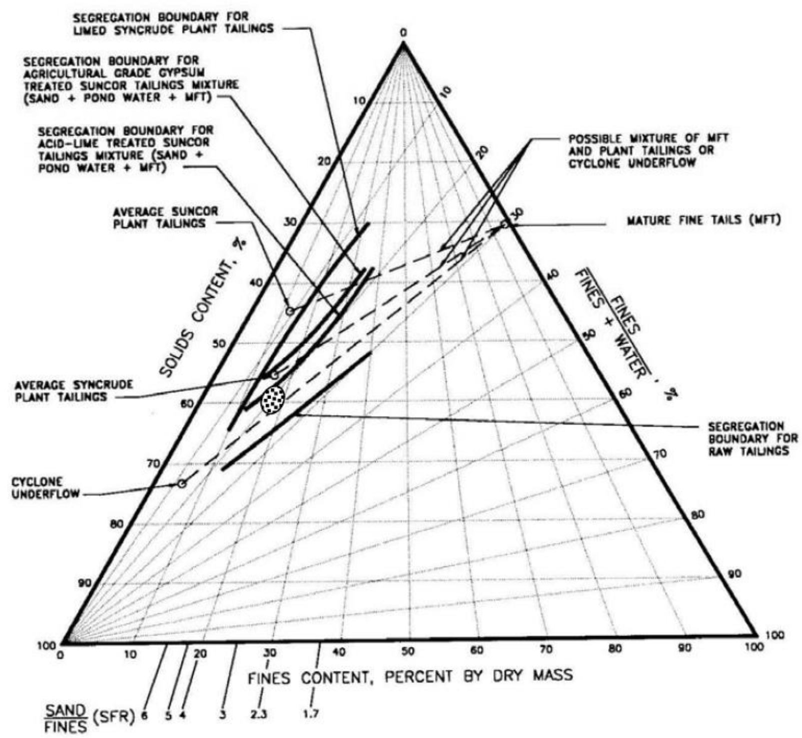

Figure 2.8. Slurry Properties Diagram (modified from FTFC, 1995)

This trial demonstrated that non-segregating tailings can be produced under field conditions and, if the tailings are not allowed to flow too quickly during deposition, the amount of segregation would be minimal (Caughill at al., 1994). The laboratory tests conducted at the University of Alberta on Suncor non-segregating tailings indicated that the rate of consolidation depended mainly on the fines content of the tailings. Decreasing the SFR from 5 to 3 reduced the consolidation rate significantly (Liu et al., 1994). The consolidation parameters measured in the laboratory were used as input for a finite strain consolidation program and the values predicted for solids content of the deposit six months after deposition were in reasonable agreement with the values measured at the pilot scale plant (Caughill at al., 1994).

Syncrude started an extensive laboratory program in 1993, and following that conducted a field pilot trial of the CT process in 1995 and a full-scale prototype demonstration of CT in 1997/98 (Matthews et al., 2002). As a readily available alternative to lime and acid-lime, in these programs gypsum was used as a coagulant. Later gypsum was selected as an affordable and effective coagulant for the commercial application of CT at Syncrude. The geotechnical performance observed from the 1995 and 1997/98 trials lead to recalibration of the consolidation and permeability models developed from laboratory experiments (Matthews et al., 2002). While a primary incentive of producing CT is to create a non-segregating tailings with higher fines content (i.e. lower SFR) and to reduce the fluid fines inventory by consuming more MFT, a target SFR of 4:1 was chosen for commercial implementation at Syncrude by a desire to optimize the rate of consolidation. The Syncrude field trial provided confidence that SFR of 4 would result in adequate geotechnical performance without sacrificing the planning needs (Matthews et al, 2002).

2.8.1.2. Commercial Production of CT/NST

Figure 2.9 shows the process flow diagram for making CT. As illustrated, MFT (at ~30% solids content) is dredged from the tailings pond and is mixed with a slurry/solution of gypsum. The resultant treated material is added to the sand from cyclone underflow (at ~70% solids content) to produce CT at about 60% solids content and a sand to fines ratio (SFR) of 3 to 5. Although laboratory tests show that about 600ppm to 1000ppm gypsum[5] could result in a non-segregating CT, but field production of CT usually requires up to two times higher gypsum (Matthews et al., 2002; Jiravipoolvarn; 2010). One reason for this discrepancy could be the additional acceleration/force that the sand particles experience during flow and deposition of CT in the field. Also, the flow/deposition process can break the agglomerated clay particles, resulting in lower viscosity/yield strength of the carrier fluid.

[5] 600 ppm: 600gr of gypsum per 1000 kg of slurry

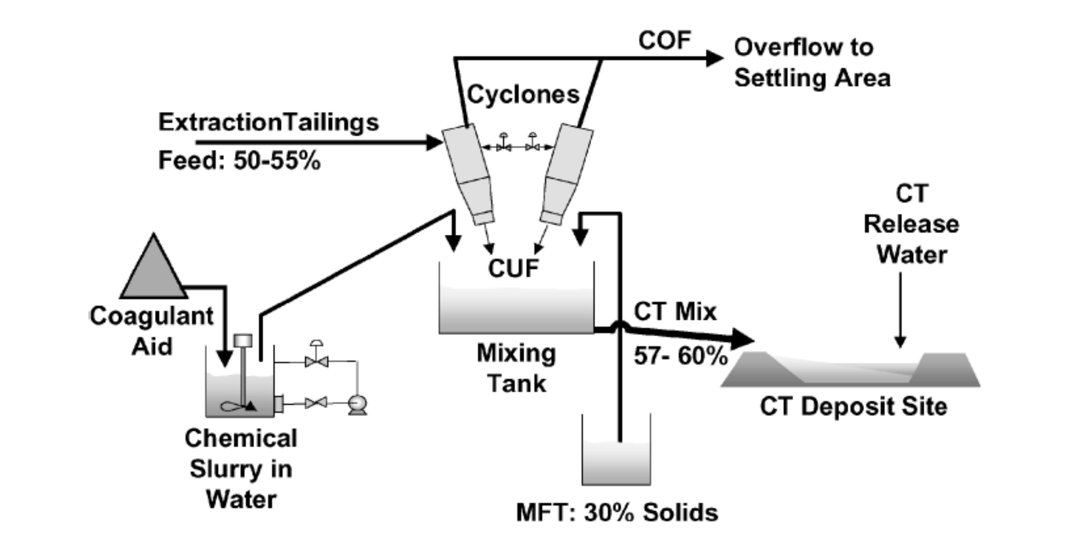

Figure 2.9 – Schematic illustration of the CT Process. Solids contents of the streams are shown in weight percentage (after MacKinnon et al., 2001).

CT (Consolidated Tailings) was first implemented on a commercial scale by Suncor in Oct. 1995 (Mikula et al., 1998). Syncrude started placement of CT (Composite Tailings) into its former east mine in 2000 (Syncrude Canada Ltd. website, 2011). Suncor has used gypsum ($CaSO_4.2H_2O$) [available as a by-product of its flue gas desulphurization unit] for treatment of MFT (NEB, 2000; Mikula et al., 1998). Other inexpensive sources of gypsum are phosphogypsum (PG: a by-product of processing phosphate ore into fertilizer with sulfuric acid) and agricultural grade gypsum (AGG) (Boratynec, 2003; Wikipedia, 2011). Addition of gypsum to MFT will release Calcium ions (Ca^{2+}) with the release water:

$$CaSO_{4\,(s)} \rightarrow Ca^{2+}_{(aq)} + SO_4^{2-}{}_{(aq)}$$

Divalent calcium ions replace the sodium ions on the surface of clay particles and result in reduction of the pH, collapse of the electric double layer and reduction of the net inter-particle repulsion. Consequently the clay particles (previously in a dispersed state) bond together and form a flocculated structure. This increases the viscosity/yield strength of MFT, enabling it to support the coarse fraction. Also, flocculation of the clay particles leads to higher hydraulic conductivity of the fine tailings on a macro scale (Caughill, 1992; Caughill et al., 1993; Mikula et al., 1998; Jeeravipoolvarn, 2010; Miller et al., 2010).

In the CNRL Horizon mine operations, cyclone underflow sand at a solids content of ~72%wt is mixed with thickener underflow (>46%wt) and CO_2 is added to the pipeline containing this mixture at a rate of 250 to 1000 ppm. Addition of carbon dioxide generates carbonic acid and lowers the pH. This results in flocculation of the fine particles and increases the viscosity of carrier fluid (Chu et al., 2008). [For definition of flocculation and coagulation see section 2.9.1].

2.8.1.3. Advantages of CT/NST Technology

The main advantage of CT/NST is its improved dewatering behavior (Figure 2.10). Weight of the sand particles retained by the fines matrix acts as a driving force and causes faster release of water during the hindered settling and self-weight consolidation. This results in decrease of the void ratio from approximately 2 to 1 after only several days (Boratynec, 2003).

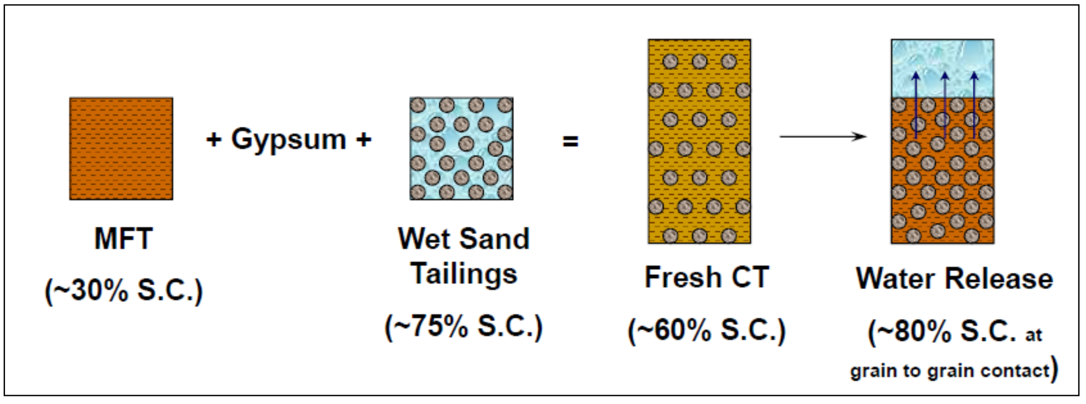

Figure 2.10- Schematic illustration of CT components and its dewatering.

According to Mikula et al. (1998) *"…the CT release water is significantly less toxic than CHWE process recycle water and this will be a significant benefit for the final reclamation of the mine site when some water will be released to the environment"*.
MacKinnon et al. (2001) observed a loss of 20-30% of the naphthenic acids in the CT release water in comparison to pre-treatment levels, also a reduction in its acute toxicity. They stated that chronic toxicity of the water released from gypsum-produced CT significantly improved with time. After just one year of aging under natural conditions, the release water passed a battery of acute and chronic bioassays. Little evidence of trace metals or organic impacts has been observed. The major issue of CT release water with regard to its use for vegetation is its salinity (MacKinnon et al., 2001).

The CT release water (having elevated calcium levels) can be mixed with the cyclone overflow to enhance the settling behavior of the fines discharged in the tailings pond. Rapid settling of the fines will provide solids free recycle water in a very short time in comparison to conventional operations, and this reduces the requirement for make-up river water (Mikula et al., 1998). Also, production of CT provides an opportunity to consume the legacy tailings, which leads to reduction of the volume of tailings ponds and improves the land reclamation process (Morgenstern and Scott 1995; Boratynec et al. 1998; Mikula et al., 1998; Matthews et al., 2002; Beier et al., 2009).

2.8.1.4. Deposition and Reclamation of CT/NST

The ideal method for deposition of CT/NST would be the sub-aerial disposal of thin layers suggested by Qiu and Sego (1998). As illustrated in Figure 2.11, in this technique the tailings impoundment area is divided into a number of deposition cells and the tailings are discharged by means of a spray bar or spigot to provide a gentle flow over a beach in one cell. Upon coverage of the cell with a thin layer of tailings, the discharge point is transferred to the next cell and the thin layer of material is allowed to settle and dry before being covered with the next fresh layer. Each layer of the deposited tailings experiences dewatering through the stages of sedimentation, consolidation and desiccation. The decanted water drains to the pool located at a low point where it may be pumped back for recycling into the processing system, or drained to a pond for treatment before release to the environment (Qiu and Sego 1998). [As will be explained in section 2.8.3, treated fine tailings and thickened tailings can also be deposited in thin layers sub-aerially].

Conventionally, CT/NST has been transported to the disposal areas by pipeline and discharged by beaching (Sobkowicz and Morgenstern, 2009, 2010). The disposal areas may include constructed cells within the in-pit cells or an External Tailings Facility (ETF). Coarse tailings from cyclone underflow, overburden materials or lean oil sands may be used for construction of the cell (Beier et al., 2009). In order to minimize the segregation and to create a stable CT deposit with maximum potential of fines capture, a low energy depositional environment is required. Controlling the shear rate during transport and discharge is an issue that the oil sands industry has not fully addressed yet (Sobkowicz and Morgenstern, 2009, 2010).

After deposition of multiple thin layers of CT/NST, a thick cap of sand and overburden may be placed on the surface of the CT/NST deposit to increase the vertical effective stress and frictional strength at the top of the deposit in a short period of time (weeks). This will allow access for further land farming and reclamation activities (Beier et al., 2009; Sobkowicz and Morgenstern, 2010).

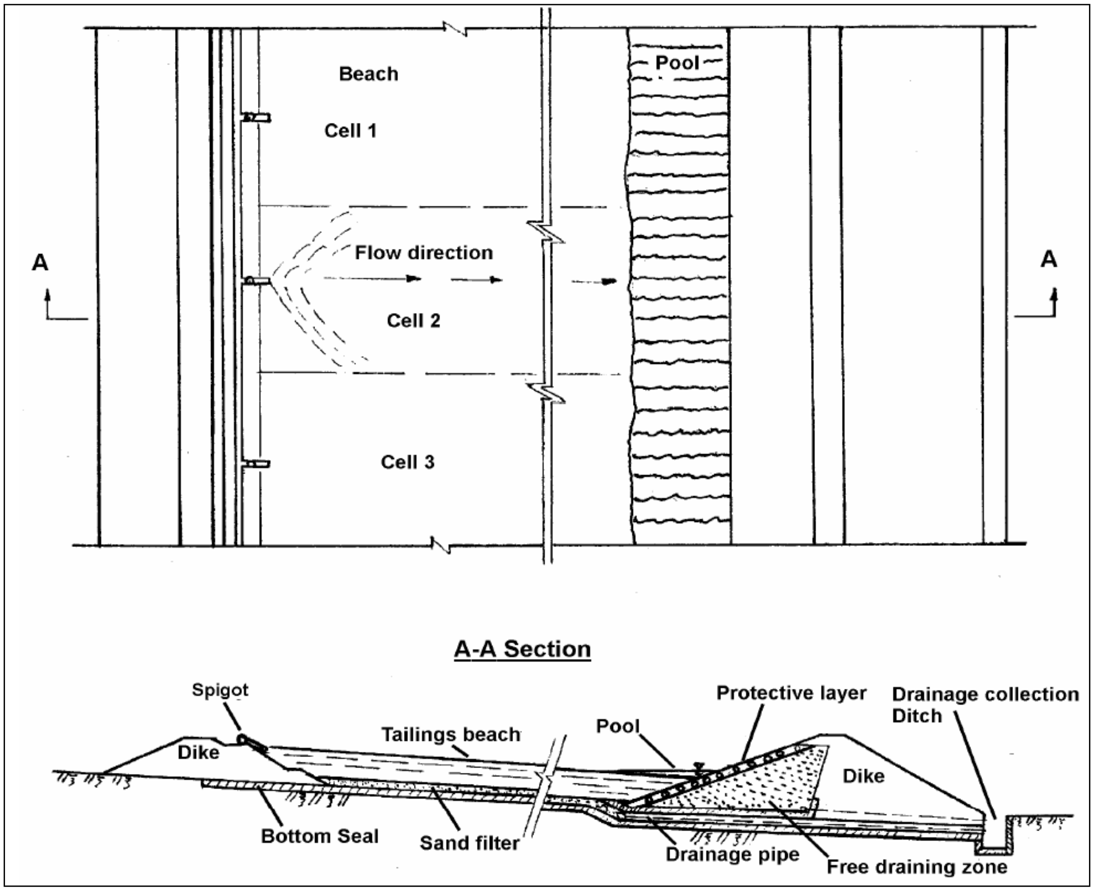

Figure 2.11 - Sketch of the sub-aerial tailings disposal method (after Qiu and Sego, 1998)

2.8.1.5. Challenges of CT/NST

Although it is more than a decade that the oil sands industry has produced CT/NST at a commercial scale, this technology has not performed as anticipated. This engineered waste stream was expected to be non-segregating when discharged, but in practice it was not particularly robust and partial segregation has been observed, resulting in release and re-suspension of fines following deposition. Another challenge for the industry has been achieving a geotechnically stable deposit in a timely manner, but the dewatering rates of this material have been lower than expected and this has prevented the deposit from reaching the strength required to support reclamation (Sego and Morgenstern - Personal Communication, 2005; Moussavi Nik et al., 2008; Beier et al., 2009).

Fluctuations in the solids content of the sand (cyclone under flow), variable clay content of the fine tailings due to heterogeneity of the oil sands ores, and difficulties in controlling the energy of the depositional environment are the factors that contribute to segregation of CT/NST (Moussavi Nik et al., 2008; Beier et al., 2009).

In addition to performance issues, another concern of the industry regarding CT/NST has been limited availability of the sand, which is also required for construction of tailings dykes/cells (Halferdahl – Personal Communication, 2007).

2.8.1.6. Previous trials for improving CT/NST quality

As stated in Chapter 1, to obtain a more robust CT/NST, its solids content must be increased. The possibility of using thickeners for dewatering CT has been studied previously, but the results have not been promising (Matthews – Personal Communication, 2007). Some of the primary challenges anticipated with the concept of using thickeners to further enhance CT solids concentration would be: very high torque management issues; the large volume of material and the need for a lot of settling area to reduce the expected long residence time for water release; and handling the thickened underflow in terms of feeding a pump and management of transport of the thickened material to the point of discharge.

Due to shortcomings observed in implementation of the CT/NST technology, the industry is looking into alternative tailings management strategies. In the following sections, a brief review of these alternative approaches is presented.

2.8.2. Chemical and/or Mechanical Dewatering of Fine Tailings

2.8.2.1. Thickening[6]

While the fine tailings from cyclone overflow could be permanently stored at the bottom of an end-of-pit pond, the current practice is to treat it with polymer flocculants and introduce it into a thickener. Addition of flocculants will enhance the settling rate of the fines. [More details about the role of flocculants is provided in section 2.9]. The thickener underflow referred to as TT (Thickened Tailings) can have a solids content of up to ~50%. As previously explained, TT can be combined with sand to produce NST or may be deposited as a separate stream to go through self-weight consolidation and natural dewatering (evaporation and freeze-thaw). In practice, the solids content of TT can be quite variable. One major reason is that thickeners also act as water clarifier and heat recovery unit for the extraction plant. As a result, the feed flow rate and residence time of the thickener are adjusted to obtain higher volumes of clear warm water, and this is at odds with producing underflow with higher solids content (Sobkowicz and Morgenstern, 2009).

Lord and Liu (1998) presented the results of geotechnical and depositional tests conducted on the underflow of a continuous thickener at the Syncrude Research Centre. The fine tailings used as feed to the thickener was obtained from the Clark Hot Water Extraction (CHWE) process and the Low Energy Extraction (LEE) process. For the feed with 32 to 37% solids content and ~50% sand content, they reported a thickener underflow of 60% to 62%, reaching to 70 to 72% solids content within 1-2 weeks of deposition. For “de-sanded” tailings, with initial solids content of 12-13% and ~5% sands content, the thickener underflow had a solids content of 32% and 48% for CHWE and LEE tailings accordingly. These thickened tailings were deposited into a 300mm wide and 9m long flume and formed a slope of 1.6% and 2.8% accordingly. Lord and Liu (1998) reported the initial vane shear strength of the freshly deposited thickened tailings reached ~50Pa, which increased to 2-5 kPa during 2-3 weeks of deposition due to thixotropy, self-weight consolidation and natural evaporation. By conducting [large strain] consolidated undrained triaxial compression tests on the thickened tailings samples (95% fines), these researchers concluded that the tailings streams typically behave like a normally consolidated clay.

[6] For details of the operation and different types thickeners, refer to section 3.2 in Chapter 3.

In 2009, Syncrude issued a review of their trials for developing the TT (Paste) technology from 2000 forward (Yuan and Lahaie, 2009). They used a shear enhanced paste thickener for their pilot tests in 2005. For feed with ~12-13% solids content and ~50% fines, a thickener underflow (paste) at 58% to 60% solids content was obtained. The unsheared and sheared yield stress of the thickened tailings samples were reported ~400Pa and ~110Pa accordingly, indicating the shear-thinning characteristic of the thickened tailing (paste). A centrifugal pump was used to transport the resultant TT (paste) into a flume to determine the deposit slope and its consolidation rate.

In addition to the pilot thickener tests, Syncrude also completed a series of field tests from 2001 to 2008, using a 10m conventional (high rate) thickener, a 1.5m deep cone paste thickener and a 4m high compression thickener. In 2003, the thickener underflow was pumped into a large deposition cell at an initial solids content of 47-53% and SFR of 0.6 to 1.5 and formed a 1m thick layer on a previously deposited [semi-dry] layer (Figure 2.12). After one month the solids content reached to 60-65%. After about 8 months of desiccation and freeze thaw, the solids content reached to ~70-75%. According to Yuan and Lahaie (2009) the pilot and field trials showed that the TT (paste) technology could be an effective tailings management alternative, however, a number of unknowns such as optimal thickness of the lifts, the life cycle of polymer and fate of polymer in thickener overflow and the TT deposit, and also the impairing effect of bitumen accumulated in the thickener feedwell on the flocculation process need to be addressed.

Shell Canada (Albian Sands Energy) and CNRL use thickeners for enhanced dewatering of cyclone overflow and production of Thickened Tailings (Matthews, 2008; Chu et al., 2008). The resultant thickener underflow is a component for production of NST. Matthews and Masala (2009) presented the results of field trial deposition of TT (Solids Content=58%, SFR=0.68) and NST (Solids Content=77%, SFR=4-4.7) at Shell Canada Tailings Testing Facility (TTF) in 2007 and 2008. The average fines capture per cubic meter of NST and TT deposits were ~325kg and 700kg accordingly.

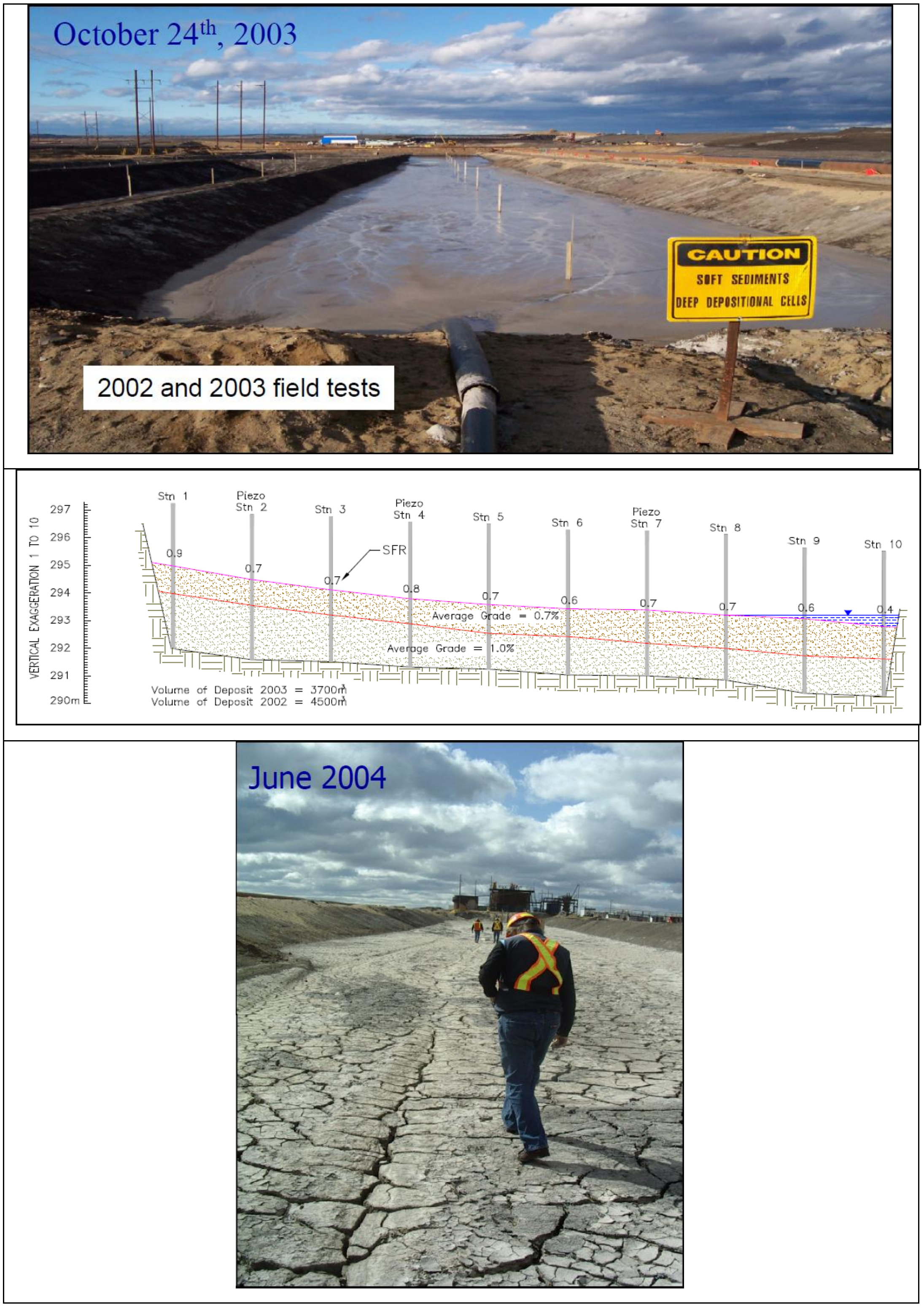

Figure 2.12 – Syncrude field trials for deposition of thickened tailings into a containment cell (Modified from Yuan and Lahaie, 2009).

At CNRL, 70m diameter thickeners with high torque rakes are utilized. Prior to addition of the polymers and flocculation, the solids content of the feed is reduced from ~28% to 10% – 15%. The underflow solids content is predicted to be between 46% to 60%. According to Chu et al. (2008), the yield stress of 150 Pa is the upper limit for pumping the thickener underflow with a centrifugal pump.

2.8.2.2. In-Line Thickening

Another approach for thickening the cyclone overflow is In-Line Thickening. As explained in section 2.7, the concept of producing In-Line Thickened Tailings (ILTT) is very similar to production of TT. In this method the tailings stream is mixed "in-line" with some chemical additives and the resultant treated stream is deposited into a settling pond/cell. Yuan and Shaw (2007) introduced a three stage chemical amendment for Syncrude fine tailings. In this method, the fine tailings stream is mixed with a sequence of a flocculant, coagulant and floculant (FCF), resulting in large aggregates of fine particles with improved settling rates (Yuan and Shaw, 2007; Jeeravipoolvarn, 2010). Details of the geotechnical field investigation conducted on ILTT produced at the Syncrude pilot ponds is provided by Jeeravipoolvarn (2010).

2.8.2.3. Centrifugation

Review of literature shows that centrifugation of oil sands tailings has been tried since the late 60's. Baillie and Malmberg (1969) proposed centrifugation of chemically flocculated pond sludge. Corti and Falcon (1989) patented a process for centrifugation of oil contaminated sludge in multiple stages. These early studies suffered from difficulties to design a feasible and economic process that would be acceptable to the industry (Kasperski, 1992).

In recent years, and specially after introduction of the new regulatory requirements for reduction of the fluid fine tailings[7], this method of dewatering has received more detailed attention from the oil sands operators.

Syncrude, with the help of CanmetENERGY, conducted some bench scale trials of centrifuging MFT in 2005. To initiate the feasibility studies, in 2007 Syncrude used

[7] In Feb. 2009, ERCB (Energy Resources Conservation Board) introduced Directive 074, stating new requirements for the regulation of tailings operations associated with mineable oil sands.

relatively large oilfield centrifuges and conducted a pilot scale trial. In 2008, Syncrude conducted a two month field trial to study MFT flocculation and centrifuging process, also to investigate transportation of centrifuge cake (using conveyors, positive displacement pumps and pipelines) and to produce bulk dewatered material for further geotechnical and environmental studies (Ahmed et al., 2009). The field pumping trials confirmed that centrifuged MFT at 55% solids content, if initially sheared in a mixer, can be pumped using positive displacement (PD) pumps. Also to realize the rheological characteristics of centrifuge cake, on-site flow loop testing was conducted which showed that this material followed a Bingham Plastic model.

In 2010 Syncrude used three parallel centrifuges, two with bowl diameter of 60cm and one with bowl diameter of 100cm. The centrate was sent back to the tailings pond for future reuse in the extraction process and the cake was conveyed to trucks and then dumped to form a deposit. After a period of about three weeks a relatively dry crust formed over the deposited cake. According to the Syncrude website (2011) after a period of 12 months due to evaporation and freeze-thaw processes, the underlying softer layers gains enough strength to support [light] vehicle traffic or human weight. At this stage either subsequent layers of cake can be deposited or the reclamation activities can begin. Syncrude does not comment on the maximum thickness of the cake that can reach a particular strength during a period of 12 months. From their 2010 campaign, Syncrude found that in addition to pumps, trucks can also be utilized as a method of transportation and disposal of the centrifuged cake. Figures 2.13 illustrates the appearance/consistency of a sample of centrifuge cake obtained in the Syncrude 2010 campaign (Syncrude website, 2011).

Figure 2.13 – Centrifuge cake sample from Syncrude 2010 campaign (snapshots taken from a video available on Syncrude website, 2011).

2.8.2.3. Filtration

The possibility of using filtration technology has been studied since the early years of oil sands extraction operations. Hepp and Camp (1970) patented a vacuum pre-coat filtration method for dewatering flocculated fine tailings. In this method, the fine tailings pumped from the tailings pond is initially amended either by organic sequestering agents (e.g. aluminum sulfate (alum), sulfuric acid, etc.) or by high molecular weight acrylamide polymers (e.g. polyacrylamide). As illustrated in Figure 2.14, this treated slurry is introduced to the pre-coat vacuum filtration assembly, composed of a vessel, a rotary filter drum, a shaving blade and a filtrate receiver. The cylindrical filter drum is covered with a coarse weave fabric supporting a pre-coat of porous material. Hepp and Camp (1970) used a one inch thick layer of diatomaceous earth (silica) with an average particle diameter of 4 microns as the pre-coat layer. These researchers also indicated that the same granular material could be added to the treated fine tailings to act as a filter aid and increase the filter cake porosity. They conducted several filtration tests using filter aids ranging from 4 to 12 microns and concluded that conventional filter aids of average particle diameters higher than 6 microns were ineffective for increasing filtration rate.

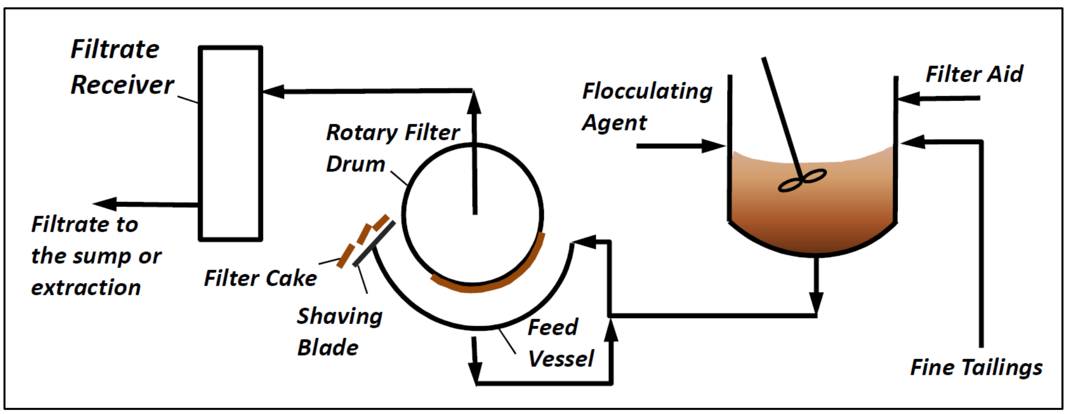

Figure 2.14. Schematic view of the vacuum pre-coat filtration method (modified from Hepp and Camp, 1970).

Liu et al. (1980) gave consideration to applying the process introduced by Hepp and Camp (1970) to the whole tailings, but they determined it was impractical due to the large filtration area and energy requirements. Experiments studying the feasibility of direct vacuum filtration of the untreated whole tailings were also unsuccessful: the coarse particles would build up a thick porous filter cake relatively quickly, and the fines would gradually form a layer on the surface of this cake and blind it (Liu et al, 1980). At the next stage Liu et al. (1980) tried adding a flocculating agent to the whole tailings prior to direct vacuum filtration. They found that agglomeration of the fines and coarse particles resulted in more uniform distribution of the fines throughout the filter cake, allowing relatively continuous filtration. Liu et al. (1980) used different chemical additives, particularly calcium salts, and showed that lime (CaO) was the most beneficial one considering its availability and cost. They recommended to avoid severe agitation of the treated slurry, as the agglomerates were relatively fragile and could break up, to the detriment of the process.

According to Kasperski (1992), filtration technology had difficulty to design a feasible and economic process that would be acceptable to the industry. However, this method has received renewed attention in the recent years.

Xu et al. (2008) conducted a series of bench-scale pressure filtration tests on unflocculated and flocculated samples to investigate the feasibility of oil sands tailings filtration. To prepare the tailings samples, they implemented the batch extraction process on an oil sands ore sample and obtained two tailings streams: a fine tailings stream with 7.9% solids content, 96% fines content and 0.72% residual bitumen; and a coarse tailings stream with 85% solids content, 11.8% fines content and 0.24% bitumen. By mixing different proportions of coarse tailings with fines, samples with varying fines content were prepared. To obtain coarse tailings samples with fewer fines than the original 11.8%, the coarse tailings samples were washed with tap water. An anionic, high molecular weight, polyacrylamide-based polymer was used as a flocculant.

Xu et al. (2008) concluded that filterability of a tailings sample is strongly affected by its fines content. Figure 2.15 shows the specific resistance to filtration as a function of fines content for flocculated and unflocculated samples. As illustrated, for raw (untreated) samples, increasing the fines content from 4.3% to 20% caused an increase of four orders of magnitude in resistance to filtration. Xu et al. (2008) stated that beyond 20% fines content, all the pores of the cake were filled with the fine particles so increasing the fines content will increase the resistance at a lower rate. These researchers indicated that it was possible to filter coarse untreated tailings with ~4.3% fines content; however, considering

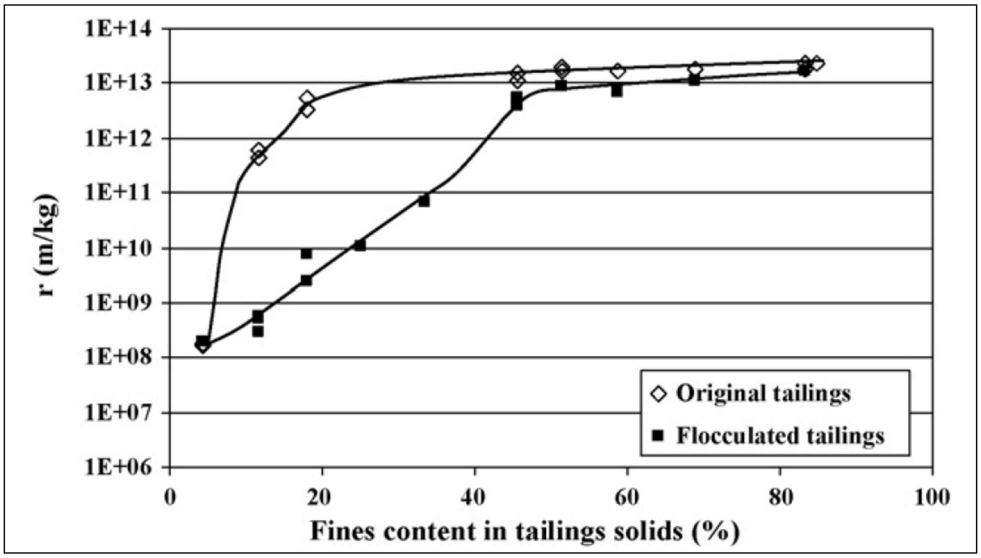

Figure 2.15 - Specific resistance to filtration for untreated and flocculated tailings obtained at 150kPa by Xu et al. (2008).

the extremely large volume of oil sands tailings, filtration of raw tailings with higher than 8% fines content would be impractical. For flocculated samples with up to ~20% fines content they observed significantly improved filterability in comparison to untreated tailings. Xu et al. (2008) indicated that the unrecovered bitumen present in the tailings may cause blinding of the filter cloth and blocking of the filtration channels in the cake. However, for the small amount of residual bitumen in their samples, they noticed that the residual bitumen was flocculated with the solids. They did not observe any bitumen coating on the filter paper, but emphasized the need for further studies on the role of residual bitumen in the filtration performance.

In their filtration tests, Xu et al. (2008) found an optimal dosage for the polymeric flocculants used for treatment of the tailings. Addition of the polymer beyond this optimal dosage had very little impact on the filtration resistance. They also indicated that the cake had its maximum solids content at this optimal dosage and increasing the flocculant caused reduction of the solids content. Further discussion about the cause of this behavior is presented in section 2.9. Also, in section 5.5.2.2 the effect of dosage of gypsum on solids content of the cake is addressed based on the tests conducted in the present research.

2.8.2.4. Centrifugal Filtration

The possibility of using a filtering centrifuge for dewatering of oil sands tailings was studied for the first time by Nik et al (2008, 2010). Observations from a series of batch centrifugal filtration tests revealed that in this dewatering method the majority of the unrecovered bitumen/asphaltene formed a separate internal layer close to the centre of rotation. This indicates that in this method of filtration the bitumen has less opportunity to be in touch with the filter medium and blockage of pores in the filter cloth is significantly reduced. Several filtering centrifuge tests with a variety of test conditions were conducted on the MFT samples received from Syncrude, Suncor and Albian Sands companies. The test results showed that a significant percentage of the MFT fed into the system could be collected as a cake with solids content ranging from 43%wt to 65%wt, suitable either for making a robust CT/NST or for deposition as a thick slurry/paste. The flow behaviour and robustness of CT/NST made from the resultant cake was evaluated by conducting laboratory scale flume tests (Nik et al, 2008, 2010). Chapters 5 and 6 of the present dissertation present the details of this research.

2.8.2.5. Cross Flow Filtration

In cross flow filtration (CFF), the slurry passes through a rigid porous pipe or a flexible hose made of a filter cloth. The porous pipe/hose, as illustrated in Figure 2.16, acts as a filter medium, i.e. the liquid permeates through the pipe wall as filtrate, and the solid particles are retained by the pipe wall forming a cake layer. While in conventional filtration the slurry and the filtrate have the same flow direction (see section 3.4 in Chapter 3), in CFF flow direction of the slurry is perpendicular to the building-up of the filter cake and filtrate flow. The tangential flow of the slurry applies a shear force on the cake layer. As a result thickness of the cake (and its resistance against filtration) is limited to a certain value. Therefore, contrary to the conventional pressure or vacuum filtration in which filtrate flux rate reduces with time, in CFF almost a constant filtration rate can be maintained (Yan et al., 2003; Zhang et al., 2009).

Beier and Sego (2008) studied the possibility of using cross flow filtration for dewatering oil sands tailings. To simulate the whole tailings, they used a mixture of water, sand and kaolinite with 55%wt solids content and 15%wt fines content. Using two different filter pipes, a polyethylene porous pipe and a PVC slotted pipe, they conducted a number of

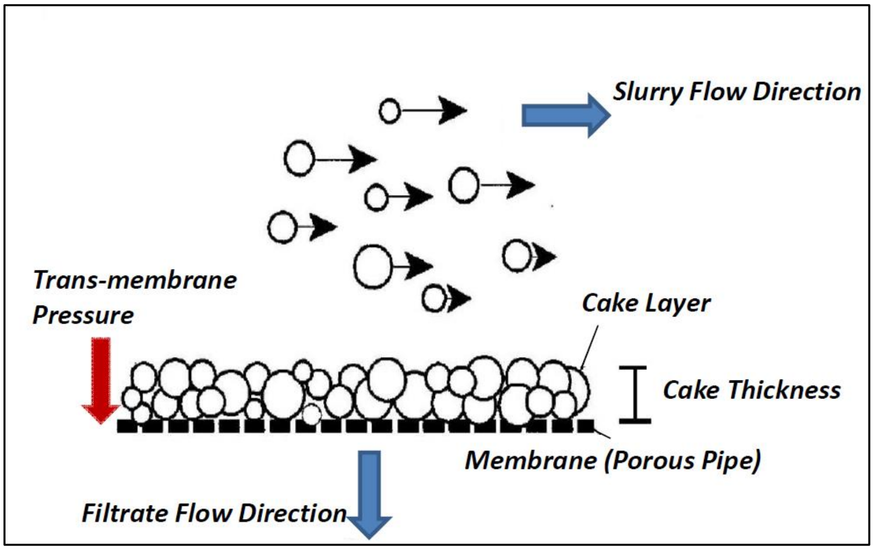

Figure 2.16. Mechanism of Cross Flow Filtration (modified from Ripperger and Altmann, 2002; Zhang et al., 2009).

CFF tests and achieved suitable filtrate quality and quantity in their experiments. They found that increasing the initial solids content did not affect the CFF performance; however, to maintain the filtrate flux rate for concentrated slurries a higher pipeline pressure might be required. Their experiments indicated that CFF could be a promising method for dewatering actual oil sands total tailings (Beier and Sego, 2008; Zhang et al., 2009).

Zhang et al. (2009) used a mixture of MFT, tap water and two types of beach sand (one with coarser gradation) to create two total tailings streams of 55% solids and 15% fines content. To conduct CFF tests on these tailings streams, they utilized two different filter pipes: a stainless steel porous pipe with 49% porosity and 40μm nominal pore size, and a stainless steel slotted pipe with 13% porosity and 250mm slot width (Figure 2.17). Summary of the findings by Zhang et al. (2009) can be listed as following:

- The coarser total tailings stream resulted in a higher flux rate.
- Performance of the CFF was not affected by increasing the tailings solids content.
- The unrecovered bitumen present in the total tailings can reduce the performance of CFF. Particularly for the porous pipe with smaller pore size, higher percentage of the pores could be plugged by bitumen in comparison to the slotted pipe.
- The larger the pore sizes, the longer it takes to obtain a clear filtrate.

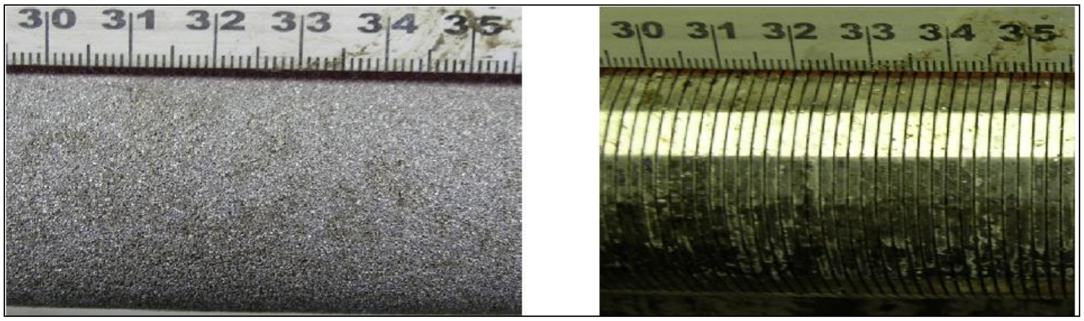

Figure 2.17. View of the two stainless steel pipes used by Zhang et al (2009) for CFF tests: Left: Porous pipe with 49% porosity; Right: Slotted pipe with 13% porosity.

2.8.3. Thin lift dewatering of oil sands tailings

The sub-aerial deposition of tailings in thin layers, as defined by Knight and Haile (1983, cited by Qiu, 2000) is systematic deposition of a solid-liquid suspension in a thin layer, allowing the solids to settle, the released liquid to drain, and the deposited material to partially air dry prior to placement of the next layer of fresh tailings. The physical processes of solid-liquid separation that are involved in this technique are sedimentation, consolidation and depending on the climatic conditions, evaporation-desiccation and/or freeze-thaw. The fundamentals of sedimentation and consolidation concepts are covered in section 2.10. The evaporation-desiccation and freeze-thaw processes are explained in the following section with reference to their application in oil sands tailings management.

In section 2.8.1.4, the sub-aerial deposition of thin layers was explained for CT/NST (Qiu and Sego, 1998). The same deposition technique can be utilized for enhanced dewatering of TT (see section 2.8.2.1 and 2) and MFT. In this method the thin layer of deposited material is preferred to be capable of holding a gentle slope, so the released water can flow towards the drainage system with no ponding on the surface (Figure 2.11). CT/NST and TT, if produced on-spec, show enough yield stress to form a gentle slope upon deposition (FTFC, 1995). However, untreated MFT due to its lower solids concentration and yield stress behaves like a fluid, showing no angle of repose when deposited. It is required to apply a chemical treatment to MFT to increase its yield stress and to enable it to form a gentle slope.

In recent years some oil sands operators in northern Alberta have introduced thin lift dewatering of treated MFT as one of their alternative tailings management options. At Suncor this method is referred to as TRO (Tailings Reduction Operations) (Wells et al.,

2011) and at Shell Canada this technology is called AFD (Atmospheric Fines Drying) (Shell Canada website, 2012).

As stated by Wells et al. (2011), during initial trials at the Suncor plant (in 2007) hydrated lime and gypsum were used for treatment of MFT. Although addition of these coagulants increased the shear strength of the MFT prior to its deposition, it did not particularly improve dewatering of the material during the sedimentation/consolidation stages. Instead, most of the water was lost through evaporation or freeze-thaw processes. In search for an alternative chemical additive that could provide improved dewatering characteristics in addition to enough shear strength, Suncor conducted a research project in collaboration with a chemical company. The result was development of a new polymer capable of generating an MFT slurry with enough yield stress[8], resistance against shear and a highly permeable floc structure. The prolonged resistance to shear allowed some flexibility to transport the flocculated MFT though pipelines towards the deposition cells. The flocculated structure of the treated MFT promoted its initial dewatering [due to sedimentation/consolidation] and the yield stress of the treated material allowed its deposition on a sloped beach, allowing the supernatant water to be collected at a low point down the slope. When optimum polymer dosage and proper mixing duration was applied, about 20% to 25% of the MFT water was released immediately as supernatant water (Wells et al., 2011). It should be noted that the new polymer can be injected in-line to the MFT slurry and except for the polymer make-up water no additional dilution of the MFT is required. The previous applications of polymers for flocculation of oil sands tailings was limited to fine tailings streams with low solids contents like the cyclone overflow (Jeeravipoolvarn, 2008; Matthews, 2008). Figure 2.18 shows the effect of polymer addition to a sample of MFT from Suncor ponds.

According to Wells et al. (2011), the dewatering and strength performance of the flocculated MFT can be greatly affected by the shear energy applied to it. Insufficient shear leads to formation of a strong flocculated structure that does not collapse/settle and as a result, does not release the water entrapped within the pores. On the other hand, excess shear breaks the bonds within the flocs and results in a MFT-like material with

[8] By enough yield stress it is implied that the treated MFT must not be too viscose, so it can be pumped easily, yet it must show enough shear strength to form a gentle slope upon deposition.

(1)	(2)	(3)

Figure 2.18- (1) Addition of polymer to an MFT sample in a beaker; (2) mixing and generation of flocs; (3) release of water (snapshots taken from an online video by Suncor, 2011).

poor dewatering characteristics. To study the effect of mixing time (i.e. shear duration) on the yield stress and dewatering characteristics of the treated MFT, Wells et al. (2011) used a rheometer and a capillary suction time[9] (CST) apparatus and measured the yield stress and CST at different times during the mixing process. As illustrated in Figure 2.19, they identified four stages in the "shear progression curve" (Wells et al., 2011):

- Stage 1- Polymer dispersion and conditioning. At this stage the flocs are formed and the yield stress is rapidly increased but water release is negligible.
- Stage 2- Rearrangement of the flocs: The solid-liquid slurry is at a gel state with high yield stress and roughly equal rate of floc formation and breakdown. Depending on the solids content of the MFT and applied shear rate, this stage can appear as a peak point in the shear progression curve or as a plateau.
- Stage 3- Breakdown of the flocs and dewatering: The flocculated structure collapses, the yield stress decreases and a significant volume of polymer-free water is released. As indicated in Figure 2.19, the capillary suction times recorded during this stage have their minimum values. This stage is the target design basis for deposition.

[9] Capillary Suction Time (CST) is a method of filtration/permeability measurement that utilizes the suction (negative pressure) created by capillaries within an absorbent paper. A sample of slurry is placed on a thick filter paper and the time that it takes the water/liquid to percolate between two electrodes located at a certain distance in the filter paper is measured. A low capillary suction time indicates the high filterability/permeability of the slurry (Gale, 1977: Optimizing the use of pretreatment chemicals, book chapter in Solid/Liquid Separation Equipment Scale-Up, edited by Purchas, 1977).

- Stage 4- Over-shearing of the flocs: The flocculated structure reverts to a dispersed (MFT-like) state. This stage is characterized by rapidly decreasing yield stress and very little water release values.

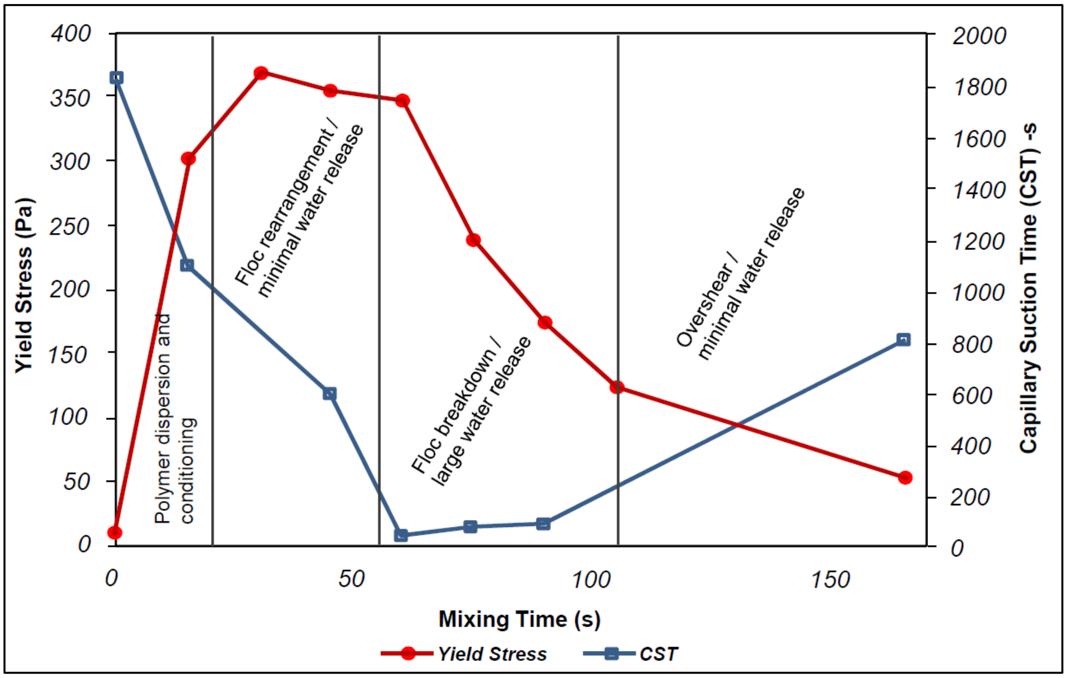

Figure 2.19- Shear progression curve of flocculated MFT (modified from Wells et al., 2011)

After using a variety of polymer dosages, Wells et al. (2011) concluded there is an optimal dosage of polymer that would result in a preferred permeability and water release during the third stage. Under-dosed and over-dosed treatment would fail to release free water and dewatering will mainly rely on evaporation. They also stated that the strength gain and dewatering effects observed for the specific polymer they used can be achieved by utilizing other standard Anionic Polyacrylamide (APAM) polymers, however the dispersion time and the shear stress response of these alternative polymers might be different.

2.8.4. Natural dewatering of oil sands tailings

Subsequent to sub-aerial disposal of the thin layer of tailings and removal of the water released during the sedimentation/consolidation stages, the tailings layer is exposed to the atmosphere. Depending on the climatic conditions, further dewatering may occur due to evaporative drying/desiccation or because of freeze-thaw. To achieve maximum dewatering due to these natural processes, it is necessary to predict the optimum tailings deposition thicknesses for varying climatic conditions. In the following sub-sections, the main factors affecting these natural dewatering processes are briefly reviewed.

2.8.4.1. Desiccation

Desiccation, the process of extreme drying, is a useful natural mechanism for further consolidation at the surface of tailings deposits and can provide the necessary strength required for reclamation activities (Robinsky, 1999). Both evaporation at the tailings surface and seepage into the underlying tailings layers can drive the desiccation procedure (Simms et al., 2009). The main processes that affect desiccation of tailings are evaporation, shrinkage and crack formation (Qiu, 2000).

Robinsky (1999) explained the process of strength gain due to evaporation in the following terms:

"…as evaporation takes place, menisci form in the pores at the surface of the tailings. Water tensile stresses develop which pull the water out of the pores, reducing the pore size. As pore sizes reduce, tensile suction stresses increase even more. The extruded water continues to evaporate and the soil continues to shrink, while remaining saturated throughout. Reduction in the pore size is, in fact, consolidation. Very high compressive stresses are developed during drying. Water content decreases, percent solids increases and strength increases…" (Robinsky, 1999)

For a tailings deposit, the rate of drying due to evaporation is affected by three main factors (Song et al., 2011; Newson and Fahey, 2003):

- Environmental factors, including the sources of radiation energy (sun, sky and clouds and the sensible heat transferred from the adjacent soil or air), relative humidity, wind speed (the ability of air to move the water vapour away from the soil surface), and precipitation intensity and duration.
- Characteristics of the tailings including hydraulic conductivity and the prevailing moisture content, which affect the availability of water at and below the evaporation surface; salt concentration in the pore fluid and its potential to form a crust.

- Tailings depositional conditions, including thickness and frequency of each deposited layer, the chosen layout for the discharge spigots (Robinsky, 1999), capillary barrier effects and under-drainage conditions.

It should be noted that the residual bitumen present in the oil sands fine tailings may gradually form a coating on the evaporation surface and impede the moisture transfer to the atmosphere, resulting in a reduced evaporation rate (Beier et al., 2009).

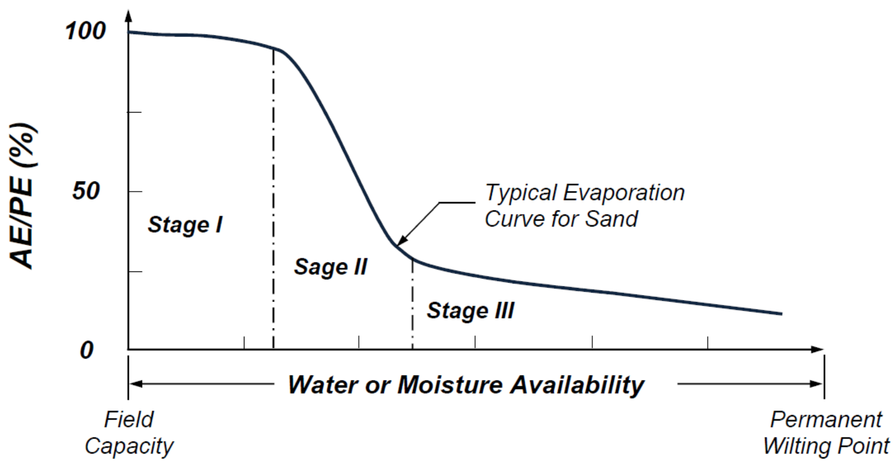

Figure 2.20 – The ratio of Actual Evaporation to Potential Evaporation (Ea/Ep) vs. water availability (modified from Wilson et al., 1994).

Evaporation occurring at the surface of tailings resembles the classic evaporation behavior in soils (Simms et al., 2009). Figure 2.20 (modified from Wilson et al., 1994) illustrates the three stages of evaporation for sand. Similar curves have been presented for clay surfaces (Gray, 1970 cited by Wilson et al., 1994). Stage I drying occurs when the soil surface is at or near saturation and the actual rate of evaporation (E_a) is approximately equal to the potential rate (E_p). When the conductive properties of the soil no longer allow a sufficient flow of water to the surface and the maximum potential rate of evaporation cannot be maintained, Stage II drying initiates. During this stage the rate of evaporation continues to decrease until it reaches a slow residual value known as Stage III drying (Wilson et al., 1994). At this stage the liquid-water phase becomes discontinuous due to desiccation of the soil surface. Hence, there will be no more flow of liquid water to the drying front and migration of the water molecules occurs through the process of vapour diffusion (Hillel, 1980 cited by Wilson et al., 1994).

The potential rate of evaporation[10] during Stage I can be calculated from climatic parameters (temperature, relative humidity, wind speed, and net radiation). A number of methods have been presented for calculation of E_p, among which the Penman method (1948) is widely used. The actual rate of evaporation (E_a) during Stage II is a function of climatic parameters and soil characteristics like unsaturated hydraulic conductivity and vapour diffusivity (Wilson et al., 1994). Given proper characterization of the tailings, conventional unsaturated flow models can be used for evaluation of the Stage II evaporation and seepage (Simms et al., 2007, 2009).

As previously stated, in addition to evaporation, shrinkage and crack formation are two other processes involved during tailings desiccation. The shrinkage behavior is due to presence of the clay minerals such as kaolinite, illite and montmorillonite. Extreme drying causes the water films surrounding the clay platelets to escape; as a result these platelets approach one another and shrinkage of the soil aggregates happens. The shrinkage and volume decrease of the soil results in development of tensile stresses. When these stresses exceed the tensile strength of the soil, tension cracks are formed (Qiu, 2000).

Several theoretical models haven been developed for prediction of the desiccation process in soils/tailings. Qiu (2000) has provided a comprehensive review of these models. For optimum sub-aerial deposition of the tailings, Qiu (2000) developed a theoretical model and its numerical implementation (called "DOSTAR"). This model used a unified sedimentation-unsaturated consolidation theory coupled with the linear elastic fracture mechanics (LEFM) theory and semi-empirical desiccation deformation theory. His model was capable of predicting sedimentation, consolidation and desiccation, along with crack initiation, propagation, spacing, depth and width, also the volume of tailings and the released water suitable for recycling (Qiu, 2000). Vogel et al. (2005) presented a model for crack formation in clay soil. In their model the clay layer was presented by a two dimensional triangular network of simple Hookean springs with

[10] Typical definition of the potential evaporation is provided by Penman (1948) as *"the theoretical evaporation that would occur from an infinite surface, adequately supplied with moisture when exposed to specific climatic conditions that remain unaltered by the evaporation itself."*(cited by Newson and Fahey, 2003).

finite strength. Desiccation was simulated by reducing the relaxed length of these springs. Once the relaxed spring length fell below a critical value, it would break and crack formation initiated.

2.8.4.1.1. Deposition thickness for drying oil sands tailings

In a recent study, Song et al. (2011) used a simplified methodology to determine the 'maximum' lift thickness of NST, TT and MFT deposits to achieve a vertical effective stress of 20 kPa[11] after evaporative drying in a certain time (~ one month). Based on meteorological data, consolidation properties and initial solids content/void ratio of the tailings, the deposition thickness was determined in the context of *"the exceedance probability of achieving the desired solids content (and hence undrained shear strength)".* The desired solids content for NST, TT and MFT was considered 79%wt, 74%wt and 72%wt accordingly. Song et al. (2011) assumed that after deposition of each tailings stream, dewatering (and strength gain) occurs due to sedimentation/consolidation and only Stage I drying; i.e. the tailings deposit was considered to be saturated at its final state. Using a 100-year climate database developed for Shell ASE site at Northern Alberta, the potential evaporation (E_p) for each month of the year was calculated through Penman method. The tailings deposition thickness year round was calculated through a trial and adjustment method for a variety of scenarios, covering different surface runoff management, tailings initial solids content and evaporation conditions. Although downward drainage to the foundation materials underlying the tailings deposit can play an important role for dewatering (Wilson et al., 2011), this factor was not included in the studied scenarios (Song et al., 2011). Figure 2.21 shows the sample calculated deposition thickness of MFT for a number of scenarios. In this figure the maximum monthly thicknesses are achievable when all precipitation is considered as runoff.

[11] Assuming the ratio of undrained shear strength over vertical effective stress equal to 0.25 (Hyndman and Sobkowicz, 2010 cited by Song et al., 2011), this would be equal to an undrained shear strength of 5 kPa, enough to support a pedestrian.

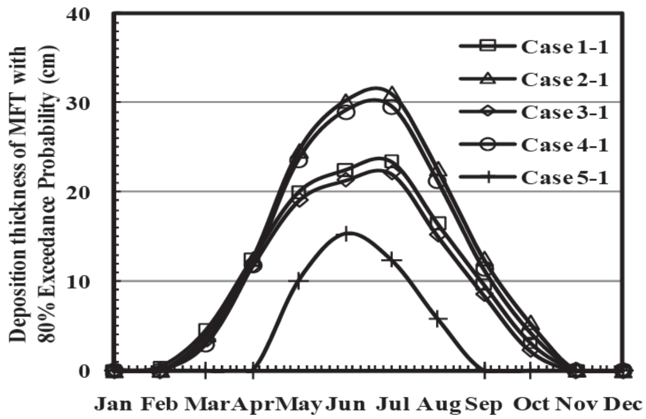

Figure 2.21 – Monthly deposition thickness of MFT with 80% exceedance probability (adapted from Song et al., 2011)

Based on their study, Song et al. (2011) concluded for the scenarios that most likely reflect the site conditions, annual tailings deposition thickness (i.e. sum of monthly thicknesses, assuming an 80% probability exceedance) would be ~140-180cm for NST, ~115-145cm for TT, and ~105-135cm for MFT. To increase the tailings deposition thickness, they suggested proper surface slope control for efficient management of surface runoff, mud-farming activities for maximum utilization of evaporation, and increasing the initial solids content of the tailings prior to deposition (Song et al., 2011).

It should be noted that in a series of laboratory studies on drying of oil sands fine tailings, Blanchard et al. (2000) found that continuous mechanical treatment (stirring) of the fine tailings significantly reduced the drying time. This was attributed to breakdown of the gel network in the fine tailings and renewal of the surface available for drying. Also in a recent study conducted at the Delft University of Technology, the possibility of using mud-farming for further dewatering of oil sands fine tailings was explored (Yao et al., 2010). The composition and dewatering characteristics of TT samples received from Shell Canada MRM operations were compared with the ones of the Rotterdam harbor dredged sludge. Based on this comparison and considering the annual average temperature and precipitation at Fort McMurray, Yao et al. (2010) concluded that the mud-farming technique can be applied to ripen oil sands fine tailings during the summer period (mid-April up to end of September), in combination with freeze-thaw during winter months. Figure 2.22 illustrates the “Amphirol” vehicle the Dutch have experimented with mud-farming of the dredged sludge.

Figure 2.22 – Amphirol used for mud-farming of dredged sludge (adapted from Yao et al., 2010)

2.8.4.2. Freeze-thaw dewatering of oil sands fine tailings

The freeze-thaw process has been recognized as an effective method for dewatering fine grained slurries. Exposure of such slurries to below freezing temperatures creates negative pore water pressures between the ice filling the voids and the unfrozen water surrounding the mineral particles. The reason for development of this negative pore pressure (suction) is the surface tension differences between ice and unfrozen liquid water. As a result of this suction, the liquid water moves towards the growing ice crystals and a distinct segregated reticulate ice/fine-grained "ped" structure is formed. The segregated ice/fine-grained systems can be formed in two different classes. When freezing occurs in stratified soils with higher permeability and an open groundwater system beneath the freezing plane, horizontal ice lenses form just above the 0^oC isotherm as the water migrates upward from lower unfrozen soil layers. When freezing takes place in a closed system of low permeability structure-less soils (with no access to free water), a three dimensional reticulate ice vein network forms by removing the pore water from the matrix of freezing soil (MacKay, 1974; Dawson et al., 1999). Figure 2.23 (modified from MacKay, 1974) illustrates a schematic cross section of clay blocks surrounded by the ice veins. According to MacKay (1974), the ice veins are formed primarily by removing the pore water from the adjacent freezing clay blocks. During thaw this reticulated ice structure melts and dewatering occurs through the remnant ice fissures.

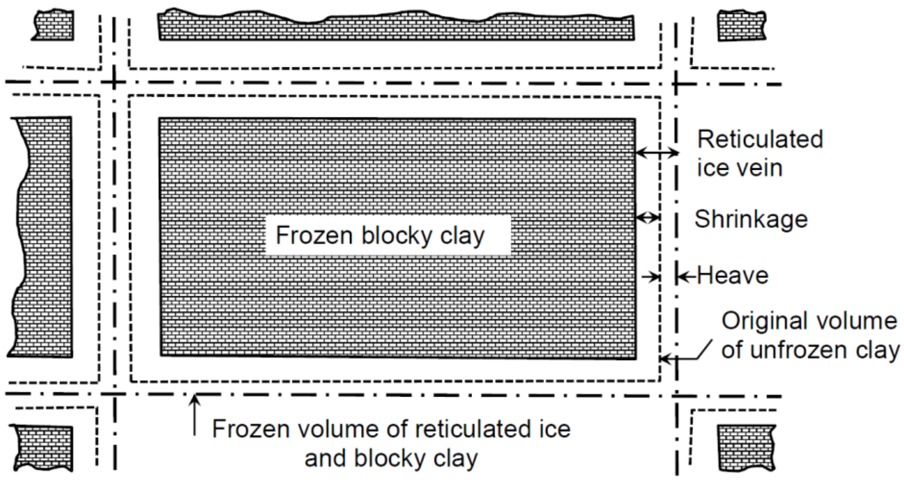

Figure 2.23 – Cross section of a frozen clay block and the ice veins (modified from MacKay, 1974)

This three-dimensional network of fissures provides an increased post-thaw hydraulic conductivity. The previously frozen fine grained peds/blocks form a soil mass with higher solids content (Proskin, 1998; Dawson et al., 1999; Beier, 2009).

Since the late 1980's extensive laboratory and field research has been carried out to investigate the freeze-thaw dewatering properties of oil sands fine tailings. Johnson et al. (1989, 1993), researchers at the Alberta Environmental Centre, found that small scale samples of Syncrude MFT with an initial solids content of 29% to 35% obtained a solids content of 52% to 54% after one cycle of freeze-thaw. Slightly higher solids contents (~56%) were achieved in larger scale experiments. The field tests showed that 2 m thick layers of frozen MFT could thaw under ambient Fort McMurray conditions. The released water during thaw could be drained from a V-notch ditch considered along one side of the deposition cell. The thawed fine tailings was fertilized and Reed Canary grass was successfully cultivated on it, which assisted further dewatering of the tailing by evapotranspiration (Johnson et al., 1989, 1993 cited by Dawson et al., 1999; and Beier et al., 2009).

In a series of bench scale lab tests conducted by Sego (1992, cited by Beier et al., 2009), 15 cm thick layers of fine tailings were frozen in cells with top and bottom cold plates at temperatures of -15 and -8^{o}C, respectively. After thawing the frozen MFT and removing the water released due to thaw strain, the solids contents of the dewatered tailings were measured. Figure 2.24 illustrates the results obtained for samples obtained from Syncrude, Suncor and OSLO operations. The different thaw strain[12] behavior observed in this figure was attributed to different concentrations of major dissolved cations in the tailings pore water. Based on X-ray diffraction analyses mineralogy of all three MFT samples were similar (Proskin, 1998). However, the sodium concentration in the pore water of OSLO tailings was significantly lower than the other two samples. This was attributed to the different extraction process of the OSLO method, which does not involve addition of sodium hydroxide. This observation led to additional research regarding the effect of chemical amendment of MFT on its freeze-thaw dewatering behavior (Sego and Dawson, 1992 cited by Dawson et al., 1999). By adding sulfuric acid (H_2SO_4) and quick lime (CaO) to Suncor MFT prior to its freezing, Sego and Dawson (1992) observed an 18% additional increase in the solids content of the thawed material. The water released after freeze-thaw of these chemically treated samples had no measurable solids compared to the similar tests conducted on untreated MFT, in which the decanted water had a solids content of 2.5% (Sego and Dawson, 1992 cited by Beier et al., 2009).

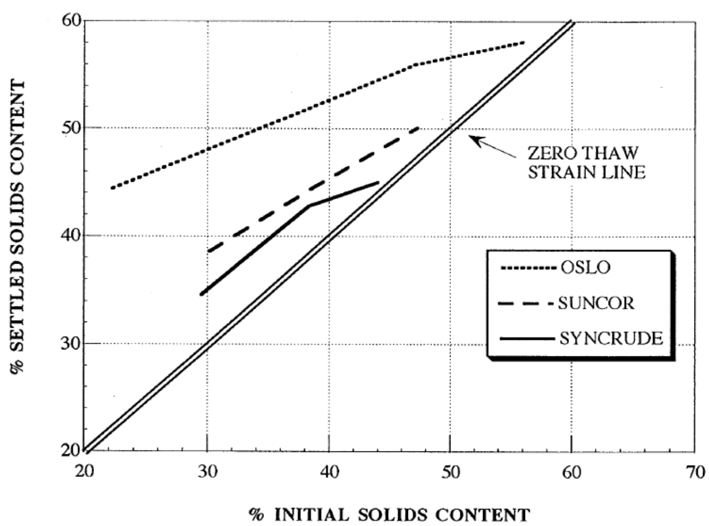

Figure 2.24 – Enhanced solids content of thaw dewatered fine tailings samples tested by Sego and Dawson (1992) (adapted from Dawson et al., 1999).

[12] Thaw strain: Ratio of change in volume of thaw dewatered tailings sample to its initial volume prior to freezing.

Using the same chemical additives, Proskin (1998) conducted thin layer freeze-thaw tests on Suncor MFT at field scale. Two test ponds (2A and 2B), each 175m long and 45m wide, were constructed on the beach of Suncor's tailings pond 2. The perimeter dyke had a height of 3m. During the first year of tests (1992-93), Pond 2A was filled with 9 lifts of treated MFT, to a total height of 1.68m and Pond 2B was filled with 8 lifts of treated MFT, to a total height of 1.73m. The deposition took about 2 months, from late December of 1992 to late February of 1993. The thawing process had been completed by August of 1993 and a significant volume of water had been released. The thawed tailings were allowed to go through post-thaw consolidation, surface drainage and surface drying for two additional months. During the October 1993 sampling program, it was observed that the solids content of MFT had increased from 28% to 69% and the volume was reduced by 61%. Also the field vane tests indicated that undrained shear strength of MFT had increases from ~0.02 kPa to an average value of 2.9 kPa. The second year of field tests (1993-94) were conducted to investigate freeze-thaw dewatering of a deposit composed of a new deposit of MFT placed on the previously frozen-thawed MFT of last year. The tests results indicated that the combined solids content of the both deposits (the 1992-93 and the 1993-94 together) increased from 47% to 75% after thawing, surface drainage and some atmospheric drying. The average undrained shear strength for the deposit in Pond 2A increased to 6.9kPa from the previous year value of 2.9kPa.

Dawson (1994) conducted post-thaw consolidation tests on a number of fine tailings samples. The samples were prepared from the cores obtained at a frozen pond containing OSLO cold water bitumen extraction (OCWE) process fine tailings. Comparison of the compressibility (void ratio versus effective stress) and permeability (void ratio versus permeability) behaviour of these samples with the associated values for never frozen fine tailings indicated that (Dawson et al., 1999):

- *"Thawed fine tailings behave like an overconsolidated soil and approach the never frozen fine tails compressibility line (virgin consolidation line) at stresses in excess of l0 kPa."*
- *"The thawed fine tails exhibit enhanced permeability values up to two orders of magnitude greater than those of the never frozen fine tails at similar void ratio upon thaw."*

Considering the average air temperature and duration of freezing and thawing seasons for Fort McMurray, Dawson et al. (1999) used some thermal models to estimate the design thicknesses for freeze-thaw dewatering of fine tailings. Their study revealed that in the Fort McMurray area a thin lift freeze-thaw dewatering system is governed by thawing considerations. The average yearly thaw thicknesses for ambient and enhanced warm water cap thaw conditions were calculated to be 3.0 and 4.5 m respectively. Although conceptual design calculations for a modest sized oil sands mine indicated that very large areas would be required for thin lift freeze-thaw dewatering of the fine tailings, Dawson et al. (1999) envisaged that in practice other management technologies would be coupled with this method. Recent advances in production of polymeric flocculants and thin lift dewatering of flocculated tailings (as stated in section 2.8.3) have caused renewed interest in taking advantage of the effect of freeze-thaw.

2.9. Clay-Water Interaction

As stated in section 2.6, typically over 95% of the solids in MFT are fine particles with 30 to 50% of them clay sized. Previous research has demonstrated that it is the clay fraction, both as a size and in the mineral form that defines the fine tailings properties and in particular their dewatering characteristics (Mikula et al., 2008). This section provides a brief review of the colloid chemistry of clay.

Colloid particles are classified as those in the size range of 10^{-9} and 10^{-6} m. A dispersion of these particles in a fluid is called a "colloidal dispersion" or a "sol". Dispersions of larger particles however are called "suspensions" (Hughes, 2000). Based on this definition MFT is a suspension that includes particles of colloidal dimensions (sub-micron) along with larger micron-sized particles. There are two major classes of colloidal dispersions: "lyophilic" colloids in which the solids show an affinity for water or some other dispersion medium; and "lyophobic" colloids where solid particles exhibit a low affinity for the host medium (Hughes, 2000). When the dispersion medium is water, these two colloidal systems are called "hydrophilic" and "hydrophobic", accordingly. Clays are an example of hydrophobic colloids. Hydrophobic dispersions are particularly sensitive to the addition of electrolyte salts and will flocculate upon such additions (van Olphen, 1977; Hughes, 2000).

Clay particles carry a net negative charge on their surface. This is due to the defective lattice of this crystalline material and presence of a net excess of anions at its surface (Hughes, 2000). When immersed in an aqueous solution, the negative surface charges of clay can be balanced by a cloud of counter-ions to create an electric double layer (EDL). Figure 2.25 shows schematic of the electric double layer model developed by Stern (1924) and Grahame (1947) (modified from Li, 2007). [It should be noted that the general model presented in Figure 2.25 shows positive charges at the particle surface and does not represent a clay particle]. As illustrated, the EDL is composed of an internal Stern Layer (the counter-ions bound to the particles surface) and an outer Diffuse Layer (the remaining counter-ions loosely associated with the particle) (Li, 2007). In the EDL model, the plane of slip between the double layer and the bulk media is referred to as the shear plane. The electric potential existing between the shear plane and the bulk phase is known as the zeta potential, ζ. Measurement of the zeta potential is a practical way to characterize the double layer (Hughes, 2000).

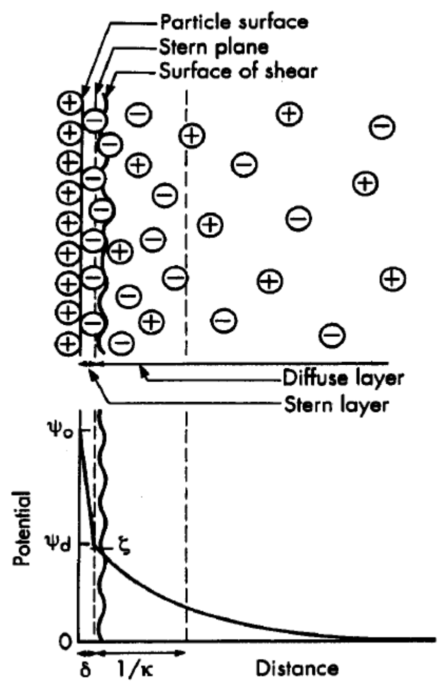

Figure 2.25 – Electric double layer model developed by Stern (1924) and Grahame (1947) (adapted from Li, 2007)

For two adjacent clay particles, attractive forces such as the London and van der Waals are opposed by the repulsive forces resulted from interaction of the negative charges distributed over each particle (Hughes, 2000). In a colloidal system, when the attraction and repulsion forces are in an equilibrium state, the particles remain dispersed and form a stable structure (Tang, 1997). A basic requirement for improving the dewatering characteristics of such a colloidal system (like MFT) is to bring the clay particles together and form larger aggregates.

2.9.1. Coagulation and Flocculation

Different definitions have been presented for the coagulation and flocculation processes. In colloid chemistry, the two terms are used interchangeably and are referred to the formation of aggregates in a colloidally unstable sol (IUPAC, 2012). However, some authors distinguish between coagulation and flocculation. Stocks and Parker (2007) state that it is necessary to make such a distinction because each term refers to a different process:

- In the coagulation process, the predominant mechanism is reduction of the repulsive potential of the electrical double layer, so that the attractive forces can bring the particles together to form small aggregates. Common chemical additives used for this purpose are multivalent inorganic coagulants like lime, alum, ferrous sulphate and ferric sulphate, or highly charged polymers of low molecular weight.
- In the flocculation process, long-chain polymers form a bridge between two or more particles and unite these particles into a random, three-dimensional, loose and porous structure. High molecular weight water-soluble polymers are used in this process.

According to Stocks and Parker (2007), during the flocculation process surface charge of the particles may or may not be changed. When the particles are in a state of natural coagulation, either due to the effect of naturally present inorganic salts or due to low surface charges, initial neutralization of the charged particles through the coagulation process would not be required, and the flocculation process can be accomplished without initial coagulation.

Hogg (2000) defines flocculation as the process of aggregating dispersed fine particles into larger units (flocs). He considers three principal steps for this process:

destabilization, floc formation and growth, and floc degradation. A brief description of these steps is provided in the following.

Destabilization: The purpose of this step is to destroy the stable structure of the colloidal system and to let the particles approach each other. This can be achieved by eliminating the electrical charges (neutralization) or by shielding these charges (double-layer compression) on the mineral particles. Adjusting the pH of the solution can usually be used to control the charges on the particles. At some pH (known as the isoelectric point) the particles have no net charge and are unstable. However, the pH adjustment may be an impractical method of destabilization if the isoelectric point occurs in an inconvenient pH range. The alternative approach would be shielding the charges on neighboring particles from one another by introducing relatively high concentration of ions in the solution. Multivalent ions resulting from reagents like alum, lime, etc. are especially effective for this purpose (Hogg, 2000). Figure 2.26 (modified from van Olphen, 1977 and Stocks and Parker, 2007) illustrates the effect of electrolyte concentration on the net potential energy between two particles in a suspension.

It should be noted that the “destabilization” process described by Hogg (2000) and the “coagulation” process defined by Stocks and Parker (2007) are in fact two terms used for the same identical process.

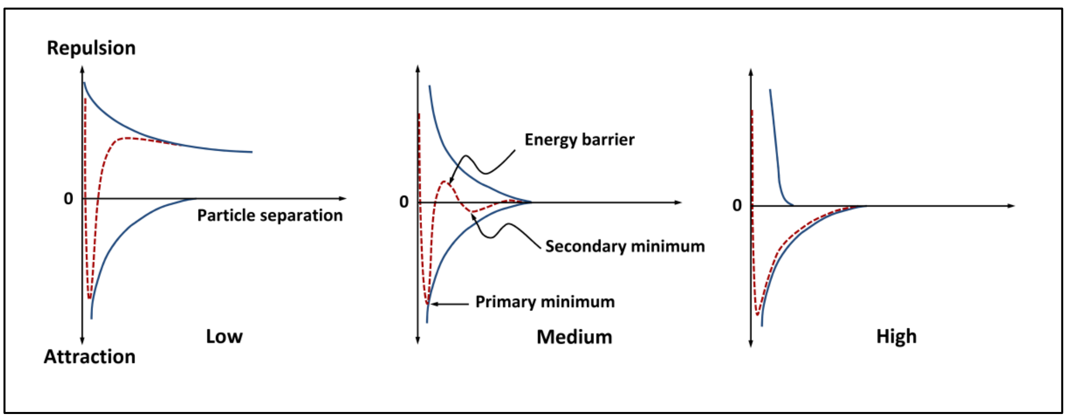

Figure 2.26- Net potential energy curve and the energy barrier between two particles in suspension at low, medium and high electrolyte concentrations (modified from van Olphen, 1977 and Stocks and Parker, 2007)

Floc development: After the destabilization stage, flocs can form as a result of collisions between particles due to Brownian motion, mechanical agitation and differential settling of individual flocs or particles. In the initial stages after destabilization, Brownian motion is the effective mechanism for formation of the flocs from very small particles. In the later stages agitation plays the main role in forming larger units through aggregation of existing flocs. Under quiescent conditions of a flocculated suspension (as in a clarifier/thickener) differential settling can be an effective factor for formation of larger flocs (Hogg, 2000).

Floc degradation: Previous research has shown that agitation of destabilized suspensions at high shear rates leads to very rapid flocculation, but the flocs formed cannot grow larger than a certain limit (Rattanakawin, 1998 cited by Hogg, 2000). As stated by Hogg (2000) the limiting factor appears to be floc breakage. The larger the floc sizes and the higher the agitation intensity, the more the flocs are susceptible to breakage. The limiting floc size occurs when the rate of floc growth and breakage are almost equal. Addition of high molecular weight polymer flocculants can improve the strength of flocs against breakage and increase the limiting floc size. Hogg (2000) has provided a detailed review of the different conditions that affect size of the flocs (e.g. mixing intensity and duration, flocculant dosage).

2.9.2. Application of coagulation and flocculation in fine tailings management

As stated in section 2.8, most of the technologies developed for management of the fine tailings (e.g. CT/NST, thickening, centrifugation, filtration and thin lift dewatering) take advantage of the coagulation and/or flocculation processes to enhance the dewatering characteristics of fine tailings. A comprehensive review of the different factors affecting the flocculation of oil sands fine tailings, including the effects of polymer dosage and charge density, particle size and concentration, water chemistry and mixing conditions is presented by Salehi (2010). A recent study by Yuan and Shaw (2007) indicated that another factor affecting the dewatering characteristics of fine tailings is the sequence of addition of flocculants and coagulants. They showed that a flocculation stage preceded and followed by coagulation (CFC), or a coagulation stage preceded and followed by flocculation (FCF) resulted in super-flocs and significantly improved the initial settling rate of the solid particles. This treatment method also resulted in a clear supernatant with a solids content of less than 0.13%wt (Yuan and Shaw, 2007; Salehi, 2010). As stated in section 2.8.2.2, the FCF treatment sequence was applied to the Syncrude fine tailings during an ILTT pilot scale study (Jeeravipoolvarn, 2010).

2.10. Process of soil formation

The genesis of soil deposits, and similarly deposition of hydraulic fills, is comprised of sedimentation and consolidation stages[13] (Schiffman et al., 1988). When the thin slurry of soil or mineral wastes is composed of clay sized particles, an initial stage of flocculation would also exist prior to the settling stage, during which no sedimentation takes place but the flocs of fine particles are generated. Figure 2.27 illustrates the generalized sedimentation characteristics of a clay-water mixture presented by Imai (1981).

Upon discharge of a thin slurry of mineral wastes into a containment area, the solid particles are carried in suspension in moving water until the flow velocity reduces enough to let the particles/flocs settle. This is the start of sedimentation stage in which the settling soil particles/flocs gradually form a sediment layer on the bed or on a previously settled layer of particles. A network of flocs with grain to grain contacts is formed and as additional material settles on top, the spacing between the flocs decreases further due to the weight of the above layers. This decrease in the volume between the flocs is associated with the expulsion of pore water from inside and between the flocs. This is the transitional stage from sedimentation to consolidation, where a soil framework with associated effective stresses is developing. At this stage, the soil skeleton is still very soft and compressible and the strains are comparatively large (Been and Sills, 1981). The conventional theory of consolidation developed by Terzaghi (1923) cannot be used for prediction of the rate of excess pore pressure dissipation in such deposits, because it assumes infinitesimal strains, neglects consolidation due to the body forces (self-weight) of the particles and assumes the coefficients of compressibility and consolidation remain constant in each load increment (Carrier et al., 1983; Schiffman et al., 1988). The following sections provide a review of the theories that have been developed for modeling the sedimentation and consolidation of slurries and soft soils.

[13] During the consolidation stage, if the water level is lowered and surface of the soil/tailings deposit is exposed to the fresh air, then desiccation can occur. As explained in section 2.8.4.1this process will lead to further consolidation of the soil surface layer.

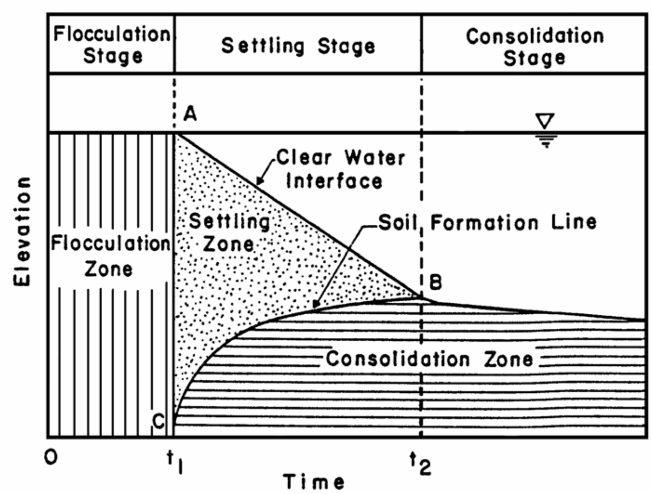

Figure 2.27 – The generalized sedimentation characteristics of a clay-water mixture (adapted from Imai, 1981).

2.10.1. Sedimentation of fine particles

Sedimentation is settling of a particle, or a suspension of particles, in a fluid due to the effect of gravity, centrifugal force or any other external body force (Concha, 2009). Suspensions of coarse particles behave rather differently from suspensions of fine particles. Coarse particles have a much lower specific surface and consequently, the surface forces and electrical interactions between the particles are of less significance in comparison to the fine particle systems. Flocculation does not occur for the coarse particles and, generally, rheology of the liquid will not be influenced by them (Richardson et al., 2002).

As previously explained, in the oil sands operations large volumes of fluid tailings containing silt and clay sized particles are produced. In the following sections, only sedimentation of the fine particles will be reviewed.

2.10.1.1. Particulate settling

When concentration of the fine particles in a liquid phase is very low, or when the solid particles are not surface-active (usually silt-sized or larger) and their distance is much larger than their size, the particles may settle individually, without interaction with each other. This is referred to as particulate settling. Under free settling conditions, the terminal falling velocity of a particle can be calculated according to the Stokes law:

$$V_s = \frac{2}{9}\frac{r^2 g(\rho_p - \rho_f)}{\eta} \tag{2.0}$$

In this equation V_s is the settling velocity of a single particle, r is the Stokes radius of the particle, g is the acceleration of gravity, ρ_p and ρ_f are densities of the particle and fluid accordingly, and η is viscosity of the fluid. In geotechnical engineering the Stokes law is used in the hydrometer analysis to determine the size of particles passing sieve #200.

2.10.1.2. Hindered Sedimentation

In many industrial and mining operations, the concentrations of suspensions are high enough to cause significant interaction between the particles. As a result of the modifications of the flow pattern, the frictional forces exerted at a given velocity of the particles relative to the fluid may be greatly increased, so that hindered sedimentation occurs and the particles settle together en-masse. The sedimentation velocity of a particle in hindered settling conditions may be considerably less than its terminal velocity under free settling conditions (Richardson et al., 2002).

Coe and Clevenger (1916) studied the settlement of metallurgical slimes and concluded that settling of an initially homogenous concentrated suspension gives rise to four settling zones, as illustrated in Figure 2.28. In this figure, “A” is a clear water zone, “B” is a zone of constant initial concentration, “C” is a transition zone of variable concentration and “D” is a compression/consolidation/sediment zone. Coe and Clevenger (1916) also observed a second and less common mode of sedimentation, in which zone “C” extends from the top interface to the layer of sediment and the zone of constant composition is absent. This case is obtained when the range of particle size in the suspension is very great (Richardson et al., 2002, Concha and Burger, 2003). According to Tan (1995), usually zones “B” and “C” are idealized to be undergoing sedimentation where no effective stress is assumed to be present, while zone “D” is assumed to be undergoing consolidation. Based on the macroscopic balance of the solid and fluid in a sedimentation vessel, Coe and Clevenger (1916) presented one of the first methods of designing thickeners. Section 3.2.2 of Chapter 3 briefly reviews their design method.

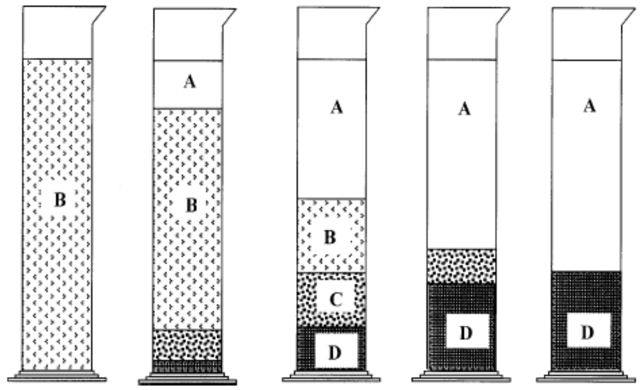

Figure 2.28 – Batch settling of a compressible pulp according to Coe and Clevenger (1916): A) Clear water zone; B) Zone of constant initial concentration; C) Transition zone of variable concentration; D) Compression zone (adapted from Concha and Burger, 2003).

2.10.1.2.1. Kynch theory of sedimentation

The first theory of batch sedimentation was developed by Kynch (1952), a mathematician at the University of Birmingham. This theory is based on the propagation of concentration waves in the suspension and the basic assumption that, at any point in the flow field, the settling velocity (v) of any particle is only a function of the local concentration (ρ) of particles in its immediate neighborhood. Kynch (1952) considered the suspension a continuum, called ideal suspension, and assumed that all the particles have the same size and shape. Another assumption was that everywhere the concentration would be the same across any horizontal layer. He introduced the particle flux as following:

$$S = \rho v \tag{2.1}$$

This parameter shows the number of solids particles crossing a horizontal section per unit area per unit of time.

Kynch (1952) considered two layers at elevations *x* and *x+dx* above the bottom of settling column and during time *dt*, calculated the accumulation of particles between these two layers as following:

$$\frac{\partial}{\partial t}(\rho dx)dt = S(x+dx)dt - S(x)dt \tag{2.2}$$

The right side of this equation is the difference between the flow of particles “in” through the upper layer and the flow “out” through the lower layer. Dividing by *dx.dt*, he derived the continuity equation of the solid phase:

$$\frac{\partial \rho}{\partial t} = \frac{\partial S}{\partial x} \tag{2.3}$$

Considering Equation (2.1), the continuity equation would be:

$$\frac{\partial \rho}{\partial t} + v(\rho)\frac{\partial \rho}{\partial x} = 0 \tag{2.4}$$

and $v(\rho) = -{dS}/{d\rho}$

If the initial concentration of the suspension $\rho(x,0)$ and the form of the particle flux function are known, then equation (2.4) can be solved by the method of characteristics (Kynch, 1952; Concha and Burger, 2003).

Based on the Kynch theory, Talmage and Fitch (1955) proposed a method of thickener design that has been extensively used in the industry (Concha and Bustos, 1987) (see section 3.2.2 in Chapter 3). According to Concha and Bustos (1987) the Kynch theory can describe the sedimentation of incompressible solid particles and non-flocculated mineral particles quite well. However, since this theory does not take into account compressibility, the sedimentation of flocculated suspensions [commonly encountered in the mineral industry] cannot be described using this theory. To account for compressibility, Bustos and Concha (1987) proposed a modification for the boundary condition used by Kynch.

An experimental verification of the Kynch theory in geotechnical engineering was first provided by McRoberts and Nixon (1976) for dispersions of silt and sand sized particles. Been (1980), Been and Sills (1981) and Imai (1980, 1981) also conducted experimental and theoretical studies on settling and sediment formation of clay materials. These studies and a large number of other literature [cited by Schiffman et al. (1988)] recognize the simultaneous presence of sedimentation and consolidation (Figure 2.27). In the following section first the conventional theory of consolidation and its shortcomings for prediction of settlement in hydraulic fills will be briefly reviewed; then the theory of large strain consolidation developed by Gibson et al. (1967) will be discussed and finally some theories suggested for linking the simultaneous processes of sedimentation and consolidation in soil suspensions will be presented.

2.10.2. Consolidation

2.10.2.1. Small Strain Consolidation

For a saturated soil, consolidation is defined as reduction of the soil volume with time under the applied stresses due to dissipation of the excess pore pressures. The conventional theory of consolidation was developed by Terzaghi in 1923 (Schiffman et al., 1969). This theory is based on the following assumptions (Qiu, 2000):

- The soil is fully saturated with water.
- The pore water and the soil particles are incompressible.
- Darcy's law governs the fluid flow within the pores.
- A linear time-dependent relation between the void ratio and effective stress controls the strains of the soil skeleton.
- The theory is quasi-static and strains, stress increments and velocities are small.
- The soil is considered homogenous.
- During consolidation, the compressibility and permeability of the soil remain constant under a particular increment of load (Gibson et al., 1967).

The mathematical expression for theory of one-dimensional consolidation is as following:

$$c_v \frac{\partial^2 u}{\partial z^2} = \frac{\partial u}{\partial t} \qquad (2.5)$$

In this equation u is the excess pore pressure, t is time, z is the vertical dimension and c_v is the coefficient of consolidation.

In conventional geotechnical engineering where the assumptions of infinitesimal strains and constant material properties during each load increment are valid, the above theory is commonly used to predict the rate of excess pore pressure dissipation. For soft soils like sediments of mine tailings however, the consolidation process is associated with large strains and nonlinear changes of compressibility and hydraulic conductivity (Jeeravipoolvarn, 2010). Carrier et al. (1983) and Schiffman et al. (1988) showed that use of the conventional consolidation theory would provide erroneous results for calculation of degree of consolidation in hydraulic fills and mineral waste slurries. They indicated that the nonlinear finite strain consolidation theory developed by Gibson et al. (1967, 1981) must be used instead.

2.10.2.2. Finite Strain Consolidation Theory

Gibson et al. (1967) introduced a one-dimensional non-linear finite strain theory of consolidation for homogenous layers of saturated clays in the following general form:

$$\pm\left(\frac{\rho_s}{\rho_f}-1\right)\frac{d}{de}\left[\frac{k(e)}{1+e}\right]\frac{\partial e}{\partial z}+\frac{\partial}{\partial z}\left[\frac{k(e)}{\rho_f(1+e)}\frac{d\sigma'}{de}\frac{\partial e}{\partial z}\right]+\frac{\partial e}{\partial t}=0 \tag{2.6}$$

In this equation, ρ_s and ρ_f are solids and fluid density accordingly, e is void ratio, k is hydraulic conductivity expressed as a function of e, σ' is the vertical effective stress which controls the void ratio, and z is a reduced coordinate based upon the volume of soil particles between the datum plane and the point being analyzed. In derivation of the above equation, Gibson et al. (1967) removed the limitation of small strains and considered the changes in soil permeability and compressibility during consolidation. They also adopted the Lagrangian[14] coordinate system; i.e. an element of soil skeleton whose boundaries always encapsulated the same soil particles was considered. Then the equations of equilibrium for the solids and fluid occupying this element, continuity of each of the solid and liquid phases, and the pore fluid flow (in accordance with Darcy's law with consideration of the drag forces on the soil skeleton) were combined to yield equation (2.6). It should be noted that Been (1980) demonstrated that the theory of hindered sedimentation (Kynch, 1952) can be deduced from the large strain consolidation theory (Gibson et al., 1967) by setting the effective stresses to be zero (Been, 1980; Pane and Schiffman, 1985).

[14] A comprehensive definition of the Eulerian and Lagrangian coordinate systems and their application in the small and large strain consolidation theories is provided by Gibson et al. (1981) and Schiffman et al. (1988).

For thin layers of clay, where the influence of self-weight of solids and pore fluid on the consolidation process is unimportant in comparison to the effect of applied stresses, Gibson et al. (1967) assumed $\rho_s = \rho_f$ and showed that the void ratio obeyed a weakly non-linear equation of the parabolic type. Later Gibson et al. (1981) presented the finite consolidation theory for thick homogenous layers of clay where stresses arising from self-weight of the soil skeleton and the pore fluid were also taken into account. From comparison of this theory and the conventional consolidation theory; they showed that the conventional theory overestimated the time of consolidation, but underestimated the amount of excess pore pressure at a given time which could lead to an overestimation of the shear strength within the deposit (Gibson et al., 1981).

2.10.3. Linking the Sedimentation and Consolidation

As previously stated in section 2.10.1.2.1, studies by Imai (1981), Been and Sills (1981) and other researchers (cited by Shiffman et al., 1987) recognize that during settling of a clay-water mixture, the sedimentation and consolidation phenomena are simultaneously present. In Figure 2.27, the boundary between the sedimentation and consolidation zones (marked as line CB) is known as the *soil* formation line. According to Shiffman et al. (1987), a *soil* "*is a deformable porous medium where the mineral skeleton has a definable stress-strain relationship*." In classical/conventional geotechnical engineering, the state of stress responsible for deformation of the porous mineral skeleton is called the effective stress σ'. Assuming that the porous medium is a two-phase system composed of an incompressible liquid (water) filling a deformable mineral skeleton, the effective stress principle can be written as (Shiffman et al., 1987):

$$\sigma = \sigma' + u_w \tag{2.7}$$

where σ is the total stress and u_w is the pore-water pressure.

In Figure 2.27 the material in the consolidation zone (i.e. below the soil formation line) can be defined as a soil. However, measurements at the top of the settling zone have shown that the total stress and the pore-water pressure are equal; in other words the effective stresses are zero and a particle aggregation has not been established (Shiffman et al., 1987). According to Imai (1981), the water content or void ratio at which a solid-liquid mixture converts into a soil/sediment is not uniquely determined. Similarly, Been and Sills (1981) stated that the concept of a unique void ratio corresponding to zero effective stress would be inaccurate. Rather than a sudden change from a zero effective stress suspension to an effective stress dominated soil, they suggested considering a transition zone or an intermediate phase, where the flocs in suspension come into contact and start breaking up (Been and Sills, 1981). These observations led Schiffman et al. (1984), Pane (1985) and Pane and Schiffman (1985) to link the sedimentation and consolidation theories by reformulating the effective stress principle in the following general form:

$$\sigma = \beta(e)\sigma' + u_w \tag{2.8}$$

where β is an interaction coefficient expressed as a monotonic function of the void ratio. Figure 2.29 illustrates two kinds of (β, e) constitutive relationships suggested by Pane and Schiffman (1985). For the values of void ratio greater than e_m (i.e. when the particles or aggregates of particles are far enough apart that their interaction is negligible), the interaction coefficient β is equal to zero. At $e=e_m$ the interaction coefficient may be defined as a step function (case “a” in Figure 2.29) with an abrupt change from zero (suspension) to unity (soil), or as a continuous function of void ratio varying from zero to one in the transition zone of $e_s<e<e_m$ (general case “b” illustrated in Figure 2.29) (Pane and Shiffman, 1985).

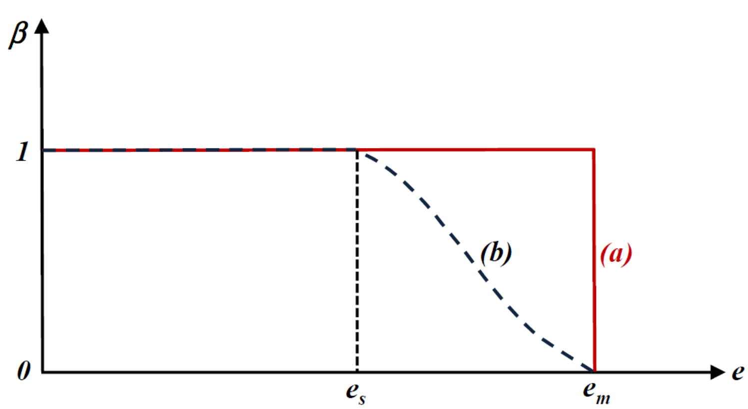

Figure 2.29 – Two forms of the (β, e) constitutive relationships (modified from Pane and Schiffman, 1985)

According to Schiffman et al. (1988), for hydraulic fills composed of sand and silt sizes particles, the interaction coefficient β is either zero or close to it. When the suspension includes fine and clay sized particles, β may change from 0 to 1 during transition from sedimentation to consolidation.

Using the modified effective stress equation, Pane (1985) presented the governing equation of a linked theory of sedimentation and consolidation as following (Pane, 1985; Schiffman et al., 1988; Qiu, 2000):

$$\frac{\partial}{\partial z}\left\{a(e)\left[\sigma'\frac{d\beta}{de}-\frac{\beta(e)}{a_v(e)}\right]\frac{\partial e}{\partial z}\right\}\pm f(e)\frac{\partial e}{\partial z}=\frac{\partial e}{\partial t} \tag{2.9}$$

where

$$a(e)=-\frac{k(e)}{\gamma_w(1+e)} \tag{2.9.a}$$

and

$$f(e)=(\frac{\gamma_s}{\gamma_w}-1)\frac{d}{de}\left[\frac{k(e)}{(1+e)}\right] \tag{2.9.b}$$

where k(e) is the saturated hydraulic conductivity expressed as a function of void ratio.

In the last two decades a number of numerical models have been presented to simulate the coupled sedimentation and consolidation; and validity of these models has been verified by means of experimental studies (e.g. Concha and Bustos, 1987; Auzerias et al., 1988; and Eckert et al., 1996 in chemical engineering and Masala, 1998; Bartholomeeusen, 2003; and Jeeravipoolvarn, 2010 in geotechnical engineering). Bartholomeeusen et al. (2002) presented the results of an international prediction exercise in which different numerical modellers (including Masala and Chan from University of Alberta) compared the settlement curves they had obtained for a silty soil of intermediate plasticity. Comparison with the experimental results indicated that the long term consolidation behavior predicted by all of the models was almost similar, and the settlement in the initial stages of the consolidation process was over-predicted by most of the models (Bartholomeeusen et al., 2002; Bartholomeeusen, 2003).

2.11. Summary

The hot water extraction process used to separate bitumen from the mineable oil sands in northern Alberta generates a large volume of mineral waste known as Mature Fine Tailings or MFT. This waste material is a stable suspension of fine particles in process affected water along with some unrecovered bitumen and solvents. The conventional approach for management of this material has been storing it in in-pit cells and out-of-pit tailings ponds. However, poor water release characteristics of MFT requires large retention structures that need to last for decades or probably hundreds of years. In addition, long-term storage of MFT poses a major environmental liability.

In recent years the trends in tailings management has been to eliminate the ponds by dewatering the fine tailings and incorporating them into a solid deposit used for creation of a trafficable landform. A major part of this chapter (section 2.8) reviews the different technologies previously developed or currently under study to create a dry landscape. One of these technologies that was developed two decades ago at the University of Alberta and is the focus of the present research is production of CT (Composite/Consolidated Tailings) or NST (Non-Segregating Tailings). CT and NST are engineered tailings streams obtained by recombination of fines (MFT or TT) and coarse tailings (sand) plus a chemical amendment. If produced on-spec, the main advantage of CT/NST would be its improved dewatering behavior and rapid release of relatively clear water during the hindered settling and self-weight consolidation, while a majority of the fine particles are entrapped within the matrix of its coarser fraction.

Production of on-spec CT/NST at a commercial scale has been a challenge for the oil sands industry. While this engineered waste stream is expected to be non-segregating when discharged, in practice it is not particularly robust and partial segregation is observed, resulting in release and re-suspension of fines following deposition. The major factors that result in a CT/NST with undesired robustness are fluctuations in the solids content of the sand (cyclone under flow), variable clay content of the fine tailings due to heterogeneity of the oil sands ores, and difficulties in controlling the energy of the depositional environment. To enhance the robustness of CT/NST and reduce its susceptibility to segregation, it needs to be produced with higher solids contents. The present research looks into different methods of solid-liquid separation and their possible application for improving the quality of CT/NST.

Chapter 3
Methods of Solid-Liquid Separation

3.1. Introduction

Many of the process industries that deal with particulate slurries use some method of solid-liquid separation. Purpose of the separation can be recovering the solids, recovering the liquids, or both. The separated phases may be used for recycling/reusing in the process (e.g. reusing the clear water formed on top of the oil sands tailings pond in the extraction process) or for depositional purposes (e.g. using the sand from cyclone underflow for construction of the dykes).

Solid-liquid separation covers a wide range of mechanical separation processes that can be categorized in two main groups: Sedimentation techniques and Filtration techniques. Figure 3.1 (modified from Purchas, 1977 and Svarovsky, 2000) illustrates a pictorial summary of the different methods of mechanical separation in each group. In the first group, the liquid is constrained in a vessel (either stationary or rotating) and the solid particles move within the liquid. The mass forces acting on the particles because of an acceleration field (gravity, centrifugal or magnetic) lead to separation of the two phases. In the second group, the solid particles are constrained by a medium and the liquid can flow freely through the medium. Density difference between the solid and liquid phases is not necessary in this group for the separation to take place. Usually a continuously operating system is easier to achieve in the first group, at lower costs (Svarovsky, 2000).

There are many chemical engineering or mineral processing handbooks that cover the theoretical and operational aspects of separation equipments (e.g. Perry's Chemical Engineers' Handbook edited by Perry and Green, 2007; Solid/Liquid Separation Equipment Scale Up edited by Purchas, 1977; Coulson and Richardson's Chemical Engineering, Vol. 2, edited by Richardson et al., 2002; Solid-Liquid Separation edited by Svarovsky, 2000; Wills' Mineral Processing Technology by Wills, 2006). In this chapter, a brief review of the following separation equipments, some already being used in the oil sands industry and some with the potential to be used, will be presented:

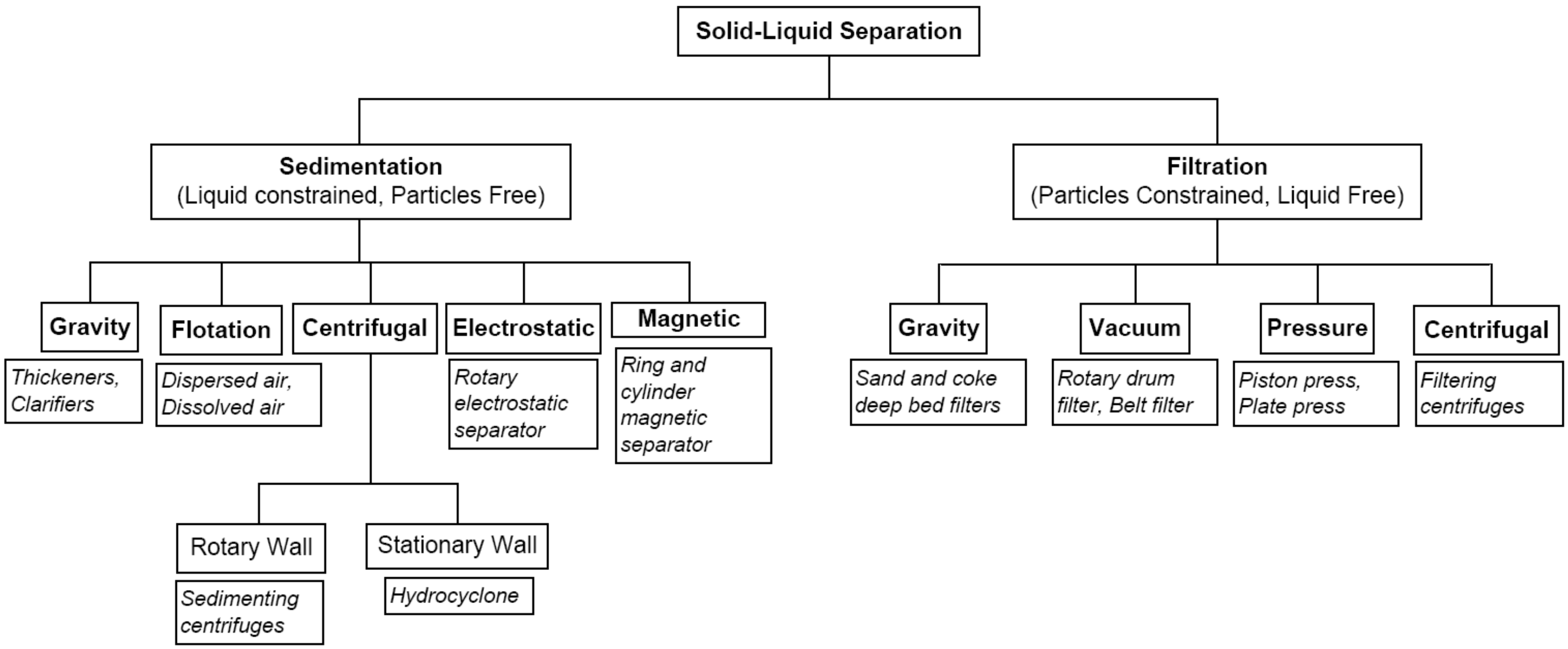

Figure 3.1. General classification of Solid-Liquid separation processes (modified from Purchas, 1977 and Svarovsky, 2000)

- Thickeners;
- Inclined plate settlers;
- Filters;
- Solid bowl centrifuges;
- Filtering centrifuges; and,
- Hydrocyclones.

The theory of centrifugal filtration will be presented in more detail, considering that in the present research this method was utilized for dewatering MFT. In Chapter 2, application of the solid-liquid separation methods in the oil sands industry was briefly reviewed.

3.2. Thickeners/Clarifiers

3.2.1. General

In thickeners and clarifiers, separation of the solid and liquid phases takes place by particle settling due to gravitational forces. A detailed description of the different stages of settling (particulate settling, hindered sedimentation and consolidation) is provided in Chapter 2. In gravity separation, when the purpose is to achieve the solids in the form of a highly concentrated slurry, the process is called thickening. When the purpose is to obtain a clear liquid, the process is called clarification. It is possible to accomplish both clarification and thickening in one stage, if the thickener is correctly designed and operated (Svarovsky, 2000). In this section a brief review of the thickeners, their operation and design is presented.

Figure 3.2 shows a schematic design of the most common thickener with a cylindrical settling tank and a slightly conical bottom, originally patented by J.V.N. Dorr in 1906 (Fitch and Stevenson, 1977). According to Concha and Bürger (2003), the invention of the Dorr thickener in 1905 can be considered as the starting point of the modern thickening era. The basic components of this thickener are (Fitch and Stevenson, 1977):

- a tank to provide the volume and area required for clarification and/or thickening;
- feed piping and feed well to disperse the feed stream gently into the thickener;

- a rake mechanism, slowly turning around the centre column, to promote solids densification and to assist in moving the concentrated solids towards the bottom central opening;
- an underflow solids withdrawal mechanism; and,
- an overflow launder.

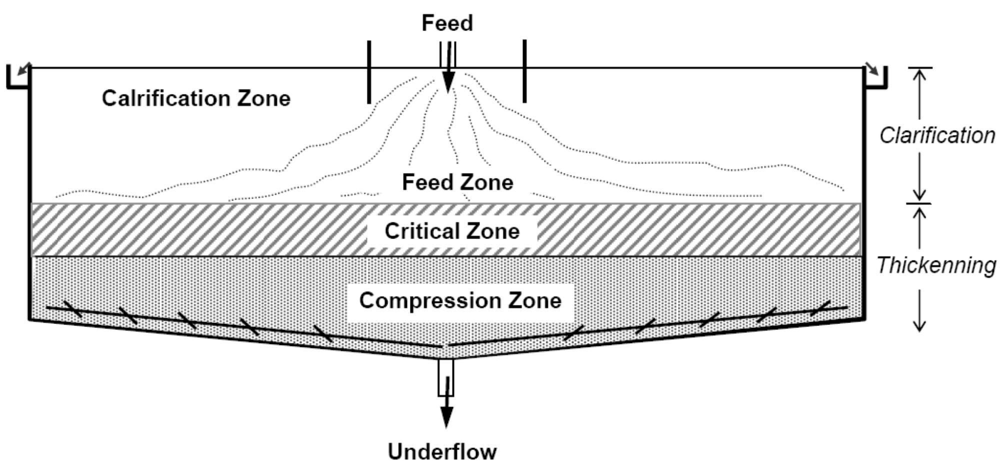

Figure 3.2. Continuous clarifier/thickener with a circular basin. The zones of different settling regimes are schematically illustrated (modified from Fitch and Stevenson, 1977).

Generally the feed slurry is mixed with a flocculating agent. After introducing this mixture through the central feed well, it falls down to the level of its hydrostatic equilibrium (where its density matches the density of the surrounding suspension) and spreads out horizontally. As illustrated in Figure 3.2, three zones of different settling regimes can be distinguished in a thickener: a clarification zone (particulate and flocculating settling), a critical zone (with a concentration in the hindered or zone settling regime) and a compression zone[1]. Due to addition of the flocculating agents, the feed is usually in the zone settling regime upon entering the thickener. Solids concentration increases downwards and additional weight of the above layers in the critical and compression zones leads to compaction or thickening of the material (Fitch and Stevenson, 1977). The clarified liquid flows upward and is collected through the overflow launder around the periphery of the tank.

[1] Comings et al. (1954) also considered a fourth zone at the very bottom, distinguished as the rake action zone (Concha and Bürger, 2003).

3.2.2. Thickener Design

A thickener designed properly should discharge a clear liquid at the top and an underflow with the required solids content at the bottom, and also, should have the smallest settling area for the required capacity (Bustos et al., 1999).

Conventional gravity thickeners are usually designed according to the batch settling tests on suspensions in the zone settling regime. According to Svarovsky (2000) the assumptions behind the conventional design methods are:

- The settling velocity of the slurry interface is only a function of its concentration (i.e. Kynch's theory).
- Concentration of the feed slurry is in the zone settling regime (i.e. hindered sedimentation conditions).
- The largest required area is controlled by the zone settling layer.
- Data obtained from laboratory batch sedimentation tests are representative of the plant conditions in a continuously operating thickener.

One of the first design methods for thickeners was presented by Coe and Clevenger (1916). This method was based on a macroscopic balance of the solid and fluid in a sedimentation vessel. Coe and Clevenger (1916) argued that at a certain concentration between the feed and the discharge concentrations, the solids flux[2] has its maximum value (Concha and Bürger, 2003). This maximum value is also known to as the critical settling flux. They developed the following equation for design of continuous thickeners, which with certain corrections, continues to be the most reliable method of thickener design to date (Concha and Bürger, 2003):

$$UA = \frac{D_k - D_D}{\rho_f v_f (D_k)} \tag{3.1}$$

where UA is the required area per unit filter flow, ρ_f is the density of the fluid, v_f is the velocity of appearance of the supernatant water in a batch settling test, D_D is the desired

[2] Solids flux is the mass rate of solids flow per unit area, which is equal to the product of the solids concentration and the downward velocity of solids in the thickener (Fitch and Stevenson, 1977).

underflow dilution, and D_k is the limiting dilution corresponding to the critical settling flux.

To evaluate the required settling area, the critical settling flux must be determined. This parameter is either calculated by the Coe and Clevenger method (1916) or the Talmage and Fitch procedure (1955). In the Coe and Clevenger method a series of settling tests at a variety of initial solids contents are conducted and the rate of settlement is determined for each concentration. Then the solids flux, which can be calculated from the rate of settlement, is plotted with regard to the solids concentration and eventually the upper boundary for solids loading and the minimum required area for the thickener are determined. The Talmage and Fitch procedure is less laborious as it requires only one test at any concentration in case that it is in the zone settling regime (Fitch and Stevenson, 1977). According to Fitch and Stevenson (1977), generally "Coe and Clevenger tests overestimate thickener fluxes and lead to underdesign of the thickener area; while the Kynch-based Talmage and Fitch analysis underestimates critical fluxes and leads to overdesign." It should be reminded that in comparison to the cumbersome method of Coe and Clevenger, a simpler method was proposed by Yoshioka et al. (1957) which does not require repeated plotting of the total flux curve and uses the flux-density function to interpret operation of a continuous thickener (Concha and Bürger, 2003). Details of this method can be found elsewhere (Svarovsky, 2000; Richardson et al., 2002).

In a comprehensive paper, Concha and Bürger (2003) reviewed the development of thickening theory and practice during the 20th century. In this review they state that Kynch's theory had the greatest influence in development of the thickening. However, the experience of several researchers during late 1950's to 1970's indicated that, although this theory accurately predicted the sedimentation behaviour of a suspension of equally-sized small rigid particles, it was not capable of a precise prediction for compressible (i.e. flocculated) suspensions. Concha and Bürger (2003) mention the work of several researchers who tried to modify Kynch's theory to account for the compressive effects: Shirato et al. (1970) were the first to solve the combined sedimentation-consolidation problem. They used material coordinates to obtain settling curves and excess pore pressure profiles. Adorjan (1975, 1976) introduced the first satisfactory method of thickener design by presenting his ad-hoc theory of sediment compression. During 1970s and 1980s several researchers used the phenomenological theory of sedimentation, which is based on "Theory of Mixtures" of continuum mechanics, to address the effect of consolidation in compressible sediment layers (e.g., Buscall and White (1987) and Auzerais et al. (1988)). Bustos and Concha (1988) and Concha and Bustos (1991) used the method of characteristics to construct entropy weak solutions of Kynch's problem, in which zones of constant concentrations were separated by shocks, rarefaction waves or combinations of these.

A widely used model that considers sedimentation and consolidation in a thickener was presented by Bürger and Concha (1998), Bürger et al. (1999) and Bustos et al. (1999). They used the local mass and momentum balances together with constitutive equations for the stresses and forces to obtain a nonlinear degenerate parabolic differential equation for sedimentation of the flocculated (i.e., compressible) suspensions in an ideal continuous thickener[3]:

$$\frac{\partial \phi}{\partial t} + \frac{\partial}{\partial z}(q\phi + f_{bk}(\phi)) = \frac{\partial}{\partial z}\left(-\frac{f_{bk}(\phi)\sigma_e(\phi)}{\Delta\rho\phi g}\frac{\partial \phi}{\partial z}\right) \tag{3.2}$$

where:

q is a constant equal to the volume average velocity;
$f_{bk}(\phi)$ is the batch Kynch flux density function; and,
$\sigma_e(\phi)$ is the effective stress of the solids.

The constitutive equations for the flux (f_{bk}) and effective stress (σ_e) functions must be postulated. Concha and Bürger (2003) presented the following functions proposed by Michaels and Bolger (1962) and Tiller and Leu (1980) as examples:

$$\begin{aligned} & f_{bk} = u_\infty \phi (1 - \phi / \phi_{\max})^c , \\ & \sigma_e = 0 \quad \text{for} \quad \phi \le \phi_c \\ & \sigma_e = \sigma_0 ((\phi / \phi_c)^n - 1) \quad \text{for} \quad \phi > \phi_c \end{aligned} \tag{3.3}$$

with n > 1 and $\sigma_0 > 0$.

[3] An ideal thickener is a vessel with no friction at the walls. For batch sedimentation it is called *settling column* and for continuous sedimentation it is called *ideal continuous thickener* (Concha and Bürger, 2003).

In the above equations, u_∞ is the settling velocity of a single floc in an infinite medium, ϕ_{max} is the maximum concentration attainable, ϕ_c[4] is the critical concentration and c is a number >1.

From (3.3), when $\phi \le \phi_c$, the right side of equation (3.2) will be equal to zero and it will reduce to the first order hyperbolic equation (continuous Kynch equation):

$$\frac{\partial \phi}{\partial t} + \frac{\partial}{\partial z}(q\phi + f_{bk}(\phi)) = 0 \qquad \text{for } 0 \le \phi \le \phi_c$$

(3.4)

Equation (3.4) indicates that for the regions that the solids concentration is less than the critical concentration (ϕ_c), Kynch's theory is valid for both compressible and incompressible suspensions.

In a recent study, Jeeravipoolvarn (2010) used the finite strain consolidation theory to model a continuously operating thickener. He compared the results of this model with a fluid dynamics based model from the literature and obtained quantitatively good agreement (Jeeravipoolvarn, 2010).

3.2.3. Thickener Types

Increasing the efficiency of flocculants has lead to design of thickeners with smaller area and higher underflow solids content. Figure 3.3 illustrates the evolution of thickeners, which can be classified into four general categories (Bedell et al., 2002; Perry and Green, 2007):

- Conventional: With slow settling rate and large area includes most of the thickeners that have served industry for the last 100 years.
- High Rate: Due to effective use of flocculants, has better settling rate, smaller area and improved underflow density. In most applications there is a threshold dosage and feed solids concentration at which a noticeable increase in capacity

[4] The critical concentration is the solids concentration at which the solid flocs start to come into contact with each other (i.e. the gel point) (Garrido et al., 2000).

begins to occur (i.e. for any given feed material, there is a feed concentration at which the flocculant behaves at an optimum).

- Ultra-High Rate (Raked and Rakeless): This type of thickener uses a tall, deep tank with a steep bottom cone and may be used with or without a raking mechanism. This combines the functions of a thickener (to provide a dense underflow) and a clarifier (to provide a clear overflow or supernatant) but is considerably taller. It is generally one-half to one-third the diameter of a conventional or high-rate thickener.
- Ultra-High Density (or Paste Thickener): Thickeners can be designed to produce underflows having very high apparent viscosity, permitting disposal of waste slurries at a concentration that avoids segregation of fines and coarse particles or formation of a free-liquid pond on the surface of the deposit. This practice is applied in dry-stacking systems and underground paste-fill operations for disposal of mine tailings and similar materials.

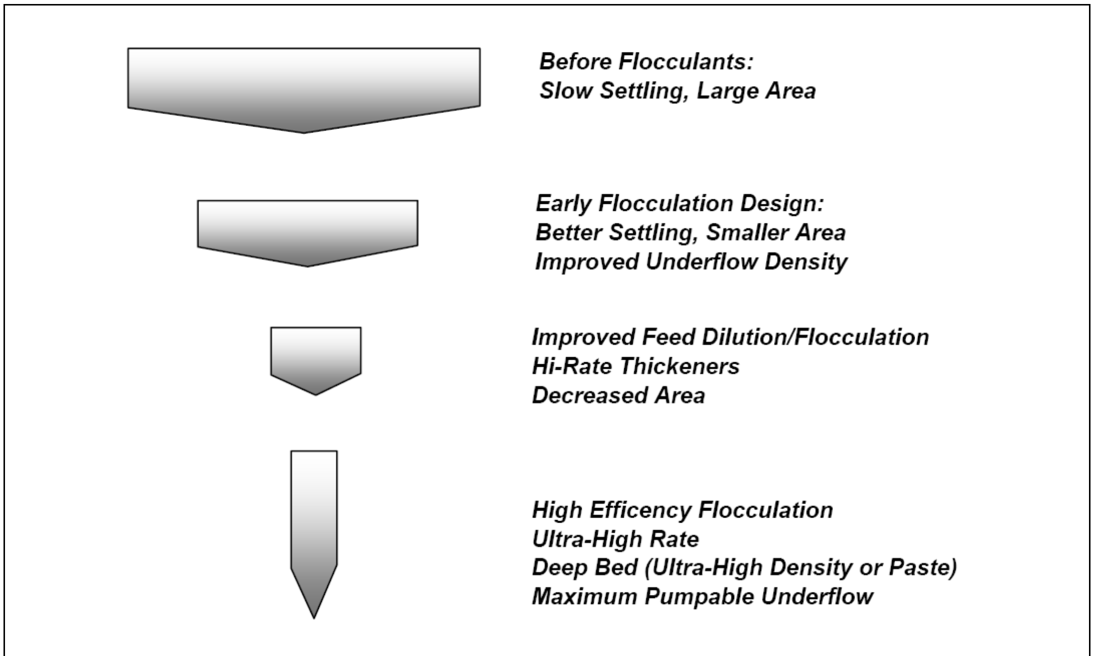

Figure 3.3 – Evolution of the Thickeners (modified from Bedell et al., 2002)

A brief review of the application of thickeners in the oil sands operations is presented in section 2.8.2.1 of the present thesis.

3.3 Inclined Plate Settlers

3.3.1. General

Inclined plate settlers, also known as Lamella Settlers (Forsell and Hedstrom, 1975 cited by Leung and Probstein, 1982) or Lamina-type clarifiers (Christensen, 1923 cited by Fitch and Stevenson, 1977), are high-rate sedimentation devices consisting of several inclined parallel plates stacked within a settling tank. Figure 3.4 illustrates the schematic design of an inclined plate settler. The basic design consists of rapid mixing and flocculation tanks prior to the inclined plate section and a sludge thickener/hopper located underneath. Similar to thickeners and clarifiers, inclined plate settlers make use of gravity sedimentation to separate the solid particles from a liquid stream. However, the space between each two plates acts as an individual channel (or inclined vessel) into which the slurry is fed for gravitational separation. The solid particles sediment on the lower (upward-facing) wall of each inclined vessel. The settled particles slide downwards and are removed as the thickened underflow.

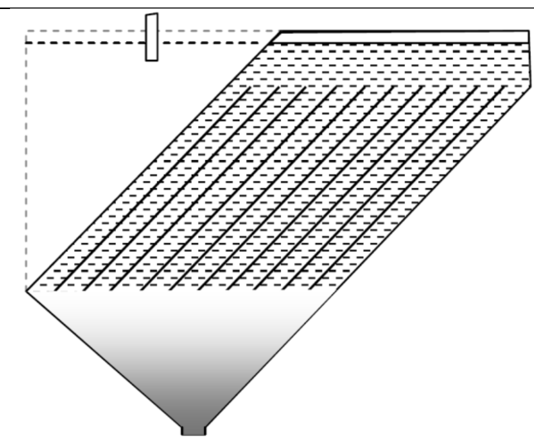

Figure 3.4 – Schematic design of an inclined plate settler (modified from Fitch and Stevenson, 1977)

One main advantage of the inclined plate settlers is the reduced plant footprint required in comparison to the regular thickeners/clarifiers. As shown in Figure 3.5, the available settling area of the tank will be equivalent to the horizontal projected area of each plate multiplied by the number of plates.

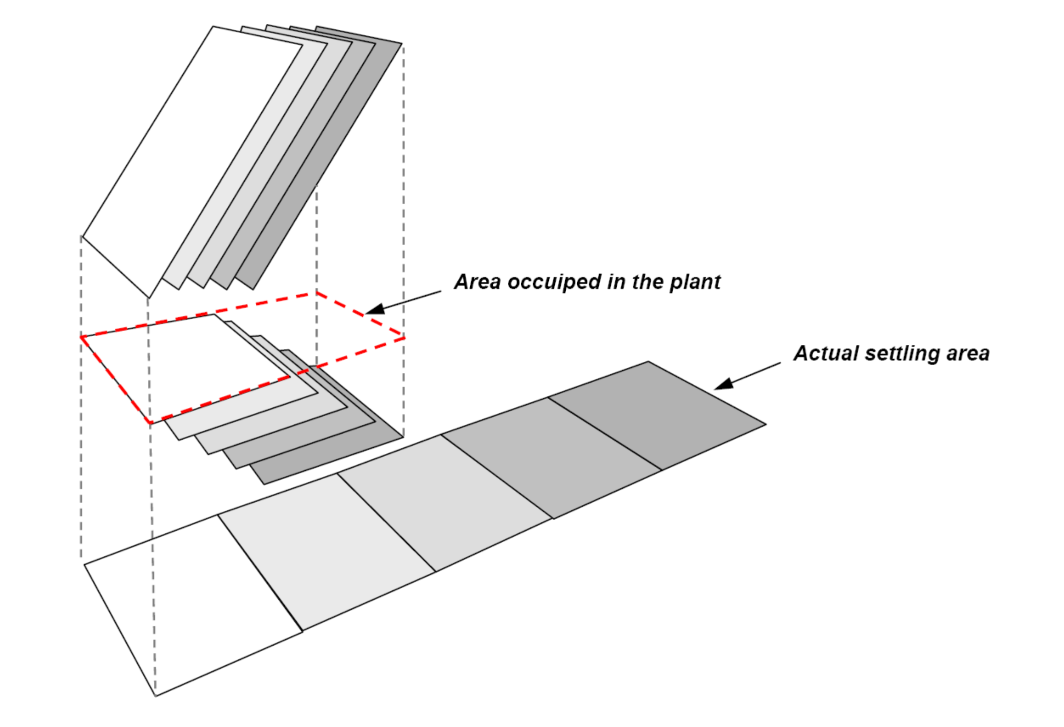

Figure 3.5 – Settling area in an inclined plate settler (modified from Parkson Co., 2009)

3.3.2 Theory of sedimentation in an inclined vessel

The inclined plate settlers are based on application of the “Boycott effect”, a curious phenomenon of settling convection first observed by Boycott (1920). The essence of Boycott’s observation was (Acrivos and Herbolzheimer, 1979):

“ … *if oxalated or defibrinated blood is put to stand in narrow tubes, the corpuscles sediment a good deal faster if the tube is inclined than when it is vertical.*”

A qualitative explanation for the “Boycott effect” is that when the walls of the container are inclined, the solid particles would take a shorter vertical distance to reach the upward-facing wall of the container. However, the process of sedimentation in an inclined vessel is more complicated than simple vertical settling (Acrivos and Hebolzheimer, 1979).

Subsequent to Boycott’s observation, many researchers studied the phenomenon of sedimentation in an inclined vessel and reported an increased rate of sedimentation (summarized by Hill, 1974). Also, the experimental observations indicated that thickness of the clear-liquid layer forming under the downward facing plate (Figure 3.6) remained small and independent of time (Acrivos and Herbolzheimer, 1979). Ponder (1925) and, independently, Nakamura and Kuroda (1937) presented a kinematic model based on the experimental observations which provided a quantitative prediction for the sedimentation rate, referred to as the PNK theory in the literature. According to these researchers, since thickness of the liquid layer under the downward-facing surface is small and independent of time, that part of the clarified liquid formed under this surface should be added to the clear liquid above the horizontal interface. The volumetric rate at which clarified liquid is formed will be equal to v_0 multiplied by (A_1+A_2) in Figure 3.6:

$$S(t) = v_0(A_1 + A_2)\,, \tag{3.5}$$

$$S(t) = v_0\left(\frac{b}{\cos\alpha} + H.\tan\alpha\right), \text{ or:}$$

$$S(t) = \frac{v_0 b}{\cos\alpha}\left(1 + \frac{H}{b}\sin\alpha\right) \tag{3.6}$$

where v_0 is the settling velocity in a vessel with vertical walls, b is the perpendicular spacing between the inclined plates, H is the height of the suspension from horizontal, α is the constant angle of inclination, $A_1 = b/\cos\alpha$ is the area of the horizontal cross section of the vessel and $A_2 = H.\tan\alpha$ is the horizontally projected area of the downward-facing wall (Fig 3.6).

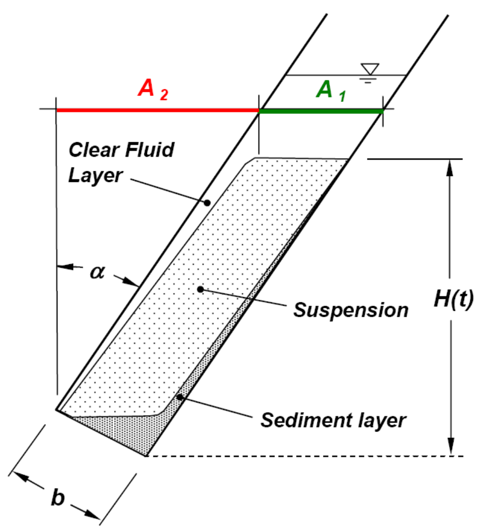

Figure 3.6 - Sedimentation in an inclined vessel (modified from Acrivos and Herbolzheimer, 1979)

Based on the PNK theory, the settling rate of the suspension in the inclined vessel can be expressed as:

$$\frac{dH}{dt} = -v_0(1 + \frac{H}{b}\sin\alpha) \tag{3.7}$$

In practice, the PNK theory often overestimates the settling rate of an inclined thickener and only under idealizing assumptions produces an acceptable approximation (Acrivos and Herbolzheimer, 1979; Harvie et al., 2002; Bürger et al., 2011). Acrivos and Herbolzheimer (1979) indicate that the PNK theory and the similar purely kinematic theories based on it suffer from two serious limitations: They can not provide any information about thickness of the clear fluid layer beneath the downward-facing wall, also such flow characteristics as velocity profiles and concentration distribution within the suspension; in addition, their range of validity is unknown and can not be used for design purposes.

As a more fundamental approach, Acrivos and Herbolzheimer (1979) used the principles of continuum mechanics to develop a theory for batch sedimentation in the inclined vessels. Current analytical theories used for description of separation in inclined settlers are generally based on their theory (Harvie et al., 2002). Acrivos and Herbolzheimer (1979) assumed laminar flow and small particle Reynolds numbers, but concentration of the suspension and geometry of the settling vessel were left arbitrary. They showed that in addition to the aspect ratio of the vessel (H/b) and the inclination angle (α), two dimensionless groups govern kinetics of the sedimentation process:

- The sedimentation Reynolds number: $R = \frac{Hv_0\rho_f}{\mu_f}$ (3.8.a)
- The ratio of a sedimentation Grashof number[5] to Reynolds number (R):

  $$\Lambda = \frac{H^2 g(\rho_s - \rho_f)\phi_0}{\mu_f v_0}$$

  (3.8.b)

[5] The Grashof number Gr is a dimensionless number in fluid dynamics and heat transfer which approximates the ratio of the buoyancy to viscous force acting on a fluid.

Acrivos and Herbolzheimer (1979) concluded that for a given geometry, as $\Lambda \rightarrow \infty$ the sedimentation rate can be predicted from the PNK theory provided that the flow (and the interface between the suspension and the clear fluid layer) remains stable. They used a boundary layer analysis to find expressions for the thickness and the flow velocity of the clear fluid layer under the downward-facing wall of the vessel.

Based on their analysis, Acrivos and Herbolzheimer (1979) explained the process of settlement in an inclined vessel as following:

Initially vertical settlement of the particles creates a layer of clear (i.e. particle-free) liquid under the downward-facing wall of the vessel. Since density of this clear fluid is lower than that of its adjacent slurry, it experiences a large buoyancy force and flows upward along the wall. The moving clear fluid layer is replaced by new fluid entrained from the suspension to the particle free layer. Flow of the fluid along the downward-facing wall creates a drag force on the particles, which balances the gravity component that tends to move them away from the wall. As a result, when $\Lambda >> 1$, the clear-fluid layer remains thin and independent of time.

According to Acrivos and Herbolzheimer (1979), a similar process occurs at the upward-facing wall on which a concentrated sediment layer forms. This sediment layer has higher density than its adjacent suspension and flows down the wall towards bottom of the vessel. As a result, when $\Lambda >> 1$, the sediment layer remains thin. The upward movement of the fluid in the clear-fluid layer and the downward slip of the sediment layer drive a convective flow within the suspension. The flow structure would be a function of R (the characteristic Reynolds number), Λ and b/H. From the kinematics analysis, these researchers concluded that enhancement to the settling rate is not a result of this convective motion but is due to the increased area available for creating particle-free fluid and for collecting settled particles. Acrivos and Herbolzheimer (1979) state that utilizing the Boycott effect for continuous systems would be possible, only if the position of the interface between the clear fluid and suspension is stationary (this would require a laminar flow and large enough Λ). Large velocities within the clear liquid layer can lead to formation of waves along this interface. These waves could cause entraining the

suspension into the clear fluid layer and eventually decrease the efficiency of the separation process (Harvie et al, 2002).
Shaqfeh and Acrivos (1986) later included bulk inertial effects to extend the theory to all values of Reynolds and Grashof numbers; and measured location of the inception point of the waves along the interface. Comparison of the geometry of clear liquid layer predicted by these analytical methods with the experimental results has shown good agreement, particularly for the most viscous cases (Harvie et al., 2002).

Leung and Probstein (1983) and Leung (1983) also examined the role of flow instability in decreasing the performance of inclined settlers. They used a three-layer model (the stratified viscous flow model of Probstein (1977)) to evaluate the performance of co-current flow lamella settlers and counter-current flow tube settlers in continuous sedimentation. They indicated that the downward movement of the settled sludge and the slurry, induces an upward flow of the clarified effluent. They showed that as the slurry concentration and the angle of the inclined plate increases, the efficiency of separation decreases. According to Leung and Probstein (1983), the efficiency decrease with settler angle principally results from flow instability.

Laux and Ytrehus (1997) used a two-fluid mathematical model and a commercial CFD (Computational Fluid Dynamics) code to simulate the batch sedimentation of moderately viscous mono-disperse suspensions in inclined rectangular vessels. They reported good agreement between their computational results, the existing theory and their experimental data for thickness of the thin clear fluid layer. They also observed a thin shear layer on top of the quasi-static particle bed.

Dorma (1998) applied accurate shock capturing techniques from computational aerodynamics to the numerical simulation of sedimentation in inclined vessels. His numerical results were in good agreement with the measurements by Herbolzheimer (1983), and the model was able to capture correctly the wavy suspension interface adjacent to the upper inclined surface.

In a recent study, Bürger et al. (2011) presented a multi-resolution finite volume scheme for the numerical approximation of velocity, pressure and solids volume fraction during sedimentation of a suspension in an inclined channel. In order to accurately resolve the sharp fronts and discontinuities in the concentration field (e.g. in the boundary between the clear water layer and the suspension), locally refined meshes were used to concentrate the computational effort on these zones of strong variation. Based on the results from numerical simulations, they conclude that their proposed scheme is robust, provides accurate results and requires substantially reduced computational effort.

The above presented review of the research work conducted on the sedimentation in inclined vessels indicates that the initial studies mainly deal with purely kinematic theories; at the next stage come the more complicated analytical theories based on fluid mechanics models, verified by experimental studies utilizing more precise measurement and photography techniques; and finally the more recent works make use of numerical analysis and computational fluid dynamics.

3.4. Filtration

3.4.1. Introduction

Separation of the solids from a liquid by passing the solid-liquid suspension (slurry) through a porous medium, which retains the solid particles, is called filtration. The fluid passing through the filter medium is referred to as filtrate. Figure 3.7.a illustrates a filtration system schematically. In this picture a layer of solids, or filter cake, has formed over the filter medium. The requirement for flow of the fluid through the filter cloth and the cake is to have a pressure difference of ΔP across the filter medium (Figure 3.7.b). The driving force for creating this pressure difference may be gravity, pressure, vacuum or centrifugation (Svarovsky, 2000).

There are two basic types of filtration processes: cake filtration for which surface filters are used and deep-bed filtration for which depth filters are used. As shown in Figure 3.8.a, in cake filtration a relatively thin filter medium is utilized and the solid particles form a cake on the up-stream side of it. Solid particles (of the same size or larger than the medium openings) build up on the filter and the initial layers create an effective filter medium, preventing the smaller particles to proceed through the filter pores and the filtrate. As the filter cake is formed, it acts as a medium for filtration of the subsequent input slurry. Surface filters are suitable for separation of suspensions with higher solids content, as the dilute suspensions can cause blinding of the medium pores (Svarovski, 2000, Richardson et al, 2001). Another mechanism of filtration, described by Wakeman (2007), is bridging filtration. This mechanism is common when the particles are at a high concentration in the feed and their sizes are smaller than the pore sizes in the filter medium. As illustrated in Figure 3.8.b several particles attempt to pass through a pore at the surface of the filter cloth, but fail to do so and make a bridge over the pore opening. This arch shaped bridge is stabilized by the flow environment around the pore opening and substantial changes of the flow velocity or direction can destabilize it (Wakeman, 2007). Bridging filtration can be considered as a kind of cake filtration, as the cake layer is formed on the up-stream side of the filter medium.

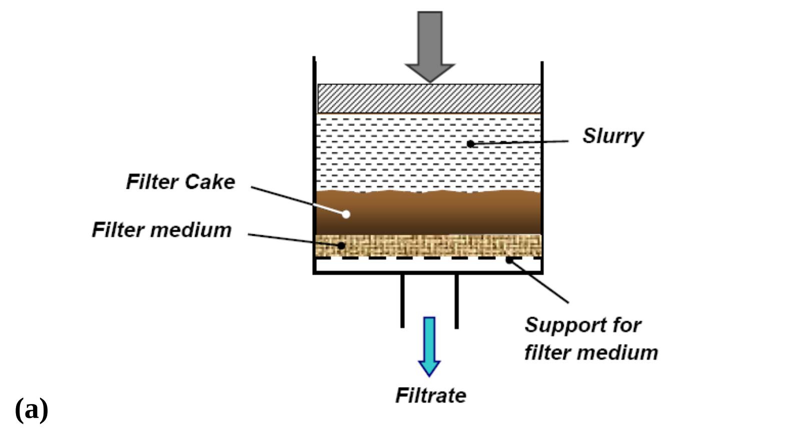

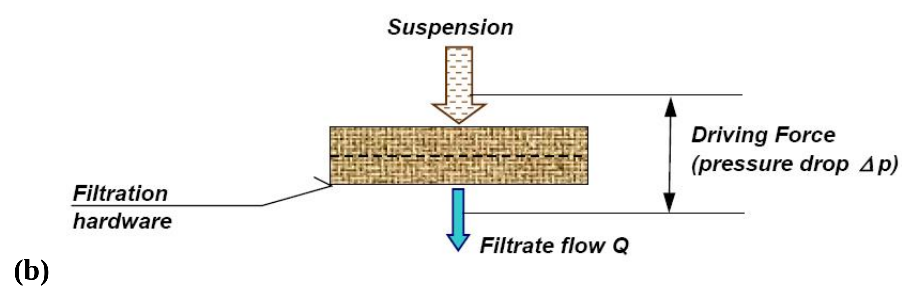

Figure 3.7.a) Schematic view of a filtration system; b) The pressure difference Δp across the filter medium (modified from Svarovsky, 2000).

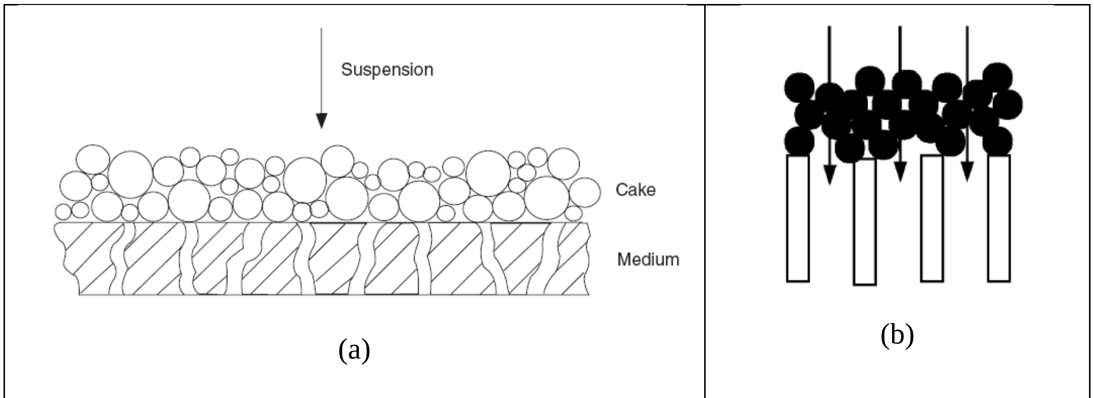

Figure 3.8 – (a) Cake Filtration (adapted from Svarovsky, 2000);
(b) Bridging Filtration (adapted from Wakeman, 2007).

In the second type of filtration, deep-bed filtration or depth filtration, the particles are smaller than the medium openings and penetrate into its pores (Figure 3.9). Molecular and electrostatic forces make the particles to attach to the filter medium. This type of filtration is used for removal of fine particles from very dilute suspensions (Svarovski, 2000). The separation mechanism in deep bed sand filters and some types of cartridge filters is depth filtration (Wakeman, 2007).

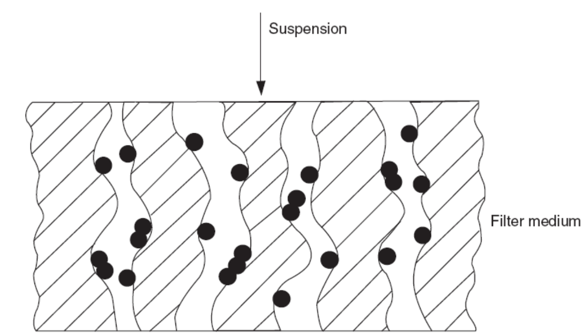

Figure 3.9 – Deep-Bed Filtration (adapted from Svarovsky, 2000)

As explained in Chapter 5, the type of filtration used in the present research is cake filtration; thus in the following section only the correlations of filtration for the surface filters will be presented.

3.4.2. Relationship between the filtration rate and pressure drop

The following parameters affect the rate of filtration (Svarovsky, 2000):

- The pressure difference from the feed slurry to the far side of the filter medium;

- The area of the filtration surface;
- Viscosity of the filtrate liquid;
- Resistance of the filter medium; and,
- Resistance of the filter cake.

Usually the pores in the filter medium and the cake are small and the rate of filtrate flow is low, therefore the laminar flow conditions are valid. Darcy's basic filtration equation can be written as following:

$$Q = \frac{A\Delta p}{\mu(R + R_c)} \tag{3.9}$$

In this equation, Q is the flow rate of the filtrate across the filter media (composed of the filter medium and the cake medium), μ is the viscosity of the filtrate, Δp is the driving pressure, R is the filter medium resistance (which is considered constant and equal to the filter thickness divided by its permeability), R_c is the cake resistance (which increases with time as the cake builds up). For the incompressible cakes, R_c can be assumed proportional to the amount of the cake formed on the medium (Svarovsky, 2000):

$$R_c = \alpha.w \tag{3.10}$$

In this equation *w* is mass of the cake deposited per unit area (kg/m^2) and α is the specific resistance of the cake (m/kg). From (3.9) and (3.10), the flow rate can be calculated as following:

$$Q = \frac{A\Delta p}{\mu.R + \mu.\alpha.w} \tag{3.11}$$

It should be noted that in gravity, pressure and vacuum filtration, the mass of cake deposited per unit area is a function of time and can be related to the cumulative volume of the filtrate V filtered in time t by:

$$wA = cV \tag{3.12}$$

In this equation c is the solids concentration of the feed. As will be explained in section 3.6.2.4, in centrifugal filtration the mass of deposited solids can not be correlated to the filtrate volume since an additional mass of cake is deposited on the filter cloth due to centrifugal forces.

From equations 3.11 and 3.12 the general filtration equation can be written as (Svarovsky, 2000):

$$Q = \frac{\Delta p A}{\alpha.\mu.c(\frac{V}{A}) + \mu.R} \tag{3.13}$$

The total volume is an integral function of the flow rate: $V = \int Q dt$ or $Q = \frac{dV}{dt}$, so rewriting the previous equation in reciprocal form will give the time per unit flow as (Svarovsky, 2000):

$$\frac{dt}{dV} = a_1 \frac{V}{A^2 \Delta p} + b_1 \frac{1}{A \Delta p} \tag{3.14}$$

Where $a_1 = \alpha\mu c$ is a constant relating the properties of the feed suspension and the suspended solids; and $b_1 = \mu R$ is a 'cloth-filtrate' constant.

In order to determine values of α and R in an experimental test, values of t/V are plotted with regard to V and a and b are calculated (Svarovsky, 2000). Figure 3.10 illustrates examples of these plots for two groups of constant pressure filtration tests reported by Wakeman (2007).

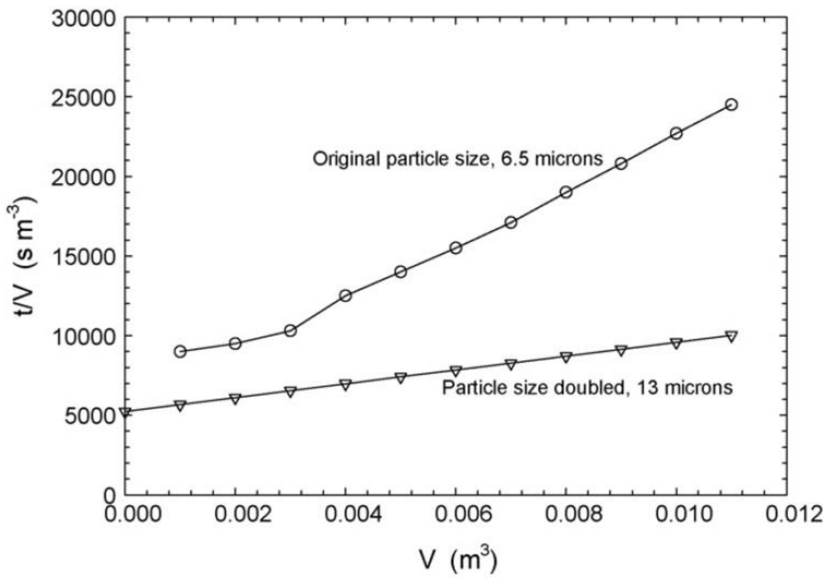

Figure 3.10. Plots of t/V versus V for constant pressure filtration tests on suspensions of calcium silicate with mean particle size of 6.5 and 13 microns. The gradient of the diagram is increased by a factor of 4 when the particle size is doubled, indicating reduction of the cake specific resistance (adapted from Wakeman, 2007).

Svarovsky (2000) has discussed the solution of Equation 3.14 for different test conditions like constant pressure, constant flow rate, variable pressure, variable flow rate, etc. which will not be covered here.

In a recent study, Stickland et al. (2005) compared the consolidation tests conducted by means of an oedometer (common in geotechnical engineering) with the filtration tests performed by a filtration rig (common in physical science) and concluded that the two test methods are essentially the same. It should be noted that the suspension samples prepared for the consolidation tests were at a volume concentration above the gel point (Stickland et al., 2005).

3.4.3. Effect of particle properties on filtration

The specific resistance of a filter cake can be significantly affected by properties of the particles present in the slurry. Wakeman (2007) has mentioned the size distribution of the particles, their shape and their interaction with the fluid as the most effective properties.

The most common particle size used in filtration operations is the surface-volume mean diameter, x_{sv}, which is equal to “sum of the volume of particles” divided by “sum of their surface area". The specific resistance of a filter cake is inversely proportional to x_{sv}^2 (Wakeman, 2007):

$$R_c \propto \frac{1}{x_{sv}^2} \tag{3.15}$$

Therefore changing the particle size can have a significant effect on the filtration performance:

R_c (after particle size change) = R_c (before particle size change). (x_{sv} (before)/ x_{sv} (after))^2

Figure 3.10 shows the results of some constant pressure filtration tests reported by Wakeman (2007). It can be seen that doubling the mean particle size of the suspension has increased the gradient of the diagram of t/V versus V by a factor of 4, indicating reduction of the cake resistance by this factor.

(In Chapter 5 of the present research, results of some centrifugal filtration tests on MFT are presented and it is discussed how chemical treatment of MFT and formation of larger agglomerates leads to formation of cakes with lower specific resistance.)

The smallest particles present in the slurry have the greatest effect in the filtration process. These have the largest contribution to the volume specific surface of the particles and interact more strongly with the ions present in the solution. Treatment of these particles with chemical additives (flocculants, coagulants) can lead to formation of larger agglomerates, lower specific resistance of the filter cake and a more flocculated and compressible cake structure. Presence of fine particles within the slurry leads to formation of smaller pore sizes in the filter cake with higher capillary pressures, and as a result higher pressure difference would be required to displace the liquid from the cake (Wakeman, 2007).

Shape of the particles is also an important factor, because it affects their specific surface. As noted by Wakeman (2007) flake shaped particles (e.g. clay) with a high specific surface, significantly increase the specific resistance of the cake.

Wakeman (2007) suggests the 5 to 10 percentile size on the cumulative particle size distribution curve as a reasonable estimate of the range of most effective particles to determine the method of treatment and the size of the filter cloth openings.

A wide range of research work has been done to study the different factors affecting filtration and the quality of the filter cakes. A series of papers titled "The role of porosity in filtration" by Dr. Frank Tiller (University of Houston) and his coworkers published during more than four decades (1970s to 2000s) have had a significant contribution to the field of filtration. Review of this literature is beyond the scope of this thesis. In section 3.6.2.3, the theory of centrifugal filtration will be presented in more detail and the differences between centrifugal filtration and compression-permeability cells will be discussed with reference to the available literature.

3.5 Centrifugal Separation

There are a wide range of situations where centrifugal acceleration is used in place of the gravitational acceleration to enhance the solid-liquid, liquid-liquid or solid-gas separations. The accelerations generated in a centrifugal field can be much higher than the gravity acceleration (g), ranging from two to five orders of magnitude (e.g. $\sim 100\times g$ in slow large-diameter basket units to $\sim 100{,}000\times g$ in analytical ultracentrifuges). The high accelerations make it possible to achieve higher rates of separation which are either not practically feasible, or even impossible, in the gravitational field (Richardson et al., 2002, Bürger and Concha, 2001).

Centrifugal fields can be generated in two different ways:

(a) By means of a centrifuge; in this case the fluid (slurry) is rapidly accelerated while being introduced into some form of rotating bowl or basket. The frictional drag within the fluid ensures that there is very little rotational slip between fluid layers within the bowl, so all the fluid tends to rotate at a constant angular velocity (ω) and a forced vortex is created. The resultant tangential velocity will be directly proportional to the radius at which the fluid is rotating.

(b) By means of a cyclone separator (e.g. a hydrocyclone); in this case a fluid with a high tangential velocity is introduced into a cylindrical or conical vessel. Contrary to a centrifuge, the vessel of the cyclone is stationary and the high speed rotational flow of the fluid creates a free vortex in which the tangential velocity varies inversely with the radius (Richardson et al., 2002).

The focus of this research has been on dewatering CT and MFT, both composed of soil particles, water and bitumen. Therefore in the following sections only "solid-liquid" separation in the centrifuges will be explained in more detail. Separation of two immiscible liquids and gas-solid phases in centrifugal fields can be found in chemical engineering handbooks (e.g. Richardson et al., 2002; Perry and Green, 2007; Svarovsky, 2000).

Prior to explaining the centrifuges and cyclones in more detail, a brief review of some dynamics related principles is provided.

3.5.1 Centripetal and Centrifugal Acceleration

Consider a body of mass rotating around a centre O with a constant angular velocity of ω (Figure 3.11). The force required to sustain this body of mass moving along a circular path (or a curve trajectory) is called centripetal force. The centripetal force acts perpendicular to the direction of motion and is directed towards the centre of rotation.

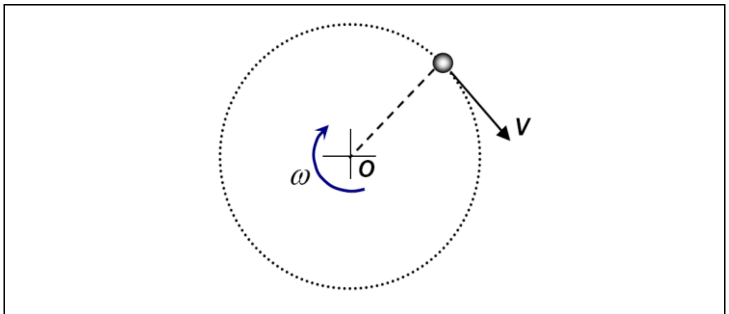

Figure 3.11 – A body of mass rotating around a centre O.

The tangential velocity of the rotating mass can be written as:

$$v_\theta = r.\omega \tag{3.16}$$

where *r* is the radius of curvature (i.e. the distance between the rotating mass and centre of rotation). The tangential velocity has a constant magnitude but its direction is continually changing. Since velocity is a vector quantity, a change in direction alone is sufficient to produce acceleration. This acceleration follows the same direction as the centripetal force and is called centripetal acceleration:

$$a = \frac{v_\theta^2}{r} \tag{3.17}$$

From Equations (3.16) and (3.17), the centripetal acceleration can be written as:

$$a = r\omega^2 \tag{3.18}$$

If the rotating body has a mass of *m*, then the centripetal force required to accelerate it towards the centre of rotation is calculated from Newton's second law as:

$$F = mr\omega^2 \tag{3.19}$$

The reaction to the centripetal force is the *centrifugal force*. An observer in a rotating frame (rotating at the same angular velocity as the body of mass) experiences a centrifugal acceleration directed radially outward from the axis of rotation with the same magnitude as centripetal acceleration (i.e. $a = r\omega^2$).

3.5.2 Motion of particles in a centrifugal field

Sedimentation in a centrifugal field is different from gravitational settling in that the centrifugal acceleration, resultant from the rotational motion, should be added to the gravitational acceleration to calculate the body force applied to the particles. In most practical cases, however, the gravitational effects are comparatively small and can be neglected. As a result, the equation of motion for the particles would be similar to that for motion in gravitational field, except that the centrifugal acceleration must replace the gravitational acceleration (Garrido et al., 2003; Richardson et al., 2002).

As stated in Chapter 2, in gravity sedimentation the Brownian diffusion forces hinder or prevent settling of very fine particles. The body forces generated in a centrifugal field are large enough to overcome these diffusion forces (Svarovsky, 2000). For a spherical particle of diameter *d*, the equation of motion in a fluid where the Stokes' law is valid[6] can be written as:

[6] The separation efficiency is mainly affected by the behaviour of the smallest particles in the solid-liquid system. Since the fine particles moving in the liquids have low Reynolds numbers (in the region of viscous resistance), it is common to assume that the Stokes' law is valid in describing the particle motion in a centrifugal field (Svarovsky, 2000).

$$\frac{\pi}{6}d^3(\rho_s-\rho)r\omega^2-3\pi\mu.d\frac{dr}{dt}=\frac{\pi}{6}d^3\rho_s\frac{d^2r}{dt^2} \tag{3.20}$$

where ρ_s is the density of the solid particles, ρ is the density of fluid, r is the radius of rotation, ω is the angular velocity and t is the time. It should be noted that in the centrifugal sedimentation, contrary to the gravitational sedimentation, the settling particle never acquires an equilibrium velocity. The reason is that as the particle moves further from the centre of rotation, the radius of rotation and consequently the magnitude of the acceleration force will increase (Richardson et al., 2002).

The right-hand side of Equation (3.20) are inertial terms and can be neglected, thus (Richardson et al., 2002):

$$\frac{dr}{dt}=\frac{d^2(\rho_s-\rho)r\omega^2}{18\mu}=\frac{d^2(\rho_s-\rho)g}{18\mu}.\frac{r\omega^2}{g}=u_g(\frac{r\omega^2}{g}) \tag{3.21}$$

where u_g is the terminal falling velocity of the particle in gravitational field (Stokes' law). Therefore in the centrifugal field, the instantaneous velocity of the particle *(dr/dt)* is equal to u_g multiplied by a factor of $r\omega^2/g$. This factor is the ratio of centrifugal acceleration to the gravity acceleration and is referred to as relative centrifugal force (RCF) or G:

$$G=RCF={r\omega^2}/{g} \tag{3.22}$$

Solution of the exact form of differential equation of motion (Eq. 5) results (Richardson et al., 2002):

$$t=\frac{18\mu}{d^2\omega^2(\rho_s-\rho)}\ln\frac{r}{r_1} \tag{3.23}$$

where t is the time that it takes for a particle to move from an initial radius of r_1 to a radius r.

3.6 Centrifuges

Two distinct groups of centrifuges are available for separation purposes:

(1) Sedimenting centrifuges; in which a difference in density of the two phases is required and the principle of sedimentation is utilized.

(2) Filtering centrifuges; in which a difference in density of the two phases is not required and the principle of filtration is utilized.

In the following sections, these two general types of centrifuges are explained.

3.6.1 Sedimenting centrifuges

3.6.1.1. General

As schematically illustrated in Figure 3.12, a sedimenting centrifuge consists of an imperforated bowl, rotating around a vertical or horizontal axis. Upon introduction of the suspension into the centrifuge, the high angular velocity generates a centrifugal field which enhances the settlement rate of the solid particles. These solid particles would settle on the wall of the bowl, forming a sediment or cake layer. The cake either remains in the bowl and is manually discharged at the end of operation (in batch systems); or is intermittently or continuously discharged during the operation. The clarified liquid (centrate) is usually removed through a skimming tube or is discharged over a weir (Records, 1977; Svarovsky, 2000).

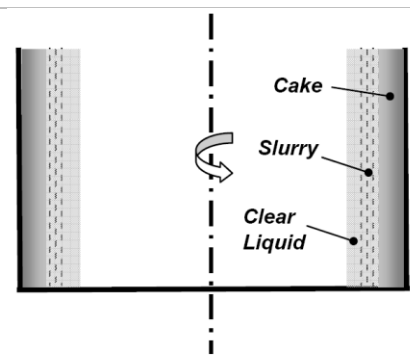

Figure 3.12 – Centrifugal sedimentation in a rotating imperforate bowl.

3.6.1.2 Comparison of gravitational and centrifugal sedimentation

Centrifugal sedimentation differs from gravitational sedimentation in the following aspects (Sambuichi et al., 1987):

- In centrifugal sedimentation, the acceleration increases linearly with radius, with its highest value adjacent to the bowl wall and zero at axis of rotation. In gravitational sedimentation the acceleration is constant (g).
- In centrifugal sedimentation, the area of the surface through which the particle has to settle increases linearly with radius while in gravitational sedimentation the cylindrical area is constant.
- The flow of liquid in a centrifugal field is radial, while in gravitational sedimentation it is one dimensional.

Therefore even with a homogenous slurry the particle flux in centrifugal sedimentation is not constant. A schematic comparison of the sedimentation in gravitational and centrifugal fields is illustrated in Figure 3.13. Because of higher accelerations present in the centrifugal field, the sediment layer is formed at a shorter time. Also, due to larger compressive forces, the thickness of a compressible sediment layer would be less in centrifugal sedimentation.

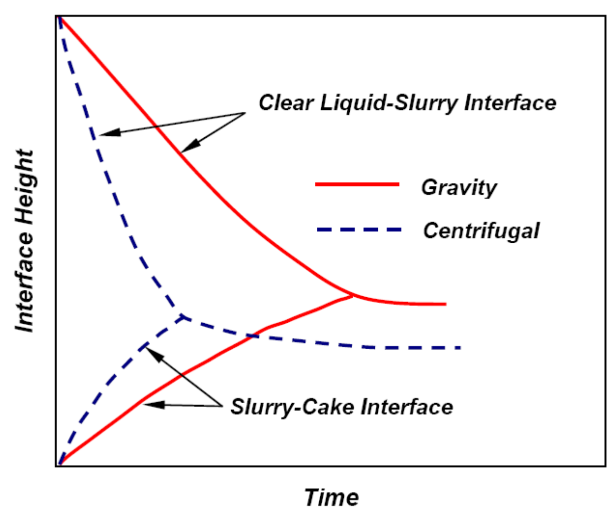

Figure 3.13- Schematic comparison of gravity and centrifugal sedimentation (modified from Sambuichi et al., 1987)

3.6.1.3 Theory of centrifugal sedimentation

Bürger and Concha (2001) presented an extension of the phenomenological theory of sedimentation-consolidation of flocculated suspensions for the centrifugal field. They considered two cases of centrifugal sedimentation (Figure 3.14):

- Sedimentation in a rotating tube with constant cross section; and,
- Sedimentation in a batch cylindrical centrifuge.

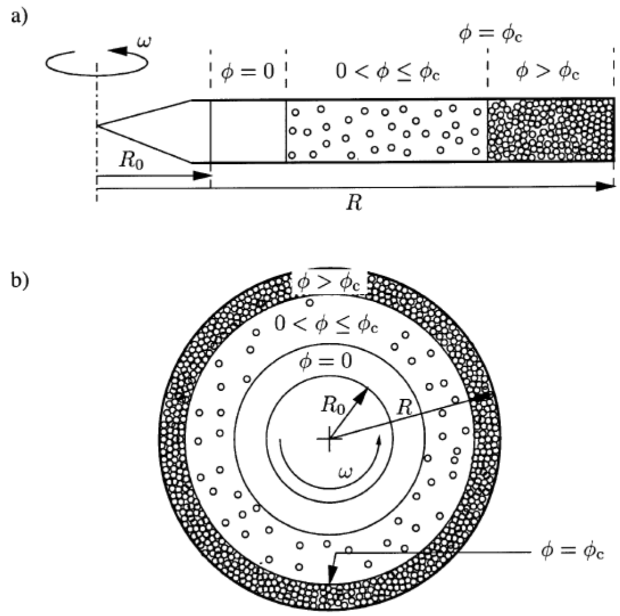

Figure 3.14. The three regions of clear liquid ($\phi = 0$), hindered settling ($0 < \phi \le \phi_c$) and compression zone ($\phi > \phi_c$) for (a) rotating tube with constant cross section; and (b) rotating axisymmetric cylinder (adapted from Bürger and Concha, 2001).

Bürger and Concha (2001) followed the usual approach of the theory of mixtures and modeled the solids and the fluid as superimposed continuous media. They wrote the mass and linear momentum balance equations for each phase in a frame of reference rotating at an angular velocity of ω. As illustrated in Figure 3.14, they assumed three regions within the centrifuge:

- a solids free or clear liquid layer ($\phi = 0$) close to the centre of rotation,
- a hindered settling zone in which $0 < \phi \le \phi_c$; and,
- a sediment compression zone with $\phi > \phi_c$.

where ϕ is the volumetric solids concentration and ϕ_c is a critical solids concentration (or gel point) such that:

$$\sigma_e(\phi) = 0 \quad \text{for} \quad \phi \le \phi_c \text{, and}$$
$$\sigma_e(\phi) > 0 \quad \text{for} \quad \phi > \phi_c . \tag{3.24}$$

The effective stress was assumed to depend only on the local volumetric solids concentration. A typical constitutive equation that Bürger and Concha (2001) suggested for the $\phi > \phi_c$ region was the "power law" function proposed by Landman and White (1994):

$$\sigma_e(\phi) = \sigma_0\left((\phi/\phi_c)^k - 1\right), \qquad \text{and} \quad \sigma_0 > 0,\ k > 1 \tag{3.25}$$

where σ_0 is a coefficient and k is an exponent in this constitutive equation.

By assuming the typical size of sedimenting space in a centrifuge equal to ~0.1m, Bürger and Concha (2001) performed an order-of-magnitude study and concluded that with the angular velocity in the range of 1000 to 10'000 rpm, the effect of gravity and Coriolis terms in the mass and momentum balance equations could be reasonably neglected. As a result, the scalar functions of concentration with time and location were expressed as following:

For flow in a rotating tube:

$$\frac{\partial \phi}{\partial t} + \frac{\partial}{\partial r}(\phi.q + \phi(1-\phi)v_r) = 0 \tag{3.26}$$

For a batch sedimenting centrifuge:

$$\frac{\partial \phi}{\partial t} + \frac{1}{r}\frac{\partial}{\partial r}(r(\phi.q + \phi(1-\phi)v_r)) = 0 \tag{3.27}$$

where q is the volume average flow velocity of the mixture defined by:

$\mathbf{q} = \phi \mathbf{v}_s + (1-\phi)\, \mathbf{v}_f$

and v_r is the solid-fluid relative velocity, which is correlated to the Kynch batch flux density function $f_{bk}(\phi)$:

$$v_r = \frac{f_{bk}(\phi)}{\Delta \rho g \phi^2 (1-\phi)}\left[-\Delta \rho \phi \omega^2 r + \frac{\partial \sigma_e(\phi)}{\partial r}\right] \tag{3.28}$$

The Kynch batch flux density function $f_{bk}(\phi)$ can be obtained by conducting batch sedimentation tests (see for example Sambuichi et al. (1987, 1991) and Garrido et al. (2000)).

In both cases of the rotating tube and the batch cylindrical centrifuge, the excess pore pressure p_e in the $\phi > \phi_c$ zone can be calculated from the following equation (Bürger and Concha, 2001):

$$\frac{\partial p_e}{\partial r} = \Delta\rho\phi\omega^2 r - \frac{\partial \sigma_e(\phi)}{\partial r} \tag{3.29}$$

Details of the boundary conditions and derivation of the above equations can be found in the reference publication by Bürger and Concha (2001). To solve Equations (3.26) and (3.27), Bürger and Concha (2001) presented a numerical algorithm and employed it to compare their analysis results with the experimental results reported by Sambuichi et al. (1991). The comparison showed that the final height of the sediment layer could be predicted precisely. However, the simulated sedimentation process took place somewhat faster than the experimental observations, and this discrepancy consistently increased with the spinning velocity (ω). Bürger and Concha (2001) attributed this discrepancy to neglect of the effect of Coriolis terms in their model.

3.6.1.4 Types of sedimenting centrifuges

Five different types of sedimenting centrifuges are common in the industry, distinguished by their design and solids discharge mechanism (Records, 1977; Richardson et al, 2002; Svarovsky, 2000):

- Bottle spinner (batch operation, manual discharge).
- Tubular bowl (batch operation, manual discharge).
- Imperforate bowl; with skimmer pipe or knife discharge (semi-continuous, intermittent discharge).
- Continuous scroll discharge (decanter) centrifuge.
- Disc centrifuge (batch, intermittent or continuous discharge).

A bottle centrifuge (bottle spinner) is a useful equipment for rapid evaluation of the dewatering characteristics of a slurry, simulation of its long term sedimentation in a tailings pond, and also, for screening the chemical additives required for enhancement of the separation (see Buscal and White, 1987; Theriault et al., 1995; Eckert et al., 1996 and, Bürger and Concha, 2001,). In Chapters 4 and 5 of the present research it is explained how this device was used for simulating centrifugal sedimentation and filtration tests, also for evaluating the effect of chemical additives for separation purposes.

Detailed description of each of the above centrifuge types can be found in the mentioned references and will not be covered here. In the following section only a brief description of the centrifugal decanter will be provided, as in recent years the oil sands industry has shown some interest in using this type of centrifuge for dewatering the oil sands fine tailings (see Chapter 2 for a brief review of the experimental studies conducted at Syncrude (Ahmed et al., 2009; Syncrude website, 2011)).

3.6.1.4.1 Continuous scroll discharge (Decanter) centrifuge

The scroll discharge centrifuge, also known as decanter centrifuge, has a conical or conical-cylindrical bowl rotating about a horizontal axis. Inside the bowl there is a close fitting helical screw (conveyor) which rotates at a slightly different speed (2 to 100rpm) relative to the bowl (Figure 3.15). This type of centrifuge usually produces a settling gravity up to 3000g. The solid-liquid mixture is fed through an axial tube at the centre of the rotor and is discharged near the centre of the device. The sedimented solids are moved by the conveyor to one end of the bowl up the gentle slope of the conical section (the beach), out of the liquid (the pond) and are discharged from the end of the conical section The clarified centrate spills over a weir fitted at the opposite end of the bowl (Records, 1977; Richardson et al., 2002).

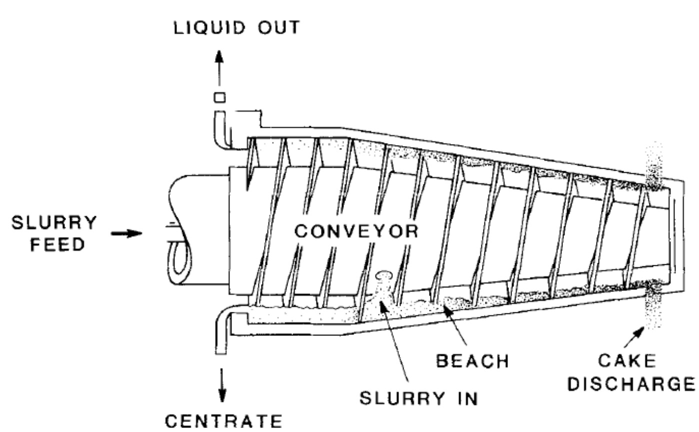

Figure 3.15. A centrifugal decanter (adapted from Sambuichi et al., 1987)

The bowl diameter in this type of centrifuge is generally from 10 cm to 150 cm and the bowl length typically varies from 1.5 to 5 times the diameter. When a clear centrate is desired, the longer bowl designs are used. Shorter machines are used to produce drier solids (Records, 1977; Richardson et al., 2002).

The cut size[7] in the decanter centrifuge is a function of solids concentration in the feed and the feed flow rate. As illustrated in Figure 3.16, at a constant feed flow rate, increasing the solids concentration higher than a certain limit will increase the cut size. Also, increasing the flow rate at a specific feed concentration would result in release of more fine particles into the centrate (Gibson, 1979; Svarovsky, 2000).

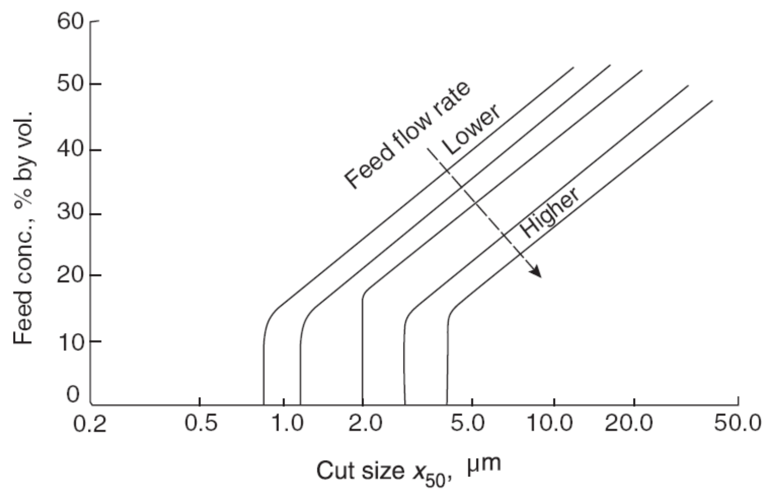

Figure 3.16. Effect of the feed solids content and flow rate on cut size (x_{50}) of the decanter centrifuge (adapted from Svarovsky, 2000; Gibson, 1979).

To increase the separation efficiency in centrifugal decanters, synthetic flocculants (polyelectrolytes) are commonly used for flocculation of inorganic or organic slurries/sludges. Depending on the type of the slurry and the flocculant, the point of treatment varies: Cationic flocculants, which react faster, are usually applied within the centrifuge, while anionic flocculants are added to the slurry at some point upstream of the centrifuge (Svarovsky, 2000; Kleine and Stahl, 1989). Breakage of the flocs can adversely affect the separation efficiency; this concept is briefly discussed in the following section.

[7] Cut size: The particle size at which separation is 50% efficient.

3.6.1.5 Floc Disintegration in Centrifugal Fields

Different factors may cause disintegration of the flocculated agglomerates: high shear forces within a turbulent flow and in the centrifuge inlet, direct collision of the flocs with rotating elements of the screw shaft, and effect of the centrifugal field on heavier components within a floc which cause them to be preferentially torn out of the floc. Shear forces may either remove the primary particles from surface of the floc or may disintegrate it (the floc) into smaller fractions (Kleine and Stahl, 1989; Bentz and Stahl, 2001).

Kleine and Stahl (1989) postulated a model of floc disintegration by mass forces in a centrifugal field and examined its validity. In this model, they assumed that the mass force acting on a floc in a centrifugal field is the sum of all the single forces acting on the individual particles within the floc. The force acting on a single particle (F_c) was considered as following:

$$F_c \propto \Delta\rho . g .(RCF). x^3 \tag{3.30}$$

where $\Delta\rho$ is the density difference between the particle and the fluid, g is the gravitational acceleration and x is the particle size. Therefore, a relatively large particle in the floc's structure experiences a significantly larger single acceleration force.

Kleine and Stahl (1989) also assumed that the single bonding forces, which attach each individual particle within the floc to its adjacent particles, result from polymer charges on the surface of the particles and therefore are a function of the corresponding particle surface area:

$$F_A \propto f . x^2 \tag{3.31}$$

where f is a surface-specific adhesion force generated by polymer action, assuming that the flocculant is uniformly distributed over the whole particle surface.

Therefore for the larger particles present within a floc, since the ratio of area to mass is lower, the ratio of F_A/F_C would be smaller. As a result, for a large enough centrifugal acceleration, particles in excess of a certain size, or specifically heavier components are pulled out from the floc structure. Use of larger quantities of polymer flocculants could reduce the level of floc destruction.

In another study, Brentz and Stahl (2001) indicate that destruction of the flocs into finer particles can result in long residence times during centrifugal filtration and blockage of the filter cloth. In Chapter 5, this concept will be discussed when results of centrifugal filtration tests on MFT conducted at lower and higher centrifugal accelerations are compared.

3.6.2 Filtering centrifuges

3.6.2.1 General

In centrifugal filtration the driving force for creating a pressure difference across the filter cloth is generated by gravitational forces in a centrifugal field. Figure 3.17 illustrates the schematic cross section of a filtering centrifuge, composed of a perforated drum (basket) covered with a filter cloth. This combination spins around a vertical axis, creating a centrifugal gravity field. Upon introduction of the solid-liquid mixture into the filtering centrifuge, the coarser solid particles settle on the filter cloth and act as a pre-coat for the finer particles. The solid phase that is retained by the filter medium gradually forms a cake. The liquid phase passes through the retained solid phase and the medium and is referred to as filtrate.

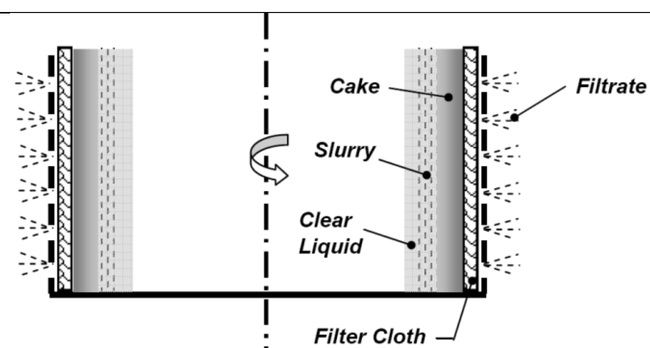

Figure 3.17. Centrifugal filtration in a rotating perforate basket.

3.6.2.2 Types of filtering centrifuges

According to their design and operation method, filtering centrifuges can be categorized as following (Hultsch and Wilkesmann, 1977):

- Batch operating systems:
    - The perforate basket centrifuge
    - The suspended centrifuge
    - The horizontal peeler centrifuge
- Continuous operating systems:
    - Oscillating centrifuge
    - Tumbler centrifuge
    - Worm screen centrifuges
    - Pusher centrifuges

The filtering centrifuge utilized in the present research was a perforate basket centrifuge with a vertical axis of spinning and batch operation. The details of design and operation of this centrifuge are presented in Chapter 5. The details of each of the above mentioned filtering centrifuges can be found in the stated references (Hultsch and Wilkesmann, 1977; Perry and Green, 2007; Richardson et al., 2002; Svarovsky, 2000).

In the following section, theory of centrifugal filtration will be reviewed and the differences between this method and other methods of filtration will be highlighted.

3.6.2.3 Theory of centrifugal filtration

This section presents a summary of the centrifugal filtration theory developed by Sambuichi, Nakakura and Osasa (1987) from Yamaguchi University together with Tiller (1987) from University of Houston. To simplify the analysis, these researchers assumed that the centrifugal basket involved only three zones: the clear liquid zone, the suspension zone and the sediment/cake zone. By correlating the changes of solid and liquid fluxes within the centrifuge to the filtrate flux exiting from the perforated bowl, they obtained equations expressing the position of interfaces between each zone as a function of time and volumetric solids content.

In the following, first these correlations are presented briefly and then the experimental approaches pursued by these researchers (to verify the validity of the equations) are explained.

3.6.2.3.1 Governing equations

In gravitational sedimentation, the downward volumetric flux of solids exactly balances the upward liquid flux:

$$u\phi + u_g\phi_s = 0 \tag{3.32}$$

In this equation u is the upward liquid velocity balanced for settling solids, u_g is the settling velocity of the slurry-supernatant interface under gravity, and ϕ and ϕ_s are the average volumetric fractions of liquid and solids respectively. Considering full saturation, then $\phi + \phi_s = 1$, and from Equation (3.32) the relative velocity of the solid phase versus the liquid phase can be written as:

$$u_g - u = \frac{u_g}{\phi} \tag{3.33}$$

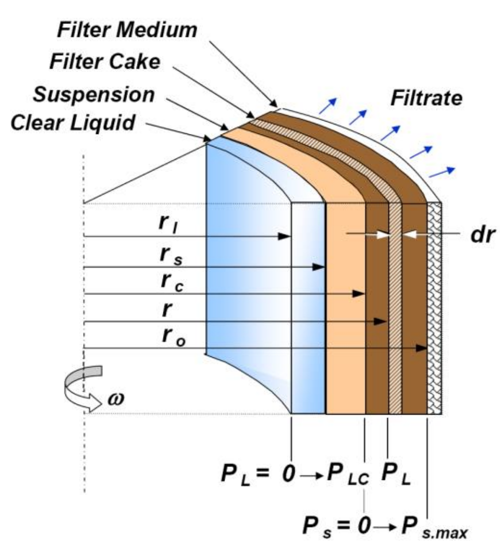

Figure 3.18. Schematic view of the clear liquid, suspension and filter cake layers in a filtering centrifuge (modified from Sambuichi et al., 1987)

It should be noted that in gravitational and centrifugal sedimentation, velocities of the liquid and solid phases have opposite signs. In centrifugal filtration, however, the liquid phase flows in the same direction as the solid particles and passes through the filter medium resulting in production of the filtrate. Flux of the filtrate exiting from the filter medium is equal to the sum of the solid and liquid fluxes at radius *r* (Figure 3.18):

$$u_g - u = \frac{u_g}{\phi} \tag{3.33}$$

$$2\pi r(u\phi + u_c\phi_s) = 2\pi r_0 u_0 \tag{3.34}$$

where u_c is the settling velocity of the slurry-supernatant interface in the filtering centrifuge, r_o is centrifuge radius (Figure 3.18) and u_o is the filtrate velocity. Solving Equation (3.34) for *u* and subtracting from u_c, would result in relative velocity of the solid phase versus the liquid phase (Sambuichi et al., 1987):

$$u_c - u = \frac{u_c}{\phi} - \frac{u_0 r_0}{r\phi} \tag{3.35}$$

As mentioned in section 3.5.2, ratio of the settling velocity in the centrifugal field to the settling velocity in the gravitational field is equal to $\frac{r\omega^2}{g}$; thus from Equations (3.35) and (3.33) we can write:

$$\frac{u_c - u}{u_g - u} = \frac{r\omega^2}{g} \tag{3.36}$$

Solving for u_c results:

$$u_c = \frac{r\omega^2}{g} u_g + \frac{u_0 r_0}{r} \tag{3.37}$$

The first term on the right side of the above equation shows the settling velocity in a centrifugal field (Equation (3.21)) and the second term indicates the increase in settling velocity due to the filtration. Therefore in centrifugal filtration, the slurry-supernatant interface settles faster in comparison to the solid-bowl centrifugal sedimentation. Figure

3.19 schematically compares the performance of a sedimenting centrifuge and a filtering centrifuge, when both systems have the same basket size (Sambuichi et al., 1987). At equal spinning velocity, the cake would build up faster in the filtering centrifuge. However, the height (and consequently the voids ratio) of the final cakes would be approximately equal in the two processes, because the centrifugal forces are the same.

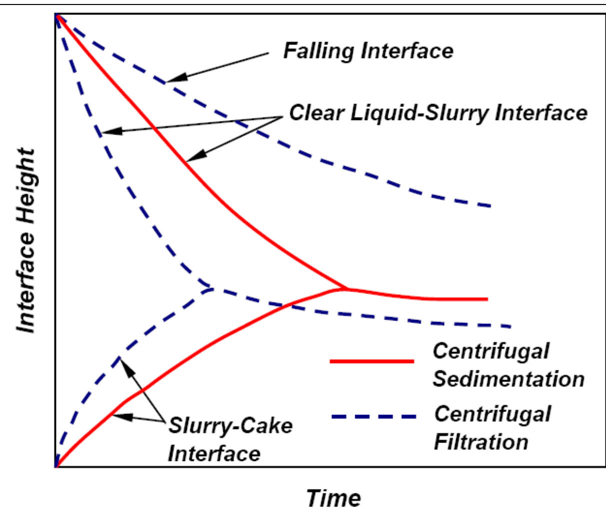

Figure 3.19- Schematic comparison of centrifugal sedimentation and filtration (modified from Sambuichi et al., 1987)

As stated in section 3.6.1.2, even with a homogenous slurry, the solids flux would not be constant in centrifugal sedimentation (Sambuichi et al., (1987, 1991)). The same concept is valid for centrifugal filtration. In Figure 3.18, equating the rate of change of solids flux across radius r to the rate of change of solids in the region between r to $r + dr$ results in (Sambuichi et al., 1987):

$$d(2\pi.r.u_c\phi_s)+2\pi.r\frac{\partial\phi_s}{\partial t}dr=0 \tag{3.38}$$

In which u_c can be substituted from Equation (3.37):

$$\frac{\partial}{\partial r}\left[\left(\frac{r^2\omega^2}{g}u_g+r_0u_0\right)\phi_s\right]+r\frac{\partial\phi_s}{\partial t}=0 \tag{3.39}$$

Assuming that the initial slurry concentration is uniform, and the settling velocity (u_g) is a unique function of slurry concentration (ϕ_s) based on Kynch's theory (Kynch, 1952), then Equation (3.39) will reduce to (Sambuichi et al., 1987):

$$\frac{d\phi_s}{dt} + \frac{2\omega^2}{g} u_g \phi_s = 0 \qquad (3.40)$$

Sambuichi et al (1987) conducted a number of gravity sedimentation tests and, for the zone settling region, found the correlation between flux ($u_s\phi_s$) and volume concentration (ϕ_s) as following:

$$u_g \phi_s = c_1 - c_2 \phi_s \qquad (3.41)$$

Putting this relation in Equation (3.40) and integration results:

$$\phi_s = \frac{c_1}{c_2} - \left(\frac{c_1}{c_2} - \phi_{sF}\right).e^{2c_2\omega^2 t/g} \qquad (3.42)$$

where ϕ_{sF} is the initial volume concentration of solids in the slurry. This equation expresses the variations of volume concentration (ϕ_s) with time (t), for the slurry (region $r_L<r<r_s$ in Figure 3.18).

The correlation between slurry concentration and position of the slurry-clear liquid interface (r_s) can be obtained from Equations (3.37) and (3.40) as following:

$$\phi_s r_s^2 - \phi_{sF} r_F^2 = 2r_o \int_0^t u_o \phi_s dt \qquad (3.43)$$

where r_s is radius of the slurry-supernatant interface and r_F is radius of the clear liquid surface at $t=0$.

Equating the volume of filtrate to the reduction in volume of the centrifuge contents results in radius of the supernatant liquid (r_L):

$$r_L^2 = r_F^2 + 2r_o \int_0^t u_o dt \qquad (3.44)$$

A solids flux balance over a volume between an arbitrary radius r within the slurry and the centrifuge radius (r_o), results in the position of the interface between the cake and slurry (r_c) as a function of volumetric solids concentration (ϕ_s):

$$r_c^2(\varepsilon_{sav}-\phi_s)-r_o^2(\varepsilon_{sav}-\phi_{sF})=\frac{r_o g}{\omega^2}\int_{\phi_{sF}}^{\phi_s}\frac{u_o}{u_g}d\phi_s \tag{3.45}$$

3.6.2.3.2 Pressure at the cake boundaries

During centrifugal filtration, the pressure applied to the surface of the cake is caused by the clear liquid and the slurry adjacent to the cake surface (Figure 3.18):

$$p_{Lc}=\frac{\omega^2}{2}\left[\rho(r_s^2-r_L^2)+\rho_{sL}(r_c^2-r_s^2)\right] \tag{3.46}$$

In this equation, ρ_{sL} is density of the slurry and can be written as:

$$\rho_{sL}=\rho(1-\phi_s)+\rho_s\phi_s \tag{3.47}$$

When all the solid particles settle to form a cake and only clear water is present adjacent to the cake, the pressure at the cake surface is:

$$p_{Lc}=\omega^2\rho(r_c^2-r_L^2)/2 \tag{3.48}$$

Figure 3.20 (modified from Sambuichi et al., 1987) illustrates distribution of the hydraulic pressure (p_L), the effective pressure (p_s) and the total pressure in a cake during centrifugal filtration (note that p_t = p_L + p_s).[8] At the surface of the cake, the liquid pressure is given by Equation (3.46). This pressure starts to decrease within the cake and reduces to p_l at the filter cloth-cake boundary (r = r_o):

$$p_1=\mu.u_o R_m \tag{3.49}$$

[8] Similar concept applies in the soil mechanics: the total stress (σ) is equal to the pore fluid pressure (u) plus the effective stress (σ’); σ = u + σ’.

where R_m is the medium resistance and p_l is the required pressure to overcome this resistance.

The effective pressure (p_s) is zero at the cake surface and increases to its maximum value at $r = r_o$.

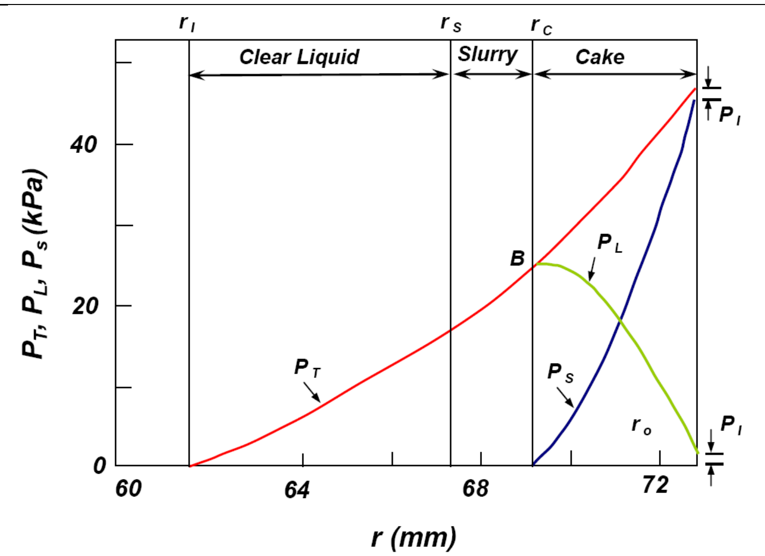

Figure 3.20. Pressure distribution in the cake during centrifugal filtration, when the liquid is present over surface of the cake (modified from Sambuichi et al., 1987. Tests conducted on slurry of $CaCO_3$ at initial solids content of 30% and spinning velocity of 2000 rpm).

In batch centrifugal filtration, as the liquid level over the cake surface decreases, the value of total pressure reduces. In the mean time, build up of the cake and reduction of the liquid level both lead to decrease of the hydraulic pressure within the cake pores. As a result, at different points in the cake the effective pressure reaches a maximum at some instant of time and then decreases. When this happens, the structure of the cake will no longer change, as its porosity and hydraulic conductivity are functions of the maximum effective pressure and cake compression is nearly irreversible (Sambuichi et al., 1987).

After the slurry zone disappears and the cake stops to grow, the remaining liquid either passes through the cake or is drained via a siphon. Figure 3.21 illustrates the pressure distribution across the cake in this stage. The solid curves correspond to the time that the particles in the suspension have just disappeared. As the level of liquid decreases, the pressure values reduce with time (the dashed curves in Figure 3.21). The cake thickness and porosity remain unchanged because the effective pressure applied to the cake structure is successively lower as time passes (Sambuichi et al., 1987).

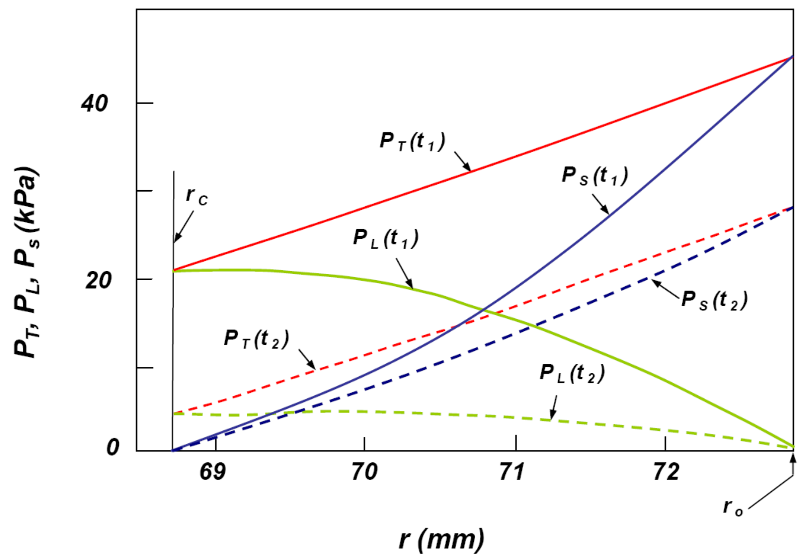

Figure 3.21. Pressure distribution in the cake during centrifugal filtration, when there is no liquid present over surface of the cake (modified from Sambuichi et al., 1987. Tests conducted on slurry of $CaCO_3$ at initial solids content of 30% and spinning velocity of 2000 rpm).

3.6.2.4 Flow resistance of the cake in centrifugal filtration

As explained in section 3.4.2, due to flow resistance of the cake and the filter medium, the pressure drops as the filtrate passes through these media. While resistance of the filter medium (R_m) is relatively constant, resistance of the cake (R_c) increases as the cake builds up. For the incompressible cakes R_c can be assumed proportional to the amount of the cake formed on the medium (Equation 3.10). For compressible cakes, however, the cake resistance is a function of the compressive pressure applied to the cake structure.

Sambuichi et al. (1987) have presented the following equation to calculate the average specific flow resistance of the cake (α_{av}):

$$u_o = \frac{\Delta p_L}{\mu(\alpha_{av} W_c / A_e + R_m)} \tag{3.50}$$

In this equation A_e is the effective filtration area and is calculated as following:

$$A_e = 2\pi . r_{av} (r_{LM} / r_o) \tag{3.51}$$

where r_{LM} is the logarithmic mean of the cake radius and r_{av} is the arithmetic average of the cake radius.

Although Equation (3.50) is similar to Equation (3.13) previously presented for constant pressure filtration (section 3.4.2), Sambuichi et al. (1987) stated that: "*... appearances are deceptive, and pitfalls must be avoided in making comparisons between calculated values for constant-pressure filtration and centrifugation.*" According to these researchers in one dimensional, Cartesian filtration, the average specific resistance of the cake (α_{av}) is assumed to be a unique function of the pressure drop (Δp_c) across the cake. On the other hand, the pressure drop (Δp_c) itself is a function of porosity and porosity is correlated to the effective stress (p_s) applied to the cake structure. Based on the discussion provided in section 3.6.2.3.2, the correlation between p_s and distance (radius) in centrifugal filtration is different from the corresponding p_s vs. distance (x) in one dimensional filtration. Consequently, even if the liquid pressure drop across the cake is the same in one dimensional and centrifugal filtration, the average filtration resistance would not be the same.

As Sambuichi et al. (1987) have stated, findings by Oyama and Sumikawa (1954) showed that "*specific resistances obtained in centrifugal filtration were larger than those of constant pressure filtration when liquid pressure drops were the same in the two processes.*" Other researchers reported differences of 20% in average resistances (Valleroy and Malony, 1960). According to Tiller and Yeh (1987), Risbud (1974) showed that cakes in C-P (Compression-Permeability) cells were highly non-uniform due to the wall friction. Liquid pressures measured as a function of distance at the wall and centre of the cell were not linear, and the values of cake permeability at the wall were higher than those at the centre. Tiller and Yeh (1987) indicate that a C-P cell provides only approximate values of specific flow resistance and porosity. Therefore the C-P cell (utilized for constant pressure filtration) is not an accurate means for development of the constitutive relationships required for scale-up of a filtering centrifuge (Tiller and Leu, 1980; Willis and Tosum, 1980; Sambuichi et al., 1987). In the following section, the experimental approach used by Sambuichi et al. (1987) to establish the constitutive equations in centrifugal filtration is explained.

3.6.2.5 The experimental method followed by Sambuichi et al. (1987)

There are two different methods to carry out centrifugal filtration tests. In one method, suggested by Hultsch and Wilkesmann (1977), initially the cake is formed by vacuum filtration of the solid-liquid mixture. Then the cake layer is placed in a filter bucket and this combination is rotated within a centrifuge. During centrifugation, pure liquid is introduced into the filter bucket and the flow rates through the fixed mass of cake are studied as a function of rotational speed. Details of this method are explained in Chapter 5, section 5.3. Considering the discussions provided in the previous two sections, one major drawback of this method is that structure of the cake layer tested would be different from the structure of cake formed during centrifugal filtration.

The other method of conducting centrifugal filtration tests, followed by Sambuchi et al. (1987), is utilizing a filtering centrifuge. These researchers considered the combined effect of sedimentation and filtration during cake formation, rather than simply flowing liquid through a constant mass of cake as suggested by Hultsch and Wilkesmann (1977).

Figure 3.22 schematically illustrates the experimental test setup utilized by Sambuichi et al (1987). These researchers used a suspension of $CaCO_3$ in water and water-glycerin and the concentrations were chosen in a way that experiments would fall in the linear region of the sedimentation diagram. For each test, a feed of 500ml of slurry was used. The basket (0.15 m ID and height of 0.083 m) of the filtering centrifuge was covered with a transparent plate, so the variations of the clear liquid and the slurry interface (r_L and r_s) could be captured by stroboscopic photography. To be able to follow the slurry interface, the operating accelerations were limited to 300g, so the slurry-supernatant interface could be observed for about two minutes. The position of the cake surface was measured by the hook gauge after completion of the test. Comparison of the positions recorded for the liquid surface and slurry-liquid interface in the experiments with the values predicted from the theoretical equations (previously presented in section 3.6.2.3.1) showed very good agreement.

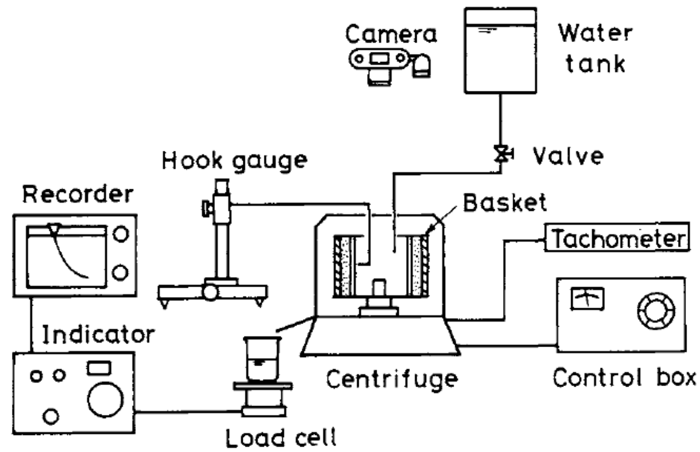

Figure 3.22. Experimental apparatus used by Sambuichi et al. (1987, 1988)

The variation of average specific resistance of the cake was calculated by determining volume of the filtrate obtained during cake formation. After completion of the cake formation, Sambuchi et al. (1987) introduced pure liquid into the filtering centrifuge and determined the average permeability at a constant centrifugal pressure (ΔP). They used the same constant pressure (ΔP) to conduct conventional C-P tests on the same slurry. The purpose was to compare the characteristics of the cake in constant-pressure and centrifugal filtration. The results indicated that the effective stress distribution in the centrifugal and constant pressure filtration were different, leading to different cake structures and accordingly, different average flow resistances.

From the above discussions it can be concluded that the C-P cell can only provide an approximate evaluation of the cake resistance in centrifugal filtration. For scale-up purposes, the method pursued by Sambuichi et al. (1987) should be followed, since the combined effect of centrifugation and filtration during formation of the cake is considered.

3.6.3. Selecting the centrifuge type

To select the appropriate type of centrifuge, the following parameters must be determined (Records, 1977):

- The physical properties of the solid-liquid mixture including: size of the solid particles, relative densities of the two phases, initial concentration of the solids in the feed and viscosity of the liquid.
- Settling velocity of the solids under normal gravity, sharpness of the solid-liquid interface and clarity of the supernatant.
- Possibility of agglomeration of the solids by addition of chemicals, sturdiness of the agglomerates under the body forces generated in the centrifuge, level of improvement on capture of the solids and necessity of conducting a flocculant study.
- The desired performance; while performance is a compromise between three variables: throughput, dryness of the sediment layer/cake; and clarity of the centrate/filtrate.
- The characteristics of the sedimented solids/cake; which is required to determine the discharge method.
- The energy consumed for recovery of unit mass/volume of the slurry.
- Temperature and pressure limits of the process; interaction of the process materials with the materials used in construction of the centrifuge.

In Chapter 5, a comprehensive review of the centrifugal filtration tests for dewatering MFT is presented.

3.7. Hydrocyclones (Cyclones)

3.7.1 General

Similar to a sedimenting centrifuge, the underlying mechanism in a hydrocyclone is utilizing centrifugal forces. However, contrary to a sedimenting centrifuge, there are no moving parts in a hydrocyclone. Figure 3.23 shows the cross section of a hydrocyclone with conventional design, composed of a cylindrical section attached to a conical portion (Trawinski, 1977; Svarovsky, 2000). In the upper part of the cylindrical section, there is an inlet opening for injection of the solid-liquid suspension. As illustrated in Figure 3.23, the combined effects of the tangential inlet and the injection of the feed under pressure generate a scroll-like flow adjacent to the inner surface of the cyclone body; this is known as the primary vortex flow. The underflow nozzle (apex) does not let discharge of the total flow and creates a secondary vortex flowing upwards into the overflow outlet nozzle. To avoid the short-circuiting between the inlet and the overflow, the outlet pipe is extended inside the hydrocyclone (Figure 3.23). This component is known as the 'vortex finder' (Trawinski, 1977).

In the primary vortex, the rotational velocities are lower and the radius of curvature is larger. As a result, the centrifugal forces generated in the primary vortex are relatively low and cause settlement of the coarser particles towards the wall. The tangential velocity in the secondary vortex is much higher and the radius of curvature is smaller, therefore higher centrifugal forces are generated which induce settlement of the finer particles. The combination of the primary settled coarse particles and the joining finer particles are discharged as a concentrated slurry through the apex nozzle, referred to as the cyclone underflow. The clarified liquid, containing the unsettled fine particles, moves along the secondary vortex towards the overflow nozzle and is known as the cyclone overflow. It can be seen that a hydrocyclone is basically a solid phase classifier rather than a solid-liquid separator (Trawinski, 1977).

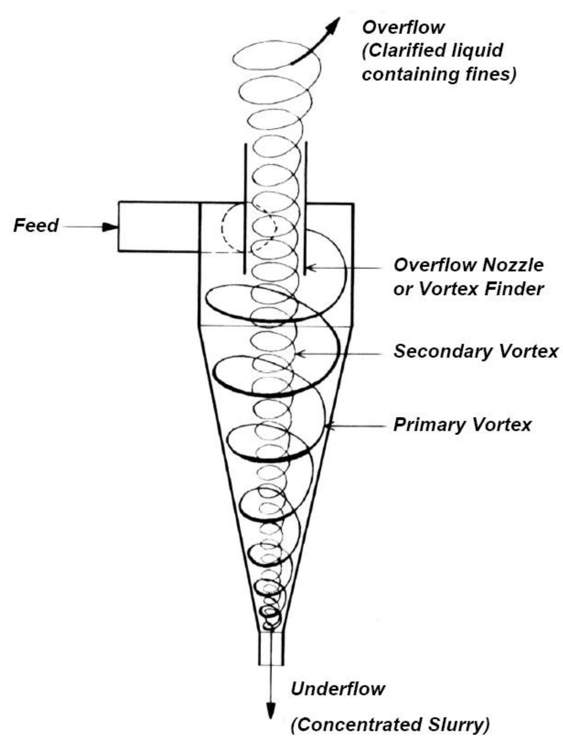

Figure 3.23. Schematic cross section of a hydrocyclone and its flow patterns (adapted from Trawinski, 1977).

3.7.2 Typical designs and performance

As illustrated in Figure 3.24, there are two basic designs of conventional hydrocyclones (Trawinski, 1977; Svarovsky, 2000):

- The long cone cyclone (or the narrow angle design); and
- The long cylinder, steep cone cyclone (or the wide angle design).

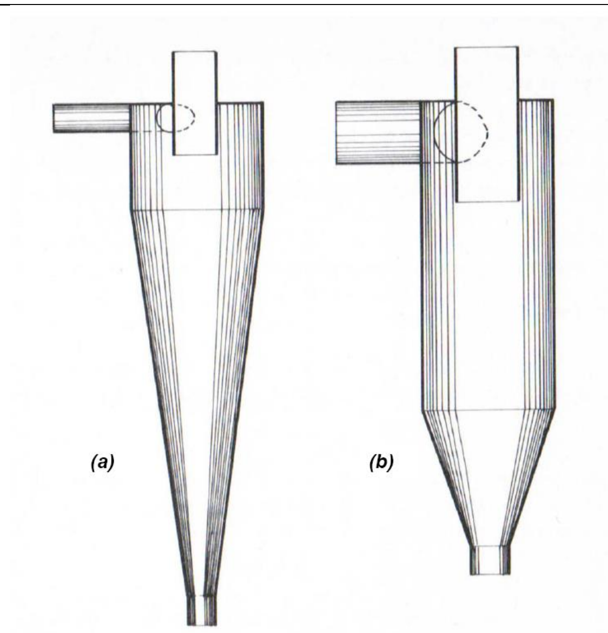

Figure 3.24. Two basic designs of hydrocyclones: (a) Long cone cyclone; (b) Long Cylinder, Steep Cone Cyclone (adapted from Trawinski, 1977).

The narrow angle hydrocyclones are more efficient for separation of fine particles and are used when a relatively low cut size is required. In the wide angle cyclones, the sharpness of cut is improved; however, only relatively coarse cuts are obtained (Svarovsky, 2000).

Hydrocyclones are available in a wide range of diameters, ranging from ~10mm to more than 2m. For a hydrocyclone with a constant body diameter, varying the cylinder length, cone angle and the diameters of the inlet and outlet nozzles would result in a wide range of units with certain performance and applications. The performance of hydrocyclones is a function of factors like density and shape of the particles, density and viscosity of the liquid and operating conditions, specially the operating pressure drop and the feed concentration. Variation in the feed pressure would affect the centrifugal field obtained. Increasing the feed concentration rapidly decreases the efficiency of separation.

Whenever high total mass recoveries are required, hydrocyclones are operated with dilute feed levels (Svarovski, 2000; Trawinski, 1977). To overcome the fluctuations of the feed and to obtain a more concentrated underflow, flapper valves and overflow siphons have been devised. Flapper valves are attached to the cyclone at the underflow apex and only open up when solid particles are present. This results in underflow streams with higher solids content (Goldup (Personal Communication, 2006); Cymerman (Written Communication, 2007)).

3.7.3 Multi-Cyclone arrangements (Multiple cyclones)

From the correlation between centrifugal acceleration and radius of rotation (presented in section 3.5.1), in can be concluded that for the same pressure drop, hydrocyclones with smaller diameter would give better separation efficiency in comparison to the larger cyclones. To make use of this advantage, it is common to utilize small cyclones as multiple units, connected either in series or parallel.

In many industrial operations, when classifications at low cut sizes are desired, clusters or banks of several identical small diameter cyclones are used in parallel to provide sufficient throughput capacity. Another application of using multiple cyclones is to split the feed slurry into a number of different size fractions. For this purpose, cyclones of different dimensions are used in serial or parallel arrangements (Trawinski, 1977; Svarovsky, 2000).

There are a number of separation theories available for the cyclones, ranging from simple fundamental theories (with no consideration of the feed concentration and feed size distribution) to empirical models (based on regression analysis of experimental data) to analytical flow models and numerical flow simulations. Review of these theories is beyond the scope of this thesis and can be found elsewhere (Svarovsky, 2000).

3.8. Summary

The Solid-Liquid separation methods can be categorized in two main groups: Sedimentation techniques and Filtration techniques. In the Sedimentation techniques, the liquid is constrained in a vessel and the solid particles move within the liquid. In the Filtration techniques, however, the solid particles are constrained by a medium and the liquid can flow freely through the medium. While in the Sedimentation techniques a density difference between the solid and liquid phases is necessary, it's not a requirement for the Filtration operations.

In this chapter a review of the theory of separation and method of operation for the following separation devices was presented:

- Thickeners; in which separation of the solid and liquid phases takes place by particle settling due to gravitational forces. Increasing the efficiency of flocculants has lead to design of thickeners with smaller area and higher underflow solids content.
- Inclined plate settlers; also known as Lamella Settlers or Lamina-type clarifiers, are high-rate sedimentation devices consisting of several inclined parallel plates stacked within a settling tank. The main advantage of the inclined plate settlers is the reduced plant footprint required in comparison to the regular thickeners.
- Filters; which are basically porous media and separation of the solids from a liquid occurs by passing the solid-liquid suspension through them. While the fluid passes through the filter medium as filtrate, the solid particles are retained and form a cake.
- Solid Bowl Centrifuges; which basically consist of an imperforated bowl, rotating around a vertical or horizontal axis. The high rotational velocity of the bowl creates a centrifugal field and enhances settlement of the solid particles.
- Filtering Centrifuges; which are composed of a basket covered with a filter cloth, rotating together around a vertical or horizontal axis. The pressure difference required for flow of the liquid across the filter cloth is generated by gravitational forces in the centrifugal field.
- Hydrocyclones; in which the underlying mechanism for enhancing the separation is utilizing centrifugal forces. However, contrary to centrifuges, there are no moving parts in a hydrocyclone and the centrifugal field is obtained by introducing the slurry with a high tangential velocity into a cylindrical or conical vessel.

Part of the present research dealt with studying the capability of different separation methods for production of more robust composite tailings streams. In Chapter 4 a brief review of some experimental work conducted for this purpose will be presented.

Chapter 4

Preliminary Dewatering Experiments

4.1. Introduction[1]

After reviewing the common methods of solid-liquid separation, this research focused on studying possibility of using some of these approaches for producing a robust non-segregating CT. This chapter first explains the possible approaches that may be followed to produce a CT/NST with high solids content. Then a review of the laboratory tests conducted to explore the practicability of dewatering CT/NST as a mixture, also dewatering MFT as its component will be presented. In addition, the dewatering and flow characteristics of some example NST samples made from centrifuged MFT will be reviewed. The last section of this chapter provides a detailed review of the vane and slump tests, as two methods for measurement of the yield stress of solid-liquid mixtures. A comparison of these methods for evaluation of the CT/NST samples at varying solids contents will be presented.

4.2. Possible Approaches for Making CT/NST with Higher Solids Contents

As stated in section 2.8.1, CT and NST are engineered tailings streams produced by recombination of fines (MFT or TT) and sand (cyclone underflow) at SFR of 3 to 5, plus a chemical additive. Different organic flocculants or inorganic coagulants may be used for production of CT/NST. Addition of the chemical additive enhances flocculation of the fines and results in a carrier fluid with higher viscosity/yield stress that is capable of supporting the sand particles and preventing their segregation. In the present research gypsum, commonly used in the Suncor and Syncrude CT operations, was utilized to make CT/NST.

---

[1] Part of this chapter has been previously published: Nik, R. M., Sego. D. C. and Morgenstern, N.R. (2010) "*Flow behavior and robustness of non-segregating tailings made from filtered-centrifuged MFT.*" Proceedings of the Second International Oil Sands Tailings Conference, Edmonton, Alberta, Canada. Dec. 2010., pp. 319 – 329.

In practice the CT produced at field operations has not been particularly robust. The solids content of this recombined tailings stream is usually not high enough to create a sufficient margin below the static segregation boundary on the ternary diagram (Figure 2.8). The proximity of CT to the static segregation boundary along with fluctuations in the solids content of the feed (cyclone underflow and MFT) and the high/uncontrolled energy of the depositional environment, all make the CT produced at field operations susceptible to segregation. To mitigate the effects of the feed fluctuations and the uncontrolled depositional energy, CT with higher solids content (located farther from the static segregation boundary) is desired.

It should be noted that the results of a study by Pirouz et al. (2006) indicate that the segregation threshold for a slurry is dependent on the rate of shearing. As the shear applied to a slurry increases, its solids concentration must also increase to show a non-segregating behavior. After the shearing rate is increased above a certain limit, turbulent mixing occurs which prevents segregation. At shear rates higher than this limit the segregation threshold decreases due to the flow turbulence (Pirouz et al., 2006). It is worthy to note that while a turbulent flow regime causes mixing (non-segregation) of the coarse and fine fractions in the pipeline[2], the flow conditions would be different after discharge and during the deposition stage. To have a non-segregating CT/NST during these stages the yield stress of the carrier fluid (i.e. fines + water) must be sufficient to support the sand particles and prevent their segregation. To obtain a carrier fluid with higher yield stress, the F/(F+W) ratio must be increased, in other words the water content of the slurry must be decreased.

The possible approaches for making CT/NST with higher solids content (i.e. lower water content) would be:

- Mixing the fine and coarse fractions to produce CT/NST and then dewatering the resultant mixture prior to deposition; and,
- Dewatering one or both of the CT/NST components (cyclone underflow and MFT) prior to mixing them together.

[2] In section 6.5.1 it is discussed that increasing the solids concentration of a slurry and changing the flow regime from turbulent to laminar would potentially reduce the pumping energy required for transferring unit weight of the material.

The following example provides a better understanding of each of the above approaches. Figure 4.1 shows a family of diagrams that correlate the solids content of the feed MFT and cyclone underflow with the solids content of the resultant CT/NST. These diagrams are obtained from parametric solution of the multiphase mass-volume relationships presented by Scott (2003) and Boratynec (2003). The horizontal axis shows the solids content of MFT, the vertical axis shows the solids content of CT and each diagram represents the correlation between these two parameters at varying solids content values of the sand. The illustrated solution in Figure 4.1 is for the specific case of SFR = 4, with the assumption that the fines content of MFT and sand (cyclone underflow) are 100% and 0% accordingly. As an example, it can be seen that mixing MFT at 30% SC with cyclone underflow at 75% SC at a SFR of 4, results in a CT with about 57.6% solids content. In order to produce a more concentrated CT (for example at about 66%), either this 57.6% CT needs to be directly dewatered to 66% using a suitable dewatering method prior to deposition (Figure 4.1), or one/both of its components are required to be dewatered prior to mixing. As marked in Figure 4.2, maintaining the MFT at 30% solids would require dewatering the sand to about 95% solids in order to obtain a CT mixture of 66% SC. Maintaining the sand at 75% SC however, would require dewatering MFT to about 45% SC as illustrated in Figure 4.3. Any combination of these two approaches (i.e. dewatering both MFT and sand) may also be followed.

It should be noted that while consistency of the CT/NST must be high enough to create a robust non-segregating tailings stream, yet it needs to allow pumping of this slurry through the pipeline. The limit of centrifugal pumping is schematically marked in Figures 4.1 to 4.3. This limit would be higher for the positive displacement (PD) pumps. In addition, the consistency (and accordingly, the yield stress) of CT/NST must allow its flow and distribution far enough beyond the discharge point (Jewell et al., 2002; Kwak et al., 2005). Further discussion on the correlation between solids content and yield stress of the CT/NST will be provided in sections 4.6.3 and 6.5.

It is worth mentioning that in addition to reducing the water content of CT/NST, another approach for creating a robust CT/NST would be increasing the dosage of coagulant/flocculant to obtain a more viscose carrier fluid. However, this approach is not desired due to the possible adverse effects of the chemicals present in the release water on the extraction process. Also formation of a very viscose carrier fluid (a very strong

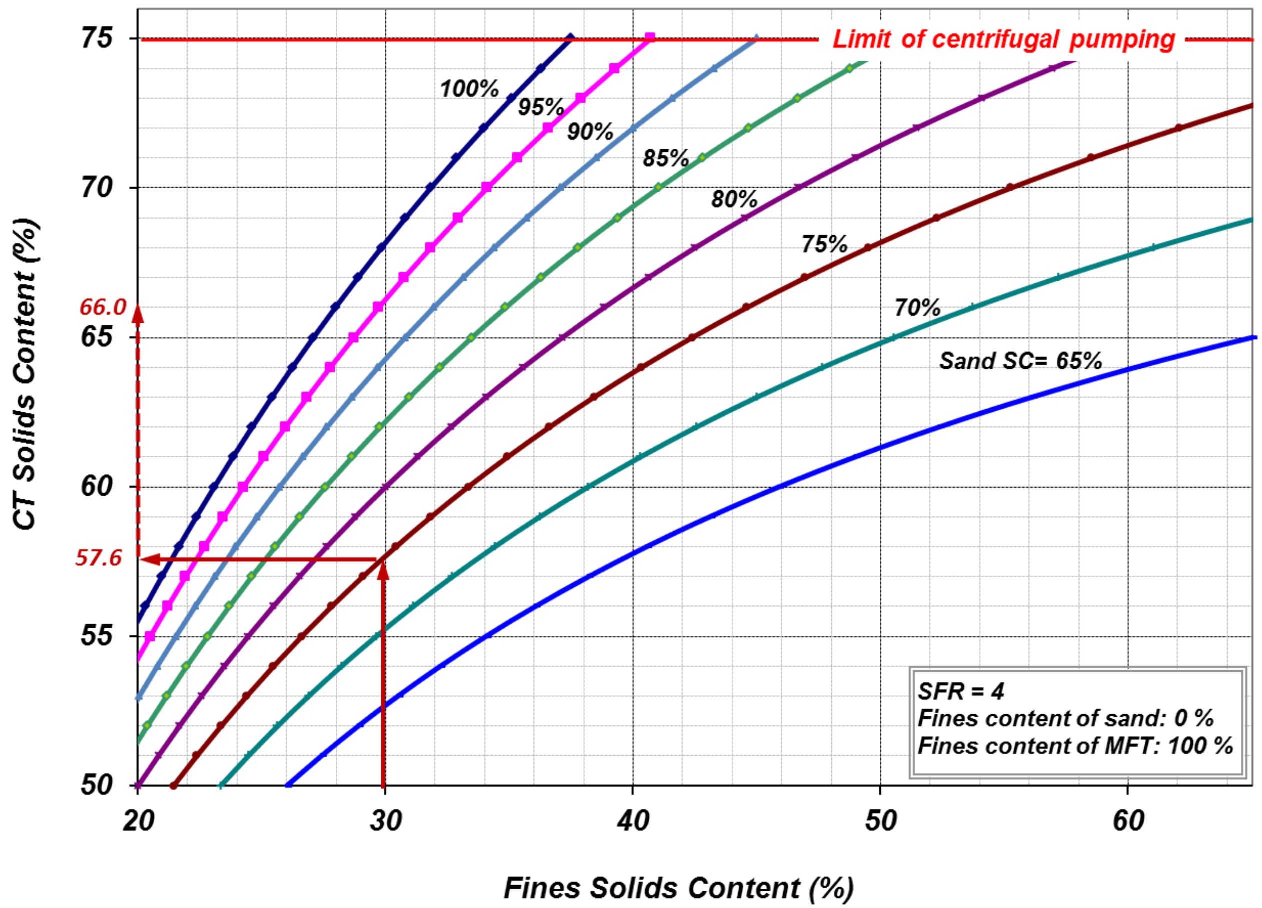

Figure 4.1. Parametric solution of the multiphase mass-volume relationships for the specific case of SFR=4, no fines in the sand and no coarse in the fines. The example arrows indicate that mixing 30% MFT with 75% sand results in CT at 57.6% solids. One approach to obtain CT at higher solids content (e.g. 66%) would be direct dewatering of 57.6% CT prior to its deposition.

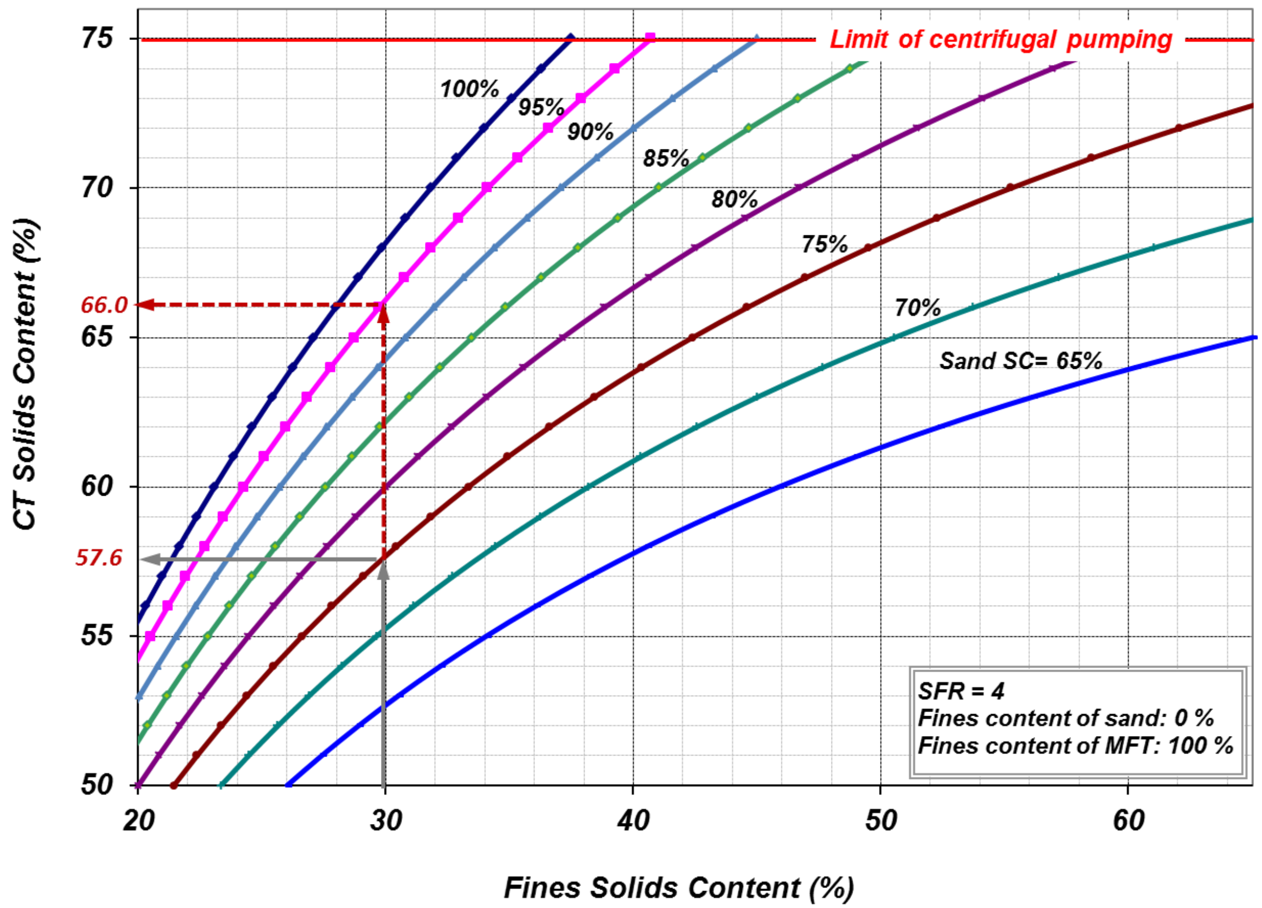

Figure 4.2. Making CT at higher solids content by dewatering the sand: The example arrows indicate that dewatering the sand from 75% to 95% solids and then mixing it with 30% MFT results in CT at 66% solids.

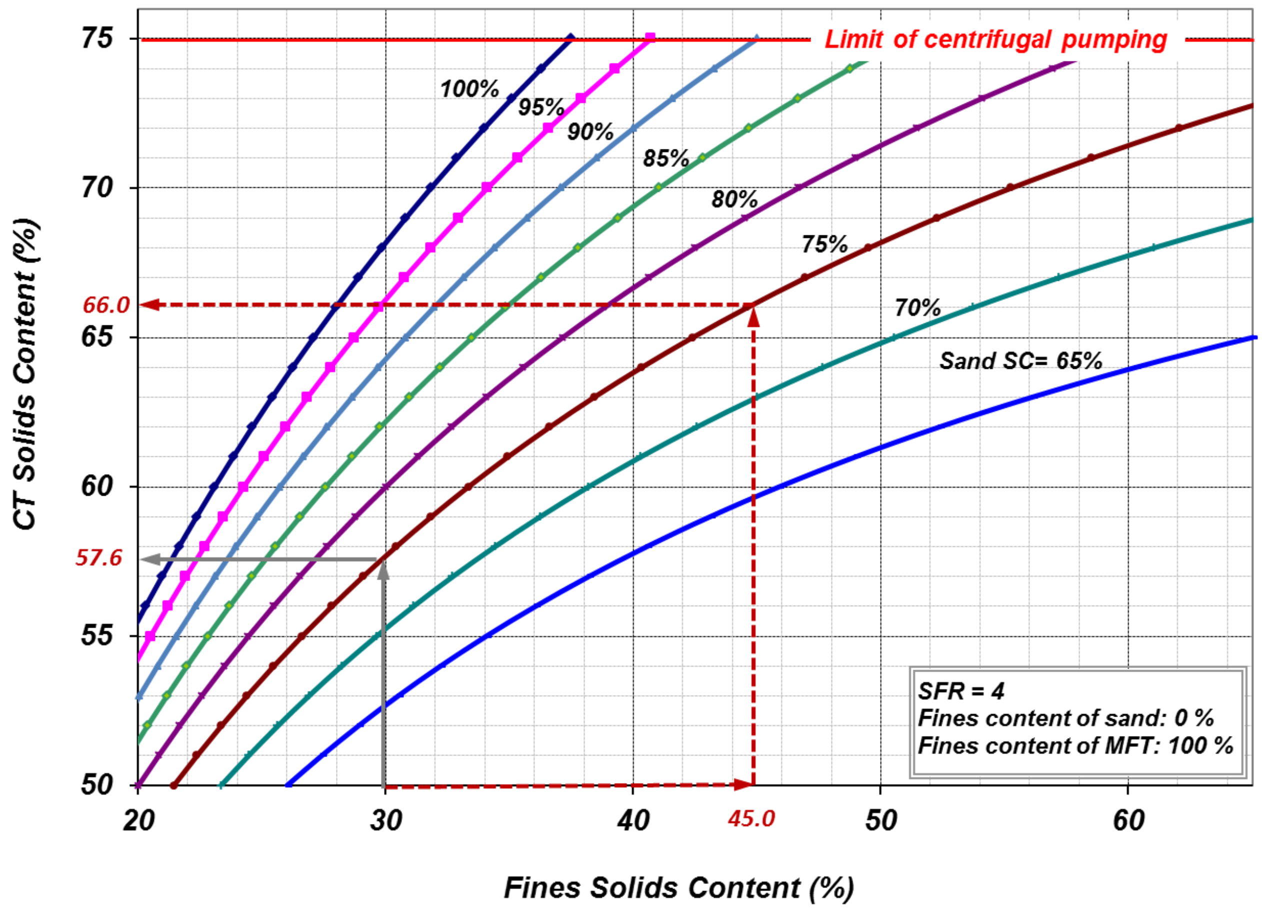

Figure 4.3. Making CT at higher solids content by dewatering MFT: The example arrows indicate that dewatering MFT from 30% to 45% solids and then mixing it with 75% sand results in CT at 66% solids content.

flocculated structure) could impede the sedimentation/consolidation of the resultant composite tailings.

4.3 Preliminary Laboratory Scale Dewatering Tests

This section provides a review of the laboratory tests conducted to study dewatering of CT as a mixture, also dewatering of MFT as a component for making CT. In the present research no laboratory tests were conducted to dewater sand (cyclone underflow), however a parallel study conducted at the University of Alberta examined dewatering of the whole tailings using cross flow filtration (Beier and Sego, 2008; Zhang et al., 2009). This method of dewatering was reviewed in section 2.8.2.5 and as will be suggested in Chapter 7, has the potential to be used for dewatering sand or CT.

4.3.1 Test Materials

The MFT used for the laboratory tests was collected from the tailings ponds of Suncor, Syncrude and Albian Sands operations. Composition of the MFT received from each company is presented in Table 4.1. The solids and bitumen contents stated in this table represent the average values for each source of MFT. The fines content values reflect the percentage of solids finer than 44 microns (i.e. passing through sieve #325). It should be noted that in calculation of the geotechnical solids content, the percentage of bitumen remaining in the samples after oven drying is considered as part of the solids. Figure 4.4 presents the particle size distribution (PSD) of each MFT sample obtained by means of sieve and hydrometer analysis.

Table 4.1. Characteristics of the MFT used for making NST

MFT Source	Geotechnical Solids Content (%)	Solids (%)	Water (%)	Bitumen/Asphaltene (%)	Fines (<44 μm) (%)
Suncor	27.0	24.62	73.3	2.08	97.2
Syncrude	36.5	34.92	63.33	1.75	97.7
Albian Sands	37	35.13	63.72	1.15	98

The sand used for making all of the CT/NST samples was sourced from the beach of Suncor tailings pond. The sand solids content and fines content were about 98.8% and 1.2% accordingly. The fines content was determined by washing the sand over sieve #325.

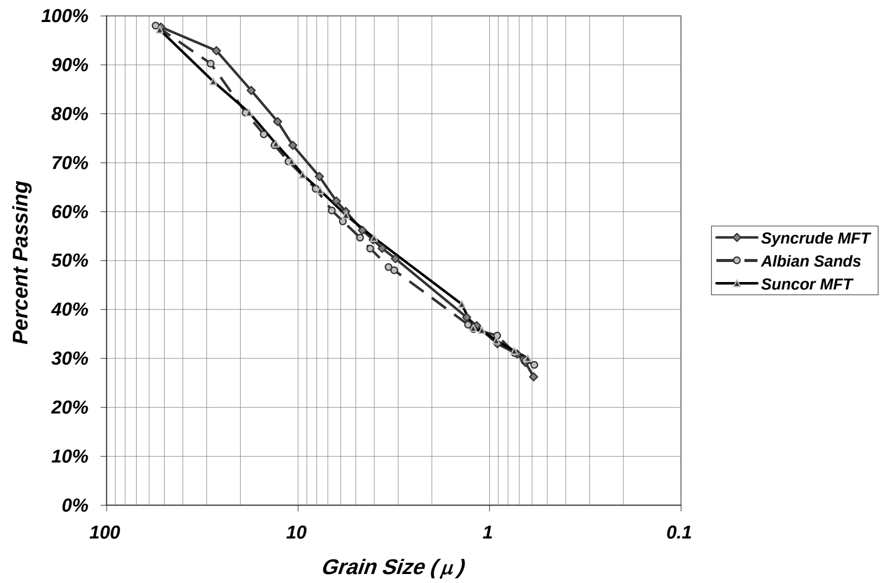

Figure 4.4. Particle Size Distribution of the MFT samples used in the present study.

4.3.2 Dewatering CT/NST as a mixture

As stated in Chapter 2, the possibility of using conventional thickeners for dewatering CT has been studied previously, but the results have not been promising (Matthews – Personal Communication, 2007). Some of the primary challenges anticipated with the concept of using thickeners to further enhance CT solids concentration would be: very high torque management issues; the large volume of material and the need for a large settling area to reduce the expected long residence time for water release; and handling the thickened underflow in terms of feeding a pump and management of transport of the thickened material to the point of discharge.

In order to investigate the concept of accelerated dewatering in vessels with inclined walls, a number of sedimentation tests were conducted on CT samples using vertical and inclined standpipes. Also the dewatering of thin layers of CT on inclined plates was experimentally studied.

4.3.2.1 Sedimentation Tests in Vertical and Inclined Standpipes

In these tests fresh CT samples were prepared and the same volume of each sample was placed in two standpipes: one at vertical position and one inclined at a certain angle from the vertical axis. Figure 4.5 illustrates a sample test conducted at the following conditions:

- Initial CT solids content: 65%
- SFR: 4
- Source MFT solids content: 28%
- Gypsum dosage: 900 ppm
- Initial density of CT (ρ_{CT}): 1650 kg/m^3
- Standpipe internal diameter: Di = 6 cm
- Initial height of slurry: L = 35 cm
- Inclination from vertical axis[3]: 27 degrees

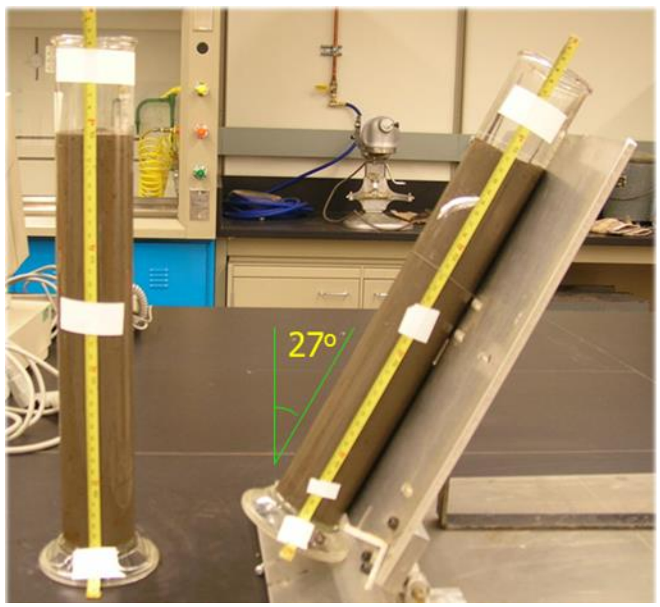

Figure 4.5. Sedimentation of CT samples in vertical and inclined standpipes.

Figures 4.5.a to 4.5.d show the gradual sedimentation/dewatering of the CT samples in the two standpipes during the first three weeks of the test. As can be observed, volume of the clear water formed over the CT sample in the inclined standpipe is higher than the one in the vertical standpipe. The diagrams illustrated in Figure 4.6 show the volume of water released in each standpipe versus time. The slope of the diagram for the inclined standpipe is significantly higher during the first couple of weeks of the test, indicating a faster dewatering rate during the sedimentation stage. Since the CT samples in both standpipes had similar composition and water content, eventually the diagrams in Figure 4.6 will reach to the same value during the consolidation stage.

[3] The parallel plates in Lamella settlers are usually inclined at a ~60^o angle to horizontal.

a) Day 0	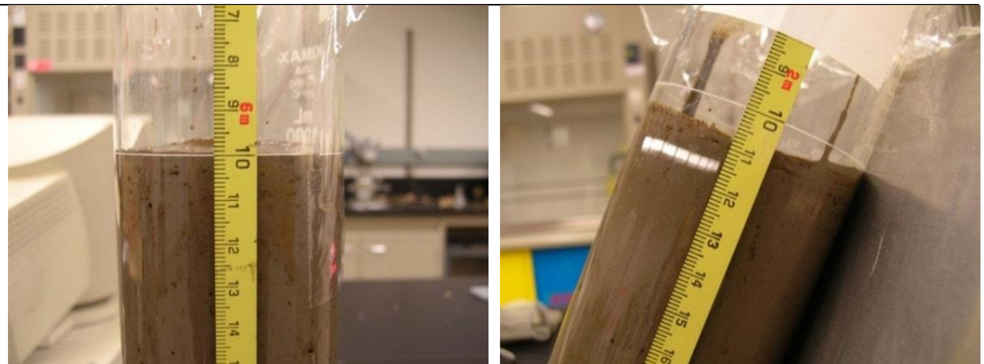
b) Day 5	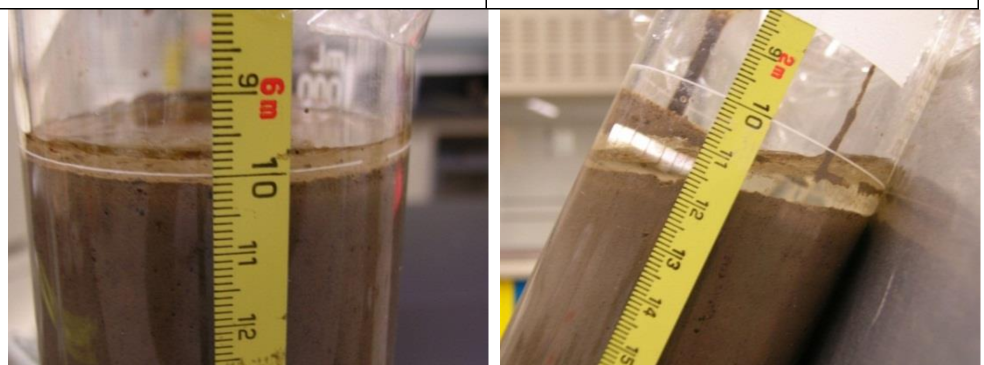
c) Day 13	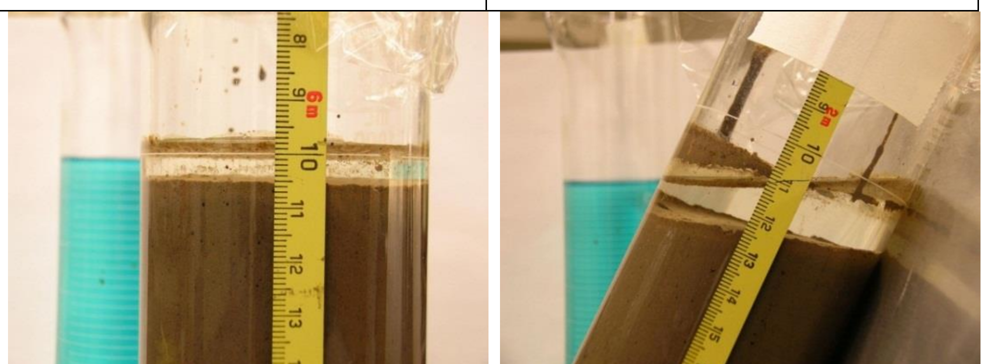
d) Day 23	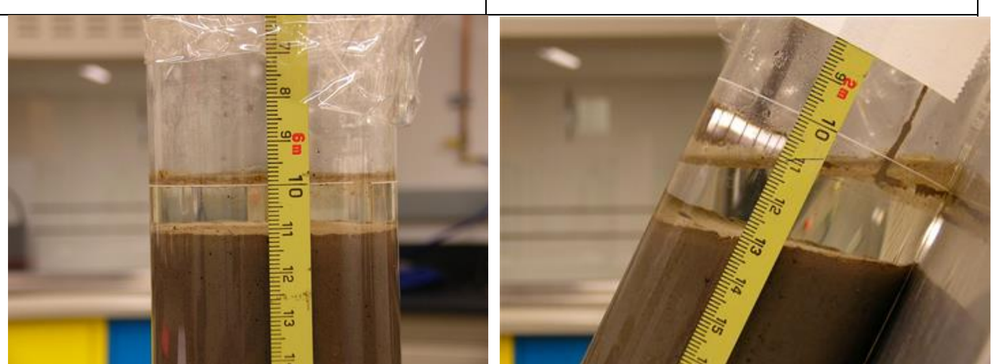

Figure 4.5.(a-d) - Gradual dewatering of CT samples in the vertical and inclined standpipes.

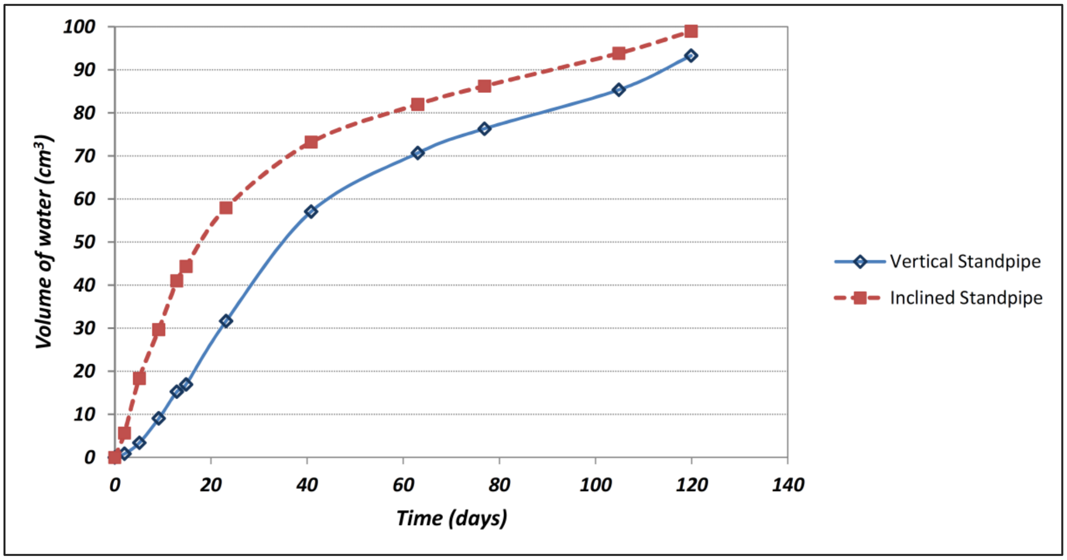

Figure 4.6 - Comparison of the volume of water released in the CT sedimentation tests in two standpipes: one vertical and the other inclined 27° from the vertical axis.

Using the PNK theory (Equation 3.7), the approximate ratio of the settling velocity in the inclined standpipe to the one in the vertical standpipe would be equal to 3.36. However, comparison of the actual settling diagrams in Figure 4.7 indicates that the settling rate in the inclined standpipe (during the first three weeks of the test) is about 2.6 times the vertical case. As previously stated in Chapter 3, the PNK theory often overestimates the settling rate in an inclined vessel (Acrivos and Herbolzheimer, 1979; Harvie et al., 2002; Bürger et al., 2011). It should be noted that in the PNK theory parameter b defines the perpendicular distance between the two inclined planes of the vessel. When the vessel used is a standpipe with circular cross section, the drainage path at the two sides of the cross section would be shorter (Figure 4.8) and parameter b in equation 3.7 would be smaller than the diameter of the standpipe.

$$\frac{dH}{dt} = -v_0\left(1 + \frac{H}{b}\sin\alpha\right) \qquad \text{(3.7 – repeated)}$$

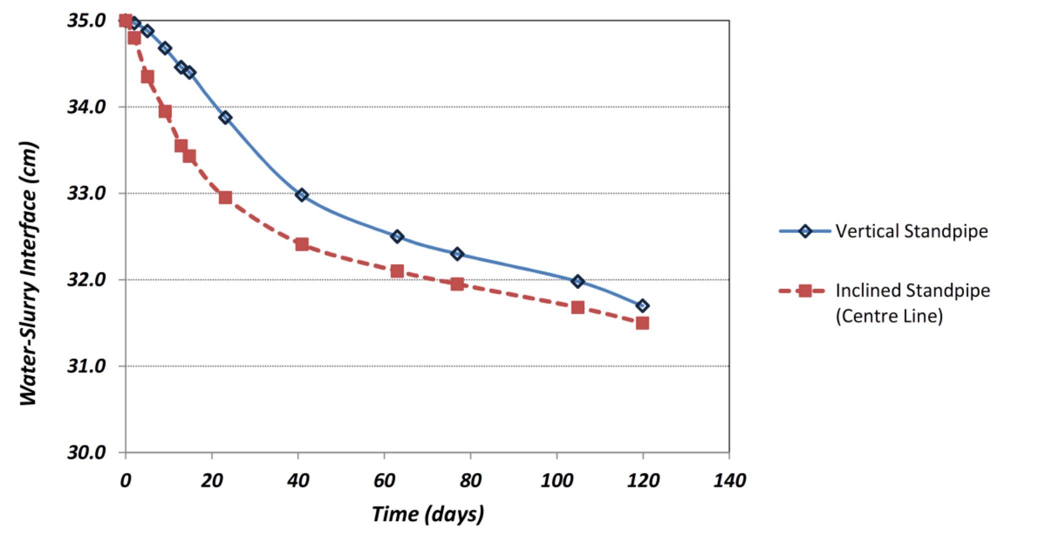

Figure 4.7 - Comparison of the settling velocity in the CT sedimentation tests in two standpipes: one vertical and the other inclined 27° from the vertical axis.

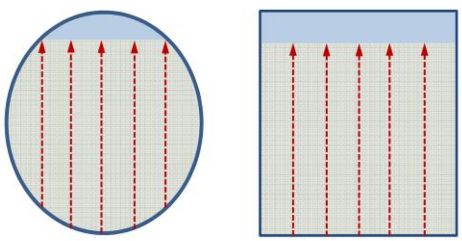

Figure 4.8. Comparison of the drainage path for the circular and rectangular vessels.

As explained in Chapter 3, during settling in an inclined vessel a thin layer of clear liquid will form under the downward-facing wall of the vessel. For the above sedimentation test with 27° inclination from vertical this layer could not be distinguished, although formation of multiple small channels directing water under the downward-facing wall of the standpipe was visible (Figure 4.9). When this test was repeated for higher angles of inclination, formation of a thin layer of clear liquid was visible under the downward-facing wall of the standpipe (e.g. Figure 4.10, 60 degrees inclination from the vertical axis).

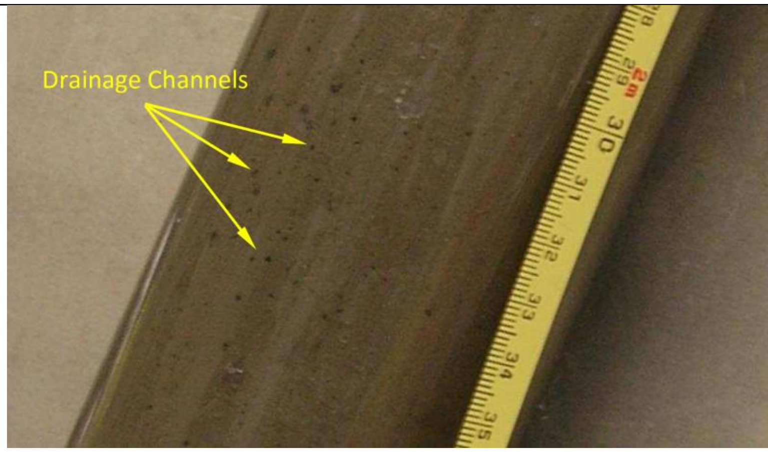

Figure 4.9. Drainage channels formed under the downward-facing wall of the standpipe inclined at 27^{o} from the vertical axis.

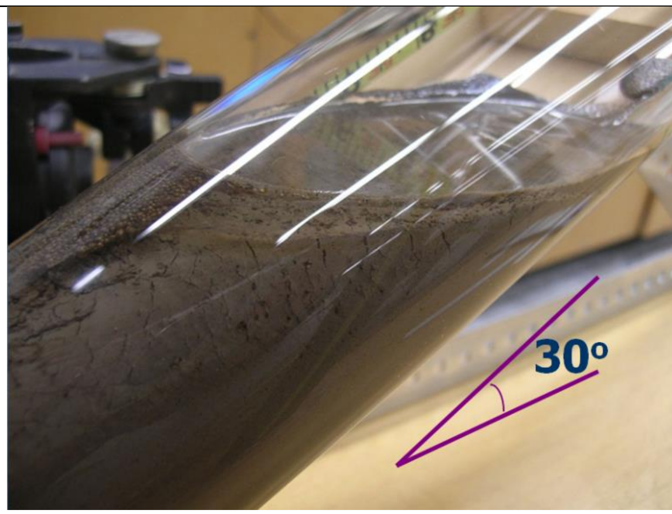

Figure 4.10. Formation of a thin layer of clear liquid under the downward-facing wall of the standpipe inclined at 60^{o} from the vertical axis.

Further increasing the standpipe inclination will extend the settling area available in it and will decrease the drainage path for the CT layer. The maximum settling area and the minimum drainage path occur when the standpipe is inclined 90 degrees from vertical (i.e. laying horizontally). However, an inclination angle is required to facilitate flow of the released water to a collection point. Also as will be explained in the following, a minimum inclination angle is required to have a self-cleaning separator. Horizontal plate separators were initially introduced in 1904 by Hazen (WSE: WaterSmart Environmental, 1999). Operation of these separators revealed that settling of the particles on the horizontal plates partially restricted the flow path of the liquid and the laminar flow conditions (desired for operation of the settler) were no longer valid because of the turbulence induced. This required regular cleaning of the horizontal plate separator to restore it to its initial efficiency. To overcome the problem of routine cleaning, the inclined plate settlers were invented in which the parallel plates were inclined at an angle greater than the angle of repose of the separated materials (WSE, 1999). To study the effect of the plate inclination and thickness of the CT layer on its dewatering characteristics, a number of experiments as explained in the following section were conducted.

4.3.2.2. Dewatering thin layers of CT on inclined plates

The test setup shown in Figure 4.11 was used to investigate the effect of layer thickness[4] and inclination angle on the dewatering rate of CT. This setup was composed of the following components:

- A flume made of 8mm (5/16") thick acrylic sheets, L: 91.4cm (36") x W: 15.2cm (6") x H: 5.1cm (2"), open at both ends and covered on top.
- An aluminum container connected to the end of the flume acting as a reservoir.
- An adjustable sliding gate separating the reservoir from the flume.
- An adjustable frame to support the flume at the desired inclination angle.
- An aluminum container placed at the base of the flume, collecting the water drained from CT samples.

To conduct each test, the flume was placed on the supporting frame holding a certain angle and freshly prepared CT was placed in the reservoir. Thickness of the CT layer flowing on the upward-facing plate (base) of the flume was adjusted by opening the sliding gate for the desired value. The solids content of CT for all tests was between 64.2% to 64.4%. The preparation conditions were identical (SFR=4 and mixing duration= 3 minutes) and the gypsum dosage was 900ppm. A number of tests were conducted for different layer thicknesses of CT (varying from 3 to 10 mm) and different angles of inclination. Details of each test follow and the results will be discussed afterwards:

---

[4] Based on the study previously conducted by Boratynec (2003) at the University of Alberta, when CT samples with the same thickness (H) were placed in standpipes with different diameters (D), increasing the Diameter to Height Ratio (DHR) would enhance the dewatering rate of CT.

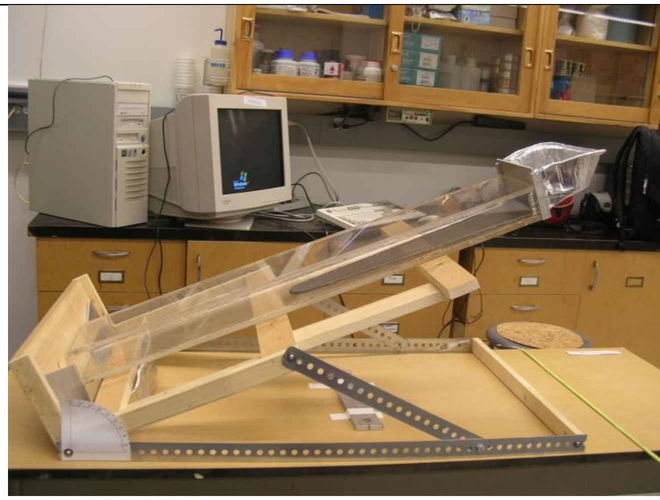

Figure 4.11. The Test setup used for dewatering thin layers of CT on inclined plates.

- Test T10-A21: A 10mm thick layer of CT was tested at an inclination angle of 21^o.
- Test T6-A21: A 6mm thick layer, tested at an inclination angle of 21^o.
- Test T6-A27: A 6mm thick layer, initially placed at an inclination angle of 21^o and after 20 minutes the angle was increased to 27^o. After slight sliding and shearing the CT layer came to rest on the inclined plate.
- Test T3-A35: A 3mm thick layer, initially tested at 30^o and after 60 minutes the angle was increased to 35^o. Some sliding and shearing of the CT layer was observed before it came to rest.
- Test T3-A39-S: To investigate the effect of high inclination angle and shearing on dewatering of the CT layer, the test for the 3mm thick layer was repeated while a sandpaper was placed on the upward-facing plate. This allowed starting the test at an inclination angle of 32^o and increasing the angle to 39^o after 25 minutes. The CT layer came to rest after some sliding and shearing.

A camera connected to a computer was programmed to take photos of the tests at one minute time intervals. By means of a computer software these images were converted to a movie for each test, which was utilized for visual comparison of the rate of dewatering.

Diagrams illustrated in Figure 4.12 show the volume of water (in drops[5]) released in each test versus time. Comparison of the tests T6-A21 and T6-A27 shows a significant increase in the volume of water released after increasing the inclination angle and this is partly due to the shearing occurred in the CT layer after increasing the inclination (Figure 4.13). Similar high rates of water release were observed for tests T3-A35 and T3-A39, both experiencing shear due to steeper angles of the plate. As marked in Figure 4.12, some delay in dewatering can be observed during the test T3-A39-S. Examining the test set-up revealed that this delay was due to absorption of part of the released water into the sandpaper. It should be noted that while a plate with a rough surface allows for steeper inclination angles and higher rate of dewatering, yet in practice it needs to be smooth enough to permit sliding down of the separated particles. Design references also recommend using non-oleophilic plates to prevent buildup of the oily particles (WSE, 1999).

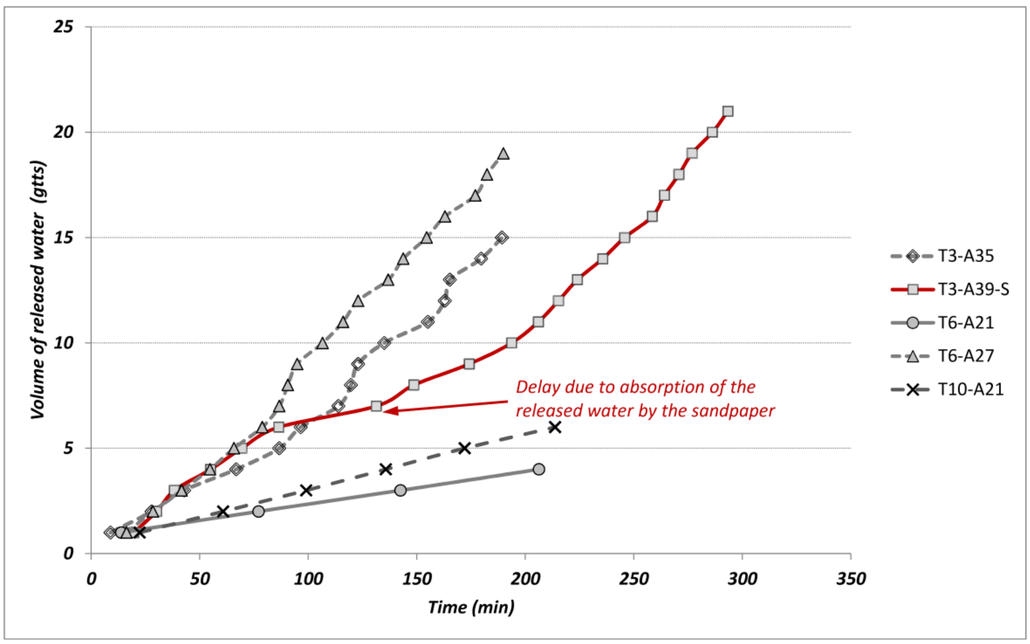

Figure 4.12. Dewatering of thin layers of CT (3 to 10 mm) on inclined plates (21° to 39° from horizontal)

[5] *gtts* (drops) is the plural of *gtt*, an abbreviation for *gutta* which is the Latin word for *drop* (Wikipedia, 2012).

(a)	(b)

Figure 4.13. (a) Initial position of the front edge of a thin layer of CT on a plate with 21^o inclination from horizontal). (b) Shearing of the CT layer resulted from increasing the inclination angle to 27^o.

While the observations made in the previous tests indicate that placing thin layers of CT on inclined plates and using vessels with inclined walls enhance dewatering of this material, practicability of using the inclined plate settlers for producing more concentrated CT in large scale operations requires further study. Based on a number of pilot scale experiments conducted on dewatering clay and silt suspensions using the inclined plate settlers, increasing the feed density will decrease the efficiency of this method of dewatering and it may not be viable for feed densities higher than 1.1 ton/m^3 (Scott, 1990 - US Army Corps of Engineers). Therefore this method of dewatering may be more suitable for a low density slurry like cyclone overflow rather than for a higher density material like CT. The possibility of combining the concept of inclined plates with thickeners for dewatering thin fluid fine tailings and producing thickened tailings should be considered for future studies.

4.4. Dewatering MFT prior to making CT/NST

To study the possibility of dewatering MFT and then using it as a component of CT/NST, two types of laboratory scale (bench-top) centrifuge tests were conducted: filtering centrifuge tests and bottle/tube centrifuge tests. These tests were conducted at the Geo-Environmental laboratory of the University of Alberta. The centrifuge device was a bench-top Heraeus Centrifuge, model Multifuge 3 L-R, by Kendro Laboratory Products (Figure 4.14). The maximum spinning velocity that was recommended by the device manual was 4150 rpm, and the distance between the center of rotation and the mid-point of the centrifuge tube/bottle was about 19.2 cm. This combination of spinning velocity and radius creates a maximum relative centrifugal force of ~3700 g (i.e. RCF = 3700 g), where g is the acceleration of gravity. As shown in Figure 4.14, two configurations of centrifuge tubes/bottles could be placed in this centrifuge: either four groups of five 50ml centrifuge tubes, or four 650ml centrifuge bottles.

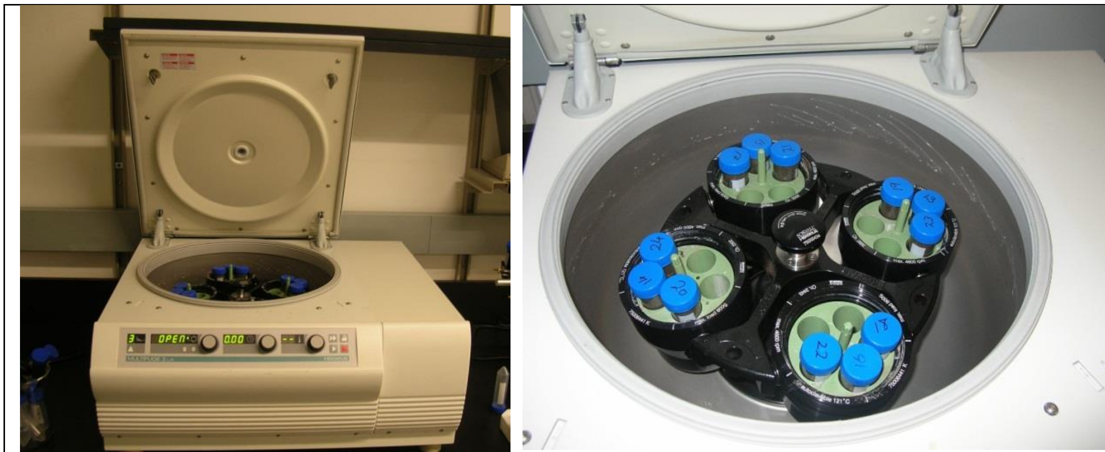

(a) **(b)**

Figure 4.14. (a) The Bench-Top Centrifuge used for laboratory scale tests
(b) Possible arrangements of the centrifuge bottles in the centrifuge.

4.4.1. Centrifugal Filtration Tests

As stated in Chapter 1, in the present research a batch filtering centrifuge designed and provided by a private industrial company was used at the OSTRF plant to dewater MFT. Prior to using this device, a bench-top clinical centrifuge was utilized to conduct small scale filtering centrifuge tests and study practicability of the filter cloth for this method of dewatering. Details of these tests are provided in section 5.3 of the next chapter.

4.4.2. Centrifugal Sedimentation Tests

The centrifugal sedimentation tests (bench-top bottle/tube centrifuge tests) were conducted with the following objectives:

- Prediction of the approximate residence time required to obtain a certain solids content in the batch filtering centrifuge.

- As a pre-screening tool for selection and evaluation of the coagulants/flocculants prior to conducting larger scale centrifuge experiments.
- Producing untreated and treated MFT at higher solids content and:
    - Using it as a component for making CT/NST with high concentration.
    - Studying the correlation between solids content and yield stress of the fine tailings and CT/NST.

It should be noted that another use of bottle/tube centrifuge tests is rapid evaluation of the dewatering characteristics of the tailings, as an alternative to settling column (standpipe) tests. Eckert et al. (1996) provide a review of the theory (developed by Buscall and White, 1987) and the test procedure for these types of centrifuge experiments along with the models obtained for the Syncrude fine tailings. For suspensions like oil sands fine tailings, settling columns with sufficient height (minimum of 3m as recommended by Scott et al. (1985)) are required and need to be monitored for years to provide meaningful results. The examples of such experiments are the 10m standpipe tests [on fine tailings and sand-fine mixtures] that were monitored at the University of Alberta for more than 25 years (Jeeravipoolvarn et al., 2009). Conducting centrifuge tests as an alternative to column sedimentation tests was beyond the scope of the present research.

4.4.2.1 Test procedure

When continuous monitoring of sedimentation of a solid-liquid mixture in a centrifugal field is desired, the ideal device would be a centrifuge with a transparent cover [equipped with a stroboscope] that allows recording the position of the slurry-water interface while it is spinning (Eckert et al., 1996). In the present research however, in addition to evaluation of the volume of clear water released, it was desired to find what percentage of the fines were in the form of a liquid slurry and what percentage were captured in a cake. As a result, the centrifuge had to be stopped at specific time intervals during the course of centrifugation to monitor the clear water-suspension interface[6], also to take samples of the slurry and cake. Prior to running each test, a sample of MFT with known initial solids-content was mixed in a beaker, and then using a 100ml syringe about 50ml of it was placed in a Fisherbrand© 50ml plastic centrifuge tube. Two equal-weight 50ml

[6] It should be noted that removal of the centrifugal force during the test can cause possible rebound of the supernatant-suspension interface (Eckert et al., 1996).

centrifuge tubes were prepared for each stage of monitoring, placed at symmetrical positions in the centrifuge with regard to the center of rotation. [This was required to balance the loads in the centrifuge as imbalance can cause catastrophic failures.] Figure 4.14.b shows an arrangement of 12 centrifuge bottles allowing 6 stages of monitoring and sampling during the sedimentation test. After spinning the centrifuge for a certain period of time and stopping it, two bottles positioned at symmetric positions were removed, the average position of the slurry-water interface was recorded and one bottle was used for measuring the volume of decanted water, also the solids content and weight of the dewatered slurry/cake. The same procedure was repeated until all the centrifuge bottles were removed from the centrifuge.

Figure 4.15 shows the images of two example centrifuge sedimentation tests conducted on untreated Suncor MFT with initial solids content of 27.6% at 4150 rpm (RCF=3700 g), and the same MFT when treated using 600ppm gypsum. Position of the slurry-water interface and the variations of average solids content of the dewatered slurry versus time are also presented in two diagrams. The results of such tests, when conducted at different treatment conditions and spinning velocities, can be used to decide about the type/dosage of chemical additive and the residence time required in larger scale solid bowl or filtering centrifuge experiments. The following sections provide further details about the use of bench-top centrifuge tests for scale-up purposes and prescreening of the chemical additives.

4.4.2.2 Prediction of the residence time required in the batch filtering centrifuge

Prior to using the batch filtering centrifuge at the OSTRF plant (Chapter 5), it was desired to have an estimation of the residence time required to obtain a certain cake consistency. In Chapter 3 it was mentioned that when a centrifugal filtration test and a centrifugal sedimentation test are conducted on identical slurries at equal spinning velocity using the same basket/bowl size, the cake would build up faster in the filtering centrifuge; however the ultimate void ratio of the dewatered cakes in both systems would be approximately equal. Therefore, at identical testing conditions the residence times obtained from the bench-top centrifugal sedimentation tests can be regarded as an upper limit for the residence times that are expected in the batch filtering centrifuge. When a slurry is tested at two centrifuge systems with different thicknesses of settling column and spinning velocities/radiuses, the ratio of the residence time between the two systems can be calculated using Equation (3.23)[7]:

$$t = \frac{18\mu}{d^2\omega^2(\rho_s-\rho)}\ln(\frac{r}{r_1}) \qquad \text{(3.23 - repeated)}$$

As mentioned in Chapter 3, t is the time that it takes a particle with diameter d to move from an initial radius of r_1 to a radius of r. The filtering centrifuge that was planned to be used at the OSTRF plant had an adjustable electric motor with a nominal angular velocity of 1750 rpm and a perforated drum with an internal diameter of 60cm and a height of 40cm. If a maximum slurry volume of 20 liters is introduced into the batch filtering centrifuge, the average thickness of the slurry on the filter cloth can be calculated as:

$H0)_1 = 20000/(\pi \times 60 \times 40) = 2.65\ cm$

For a particle with diameter d to move from surface of the slurry to the surface of the filter cloth, in Equation 3.23 parameters r, r_1 and ω will be equal to 30cm, 27.35cm (= 30 – 2.65) and 1750rpm accordingly. On the other hand, the thickness of the settling column (i.e. the tube height) in the bench-top centrifuge tests is 10cm and the distance between the center of rotation and center of sample is 19.2cm. Therefore parameters r and r_1 for this system will be equal to 24.2cm and 14.2cm (=19.2 ± 5). It is desired to run the bench-top centrifuge tests at a spinning velocity that the residence times required to obtain a certain solids content can be directly used for prediction of the residence times in the filtering centrifuge. Inserting the known parameters of the bench-top and the filtering centrifuge in the above equation and equating the residence time of both systems will result in the required spinning velocity of the bench-top centrifuge:

$$\frac{18\mu}{d^2\omega^2(\rho_s-\rho)}\ln\left(\frac{24.2}{14.2}\right) = \frac{18\mu}{d^2(1750)^2(\rho_s-\rho)}\ln\left(\frac{30}{27.35}\right)$$

$\omega = 4176.9$ rpm

[7] The time scaling between the two systems can also be calculated using the Peclet number, as discussed by Theriault et al. (1995) and Eckert et al. (1996).

Centrifugation Time	*t = 8 min*	*t = 16 min*	*t = 24 min*	*t = 32 min*	*t = 40 min*	*t = 48 min*
Suncor MFT SC = 27.6% No Additive RCF = 3700g						
Suncor MFT SC = 27.6% 600 ppm Gypsum RCF = 3700g		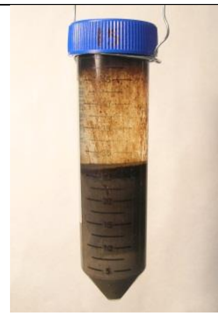				

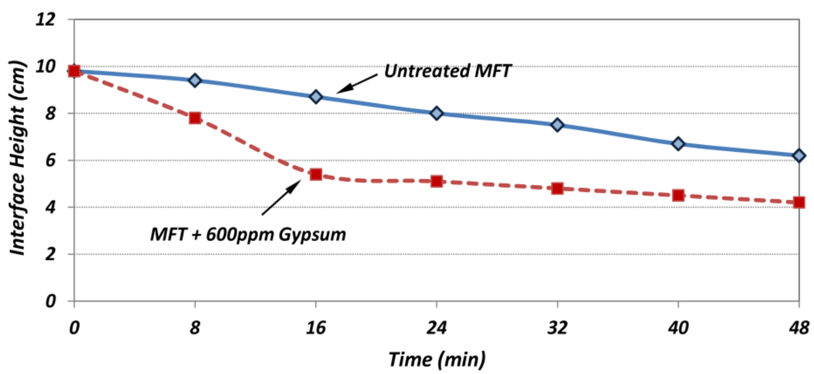

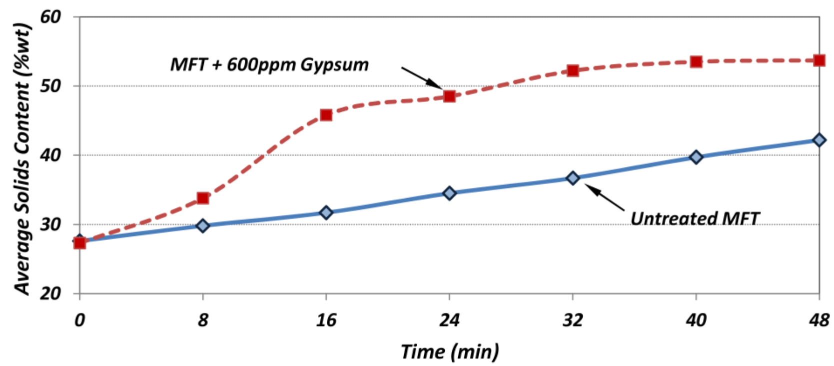

Figure 4.15. Comparison of the dewatering rate for untreated and treated MFT during centrifugal sedimentation.

As stated in section 4.4, the maximum spinning velocity of the bench-top centrifuge was limited to 4150 rpm (RCF = 3700g), which is slightly lower than the above value. It is expected that when the bench-top centrifuge tests are conducted at this spinning velocity, the observed residence times can be directly used as an upper limit for the plant filtering centrifuge tests.

As an example, the bench-top test results presented in Figure 4.15 indicate when the Suncor MFT sample is treated with 600ppm gypsum, a residence time of about 15 min in the batch filtering centrifuge (spinning at 1750rpm) should increase the average solids content to about 45%. While the results in Figure 4.15 indicate that centrifuging this treated MFT more than 30 min will not enhance the solids content significantly, in a filtering centrifuge longer residence times will create a cake with higher solids content. The remaining water will pass through the cake and the filter cloth, creating a drier cake (see Figures 3.20 and 3.21).

4.4.2.3 Using bench-top centrifuge tests to evaluate the coagulants/flocculants

Bench-top centrifugal sedimentation tests are a useful tool for pre-screening the chemical additives (coagulants/flocculants) that are to be used for treatment of the tailings in larger scale centrifugation applications. The testing procedure used in the present research [to study the effect of chemical additives on dewatering characteristics of MFT] can be summarized as following:

- The tailings sample at its as-received solids content was treated with the coagulant/flocculant at a range of dosages[8].
- For each dosage an even number of 50ml centrifuge tubes, as explained in section 4.4.2.1, were filled with the treated sample and were spun using the centrifuge. The initial test duration and spinning velocity should be estimated according to the operation conditions planned for the larger scale centrifugation trials at the plant/field.

[8] In the present research the selected gypsum dosages were aimed to be lower than the industry experience. Making a decision about dosage of a new coagulant/flocculant must be based on the chemical characterization of the slurry, its clay content and zeta potential measurements.

- At specific time intervals during the centrifugation, a couple of centrifuge tubes were removed from the centrifuge and the position of supernatant-suspension interface was recorded. The clarity of the supernatant was examined and the dewatered slurry was sampled. As illustrated in Figure 4.16, all or part of the dewatered material may be in the form of a fluid slurry, or in the form of a semi-solid cake. Records (1977) points out that the state of the dewatered material determines the method of discharge in the large scale centrifuge operations: if the dewatered solids are sufficiently cohesive, scrolling mechanism may be utilized; and if the dewatered solids are sufficiently fluid, skimming may be used.
- The amount of fines still remaining in the form of a suspension was determined. This amount was subtracted from the total fines in the sample to calculate the percentage of fines captured in the cake. A coagulant/flocculant is suitable when, in addition to enhancing the dewatering rate, it results in a clear centrate and a cake in which the majority of the fines are captured.
- Based on the results obtained, the test conditions (spinning duration and velocity, dosage of the chemical additive, and initial solids content of the slurry) may be adjusted and the above test procedure is repeated to determine the optimum dosage.

It should be noted that some coagulants/flocculants result in better flocculation of the fines when the slurry is diluted to lower solids contents. The water used for dilution of the samples must be similar to what is planned for field operations. If the process affected water is to be used, an alternative in the lab operations would be the water decanted from the tailings container or the water extracted from larger volumes of tailings in bench-top bottle centrifuge tests.

Section 5.6 in Chapter 5 provides the detailed results of some bench-top centrifuge tests conducted to evaluate the performance of an anionic flocculant versus gypsum.

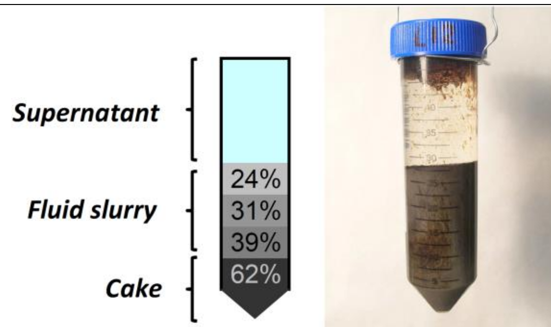

Figure 4.16. The solids content profile for a sample of Suncor MFT treated with 600ppm Gypsum and spun at RCF of 2850 g for 30 minutes. The average solids content of the dewatered part (slurry and cake) is about 41.5%.

4.4.2.4 Using bench-top centrifuge tests to produce MFT with high concentration

A previous study by Theriault et al. (1995) showed that although different physical and chemical treatment methods affect the rate of sedimentation of the fine tailings in a centrifuge, the ultimate volume fraction of the solids at the end of centrifugation was about 0.3, equal to about 50 to 55%wt. In the present research similar observations were made: when the filtrate was clear (i.e. when no segregation occurred and more than 99% of the fines were captured within the cake) the maximum solids content of the cake did not exceed 55%. The test results in Figure 4.15 indicate that after the solids content of the chemically treated Suncor MFT reaches to about 53%wt, the changes in concentration of the cake are very slow.

Based on the above observations, to produce MFT with high solids content the 650ml bottles illustrated in Figure 4.17 were filled with raw (untreated) MFT and then were centrifuged at 4150 rpm (RCF=3700g) for 2 hours. This procedure ensured obtaining a minimum solids content of 53% or higher. The centrifugation resulted a clear supernatant sitting on top of a dense cake of MFT. This clear water was decanted into a jar and was stored for future adjustments of the cake solids content or for preparation of CT/NST, as will be discussed in section 4.5.

Figure 4.17.b shows the MFT cake that was removed from the centrifuge bottle at the end of the test, having an average solids content of 53.7%. Upon removal the cake looked like a thick paste, showing a steep angle of repose on the spoon. After mixing this cake using a small dual-blade mixer, it flew as a thick fluid, indicating the effect of shear on

reducing the yield stress of the material (Figure 4.17.c). This dewatered MFT was used as a component for making high solids content CT with and without chemical treatment.

(a)	(b)	(c)

Figure 4.17. Using bench-to centrifuge to produce MFT at higher solids content: (a) The decanted 650ml centrifuge bottle including the cake; (b) The un-sheared cake sample at 53.7% solids content; (c) Appearance of the cake after being mixed by a dual blade mixer.

4.5. Making NST from Centrifuged MFT

The cake obtained from centrifuging the untreated MFT showed segregation: the silt-sized coarser fraction had settled to the bottom of the centrifuge bottle and the finer particles were on top of the coarse fraction, closer to the center of rotation. Prior to using the cake for making NST samples, it was thoroughly mixed and its solids content and SFR were determined. [Since part of the fines may not be captured in the cake, its SFR can be higher than the source MFT.] The required amount of each component for making NST (i.e. Sand, MFT Cake and Pond Water) was calculated using the multiphase mass-volume relationships developed by Scott (2003) and Boratynec (2003). An example group of diagrams resulted from parametric solution of these relationships were previously shown in Figure 4.1.

Table 4.2 presents the solids content of four example CT/NST samples made from regular/centrifuged MFT, along with concentration of the source MFT/Cake and dosage of the gypsum used. The MFT and sand utilized for making these samples was received from Suncor operations and SFR of all the samples was approximately 4:1.

Table 4.2 - CT/NST samples made from regular/centrifuged MFT (SFR=4)

Sample ID	MFT/Cake Solids Content (%)	Gypsum (PPM)	CT/NST Solids Content (%)	Small Flume Test	
				Average Slope (%)	Runout Length (cm)
CT-1	25.18 (MFT)	900	62.78	2.1	82.3
NST-1	49.44 (Cake)	900	63.14	2.4	73.3
NST-2	52.25 (Cake)	300	67.47	2.7	70.9
NST-3	53.17 (Cake)	No Gypsum	69.27	3.1	66.7

In Table 4.2 sample CT-1 was made from regular MFT and relatively dry sand, and sample NST-1 was produced by mixing centrifuged MFT and sand-water mixture at 68% solids content (i.e. simulated cyclone underflow). The solids concentration of both CT-1 and NST-1 was about 63%. The objective of making these two samples at the same solids content, but using a different method of production, was to compare their flow and dewatering characteristics. In Table 4.2 samples NST-2 and NST-3 were made from centrifuged cake and simulated cyclone underflow, one with 300ppm gypsum and the other without any chemical additive. These two samples are examples of the high solids content NST that cannot be produced at normal field operations.

A small flume device was used to compare the angle of repose of these samples after deposition. As illustrated in Figure 4.18, the flume previously used for the tests in Section 4.3.2.2 was modified by adding a reservoir (wooden box in Figure 4.18) and a sliding gate separating it from the flume. The CT/NST sample was placed in the reservoir and then the gate was opened to allow discharge of the material. The average angle of repose and final runout length of each deposited sample are presented in Table 4.2. The exceptionally high angles of repose observed in these tests were due to the small width of the flume (5.1cm or 2”) and the boundary effect of the side walls. As will be explained in Chapter 6, later a larger flume with an internal width of 18cm was built to reduce the effect of the side walls[9]. Sections 6.3 and 6.4 provide a detailed review of the larger scale flume tests and the procedure for sampling, characterization and analysis of the deposited material along the flume.

[9] Section 6.3 provides a description of the common types of laboratory flume tests used to study the beach slope of segregating and non-segregating tailings, along with a summary of the recent studies conducted by Fourie and Gawu (2010) on the effect of flume width.

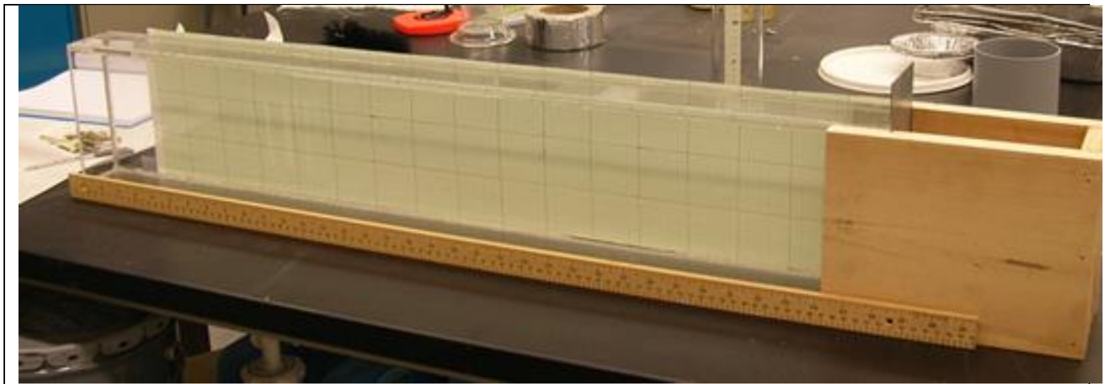

Figure 4.18. The small flume device used for the preliminary deposition tests (106.7 cm long, 5.1 cm wide and 15.2 cm high)

4.5.1. Comparison of the flow and dewatering characteristics of the CT/NST samples

The flume test results presented in Table 4.2 indicate that the solids content increase in samples NST-1 to 3 has resulted a higher angle of repose and a shorter runout length. Figures 4.19.a and b illustrate the flow profiles for samples CT-1 and NST-1. While both samples have almost the same solids content, it can be seen that NST-1 (made from centrifuged MFT) shows a steeper average slope and a shorter runout length.

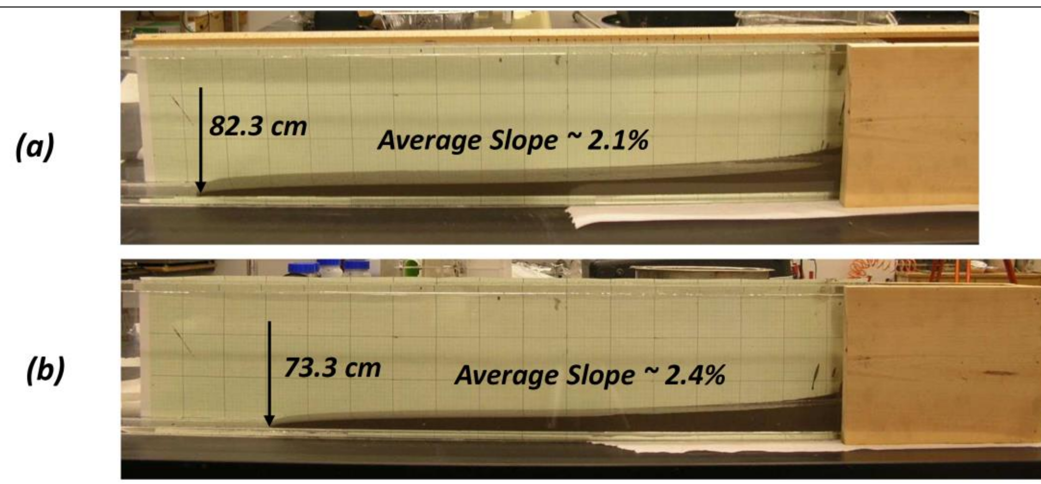

Figure 4.19. Comparison of the flow profile for samples CT-1 (a) and NST-1 (b).

To compare the dewatering rate of CT/NST samples presented in Table 4.2, standpipe sedimentation tests were conducted. The initial height of all samples was about 35cm. Figure 4.20 shows comparison of the settling rate of the CT/NST samples. The results

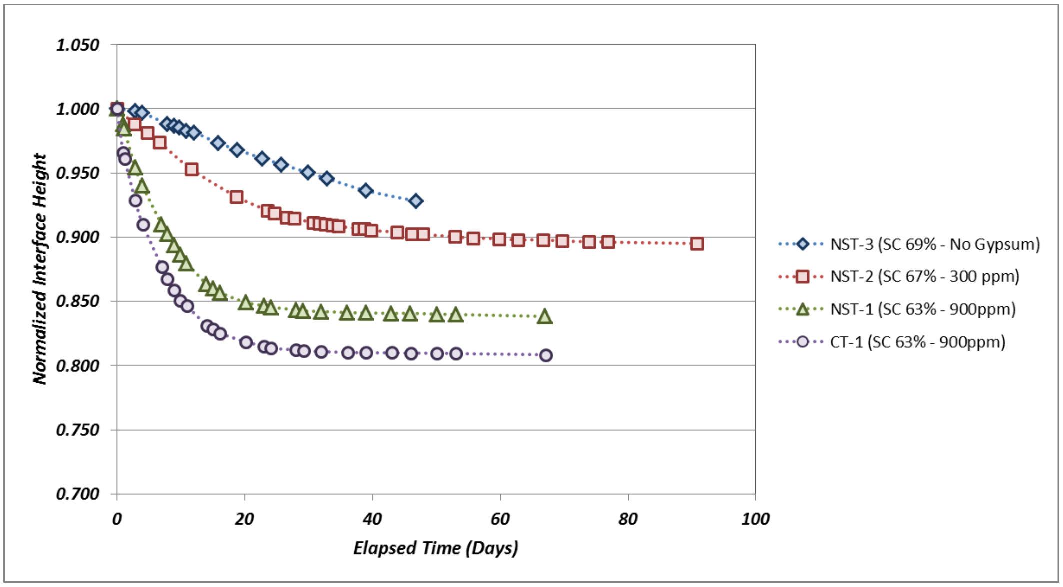

Figure 4.20 – Interface settlement versus elapsed time for CT/NST with varying initial solids content.

indicate that as the solids concentration of the slurry increases, the rate of dewatering during hindered sedimentation (slope of the linear part of the diagram) decreases. This is in agreement with the Kynch theory (1952) and the observations published by McRoberts and Nixon (1976), Been and Sills (1981) and Imai (1981). An unexpected observation made during the sedimentation tests was the different settling velocity of CT-1 and NST-1 samples. As can be seen in Figure 4.20, while both samples approximately have the same solids content, sample NST-1 that was made from centrifuged MFT showed a slower settling rate. To investigate the possible cause for this difference, two other sedimentation tests were conducted: in one test the as-received MFT, which had been used for making CT-1, was diluted to about 10% solids content and the resultant suspension was placed in a standpipe to conduct the sedimentation test. In the second test, the centrifuged cake used for making NST-1 was diluted to about 10% and a similar sedimentation test was repeated. In both cases, the centrate obtained from centrifugation of the same MFT was used for dilution and the similar mixing time and energy were used to prepare the suspension. Figure 4.21 illustrates the comparison of these two sedimentation tests. As can be observed, the suspension obtained from the centrifuge cake shows a slower settling velocity, although eventually after about 130 days both samples reach to the same solids concentration (~28.9%). These tests indicate that centrifugation of MFT (at relatively high RCF values) and consequent dilution and mixing of the cake would results in a suspension with different dewatering characteristics from the original material. Crushing of the solid particles and changes in PSD of the suspension does not seem possible at this level of centrifugal forces (Mikula, 2008; Hollander, 2012 – Personal Communication). Further investigation about the possible causes for this change in dewatering behavior was beyond the scope of this study, but should be an interesting topic for future investigations.

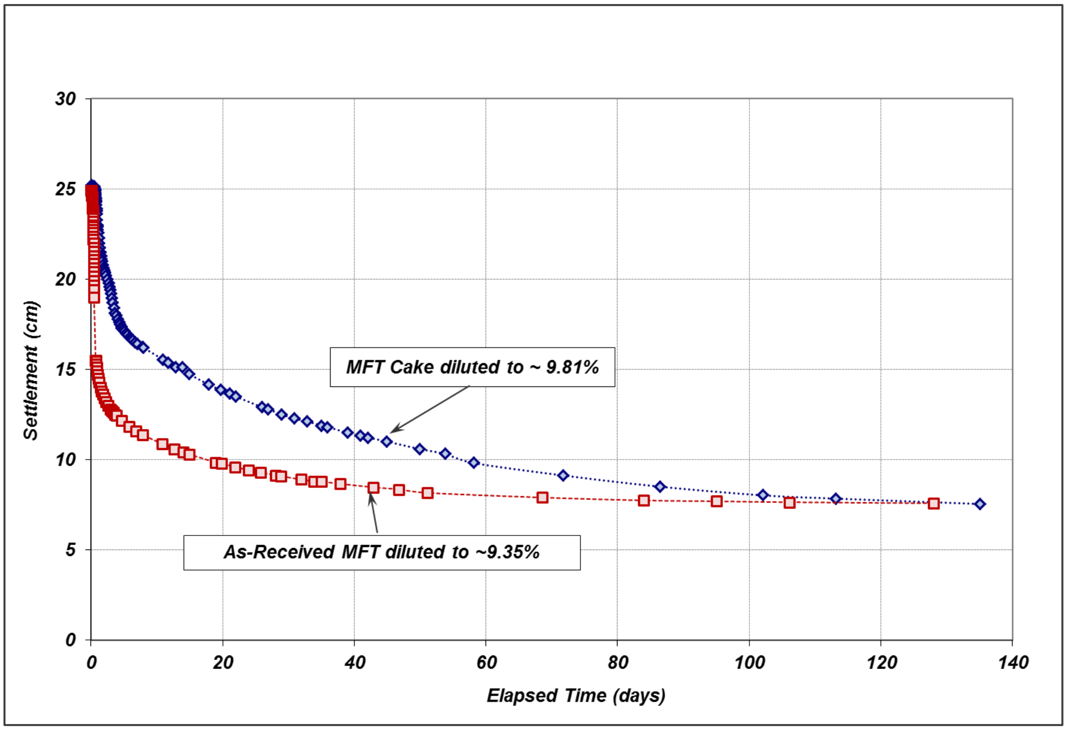

Figure 4.21 – Comparison of the settling rate for as-received MFT and centrifuge cake when both are diluted to about 10% solids content.

4.6. Yield Stress Measurement

Yield stress of a solid-liquid mixture can be defined as the minimum stress required to initiate irreversible deformation and flow of the material (Roussel and Coussot, 2005). Knowledge of this parameter is essential in engineering design and operation of the dewatered tailings systems as it affects the transportation energy and the land footprint required for disposal of the tailings (Pashias et al., 1996; Gawu and Fourie, 2004).

In the this section two methods for measurement of yield stress that were utilized in the present research will be explained: the vane method, which provides accurate results in the lab conditions and the slump method, which offers a quick approach for approximate evaluation of the slurry consistency at field operations. The results of some vane and slump tests conducted on CT/NST samples and their comparison will be provided at the end of this section.

4.6.1. The Vane Method

4.6.1.1 Background and theory

In geotechnical investigations, the field vane shear test is a common method to evaluate the in-situ undrained shear strength of very soft, fine grained soil deposits. This method also has considerable application in offshore soil exploration. The vane shear apparatus used for field investigations is made of four blades welded to a cylindrical shaft (Figure 4.22). To conduct the test, the vane apparatus is inserted into the soil stratum and the torque is applied to shear the soil around the perimeter of the vane. Usually a suitable gearing device is used to achieve a rate of 6^o of rotation per minute. The ASTM standard for the field vane test is D2573 and specifies a height to diameter ratio of 2 (Figure 4.22) for the vane (Bowles, 1997).

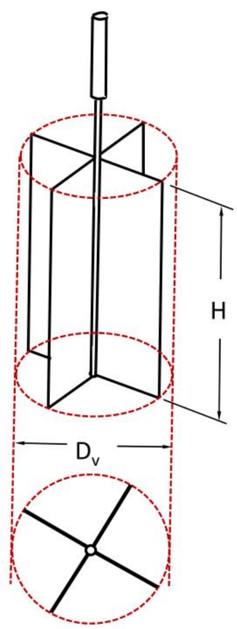

Figure 4.22 - Schematic view of the vane (modified from Nguyen and Boger, 1983).

Nguyen and Boger (1983) listed a number of different techniques/apparatus that can be used for measurement of yield stress of highly concentrated suspensions. They indicated that the success of each technique would depend on the capability of the test material to show well-defined yielding under a selected experimental condition. They introduced a new method of yield stress measurement based on the vane test developed in soil mechanics (Nguyen and Boger, 1983). As stated by Gawu and Fourie (2004), there is an emerging consensus that the vane method offers an accurate and reliable option for measurement of the yield stress in concentrated solid-liquid mixtures.

Nguyen and Boger (1983, 1985) consider the vane method superior to other direct methods of yield stress measurement, since it is quick and simple and provides reproducible results even at low or high slurry concentrations. They state that special geometry of the vane allows the material to yield under static conditions and within the material itself; also introduction of the vane blade into the suspension causes minimum disturbance to the sample. This is particularly important when thixotropic materials, that are sensitive to past shear history, are to be tested. These researchers indicated that achieving satisfactory yield stress measurements would be possible only if the vane was rotated at low rotational speeds (lower than 8 rpm). At higher rotational speeds, significant viscous resistance together with instrument inertia and insufficient damping were identified as sources of error in measurement of the maximum torque and the calculated yield stress. To minimize any unforeseen errors they carried out all their vane measurements at the lowest possible speed of 0.1 rpm (Nguyen and Boger, 1983, 1985).

When the vane test is conducted at a fixed rate of rotation, the torque-time curve [for yield stress slurries] would show a definite peak after a linear elastic deformation region (Nguyen & Boger, 1992). Figure 4.23 illustrates an example of variations of torque versus time during a vane test conducted on a CT sample in the present study. [The shear stress is calculated based on the torque measurements and the vane geometry, as explained below]. In Figure 4.23, point “A” indicates the observed peak in torque and point “B” shows the end of linear region of the diagram. According to Nguyen and Boger (1992), a group of researchers suggest that point “A” corresponds to complete breakdown of the fluid structure and therefore should be considered for calculation of the yield stress. The experimental data in other studies however, as stated by Nguyen and Boger (1992), showed that the peak value is a function of the applied shear rate and that yielding actually starts at point “B” where the torque-time (or stress-strain) curve is no longer linear. Practically, however, the peak torque would be easier to detect, and if the

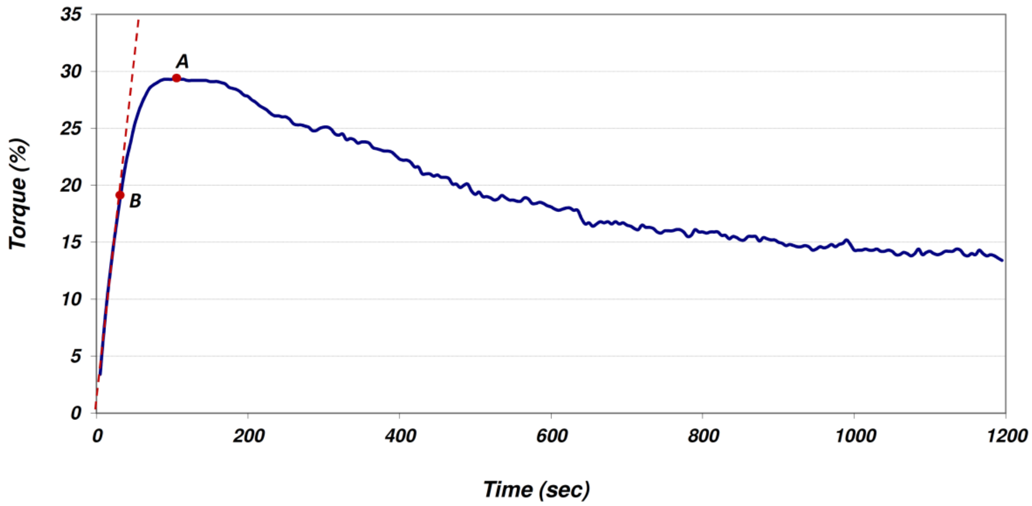

Figure 4.23 – Variations of the measured torque with time during a vane test conducted on a CT sample. The torque is expressed as percentage of the maximum capacity of the viscometer. The CT sample had a solids content of 66.9% and an SFR of 4. The vane spindle used was V-73. The calculated yield stress from point A (peak value) is 28.3 Pa and the maximum elastic stress calculated from point B is 19.7 Pa.

applied shear rate is sufficiently low to minimize the viscous effects, the shear stress calculated from the peak torque should be a reasonable measure of the yield value (Vinogradov and Malkin, 1980 cited by Nguyen and Boger, 1992). In section 6.4.5, the peak and maximum elastic stress values are compared for a number of CT/NST samples and it is explained that, for practical reasons, the peak value is considered as yield stress.

To calculate the yield stress from the maximum torque, the yield surface and the shear stress distribution around the vane blades must be known. The common approach in soil mechanics assumes that the material yields along a localized cylindrical surface defined by the vane dimensions (Figure 4.22). The total torque is therefore composed of three components: one due to the shearing on the cylindrical wall and the other two due to shearing at the two end surfaces (Nguyen and Boger, 1983):

$$T = (2\pi R_v H)\tau_w R_v + 2\left[2\pi \int_0^{R_v} \tau_e(r) r dr . r\right] \tag{4.1}$$

where T is the measured torque, H and R_v ($=D_v/2$) are length and radius of the vane, respectively; τ_w is the shear stress at the cylindrical wall, and τ_e is the shear stress distribution along the two flat circular end surfaces, which is a function of r (radial position).

Nguyen and Boger (1985) demonstrated that for vanes with $\left(\frac{H}{D_v}\right) \geq 2$, τ_e can be assumed constant (i.e. uniformly distributed over both end surfaces) and equal to τ_y (yield stress) at the yield point. As a result Equation (4.1) reduces to the following simple formula, allowing τ_y to be calculated directly from T_m (maximum torque) and the vane dimensions:

$$T_m = \frac{\pi D_v^3}{2}\left(\frac{H}{D_v} + \frac{1}{3}\right)\tau_y \qquad (4.2)$$

4.6.1.2 Vane apparatus in the present study

In the present research, a strain controlled viscometer (Brookfield Digital Viscometer - Model DV-II+) with vane spindles was used to measure yield strength of CT/NST and dewatered MFT samples. Figures 4.24.a and 4.24.b illustrate the test setup and the vane spindles utilized. As shown in Figure 4.24.a, the slurry sample was placed in a 600ml beaker[10] and the vane spindle (connected to the viscometer) was slowly lowered into the slurry by adjusting the position of the viscometer on a vertical stand. When the groove mark on the shaft of the spindle reached the surface of the slurry, the position of the viscometer was fixed and the test was started by running the vane at the rotational speed of 0.1 rpm. The viscometer measures the toque required to rotate the immersed vane spindle in the suspension. A motor drives the spindle through a calibrated spring and the spring deflection is indicated by a digital display (Brookfield Engineering Labs., Manual No. 1056-1014 10M 12/05). At the same time, the torque measurements and the time of records were sent to a computer connected to the viscometer via RS232 ports. The Microsoft Windows HyperTerminal Communication Program was used for data acquisition.

The resistance to flow (or the viscous drag) at any given viscosity is proportional to the size and rotational velocity of the spindle. As indicated in Figure 4.24.b, larger spindles are used for measurement of lower yield stress/viscosity values and smaller spindles are utilized for measurement of larger yield stress/viscosity values (Brookfield Engineering Labs., Manual No. 1056-1014 10M 12/05). Table 4.3 presents the dimensions and the

[10] To minimize the boundary effects, the diameter of the container and the depth of the suspension should be at least twice as large as the diameter and length of the vane spindle (Nguyen and Boger, 1983).

Figure 4.24.a. Test setup used for yield strength measurement of NST and MFT samples, comprised of the programmable Brookfield Viscometer with a vane spindle, and a computer to record the device readings.

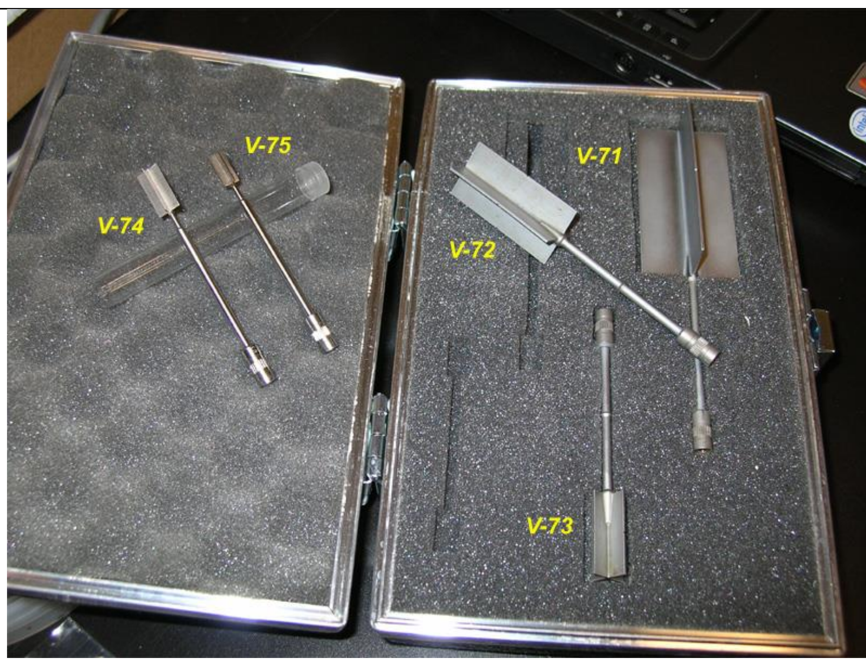

Figure 4.24.b. Vane spindles V-71 to V-75 used for measurement of the yield strength. Spindles with larger blades (e.g. V-71) are used for less viscous materials and spindles with smaller blades are used for more viscous materials.

Table 4.3 – Dimensions and shear stress range of vane spindles V-71 to V-75

Spindle	Vane Length (H) (cm)	Vane Diameter (D) (cm)	H/D	Shear stress range (Pa)
V-71	6.878	3.439	2.0	0.5 - 5
V-72	4.338	2.167	2.0	2 - 20
V-73	2.535	1.267	2.0	10 - 100
V-74	1.176	0.589	2.0	100 - 1000
V-75	1.61	0.803	2.0	40 - 400

shear stress range that can be measured by each spindle. Operating instructions for this type of viscometer are available in the Brookfield Engineering in Manual No. M/97-164-D1000. Mihiretu (2009) provided detailed description of conducting viscosity measurements on slurry mixtures of kaolinite (d_{50} ~< 1 μm), rock flour (d_{50} ~16 μm) and sand (d_{50} ~ 200 μm), also on MFT samples using this viscometer.

4.6.2. Slump Test

The slump test was originally introduced as a rapid and simple method to determine the "workability" of fresh concrete. Murata (1984) devised an analytical model to predict the yield stress of fresh concrete from conical slump tests. Rajani and Morgenstern (1991) proposed using this model and the conical slump test for determination of the yield strength for debris and other materials that behave like a Bingham fluid. Pashias et al. (1996) adapted the model presented by Murata (1984) for prediction of yield strength from cylindrical slump tests. Roussel and Coussot (2005) extended the theoretical analysis of this test by proposing analytical solutions of the flow for two asymptotic flow regimes. In the following section, details of the slump test method and the equations derived by Pashias et al. (1996) and by Rousset and Coussot (2005) for estimation of the yield stress from this test will be explained.

As illustrated in Figure 4.25, to conduct the slump test initially a cylindrical frustum (e.g. PVC pipe) with a height to diameter ratio of one (i.e. height = diameter = 76mm) was placed on a flat surface and the CT/NST sample was poured in it slowly to prevent entrapment of air bubbles. Then the cylinder was lifted off allowing the material to collapse under its weight and form a symmetrical flow. The final height and diameter of the deposited material were measured (Figure 4.25.c). The difference between the initial

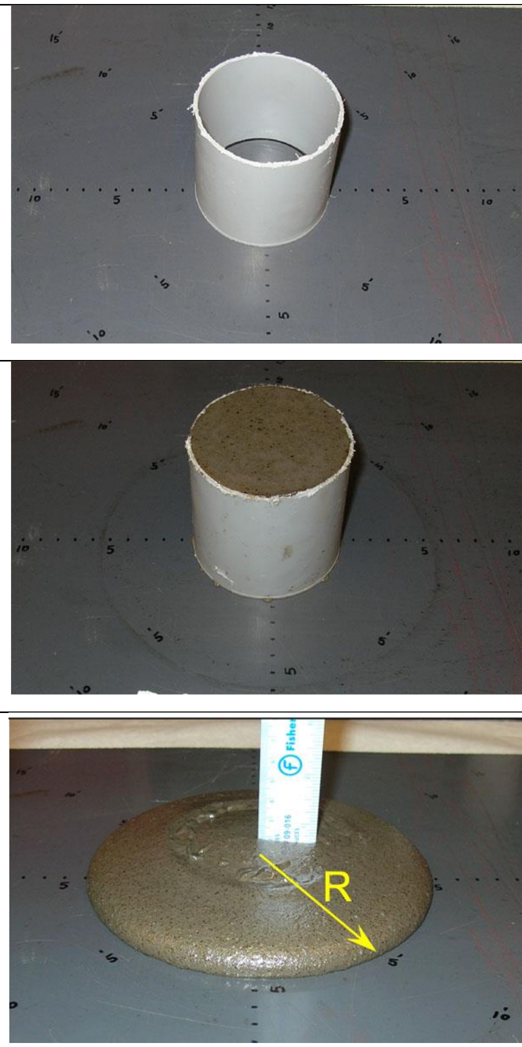

Figure 4.25. Cylindrical slump test for NST samples.

and final heights is referred to as the slump height (S). The final diameter of the collapsed sample is known as "spread" (Roussel and Coussot, 2005).

Pashias et al. (1996) defined the scaled (dimensionless) values of slump and yield stress as following:

$$S' = \frac{S}{H} \tag{4.3}$$

$$\tau'_y = \frac{\tau_y}{\rho g H} \tag{4.4}$$

where S is the slump height, H is the initial height of the sample in the cylindrical frustum, τ_y is the yield stress, ρ is the slurry density and g is the gravity acceleration. They showed that the correlation between the scaled slump height (S') and the yield stress would be (Pashias et al., 1996):

$$S' = 1 - 2\tau'_y\left[1 - \ln(2\tau'_y)\right] \tag{4.5}$$

Roussel and Coussot (2005) stated that for large slumps the above approach does not apply and the spread would be a more relevant parameter for evaluation of the material yield stress. They considered two flow regimes based on the ratio of the final height and radius of the slumped material:

(a) Pure shear flow, where the radius of the slumped material (*R*) is higher that its height (*H*) and the lubrication theory conditions are valid (see section 6.4.6). They provided the following correlation between the yield stress (τ_y), volume (Ω) and spreading distance (*R*) of the slumped material (Roussel and Coussot, 2005):

$$\tau_c = \frac{225 \rho g \Omega^2}{128 \pi^2 R^5} \tag{4.6}$$

(b) Pure elongational flow, where they considered the radius of the cylinder (R) was much smaller than its height (h) and assumed the stress variations in the radial direction were negligible. They obtained the following equation between the dimensionless (scaled) yield stress and slump (Roussel and Coussot, 2005):

$$\tau' = \frac{(1-S')}{\sqrt{3}} \qquad (4.7)$$

The second flow regime (pure elongational flow) was used by these researchers to describe intermediate cases where $R \approx H$ (Roussel and Coussot, 2005).

4.6.3. Vane and Slump test results for CT/NST samples

To investigate capability of the cylindrical slump test for evaluation of the yield strength of CT/NST, a number of CT samples with varying solids contents (ranging from ~61%wt to ~76%wt) and a SFR equal to 4.0 were prepared (Table 4.4). All the samples were made from the same source MFT (received from Albian Sands) and the amount of gypsum used for making them was 600ppm. Following the procedures explained in the previous sections, both the vane shear test and the slump test were conducted for each sample and the results were compared. Table 4.4 presents the solids content of each CT sample along with its yield stress evaluations obtained from the vane and slump tests. For the slump test, two yield stress values are presented; one was calculated using Equation (4.5) (Pashias et al., 1996) and the other one was calculated from Equation (4.6) (Roussel and Coussot, 2005). The reason for using Equation (4.6) was the high ratio of spread to thickness of the slumped samples.

Table 4.4- The slump and vane test results for a number of CT samples (SFR = 4).

CT Solids Content	Density	Thickness of the Slumped Sample	Diameter of the Slumped Sample	Slump Height : S	τ_y		
					Estimated from Slump (Pashias et al.) (Equation 4-5)	Estimated from Slump (Roussel & Coussot) (Equation 4-6)	Measured by Vane
(%)	(kg/m^3)	(mm)	(mm)	(mm)	(Pa)		
61.54	1621.2	3.2	420	72.8	4.2	0.8	9.2
64.57	1672.4	4.5	378	71.5	6.9	1.4	15.0
68.06	1735.4	7	338	69	12.3	2.6	24.6
70.25	1777.5	8	310	68	13.9	4.1	36.0
72.24	1817.5	15	242	61	33.2	14.5	56.9
75.26	1881.8	19	182.5	57	47.7	61.8	109.2
75.75	1892.7	21	169	55	55.0	91.2	145.1

The diagrams in Figure 4.26 show the variations of shear stress versus time for the vane tests conducted on the CT samples. From these diagrams it can be observed:

- As the solids content of the samples increases, the initial peak shear stress (i.e. yield stress) and also the slope of the elastic part of the diagrams increase. In other words, the CT samples with lower water content show higher yield stress and elastic modulus of deformation.
- When the shear stress reaches to its initial peak value (yield stress), the network bonds in the region of CT close to the edges of the vane blades break and a rapid falloff in shear stress happens (Nguyen and Boger, 1983). However, after a while a gradual increase in the shear strength can be observed; this is more significant for the CT samples with lower solids content. While part of this strength gain may be attributed to the thixotropic behavior of the carrier fluid (i.e. fines + water + gypsum), the author's hypothesis is that settlement of the sand-fines network and increase of the concentration at the level of the vane blade also contributes to the strength gain. For CT samples with lower solids content (e.g. CT with the initial solids content of 68.06% in Figure 4.26), the shear strength reaches to values higher than the initial peak. For CT samples with higher solids content (e.g. CT with 75.45% SC in Figure 4.26) however, this strength gain is limited since the material is already close to the sand matrix region on the ternary diagram. This is probably the cause for the fluctuations observed in the shear strength diagrams for the CT samples with higher solids contents (due to interaction of the sand particles), a behaviour that cannot be observed for CT samples with lower solids content.
- From the above discussion, it can be concluded a vane test on CT samples (particularly with lower solids content) must be conducted with minimum delay to prevent error in the results due to sedimentation.

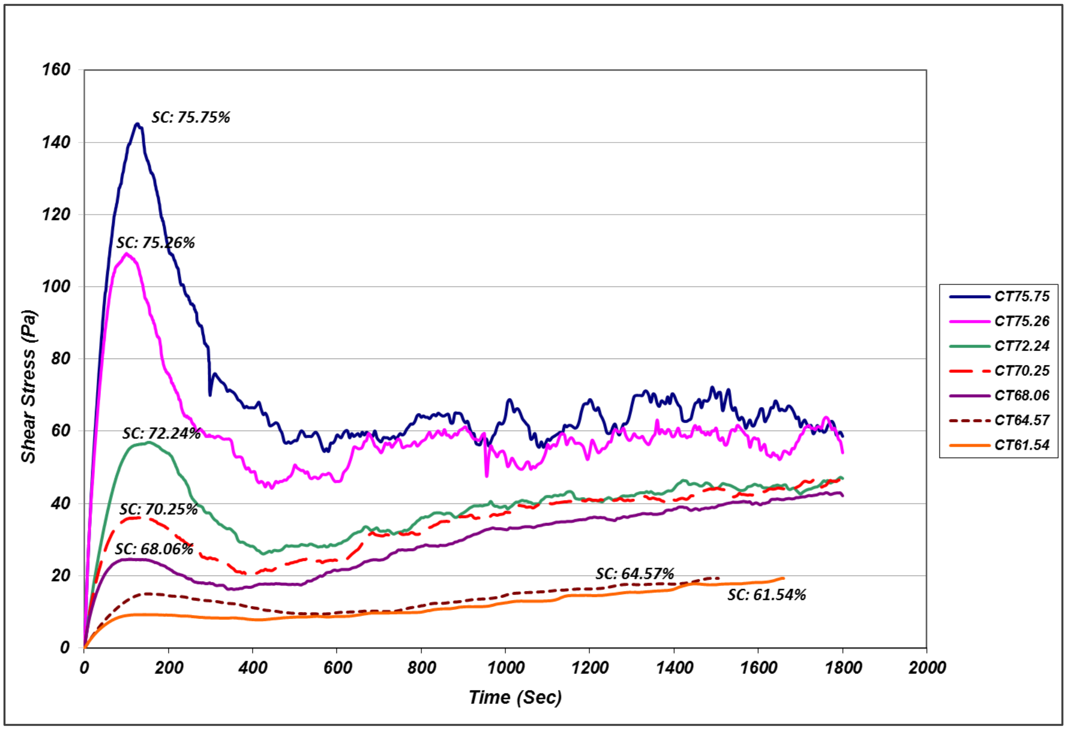

Figure 4.26. Diagrams of shear stress readings recorded during vane shear tests on seven CT samples with varying solids content and similar SFR.

In Figure 4.27, the yield stress values measured by the vane and estimated from the slump tests are plotted with regard to the solids content of the material. The diagrams shown for all three data sets indicate that shear strength of the CT can be expressed as an exponential function of its consistency. Except for the two CT samples with the highest solids content, method of Roussel and Coussot (2005) has the lowest yield stress values in comparison to the other two methods. Comparison of the trend-lines illustrated for the slump method of Pashias et al. and the vane method indicate that the two exponential functions are similar, with varying coefficients. Also Figure 4.28 shows that for vane method and the slump method of Pashias et al. a linear correlation exists between the yield stress values and the average slope (thickness to radius) of the slumped cone.

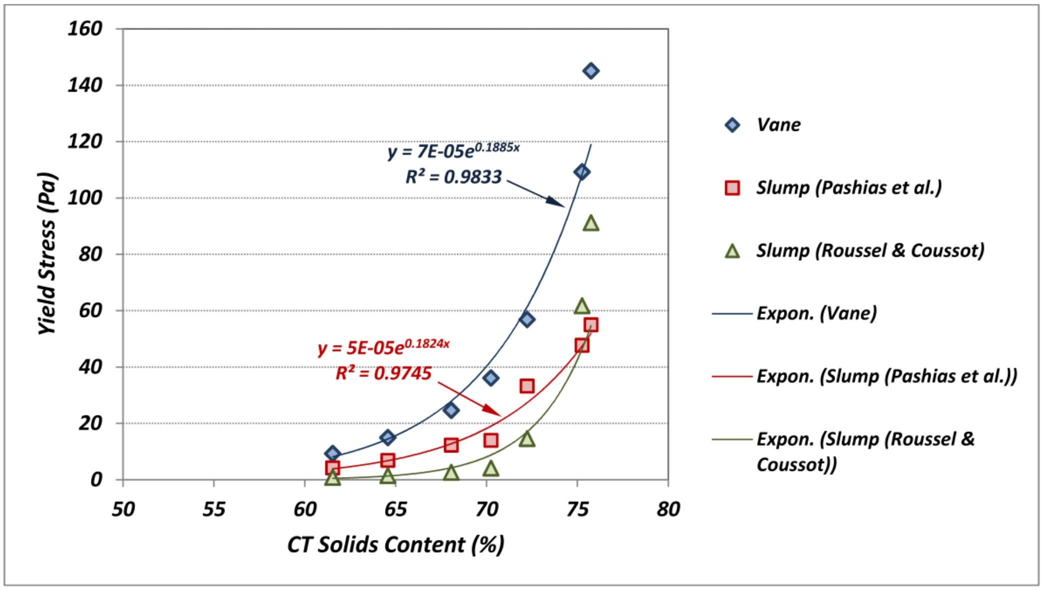

Figure 4.27. Variations of the yield stress with solids content of the CT samples.

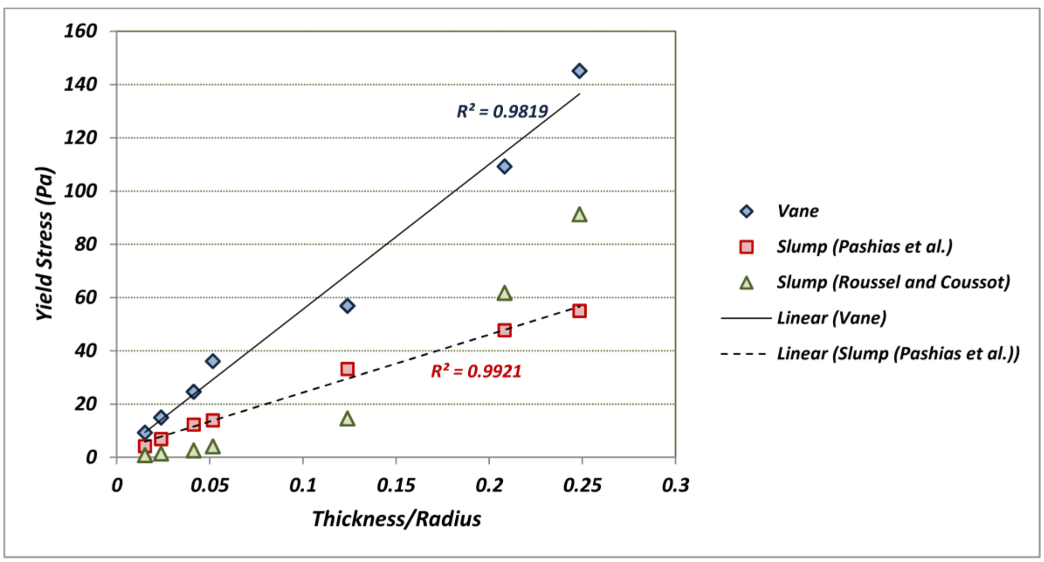

Figure 4.28. Linear correlation observed between the vane and slump test results and the average slope (i.e. thickness to radius) of the slumped CT/NST.

From the above discussion it can be concluded that the slump test is a useful tool for comparison of the consistency of the CT/NST samples taken at field operations, however the vane test should also be conducted on a representative range of solid concentrations to provide a reference data set. It is worthy to note that in a discussion paper by Crowder and Grabinsky (2005), the results of vane and modified slump tests for gold mine tailings were compared. The slump test results were consistently lower than the vane test result for yield stresses up to 200 Pa, and beyond this value the slump test results were significantly higher than the vane test results. While Crowder and Grabinsky (2005) agreed with the principle of using the slump test as an index property for frequent field measurements, they suggested that a vane test should also be used to verify the suitability of the slump test.

4.7. Summary

To have a robust CT/NST during the transportation stage, at discharge and after deposition, yield stress of the carrier fluid (i.e. fines + water) must be sufficient to support the sand particles and prevent their segregation. To obtain a carrier fluid with higher yield stress, the F/(F+W) ratio must be increased, in other words the water content of the slurry must be decreased. The possible approaches for reducing the water content of the CT/NST tailings streams are:

- Mixing the fine and coarse fractions to produce CT/NST and then dewatering the resultant mixture prior to deposition; and,
- Dewatering one or both of the CT/NST components (cyclone underflow and MFT) prior to mixing them together.

In this chapter a review of the laboratory tests conducted to explore each of the above approaches was presented. A series of laboratory experiments studying the dewatering of CT/NST in vessels with inclined walls and on inclined plates were briefly described. While CT showed accelerated dewatering in these test setups, this method of solid-liquid separation may be more practical for slurries with lower solids content (e.g. the cyclone overflow). Bench top bottle centrifuge tests were used to dewater MFT and the resultant cake was used as a component for making NST. Dewatering and flow characteristics of some example NST samples made from centrifuged MFT were reviewed. Also a procedure for pre-screening of the chemical additives by means of bench-top tube centrifuge tests was explained. In the last section of this chapter a detailed review of the vane and slump tests methods for measurement of the yield strength of mine tailings was presented. The laboratory scale filtering centrifuge tests will be presented as part of the next chapter.

Chapter 5

Centrifugal Filtration of MFT

5.1. Introduction[1]

Centrifugal filtration can be defined as a filtration method in which the driving force for solid-liquid separation is generated by gravitational forces in a centrifugal field. To study the capability of this method for dewatering MFT a batch filtering centrifuge was utilized in the present research. This device was designed and provided by a private industrial company. The filter cloth provided for this filtering centrifuge had a special coating on one side which facilitated removal of the cake. The batch filtering centrifuge tests were performed at the Oil Sands Tailings Research Facility (OSTRF) located in Devon, Alberta. Prior to conducting the batch filtering centrifuge tests, a number of laboratory tests were conducted to evaluate this method of dewatering. A filter-bucket test set-up was designed for this purpose.

The main objectives of the centrifugal filtration tests were:

- to study possibility of using centrifugal filtration for dewatering MFT and obtaining fine tailings with high solids content;
- to study the different factors that affect the dewatering process and the quality/quantity of the dewatered MFT; and,
- to produce sufficient volumes of thickened MFT to be used as a component for making CT/NST in the next stages of this research.

It should be noted that designing a filtering centrifuge and numerical simulation of centrifugal filtration of MFT are not covered in this study.

---

[1] Part of this chapter has been previously published: Moussavi Nik, R., Sego. D. C. and Morgenstern, N.R. (2008) "*Possibility of Using Centrifugal Filtration for Production of Non-Segregating Tailings*". Proceedings of the First International Oil Sands Tailings Conference, Edmonton, Alberta, Canada. Dec. 2008., pp. 200 – 208.

In centrifugal filtration of a slurry it is necessary to consider the simultaneous effect of sedimentation and filtration during the centrifugation process. Simple standpipe sedimentation tests or bottle centrifuge tests can provide information about the rate of settling of the solid-liquid interface. Also the common approach for determining the filtration rate in the pressure or vacuum filtration processes is using a Büchner funnel or a pressure filter cell (also known as C-P: Compression-Permeability Cell). But as it will be explained in the following, these are not the proper tools to study the solid-liquid separation in a filtering centrifuge.

As explained in section 3.4.2, the average filtration resistance is proportional to the mass of dry solids (cake) deposited on the unit area of the filter. While in the ordinary pressure or vacuum filtration the cake formation is due to the pressure difference across the filter cloth, in the centrifugal filtration there is an additional cake formation due to the sedimentation that has to be considered in calculation of the filtration resistance. In pressure or vacuum filtration it is customary to calculate the mass of cake from the material balance involving only the filtrate volume. Following the same procedure in centrifugal filtration leads to serious errors in calculations (Sambuichi et al., 1987).

One method of evaluating the filtration rate of the cake in a centrifugal field, suggested by Hultsch and Wilkesmann (1977), is conducting filter-bucket centrifuge tests. In the following sections, first the suggested test procedure by these researchers is briefly explained. Then the test set-up designed for laboratory scale centrifugal filtration of MFT is described and sample test results are presented. Later a comprehensive review of the batch filtering centrifuge tests conducted at the OSTRF, along with the test results and observations made are provided.

5.2. Filter-Bucket Centrifuge test method

The procedure for designing a filtering centrifuge, suggested by Hultsch and Wilkesmann (1977), is to conduct filter-bucket centrifuge tests. This testing method is introduced as a convenient tool to determine the filtrate speed (i.e. filtration rate), the filterability factor, the residual moisture content of the cake and its correlation with the time, g-factor (i.e. RCF) and the cake thickness. The above mentioned researchers considered this test method as a proper tool for selection of the type of centrifuge appropriate to a specific problem, which reduces the amount of costly pilot plant trials.

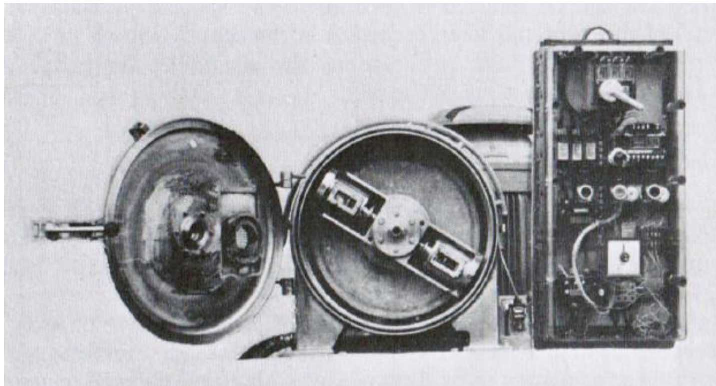

Figure 5.1 – A Filter Bucket Centrifuge (adapted from Hultsch and Wilkesmann, 1977)

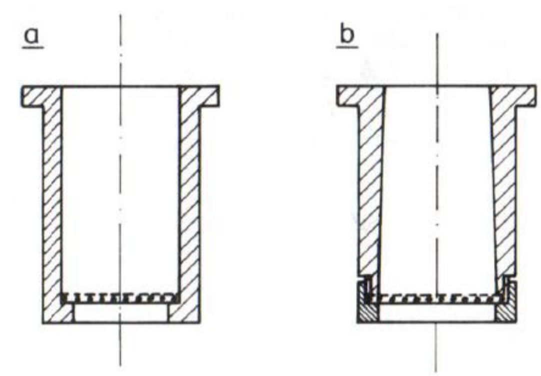

Figure 5.2 – Two Types of Filter Buckets (adapted from Hultsch and Wilkesmann, 1977)

Figure 5.1 shows a filter-bucket centrifuge with a horizontal shaft. This device has locking buckets with fluid-feed pipes and sight-glasses, which allow observation by means of a stroboscope during operation. Figure 5.2 illustrates two types of the filter buckets that are placed within the centrifuge. The filter medium is placed at the bottom of the filter bucket. Rather than feeding the slurry into the buckets by means of the fluid-feed pipes, Hultsch and Wilkesmann (1977) suggested to insert in each bucket a layer of the cake initially formed on a vacuum filter. Although the effect of sedimentation must be considered during the centrifugal filtration, by placing a cake with a specific thickness, these researchers neglected this effect for practical scale-up purposes. In the next stage, a controlled centrifuge test is conducted wherein clean liquid (i.e. filtrate from the vacuum filter) is centrifuged through this cake. This test is repeated for different rotational speeds, durations and cake thicknesses. For each test run, the flow rate and the residual moisture content of the cake are measured. Based on the results of all tests, correlations between the residual moisture of the cake, the centrifuging time and the g-factor are obtained for each cake thickness.

It should be noted that according to Hultsch and Wilkesmann (1977) this test procedure is particularly suitable for testing rapidly filtered products; where sedimentation period occurs fast and the clear supernatant fluid flows through the cake. Considering the low permeability of MFT and the slow rate of sedimentation in this material, the procedure for testing the centrifugal filtration of this material would be different from the procedure explained in this section. In sections 5.3 and 5.4, the test procedures followed for studying centrifugal filtration of MFT in the laboratory and plant scales are presented.

5.3. Centrifugal Filtration of MFT – Bench Top (or Laboratory Scale) Tests

As explained in Chapter 2, the oil sands tailings stream is composed of process water, coarse and fine minerals and residues of bitumen. One concern about using the vacuum or pressure filtration for dewatering MFT is clogging of the filter pores due to presence of bitumen. In the present research, prior to conducting the costly batch filtering centrifuge tests, it was desired to study the possibility of centrifugal filtration of MFT through some laboratory scale tests. The objectives of these preliminary tests were:

- To study if presence of bitumen could result in clogging of the filter cloth and consequently reduce the rate of filtration;
- To evaluate performance of the filter cloth; and,
- To assess the feasibility of obtaining fine tailings with high solids content using centrifugal filtration.

To achieve these objectives, a filter bucket was designed and samples of MFT were tested at a variety of test conditions.

5.3.1. Filter Bucket Design

As stated in section 4.4, the laboratory scale filtering centrifuge tests were conducted at the Geo-Environmental laboratory of the University of Alberta. The centrifuge device available for these tests was a bench-top Heraeus Centrifuge, model Multifuge 3 L-R, by Kendro Laboratory Products (Figure 4.14) in which four 650ml centrifuge bottles could be placed. To perform the filtering centrifuge tests a filter bucket was designed in a way that it could be fit inside the 650ml centrifuge bottles (Figure 5.3).

Figure 5-3 - The filter bucket set-up designed for lab-scale filtering centrifuge tests

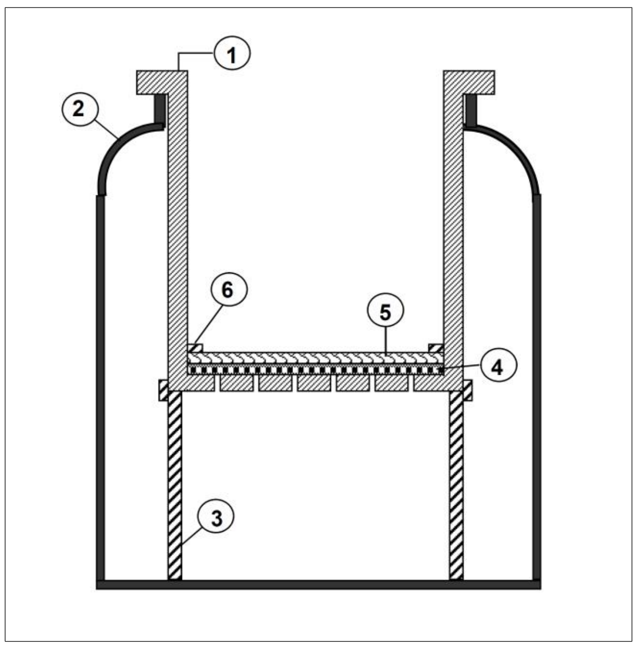

Figure 5.4 –Components of the filter bucket test set-up

As illustrated in the schematic drawing in Figure 5.4, the test set-up was composed of the following parts:

1. A cylindrical vessel with a perforated base;
2. A 650ml centrifuge bottle;
3. A four-leg support;

4. A porous disc-shaped thick cloth;
5. A piece of coated filter cloth cut in shape of a disc; and,
6. Two metal O-rings with rubber sealing on the outer perimeter (to seal the gap between perimeter of the filter cloth and the cylinder).

The reason for placing a porous thick cloth between the filter medium and the perforated base is to facilitate drainage of the filtrate. Use of the four-leg support was essential to prevent collapse of the centrifuge bottle due to the load applied by the cylindrical vessel during centrifugation.

5.3.2. Test procedure

To satisfy balance of the loads in the centrifuge, for each run two test set-ups with exactly similar specifications were prepared. Each of the test set-up components was weighed separately and then MFT, either untreated or with a desired treatment, was poured inside the cylinder over the filter cloth. After closing the lid of each centrifuge bottle, they were placed in the clinical centrifuge and the device was spun for a definite time. The temperature of the centrifuge was maintained at 21^{o}C during the test.

It should be noted that the same source MFT with exactly similar treatment must be placed into each of the test setups. This guarantees that the settling rates of both samples are equal, and consequently, the mass centre of each test setup locates at the same distance from the centre of rotation. Neglecting this point will cause imbalance of the centrifuge during spinning, which can result in dangerous vibrations and possible collapse of the rotor. The laboratory centrifuge used in this study was designed to buffer a certain degree of imbalance and was equipped with an automatic switch-off mode.

After the centrifuge completely stopped spinning, the bottles were removed and weighed. The filtrate (i.e. the fluid passing through the filter cloth) accumulated inside the centrifuge bottles. It was observed that the material inside the cylindrical vessel comprised the following layers (Figure 5.5):

- A layer of bitumen/asphaltene floating on the surface;
- A layer of almost clear water;
- A layer of thin fluid fine tailings in the middle part; and,

- A layer of thick MFT (with consistency of a thick slurry/paste) at the bottom, adjacent to the filter cloth.

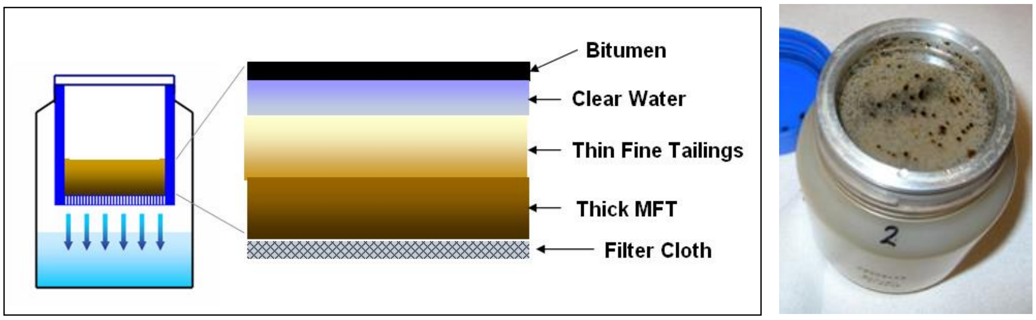

Figure 5.5 – The layering observed after centrifugal filtration

The tests were conducted using filters of different pore size, for various cases of MFT treatment. In order to evaluate the performance of each test, weight and solids content of the filtrate, the thin part (including bitumen, water and thin slurry), and the thick MFT were measured and the results were compared with weight and solids content of the source MFT.

5.3.3. Test observations and sample results

Presence of a separated layer of bitumen floating on top of the centrifuged MFT indicates an important advantage of the centrifugal filtration over the other filtration methods (e.g. pressure filtration and vacuum filtration):

During centrifugal filtration, bitumen, which has a specific gravity of about 2.6 times lower than the mineral particles, stays closer to the centre of rotation. Therefore it has less opportunity to reach the filter cloth and this significantly reduces possibility of blockage of the filter pores.

Table 5.1 presents the results of a number of sample bench-top filtering centrifuge tests. In this table, the solids content of the source MFT, the filter cloth pore size, the gypsum dosage, the spinning velocity and the solids content and weight percentage of cake, thin tailings and filtrate are presented. The filter media used for tests number 1 to 4 were MSI Nylon Membrane Filters, while for the rest of the tests the 2.5mm thick coated filter cloth, which was intended for use in the batch filtering centrifuge, was utilized. The bench top filtering centrifuge tests revealed that this type of filter cloth was quite durable, making it a suitable option for the batch filtering centrifuge tests. Figure 5.6 shows

Table 5.1 – Sample results of some bench-top filtering centrifuge tests

Test #	MFT SC (%)	Source	Gypsum (ppm)	Filter cloth opening (m)	Spinning Speed (RPM)	RCF	Duration (min)	Cake SC (%)	Cake Weight (%)	Thin Slurry SC (%)	Thin Slurry Weight (%)	Filtrate SC (%)	Filtrate Weight (%)
1	22.4	Suncor	No Gypsum	0.22	1600	500g	33	56.89	27.00	10.34	61.76	5.95	11.12
2	22.6	Suncor	No Gypsum	10	1600	500g	5	---	---	---	---	---	5.15
3	23.3	Suncor	No Gypsum	10	2850	1750g	5	51.97	28.69	7.68	57.65	---	7.92
4	22.1	Suncor	300	10	2850	1750g	5	45.75	25.85	6.23	45.30	---	12.15
5	22.5	Suncor	300	15	4150	3773g	3	47.19	31.37	7.44	38.59	10.69	16.22
6	25.2	Suncor	No Gypsum	0.8	4150	3773g	3	47.75	43.89	8.28	43.71	0.87	11.90
7	34.5	Albian	300	0.8	4000	3434g	5	44.10	59.66	23.93	33.84	1.06	5.50
8	34.5	Albian	600	0.8	4000	3434g	5	40.44	69.00	20.27	21.91	0.62	8.91
9	23.9	Syncrude	No Gypsum	0.8	800	137g	15	---	---	---	---	---	No Filtrate
10	23.9	Syncrude	No Gypsum	0.8	4150	3697g	5	42.49	---	13.82	---	---	---
11	29.5	Syncrude	No Gypsum	0.8	800	137g	15	---	---	---	---	---	No Filtrate
12	29.5	Syncrude	No Gypsum	0.8	4150	3697g	5	47.6	---	13.07	---	---	---

photos taken from the front and back side of a disc-shaped piece of the coated filter cloth with 0.8 μ openings, after it was used for 5 trials. The coating on the filter cloth allowed easy removal of the cake, leaving negligible amount of bitumen on the filter surface. This indicated that blockage of the filter pores with bitumen should not be an issue for the larger scale filtering centrifuge tests.

	
Front side (coated)	Back side (no coating)

Figure 5.6 – Appearance of the filter cloth after removal of the cake

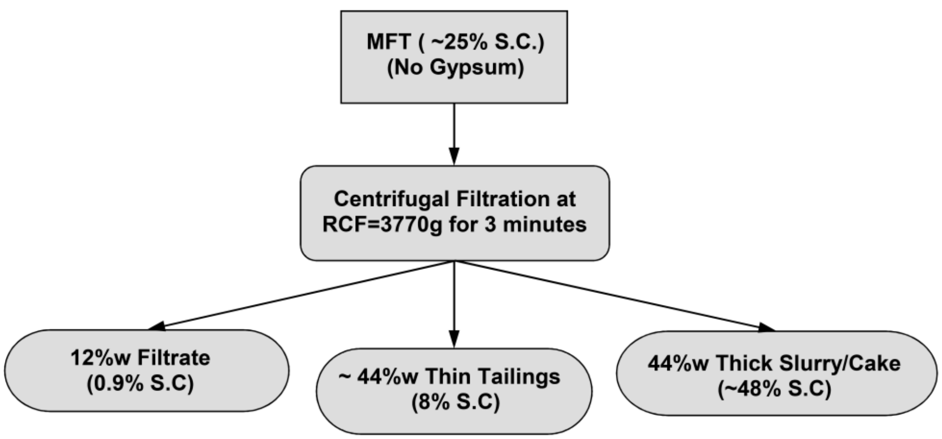

Figure 5.7 – Sample test results for a bench-top filtering centrifuge test

Figure 5.7 schematically shows the results for test #6 listed in Table 5.1. As shown in this typical example, in each test three products could be obtained: filtrate, thin tailings and thick slurry/cake. Filtrate is the relatively clear water that passes through the filter medium. Thin tailings is the runny mixture of floating bitumen, clear water and the fines suspension remaining inside the cylindrical vessel. Thick slurry or cake, however, is the dewatered material that remains over the filter cloth and has to be removed by means of a scraper. As it will be explained in section 5.4.5, the same three products are obtained in the batch filtering centrifuge tests. Detailed description of the factors affecting quality of the cake, thin tailings and filtrate will be provided in section 5.5.2 for the plant scale tests.

It was observed that running the filter-bucket tests at low centrifugal gravities (equivalent to the batch filtering centrifuge tests) did not result in any significant volume of filtrate and cake in a practicable time (e.g. tests #9 and #11 in Table 5.1). For this reason, majority of the bench-top tests were conducted at high centrifugal gravities.

The primary objective of the bench top filtering centrifuge tests was to assess this method of solid-liquid separation for dewatering MFT. Due to scale effects, extrapolation of the results obtained from the filter-bucket tests to the large scale batch filtering centrifuge tests can be misleading. In the bench-top test setup, the small size of the disc-shaped filter cloth (with a diameter of ~ 60mm) and the friction between the tailings sample and the wall of the cylinder can affect the separation performance. Tiller et al. (1972) stated that in compression permeability cells, a large portion of the pressure applied to the top portion of a compressible bed is absorbed in wall friction, resulting in the non-uniformity of cake porosity.

5.4. Centrifugal Filtration of MFT – Pilot Scale Tests

After observation of the results from the laboratory scale filtering centrifuge tests, it was decided to proceed with the pilot scale tests. For this purpose a batch filtering centrifuge[2], provided by an industrial partner, was transferred to the Oil Sands Tailings Research Facility (OSTRF) located in Devon (40 km south of Edmonton), Alberta. Details of this device along with the test set-up used at the OSTRF plant are described in the following sections. Prior to description of the test set-up, the tailings samples used as test materials for this study are described.

5.4.1 Test Materials

The MFT used for the batch filtering centrifuge tests was collected from the tailings ponds of Suncor, Syncrude and Albian Sands operations. Composition of the MFT

[2] Contrary to a continuous operating centrifuge, a batch centrifuge has an operating cycle including the acceleration, loading, centrifuging, deceleration and unloading stages.

received from each company is presented in Table 5.2. The solids and bitumen contents stated in this table represent the average values for each source of MFT. The fines content values reflect the percentage of solids finer than 44 microns (i.e. passing through sieve #325). It should be noted that in calculation of the geotechnical solids content, the percentage of bitumen remaining in the samples after oven drying is considered as part of the solids.

Table 5.2 - Characteristics of the MFT used for making NST

MFT Source	Geotechnical Solids Content (%)	Solids (%)	Water (%)	Bitumen/Asphaltene (%)	Fines (<44 μm) (%)
Suncor	27.0	24.62	73.3	2.08	97.2
Syncrude	36.5	34.92	63.33	1.75	97.7
Albian Sands	37	35.13	63.72	1.15	98

Figure 5.8 presents the particle size distribution (PSD) of each MFT sample obtained by means of sieve and hydrometer analysis. For this purpose the standard test method for particle size analysis of soils, ASTM D422, was conducted on a wet sample of MFT containing a minimum of 50g of solids.

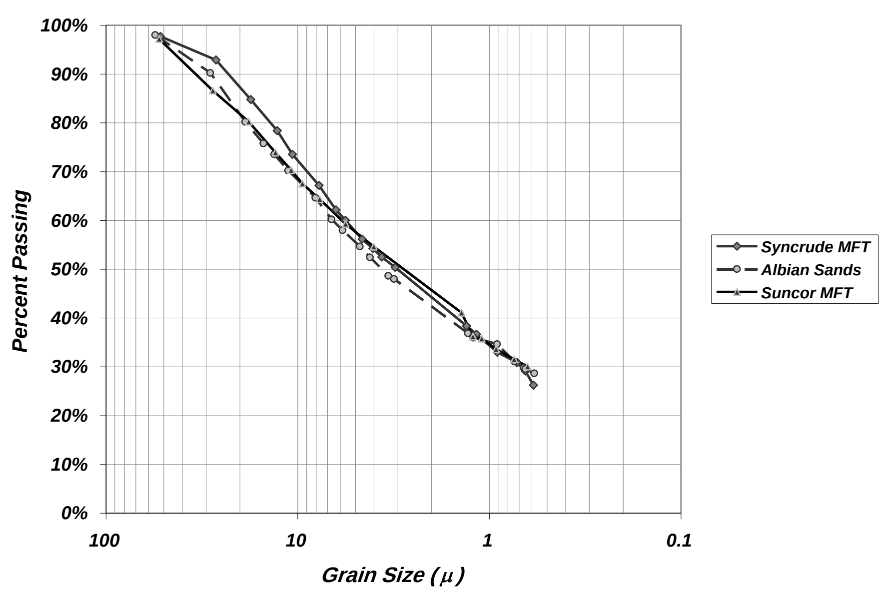

Figure 5.8 – Particle Size Distribution of the MFT samples used in the present study

The MFT received from Shell Albian Sands had been collected from depth of 7.5m in the tailings pond. Sorta and Sego (2010) reported the following Atterberg limits for this material:

LL = 53%, PL=26%.

The same source of MFT was characterized by Alam (2013 – Personal Communication), who reported the Atterberg limits as follows:

LL=60.8%, PL=27.1%.

Alam (2013 – Personal Communication) found the correlation between permeability (hydraulic conductivity) and void ratio of the Albian Sands MFT as illustrated in Figure 5.8.1.

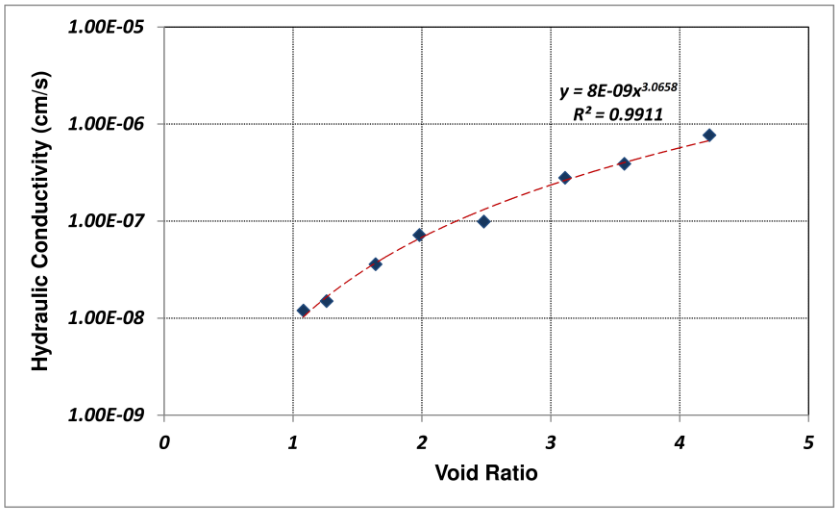

Figure 5.8.1 – Hydraulic Conductivity of Albian Sands MFT (after Alam, 2013 – Personal Communication)

5.4.2. Batch filtering centrifuge

Figure 5.9.a illustrates a picture of the batch filtering centrifuge used in this study. A schematic section of this device is illustrated in Figure 5.9.b. The main components of this filtering centrifuge are:

- a perforated drum (basket) with an internal diameter of ~600mm and height of ~400mm;
- a filter cloth that is placed inside the drum;
- the drum lid (to prevent leakage of the slurry during spinning);

(a)


(b)
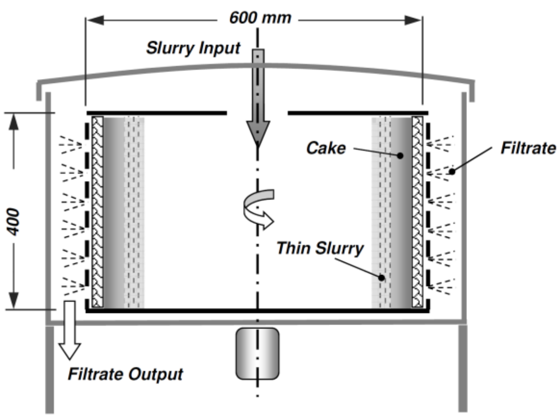

Figure 5.9: (a) The batch filtering centrifuge used in the present study.
(b) Schematic cross section of the device.

- an adjustable electric motor with a nominal angular velocity of 1750 rpm;
- an outer container and its lid which are the stationary parts;
- the inlet of the slurry feed and two nozzles at the centre of the top lid;
- the filtrate outlet devised at the bottom of the outer container; and,
- a supporting frame.

Depending on the PSD of the solid-liquid mixture and the type of treatment, filter clothes of different pore size can be used in the filtering centrifuge. In this research, two filter clothes with pore sizes of 0.8 μm and 2 μm were utilized. The provided filter clothes had a special coating with low affinity for oil and water.

As shown in Figure 5.9.b, the slurry is fed into the system through the inlet located over the lid. The electric motor spins the combination of drum and filter around a central vertical shaft, generating a centrifugal gravity field. The filtrate passing through the filter medium is collected in the space between the drum and the outer container and is discharged through an outlet devised at the bottom of the centrifuge.

The relative centrifugal force (*RCF*) applied to a sample within a centrifuge, located at a rotational radius of *R* (cm) and spinning at a velocity of *N* (RPM), can be calculated as following (Rayment and Lyons, 2010):

$$RCF = 0.00001118 \times R \times N^2 \tag{5.1}$$

In the above equation *RCF* is the ratio of the centrifugal force generated in the centrifuge to the gravitational force at the earth's surface; expressed as a factor of gravitational acceleration g. Figure 5.10 illustrates the correlation between the relative centrifugal force and spinning velocity for the filtering centrifuge used in the present study at the surface of the filter cloth (*R=30 cm*).

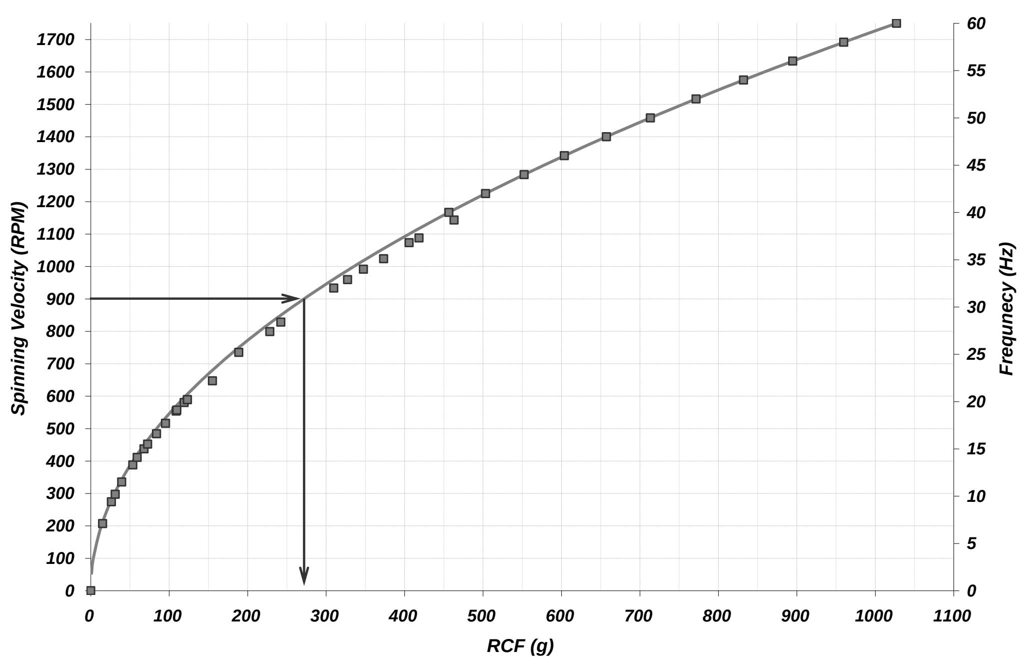

Figure 5.10 – Correlation between the spinning velocity and relative centrifugal force.

5.4.3 Pilot plant test setup

Figure 5.11 illustrates the components of the test setup used for the plant tests. A centrifugal slurry pump with an adjustable flow rate was used to feed the slurry into the centrifuge. The MFT introduced into the filtering centrifuge could be either untreated, or treated by addition of some kind of coagulant/flocculant. Depending on the method of treatment and the level of flocculation, viscosity of the MFT can change significantly and this will affect its flow characteristics and the required pumping energy. Possibility of adjusting the flow rate of the pump was particularly beneficial, considering the variety of viscosities that the feed slurry could have due to chemical treatment.

To control the rate of acceleration/deceleration and the spinning speed of the centrifuge, a Variable Frequency Drive (VFD) was utilized. This device enabled the electric motor to ramp up or ramp down to a certain RPM during a specific time frame (90 sec, 120 sec or 150 sec).

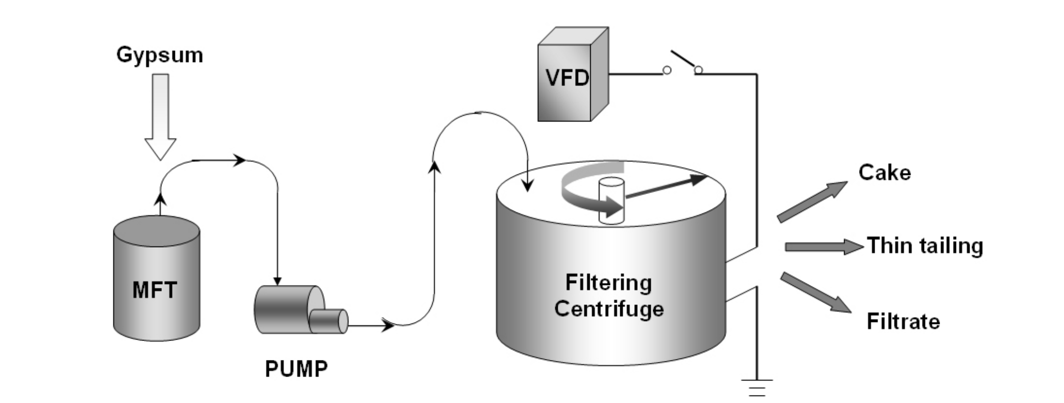

Figure 5.11 – The test setup used for the batch centrifugal filtration tests.

5.4.4 Operating cycle of the batch filtering centrifuge

Figure 5.12 shows the typical operating cycle of the batch filtering centrifuge used in the present study. At the first stage, the empty drum is accelerated from the stationary position to the loading speed (~600 rpm to 800 rpm) in about one minute. Then MFT is introduced into the system by means of the pump and the connecting hoses. After loading is complete in couple of minutes, the centrifuge is accelerated to a higher speed (~900 rpm or more) spinning for the desired test duration and finally it is decelerated in about a minute.

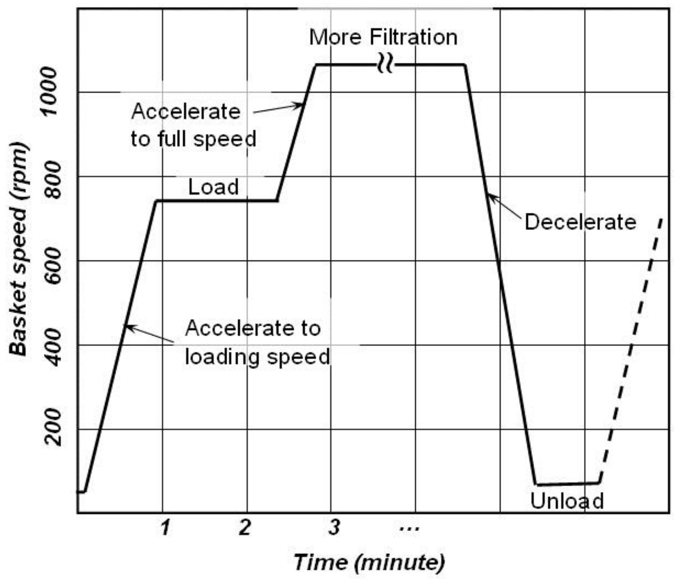

Figure 5.12 - Operating Cycle of the Batch Filtering Centrifuge

In a typical filtration operation in other industrial fields, the filtration usually continues until a relatively dry cake is obtained. In the present study, however, the goal is to achieve a thicker MFT (preferably pumpable) to be used as a component for production of CT/NST. In other words the desired state of the final product (i.e. cake) will be the main criterion for determining the duration and acceleration of the centrifugal filtration.

The advantage of using a batch centrifuge system for the plant scale tests is that duration of the filtration period and the level of centrifugal gravity are adjustable. This facilitates qualitative optimization of the final products and adjustment to varying product requirements (Perry et al. 2007).

5.4.5. Products

The MFT introduced into the filtering centrifuge results in three products:

- Cake: A layer of solid particles that is formed over the filter cloth and can have the consistency of a thick slurry to a paste like material (Figure 5.13.a).
- Filtrate: The water passing through the filter medium (comprising the porous cake and the filter cloth) that is relatively clear and has low percentage of solids. Figure 5.16.a shows samples of filtrate collected during a test.

- Thin tailings: Part of the liquid that has not passed through the filter medium and is not collected within the cake, remains inside the basket and includes a percentage of fine particles in the form of a suspension (plus unrecovered bitumen and asphaltenes). Figure 5.13.b illustrates view of the thin tailings remaining inside the centrifuge.

Figure 5.13.a – View of the cake formed over the filter cloth at the end of the batch centrifugal filtration of MFT.

Figure 5.13.b - The thin tailings (i.e. suspension of fines in water plus asphaltenes) remaining inside the filtering centrifuge

In Figures 5.13.a and b, patches of bitumen/asphaltene can be observed on the surface of the cake. The pressure difference generated by the centrifugal field causes flow of the water through the cake and filter cloth porous media, but very little bitumen can pass through these porous media. Although the bitumen extracted from the Athabasca oil sands has a specific gravity around 1.02, which is slightly higher than specific gravity of water, but at 20^{o}C the viscosity of this material is about one million times higher than viscosity of water (Figure 5.14). As previously explained in Chapter 3, according to Darcy's law volume of liquid discharged through a porous medium is inversely related to the viscosity of that liquid. This explains why majority of the bitumen/asphaltene present in the MFT cannot pass through the filter cloth.

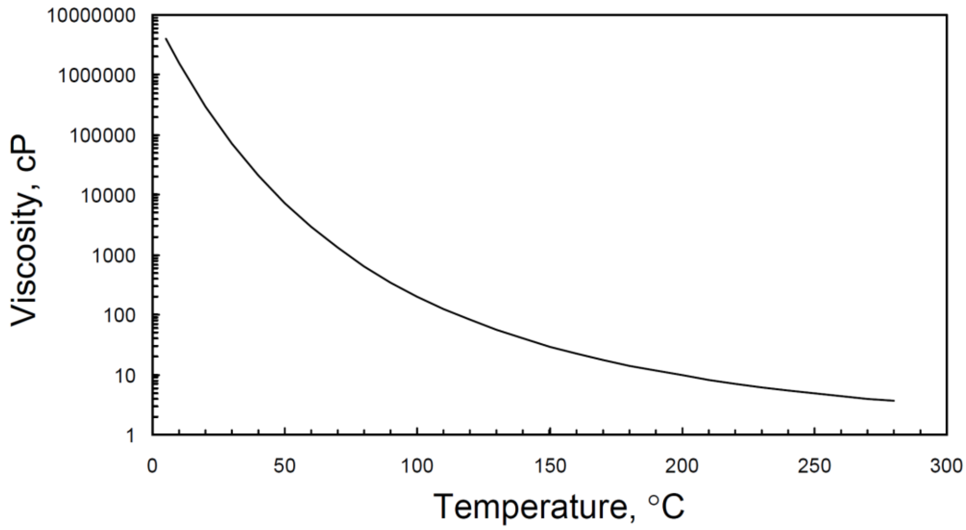

Figure 5.14 - Variations of the viscosity of Athabasca bitumen with temperature (modified from Mehrotra and Svrcek, 1986).

5.4.6. Test procedure

Prior to starting each filtering centrifuge test, the feed MFT was thoroughly mixed inside a 20 liter pail. A dual mortar mixer (Figure 5.15) was utilized for efficient mixing. For the tests that MFT treated with gypsum was to be used as the feed, a 100ml mixture of phospho-gypsum and DI (de-ionized) water was added to the MFT pail and the combination was mixed for 90 seconds. The mixing time was controlled by means of a stopwatch (chronometer). Samples of the mixed MFT (treated/untreated) were taken for the solids content and PSD analysis.

Figure 5.15- Dual Mortar Mixer

In the next stage, the operating cycle explained in section 5.4.4 was followed. It should be mentioned that for a number of tests, the MFT mixed with gypsum was instantly pumped into the filtering centrifuge and the centrifugal filtration started, while for others a delay time of 30 to 100 minutes was considered after mixing the gypsum and before start of the test. The effect of delay time after addition of gypsum will be discussed in section 5.5.2.3.

For each test, the time elapsed until start of the filtrate discharge from the centrifuge outlet was recorded. The filtrate was collected within a pail. Also during the test, a number of filtrate samples were collected from the centrifuge outlet. Figure 5.16.a shows five samples of filtrate collected during one of the filtering centrifuge tests (test SR-600-F2-70) in chronological order; the first sample appears on the left and the last one on the right. It can be observed that solids content of the filtrate samples has gradually decreased during the test (ranging from 0.76%wt to 0.15%wt, average 0.24%wt). This indicates that as the layer of cake builds up over the filter cloth, it itself acts as a filter medium, i.e., it captures the fine particles and prevents them from entering the filtrate.

(a)

(b)

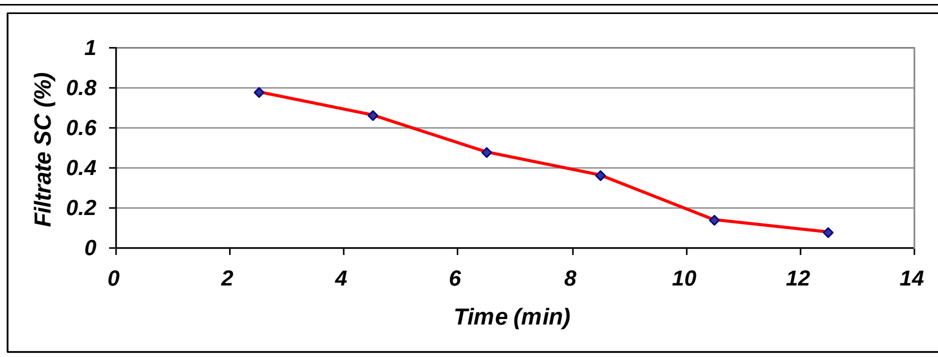

Figure 5.16.a - Samples of filtrate taken during the filtering centrifuge test SR-600-F2-70
b - Variation of filtrate solids content along the test

After each test when the filtering centrifuge fully stopped, the electricity power was disconnected, the feed hoses were unhooked from the centrifuge and the upper lid was opened. The drum lid was carefully inspected to see if any leakage of MFT had occurred. Then the lid was opened and after taking photographs from inside of the centrifuge, samples of the cake and thin tailings were collected. Corning "Snap-Seal"® 300ml plastic containers were used for collection of samples.

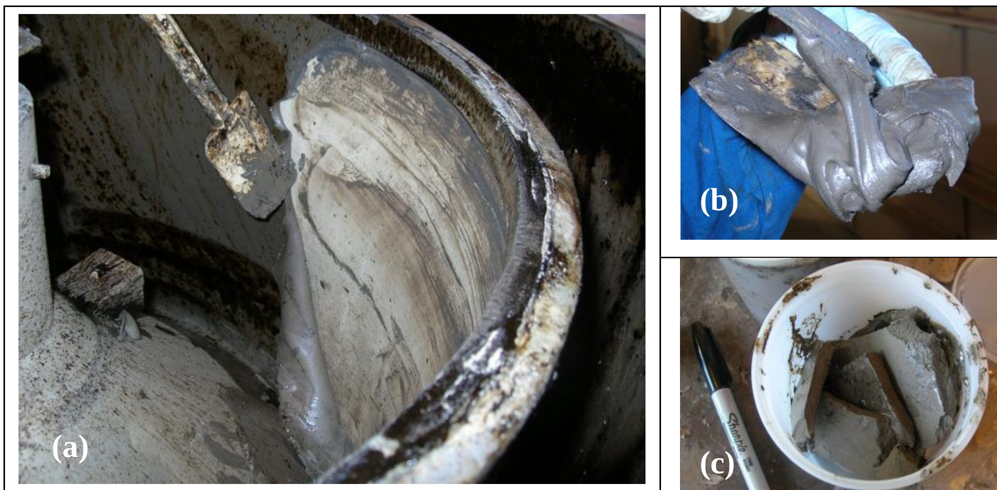

Figure 5.17. (a) Collecting the cake formed over the filter cloth
Consistency: Thick slurry, paste (b), or brittle cake (c)

The next stage was unloading the centrifuge. For this purpose, at first a vacuum cleaner (capable of vacuuming a mixture of solid and liquid) was utilized to collect all the thin tailings remained inside the centrifuge. Then, the cake sitting on the filter cloth was collected manually by means of a scraper (Figure 5.17.a) and was put inside a pail. The special coating over the filter cloth facilitated removal of the cake. Depending on the testing conditions, consistency of the dewatered MFT could vary from thick slurry to paste like material (Figure 5.17.b). At limited zones over the filter cloth brittle and relatively dry cake, as shown in Figure 5.17.c, could form. After weighing the total collected cake, the dual mixer was used to mix the cake inside the cake. The reason for mixing was to get a uniform thick slurry/paste material for further analysis and producing CT/NST, as will be explained in Chapter 6.

To evaluate performance of the centrifugal filtration tests, the total weight and the solids content of each product (cake, thin tailings and filtrate) were measured and the values were expressed as percentage of the feed material. Also for selective tests, PSD analysis was conducted on the samples taken from the feed MFT, the cake and the thin tailings left inside the drum. The purpose was to assess percentage of the fines captured within the cake in comparison to the fines percentage in the source MFT and the thin tailings. Also it was desired to determine the level of segregation occurred within the centrifuge. The test results are provided in the following section.

5.5. Filtering centrifuge test results

Table 5.3 presents the detailed information for 18 batch filtering centrifuge tests conducted at the OSTRF plant. These tests are selected as sample examples to be discussed in the rest of this chapter. For each test the following information are provided:

- Test identification (ID)
- The source of MFT (Syncrude, Suncor or Albian Sands)
- Amount of Gypsum used for treatment; untreated MFT is indicated as "No Gypsum"
- Spinning velocity of the basket during centrifugation (in RPM)
- Spinning velocity of the basket during feeding MFT (in RPM)
- Weight of the MFT fed into the centrifuge (the feed)
- Total test time
- Delay time after mixing with gypsum and before the centrifugal filtration
- Size of the filter cloth openings
- Weight percentage of the cake, thin tailings and filtrate in comparison to the source MFT
- Solids content and void ratio of the cake, also solids content of the thin tailings and filtrate

In the following sections, first a brief description about the ID selected for each test is provided and then different factors affecting the centrifugal filtration of MFT are discussed.

Table 5.3 – Test information and results of sample batch filtering centrifuge tests

Test No.	Test ID *(see section 5.5.1)*	MFT Source	Gypsum	Filtration RPM	Feeding RPM	Weight of Feed (kg)	Delay after Mixing	Total Time (min)	Filter Cloth Opening (μm)	Cake			Thin Tailings		Filtrate	
										%Wt	SC%	e	%Wt	SC%	%Wt	Avg. SC (%)
1	ASE-0-F2-ND	Albian Sands	No Gypsum	903	768	12	No Delay	0:14:39	2	49.99	69.06	1.19	39.29	18.2	10.73	11.08
2	ASE-600-F2-65	Albian Sands	16gr (600ppm)	903	768	12	65min	0:15:30	2	67.31	62.62	1.58	16.57	5.57	16.12	1.18
3	ASE-600-F08-ND	Albian Sands	16gr (600ppm)	903	768	12	No Delay	0:13:00	0.8	63.55	62.86	1.57	27.08	7.52	9.37	0.28
4	ASE-0-F08-ND	Albian Sands	No Gypsum	984	911	10	No Delay	0:16:00	0.8	59.99	63	1.56	34.66	24.61	5.35	0.70
5	SR-600-F2-70	Suncor	13gr (600ppm)	903	768	12	70 min	0:15:07	2	46.71	53.11	2.34	38.84	8.21	14.46	0.22
6	SR-600-F08-70	Suncor	13gr (600ppm)	903	768	12	70min	0:15:30	0.8	45.33	52.77	2.37	45.65	9.55	9.02	0.24
7	SD-0-F2-ND	Syncrude	No Gypsum	906	768	6	No Delay	0:21:00	2	38.46	63.37	1.53	16.31	17.85	2.8	7.01
8	SD-600-F2-95	Syncrude	16gr (600ppm)	903	768	12	95min	0:16:40	2	74.69	44.46	3.31	10.49	1.74	14.82	0.42
9	SD-300-F08-90	Syncrude	8gr (300ppm)	906	768	12	90min	0:15:38	0.8	45.62	52.47	2.40	47.48	25.3	6.9	0.21
10	SD-600-F08-100	Syncrude	16gr (600ppm)	903	768	12	100min	0:16:08	0.8	79.93	43.99	3.37	10.08	2	9.98	0.23
11	SD-300-F00-90	Syncrude	8gr (300ppm)	903	768	12	90 min	0:15:30	N/A	46.1	48.19	2.85	53.9	23.17	N/A	N/A
12	SD-300-F08-68-RPM1287	Syncrude	8gr (300ppm)	1287	768	12	68 min	0:16:42	0.8	59.84	49.88	2.66	34.89	21.43	5.28	0.45
13	SD-300-F08-37C	Syncrude	8gr (300ppm)	903	768	12	37m circulated	0:13:50	0.8	46.52	58.68	1.87	48.09	24.74	5.39	0.60
14	SD-300-F08-63	Syncrude	8gr (300ppm)	903	768	12	63min	0:14:34	0.8	86.25	43.1	3.50	9.73	2.15	4.01	1.12
15	SD-300-F08-ND	Syncrude	8gr (300ppm)	903	768	12	No Delay	0:14:00	0.8	40.55	61.38	1.67	53.44	22.58	6.01	0.65
16	SD-600-F08-ND	Syncrude	16gr (600ppm)	900	768	12	No Delay	0:14:00	0.8	77.53	48.06	2.86	18.12	5.4	4.35	0.74
17	SD-900-F08-ND	Syncrude	24gr (900ppm)	900	768	12.48	No Delay	0:16:10	0.8	65.54	48.54	2.81	29.69	18.45	4.76	0.43
18	SD-0-F08-ND	Syncrude	No Gypsum	940.2	796	12	No Delay	0:15:22	0.8	38.57	64.86	1.44	59.12	20.66	2.31	0.76

5.5.1. Test ID

In Table 5.3, each test ID denotes the following information for the centrifugal filtration tests:

- the source of MFT,
- the amount of Gypsum used for treatment,
- size of the filter cloth openings,
- delay time after MFT treatment, and;
- for some cases the maximum RPM.

For the tests that spinning velocity is not indicated, it was about 900rpm (equal to a RCF of ~270g).

The following examples explain how each Test ID should be interpreted:

- SD-300-F08-ND: Test on Syncrude MFT, with 300ppm Gypsum, using 0.8 micron filter cloth and No Delay after mixing Gypsum.
- ASE-600-F2-65: Test on MFT from Albian Sands Energy, with 600ppm Gypsum, using 2 microns filter cloth, with 65 minutes delay after mixing Gypsum.
- SR-600-F2-95: Test on Suncor MFT, with 600ppm Gypsum, using 2 microns filter cloth with 95 minutes delay after mixing Gypsum.

5.5.2. Factors affecting the centrifugal filtration of MFT

From the observations made during conducting the tests, also from the results obtained after analysis of the test samples, the main factors that affect the test performance can be categorized as following:

- Source of the MFT (method of extraction and waste production),
- Initial PSD of the feed (percentage of fines),
- Amount of the gypsum used for the same source material,
- Delay time after mixing the gypsum and before pumping the treated MFT into the centrifuge,
- Duration and speed of centrifugation (level/amount of energy applied),
- Size of the filter cloth opening

In the following sections each of these factors/parameters are described in more detail.

5.5.2.1. Source of the MFT

As stated by Miller et al. (2010, 2011) the type of bitumen extraction process, the choice of process water, subsequent chemical additions to the fine tailings, and oil sand ore all affect the compressibility, hydraulic conductivity and shear strength properties of the fine tailings. In the present research, comparison of the filtering centrifuge test results conducted on MFT samples from Suncor, Syncrude and Albian Sands tailing ponds indicated different dewatering characteristics for each source material.

Table 5.4 shows the results of three couples of tests conducted on MFT from different sources at similar testing conditions. The first two tests (tests 2 and 10: ASE-600-F2-65 and SR-600-F2-70) were conducted on Albian Sands and Suncor tailings accordingly, using the 2 microns filter cloth, 600ppm gypsum, about 65 minutes delay time after treatment and at similar spinning velocity. It can be observed that the solids content and weight percentage of the cake collected for Albian Sands MFT is higher than the values obtained for the Suncor MFT. Also for the Albian Sands MFT, the solids content and amount of thin tailings remaining inside the centrifuge is lower and the weight of filtrate obtained is higher. It can be concluded that, for the same level of energy, the Albian Sands MFT can be dewatered to a higher solids content in comparison to the MFT from Suncor tailings ponds. Similar results can be observed for the other two couples of tests listed in Table 5.4.

Table 5.4 – Comparison of filtering centrifuge test results for MFT from different sources at similar testing conditions

Test No.	Test ID	MFT Source	Gypsum	Filtration RPM	Feeding RPM	Weight of Feed(kg)	Delay after Mixing	Total Time (min)	Filter Cloth	Cake			LO		Filtrate	
										%Wt	SC %	e	%Wt	SC %	%Wt	Avg. SC (%)
2	ASE-600-F2-65	Albain Sands	16gr (600ppm)	903	768	12	65min	0:15:30	2 microns	67.31	62.62	1.58	16.57	5.57	16.12	1.18
10	SR-600-F2-70	Suncor	13gr (600ppm)	903	768	12	70 min	0:15:07	2 microns	46.71	53.11	2.34	38.84	8.21	14.46	0.22
22	SD-600-F08-ND	Syncrude	16gr (600ppm)	900	768	12	No Delay	0:14:00	0.8 micron	77.53	48.06	2.86	18.12	5.4	4.35	0.74
3	ASE-600-F08-ND	Albian Sands	16gr (600ppm)	903	768	12	No Delay	0:13:00	0.8 micron	63.55	62.86	1.57	27.08	7.52	9.37	0.28
1	ASE-0-F2-ND	Albian Sands	No Gypsum	903	768	12	No Delay	0:14:39	2 microns	49.99	69.06	1.19	39.29	18.2	10.73	11.08
12	SD-0-F2-ND	Syncrude	No Gypsum	903	768	12	No Delay	0:15:35	2 microns	38.46	63.37	1.53	35.95	21.38	6.48	17.53

To explain the reason for this different behaviour, in Figures 5.18 and 5.19 PSD of the Albian Sands and Suncor tailings in the dispersed and non-dispersed states are presented. (It should be noted that to obtain the PSD of the tailing in the non-dispersed state, the modified hydrometer analysis was utilized. In this method no dispersing agent is added to the suspension of fines, no high-speed mixing is applied, and processed water is used instead of DI water.) The diagrams indicate that the non-dispersed MFT from Albian Sands Energy has larger virtual grains (agglomerates), in other words it has a more flocculated structure. [3]

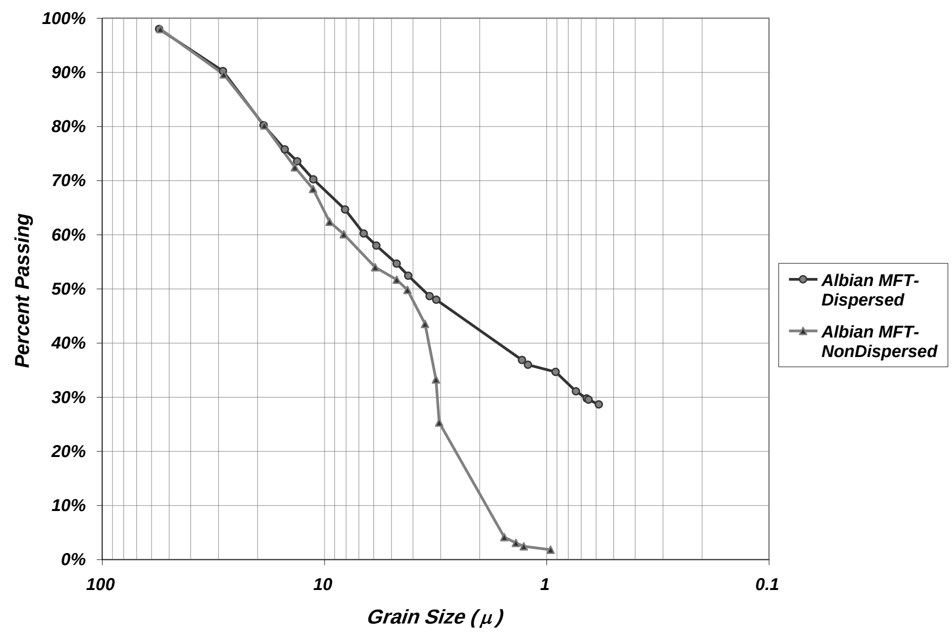

Figure 5.18. Comparison of the PSD of Albian Sands MFT in the dispersed and non-dispersed states.

[3] It should be noted that the MFT received from the Albian Sands had been collected from the TT Pond (Thickened Tailings Pond). Prior to deposition of the tailings into the TT pond, the thin fine tailings is treated by addition of a polymeric flocculating agent and then is dewatered in a thickener. Then the resultant thickener underflow is deposited into the TT pond. Since the method of extraction and waste production for Albian Sands ore is different from the Syncrude and Suncor ores, the dewatering characteristics of the resultant tailings stream for each ore is different as well. Fundamental research on the dewatering characteristics of Albian Sands MFT is in progress at the University of Alberta (Alam's thesis).

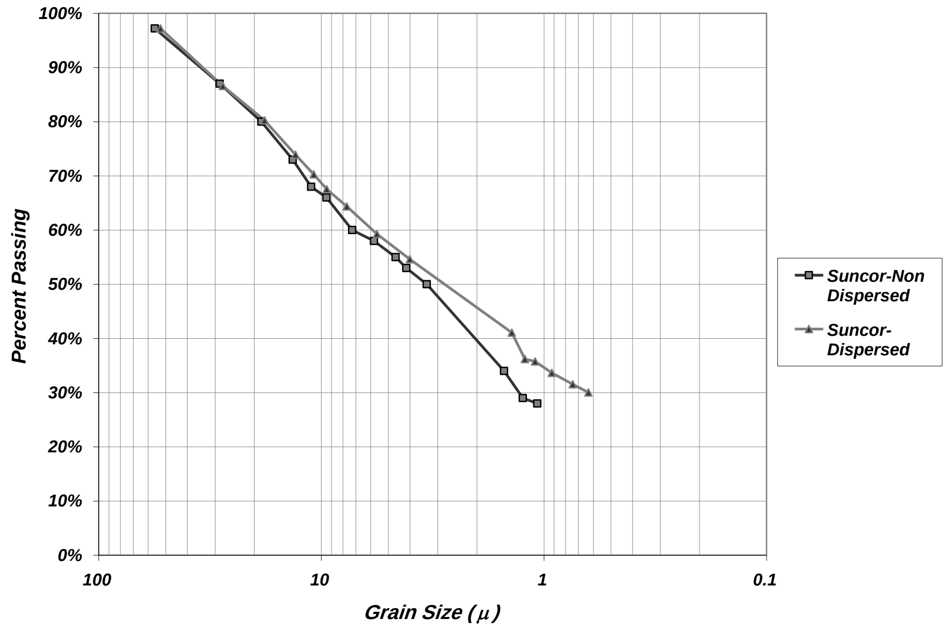

Figure 5.19. Comparison of the PSD of Suncor MFT in the dispersed and non-dispersed states.

According to Wakeman (2007), the smallest particles in the size distribution present the greatest contribution to the specific resistance of the filter cake. He suggests that size of the particles falling within the 5 to 10 percentile size on the PSD diagram ("the cumulative undersize curve") is a reasonable estimate for characterization of the filterability of material. It should be noted that in soil mechanics, D_{10} (effective size of the soil) has been empirically correlated with the permeability of fine-grained sandy soils (Hazen, 1893).

As explained in chapter 3, permeability of a filter cake is proportional to the square of effective particle size. Comparison of the PSD diagrams for the non-dispersed MFT in Figures 5.18 and 5.19 indicates that in the non-dispersed state, the D_{10} value for Albian Sands MFT is higher than the one for Suncor MFT. Presence of larger flocculated particles leads to higher permeability of the material. Therefore, for the same level of energy (same RPM and same duration of centrifugation) in the Albian Sands MFT, the solid particles settle faster and form a cake with higher consistency in which a higher percentage of the fine particles are collected. In section 5.5.2.2 more details are explained about the parameters controlling solids content and quality of the cake.

5.5.2.2. Effect of the chemical treatment on quality of the cake

Table 5.5 presents the results of four filtering centrifuge tests conducted on Syncrude MFT. All the tests are performed at a spinning velocity of ~900 rpm, using a 0.8 micron filter cloth. In the first test, no Gypsum is used for chemical treatment of MFT. In the other three tests, gypsum values varying from 300 to 900 ppm are used. After mixing the gypsum, the material is fed into the centrifuge with no delay.

According to this table and the diagram shown in Figure 5.20, as the amount of gypsum increases, the solids content of the resultant cake decreases. Yet, percentage of the dry solids captured within the cake increases.

Table 5.5- Result of filtering centrifuge tests on Syncrude MFT at different dosages of Gypsum

Test ID	Gypsum	Cake		
		%Wt	SC%	Weight of Dry Solids in the cake (kg)
SD-0-F08-ND	No Gypsum	38.57	64.86	3.00
SD-300-F08-ND	300 ppm (8gr)	40.55	61.38	2.99
SD-600-F08-ND	600 ppm (16gr)	52.39	56.36	3.54
SD-900-F08-ND	900 ppm (24gr)	65.54	48.54	3.97

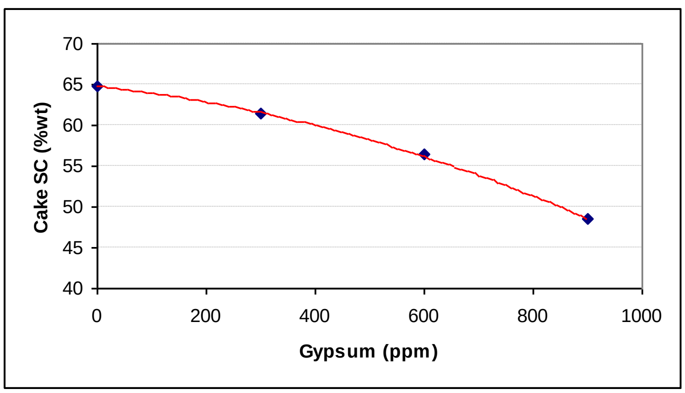

Figure 5.20 - Effect of gypsum on solids content of the cake produced from Syncrude MFT.

To investigate the role of gypsum on quality of the cake, PSD of the cake and the thin tailings remaining inside the centrifuge were compared with PSD of the source MFT. Figures 5.21.a and 5.21.b illustrate the results of hydrometer analysis for tests SD-0-F08-ND and SD-900-F08-ND (the first and last rows in Table 5.5) accordingly.

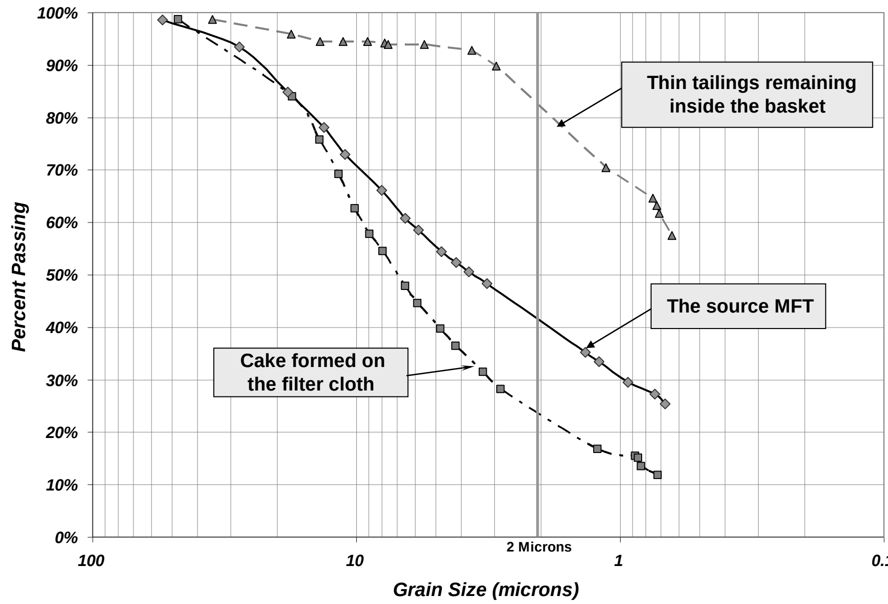

Figure 5.21.a – Results of hydrometer analysis for the test SD-0-F08-ND. The diagrams indicate segregation of the source MFT into a coarse (cake) and a fine fraction (thin tailings). About 29%wt of the fines are collected within the cake.

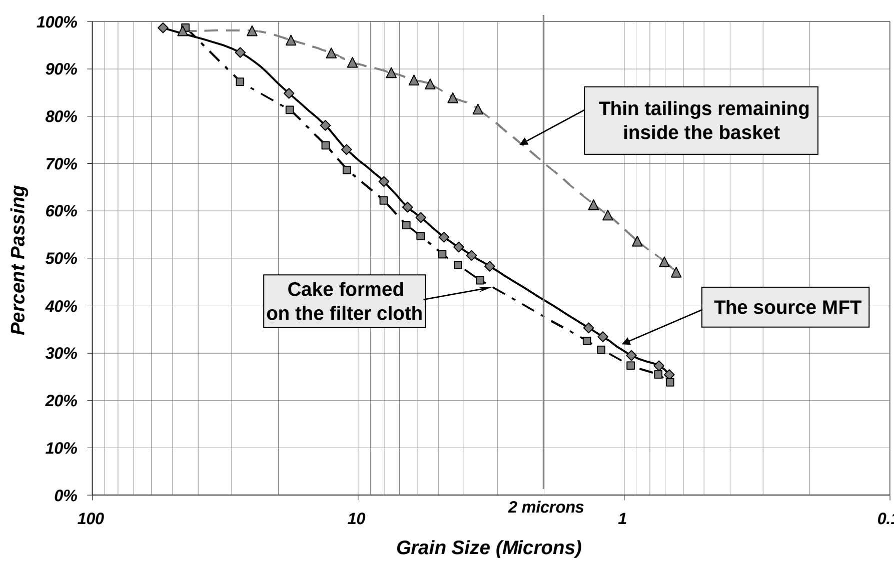

Figure 5.21.b – Results of hydrometer analysis for the test SD-900-F08-ND. The diagrams indicate lower segregation of the source MFT into a coarse (cake) and a fine fraction (thin tailings). About 58%wt of the fines are collected within the cake.

Figure 5.21.a indicates that in the absence of gypsum, segregation of the source MFT occurred within the filtering centrifuge: while the cake is composed of the coarse fraction,

the thin tailings remaining inside the centrifuge include finer particles in the form of a suspension. Based on the PSD diagrams of the cake and source MFT and the solids content values shown in Table 5.5, it can be calculated that in test SD-0-900-ND, about 29% of the particles finer than 2 microns are collected within the cake.

Figure 5.21.b shows that after treatment of MFT with 900ppm gypsum still segregation of the coarse and fine fractions occurs, but the PSD diagrams of these two fractions are closer to the PSD diagram of the source MFT. It can be calculated that about 58% of the clay sized particles are captured within the cake. As previously explained in chapter 2 addition of gypsum leads to coagulation of the clay particles. This results in formation of larger aggregates and contribution of higher percentage of the fine particles within structure of the cake.

According to Wakeman (2007) presence of higher percentage of fine particles within the cake leads to formation of smaller pores in the cake, resulting in a cake with higher moisture content. The reason is that smaller pore sizes increase the capillary pressure in the cake, leading to the requirement for higher dewatering pressures to displace the water from the cake. This explanation clarifies why increasing the amount of gypsum results in MFT cakes with lower solids content (Table 5.5).

Discussion:

There are a number of factors that affect variations of the cake solids content with dosage of the flocculant or coagulant, for instance: PSD of the slurry, percentage of the fines, initial solids content of the slurry, mineralogy of the solids and type of the chemical agent used for treatment of the slurry. As discussed in section 2.8.2.3, Xu et al. (2008) conducted a number of bench-top pressure filtration tests on oil sands tailings with fines content varying from 4.3% to 83.3% and with solids content varying from 8.7% to 69.6%. The tailings were treated with an anionic, high-molecular weight, polyacrylamid-based polymer. Figure 5.22 shows the variations of solids content of the cake versus dosage of the flocculant for a specific tailings composition with 18% fines. According to this study (Xu et al., 2008) there is an optimal dosage of flocculant for this specific tailings composition at which the maximum cake solids content can be obtained and overdosing leads to reduction of the cake solids content. In the present study, the amount of gypsum used was limited to the range of 0 to 900ppm and such an optimal dosage was not observed in this range.

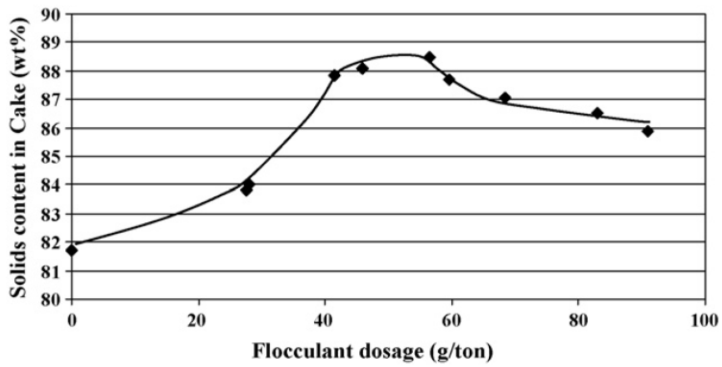

Figure 5.22 - Filter cake solids content for flocculated tailings (fines content 18%) as a function of flocculant dosage (after Xu et al. , 2008)

5.5.2.3. Effect of delay after chemical treatment, before pumping the material into the centrifuge

One interesting observation made during the filtering centrifuge tests was that mixing the MFT with gypsum and then leaving the mixture to sit for a while before being introduced into the filtering centrifuge resulted in thin tailings with very low solids content. Also a large percentage of the source MFT could be collected as cake.

Table 5.6 presents the results of three filtering centrifuge tests conducted on Syncrude MFT. The two tests SD-300-F08-63 and SD-300-F08-ND were performed at a spinning velocity of 900 rpm. In the first test (test A), 300 ppm gypsum was mixed with MFT and the mixture was left aside for one hour before being introduced into the filtering centrifuge. In test B, the same amount of gypsum was mixed with MFT and the mixture was instantly fed into the filtering centrifuge. As Table 5.6 shows, the thin tailings in the test with delay (SD-300-F08-63) has a significantly lower solids content and majority of the solids are collected within the cake. As illustrated in Figure 5.23, hydrometer analysis of the cake samples reveals that in test A, the PSD diagrams of the source MFT and the cake are exactly similar, indicating that no segregation occurred during this test. However, in test B segregation occurs and the cake has a coarser gradation in comparison to the source MFT. Similar result was observed for tests SD-600-F08-ND and SD-600-F08-30 in Table 5.3.

Table 5.6. Effect of delay after chemical treatment on the results of centrifugal filtration tests

Test No.	Test ID	MFT Source	Gypsum	Filtration RPM	Feeding RPM	Weight of Feed (kg)	Delay after Mixing	Total Time (min)	Filter Cloth	Cake			LO		Filtrate	
										%Wt	SC%	e	%Wt	SC%	%Wt	Avg. SC (%)
A	SD-300-F08-63	Syncrude	8gr (300ppm)	903	768	12	63min	0:14:34	0.8 micron	86.25	43.1	3.50	9.73	2.15	4.01	1.12
B	SD-300-F08-ND	Syncrude	8gr (300ppm)	903	768	12	No Delay	0:14:00	0.8 micron	40.55	61.38	1.67	53.44	22.58	6.01	0.64
C	SD-300-F08-37C	Syncrude	8gr (300ppm)	903	768	12	37min (Circulated)	0:13:50	0.8	46.52	58.68	1.87	48.09	27.74	5.39	0.60

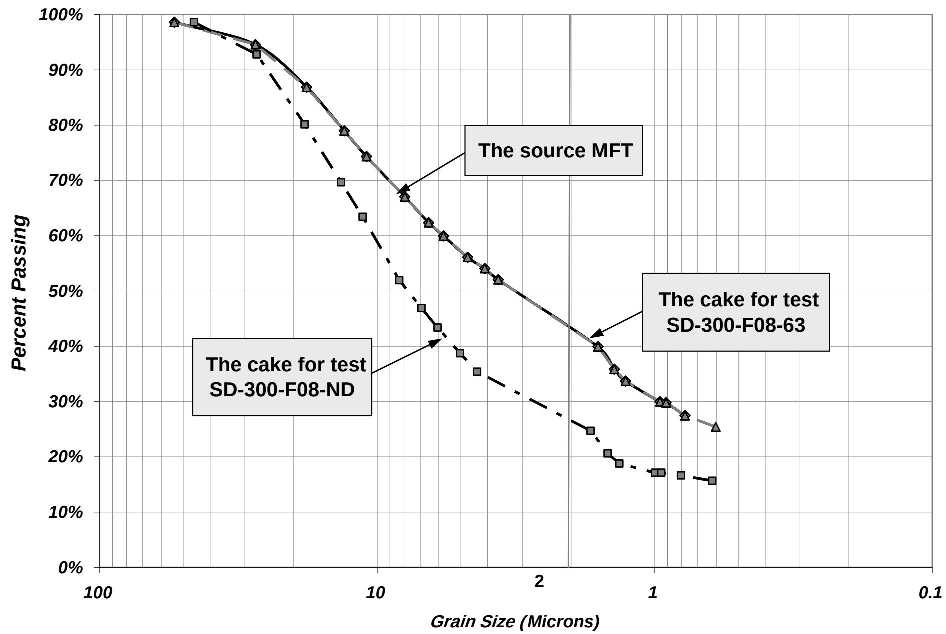

Figure 5.23 - Effect of delay time on PSD of the cake

From this observation it can be concluded that in a continuous centrifugal filtration system, devising an alternate settling tank between the mixing point and the filtering centrifuge can improve performance of the solid-liquid separation process. This tank will serve as a buffer to provide the minimum delay time required after addition of the gypsum. Figure 5.24 illustrates a schematic diagram of the suggested (dewatering) sequence/system.

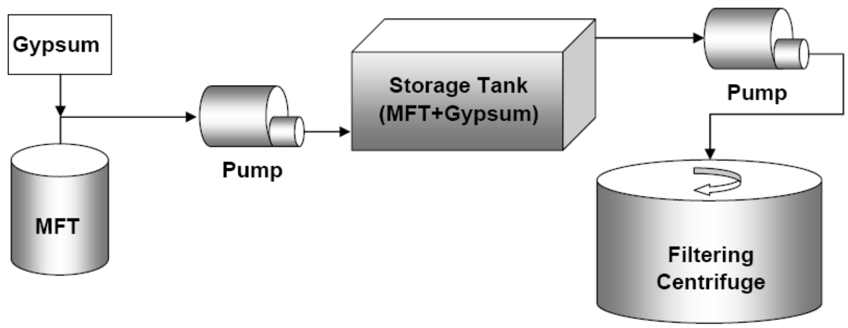

Figure 5.24 –Storage tank to increase the delay time after treatment of MFT

Review of the literature shows that one similar observation is recorded for the solid-liquid separation of the tar sands tailings. Baillie and Malmberg (1969) in their patent titled "Removal of Clay from the Water Streams of the Hot Water Process by Flocculation" indicated that mixing the clay suspension with the flocculant and then leaving the mixture to stand for a period of time surprisingly improved quality of the recovered water in the solid bowl centrifuge they had used. According to their experience, better results were achieved with a settling period of any length over immediate centrifuging. They tried settling periods of up to 30 hours with the best results; yet stated that greater periods are economically less desirable than shorter times.

Effect of delay time on PSD of the MFT:

In order to study the effect of delay time after addition of gypsum, modified hydrometer tests were conducted on samples of MFT in the following three conditions:

- Test 1: MFT without addition of gypsum;
- Test 2: MFT with addition of 600 ppm of gypsum, tested after 10 minutes of gypsum addition; and,

- Test 3: MFT with addition of 600 ppm of gypsum, tested after 80 minutes of gypsum addition.

In all three tests, the same source MFT was used. It is reminded that in the modified hydrometer analysis instead of using DI water, process water is used. The process water was sourced either by decanting the clear water sitting on top of the MFT container or by centrifuging MFT.

Figure 5.25 shows the result of hydrometer analysis for each of the Tests 1, 2 and 3. It can be observed that in the tests 2 and 3, a sudden decrease occurred in percentage of the clay sized particles (i.e. particles smaller than 2 microns). The MFT suspension in test 3, which experienced longer delay after addition of gypsum, appears to have lower percentage of ultrafine particles, indicating that higher number of these particles gathered together to form large agglomerates. Eventually this results in higher hydraulic conductivity and better dewatering characteristics of the treated slurry.

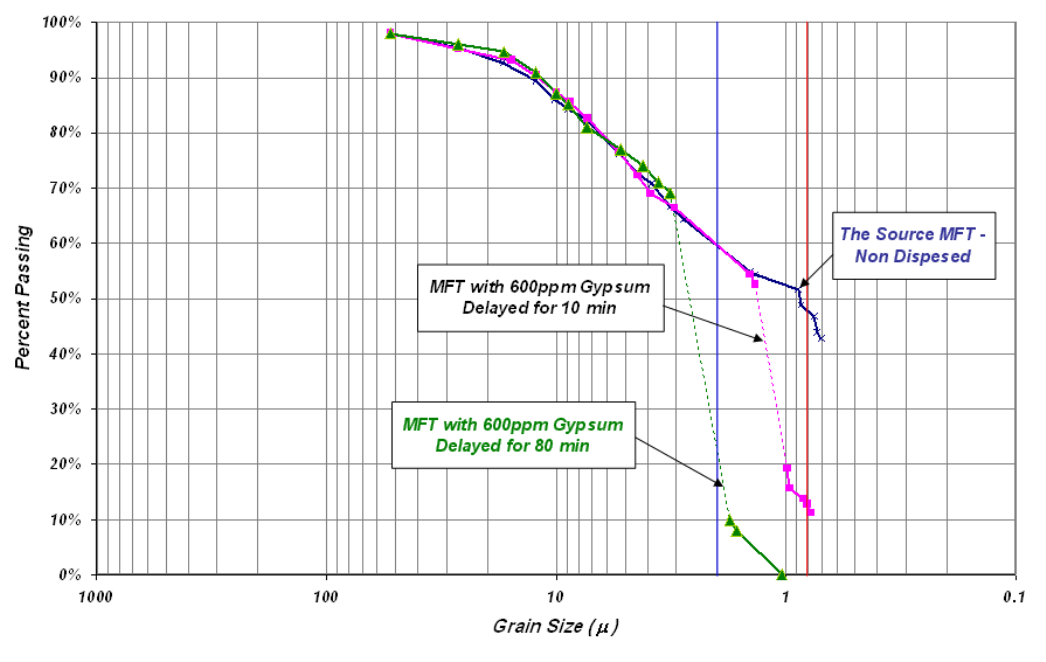

Figure 5.25 – PSD of the MFT samples in Tests 1, 2 and 3

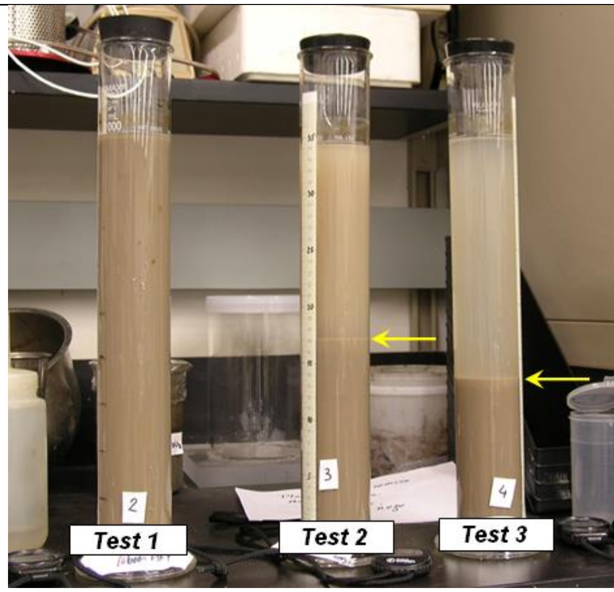

Figure 5.26 – Settlement interface in sedimentation tests 1, 2 and 3

Figure 5.26 illustrates a photo taken from the sedimentation standpipes during tests 1, 2 and 3. Although Test 3 started about 60 minutes after Test 2, it is visible that after a certain period of time, the water-slurry interface settled to a lower level, indicating higher hydraulic conductivity.

If the solubility of gypsum is increased, for instance by adjusting the temperature, by addition of chemical agents (e.g. NaOH, H_2SO_4) or by altering its physical structure (Ghorab et al., 1984; Ghorab and Fetouh, 1985; Wilson, 1998), then it is estimated that the clay particles will coagulate faster and as a result shorter delay times after treatment of the MFT will be required. This approach is not covered in the present research.

5.5.2.4. Effect of shearing on dewatering characteristics of the treated MFT

As explained in section 5.4.3, treated MFT is fed into the filtering centrifuge by means of a centrifugal pump and tubing (Figure 5.11). In field scale operations, the pipeline through which the treated MFT is transferred can be long. Also to overcome the pressure drop along the pipeline, it may be necessary to consider a number of pumps along the pipeline. Therefore the treated MFT is susceptible to 'low shear breakdown' along the pipe and 'high shear breakdown' within the centrifugal pumps.

To study the effect of shearing on the treated MFT, Test SD-300-F08-37C (test C in Table 5.6) was conducted. The test conditions were similar to the tests A and B presented in the same table, but the MFT mixed with gypsum was circulated through the pump and tubing for 37 minutes before starting centrifugal filtration. The purpose was to approximately simulate the flow within the pipeline in the field conditions. The results of this test are presented in Table 5.6. It can be seen that about half of the material is still in the form of a suspension with a high solids content of about 25%, which is not desired. These test results are quite similar to the results obtained from test SD-600-F08-ND (Table 5.6) in which treated MFT was instantly fed into the filtering centrifuge. Therefore, although in the test SD-300-F08-37C feeding the mixture of MFT and gypsum was delayed for about 37 minutes, but the shear stress due to circulation of the material caused breakage of the flocs and resulted in poor separation conditions.

Based on this observation, every attempt must be made to minimize the length of the pipeline and the number of pump stations between the filtering centrifuge and the settling tank suggested in section 5.5.2.3 (Figure 5.24). This is necessary to reduce the shear stress applied along the pipeline and to retain the flocculated structure of the material at the highest possible level.

5.5.2.5. Effect of centrifugation energy on quality of the cake

As previously explained in chapter 3, the centrifugation energy (applied to the slurry) is a factor of the spinning velocity and the duration of loading, filtration and deceleration stages. Figure 5.27 shows the variations of the cake solids content with spinning velocity for a number of tests conducted on untreated Syncrude MFT. The duration of all tests was similar. As it is expected, increasing the centrifugation energy leads to a cake with higher solids content.

It should be noted that in a filtering centrifuge, to apply a certain amount of energy to the slurry, two approaches may be followed:

- either by limiting the maximum spinning velocity and extending the centrifugation time; or,
- by limiting the centrifugation time and increasing the spinning velocity.

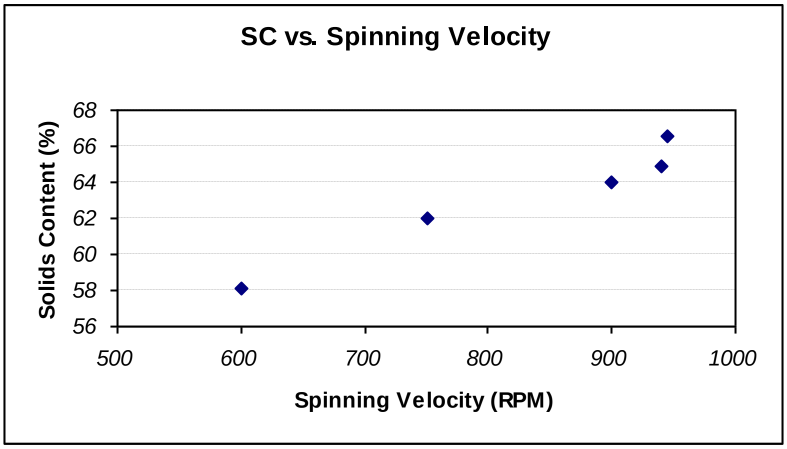

Figure 5.27 – Variations of the cake solids content with spinning velocity

For treated MFT, in which agglomerates are formed through flocculation/coagulation of the fine particles, increasing the spinning velocity higher than a certain limit may lead to disintegration of the flocs. As a consequence, segregation will occur in the centrifuge and less percentage of fine particles will be captured within the cake (see Chapter 3, section 3.6.1.5, "Floc disintegration in centrifugal fields"). Therefore one requirement in designing a slurry dewatering process by means of a centrifuge is to determine the limiting centrifugal force at different dosages of flocculants/coagulants.

Table 5.7 presents the results of two filtering centrifuge tests on Syncrude MFT. Test SD-300-F08-63 is conducted on MFT treated with 300ppm of gypsum and delayed for 63 minutes, at a spinning speed of 903rpm. Test SD-300-F08-68-RPM1287 is conducted at similar conditions except for the higher spinning speed of 1287rpm. The centrifugal force generated in the second test is almost twice the force generated in the first test. Although solids content of the cake increased from about 43.1% in the first test to almost 49.9% in the second test, but the weight percentage of the material collected within the cake decreased from 86% to about 60%. Looking into the results presented for the thin tailings remaining inside the centrifuge indicates that in the second test with higher spinning velocity, a large percentage of the material (34.9%) remains inside the filtering centrifuge as a suspension with a solids content of 21.4%. This reveals that increasing the spinning velocity caused disintegration of the flocs and release of the fines. The last two columns of the table show that weight of the filtrate produced in the second test is increased by about 30%.

Table 5.7 – Effect of increasing the spinning velocity on quality of the cake, thin tailings and filtrate

Test ID	Gypsum	RPM	Relative Centrifugal Force (RCF)	Delay after Mixing (min)	Filter Cloth Opening	Cake		LO		Filtrate	
						%Wt	SC%	%Wt	SC%	%Wt	SC%
SD-300-F08-68-RPM1287	300ppm	1287	555.5g	68	0.8 micron	59.84	49.88	34.89	21.43	5.28	0.45
SD-300-F08-63	300ppm	903	273.5g	63	0.8 micron	86.25	43.1	9.73	2.15	4.01	1.12

5.5.2.6. Effect of size of the filter cloth opening

Table 5.8 shows the results of two couples of filtering centrifuge tests. Each pair of the tests was conducted on the same source MFT with two sizes of filter cloth opening: 0.8μm and 2μm. The other test conditions including the spinning velocity, duration, dosage of gypsum and delay time after mixing the gypsum were similar. The results show that the solids content and weight percentage of the cake for both of the tests in each group is almost the same, while the amount of filtrate for the test with 2μ filter cloth is about 50% more than the test with 0.8μ filter cloth. This comparison indicates that:

- Using the filter cloth with larger openings results in higher volume of filtrate.
- Considering the similar porosity (and accordingly hydraulic conductivity) of the cake in the tests of each group, the higher volume of filtrate in the test with 2 microns filter indicates that the filter cloth with larger openings has lower resistance.
- Similar solids content of the filtrate in both tests implies that when the filter cloth openings are smaller than a certain size, then it is the porous structure of the cake that plays its role as a filter medium and determines the amount of solids suspended in the filtrate.

In Table 5.8, the combined resistance of the cake and filter cloth for each test is presented. For simplification, this average value is calculated according to equation 3.9 in Chapter 3. As expected, it is observed that the combined resistance for the tests with the 2 microns filter is smaller than the one for tests with 0.8 micron filter.

5.5.3. Comparison of the solid bowl centrifuge and the filtering centrifuge

As explained in section 3.6.2 and illustrated in Figure 3.19, in similar testing conditions, the interface between the cake and slurry settles faster in a filtering centrifuge in comparison to a solid bowl centrifuge (Sambuichi et al, 1987). Therefore for similar spinning velocity and duration, the cake obtained in a filtering centrifuge is expected to have higher solids content. To confirm this, the two tests presented in Table 5.9 were conducted. The source of MFT, treatment method, RPM and test duration were similar in both tests; however in one test a 0.8μm filter cloth was used while in the other a layer of plastic cover was placed inside the filtering centrifuge to simulate the testing conditions of a solid bowl centrifuge.

Table 5.8 - Effect of the size of filter cloth opening

Test No.	Test ID	MFT Source	Gypsum	Delay after Mixing	Total Time (min)	Filter Cloth Opening (μ)	Cake			LO		Filtrate		Weight% of Clear Filtrate	Resistance of the filter cloth and cake (1/m)
							%Wt	SC%	e	%Wt	SC%	%Wt	Avg. SC (%)		
5	SR-600-F2-70	Suncor	13gr (600ppm)	70 min	0:15:07	2	46.71	53.11	2.34	38.84	8.21	14.46	0.22	14.43	7.20E+03
6	SR-600-F08-70	Suncor	13gr (600ppm)	70min	0:15:30	0.8	45.33	52.77	2.37	45.65	9.55	9.02	0.24	9.00	1.18E+04
8	SD-600-F2-95	Syncrude	16gr (600ppm)	95min	0:16:40	2	74.69	44.46	3.31	10.49	1.74	14.82	0.42	14.76	7.48E+03
10	SD-600-F08-100	Syncrude	16gr (600ppm)	100min	0:16:08	0.8	79.93	43.99	3.37	10.08	2	9.98	0.23	9.96	1.07E+04

Table 5.9 – Comparison of the solid bowl and filtering centrifuges

Test No.	Test ID	MFT Source	Gypsum	Filtration RPM	Feeding RPM	Weight of Feed(kg)	Delay after Mixing	Total Time (min)	Filter Cloth Opening (μ)	Cake			LO		Filtrate	
										%Wt	SC%	e	%Wt	SC%	%Wt	Avg. SC (%)
9	SD-300-F08-90	Syncrude	8gr (300ppm)	906	768	12	90min	0:15:38	0.8	45.62	52.47	2.40	47.48	25.3	6.9	0.21
11	SD-300-F00-90	Syncrude	8gr (300ppm)	903	768	12	90 min	0:15:30	N/A	46.1	48.19	2.85	53.9	23.17	None	N/A

According to Table 5.9, although the weight percentage of the cake obtained in both tests is quite close, but the solids content of the cake obtained in the filtering centrifuge is more than 4% higher than the solid bowl centrifuge. Also in the filtering centrifuge, about 7%wt of the MFT is recovered as a clear filtrate with a solids content of about 0.2% which can be reused in the extraction process.

The above comparison indicates that, in similar testing conditions, the advantage of using a filtering centrifuge to a solid bow centrifuge is obtaining a cake with higher consistency for the same level of energy. The capital, operational and maintenance costs associated with each type of centrifuge can be different and are not covered in the present study.

5.6. Studying the possibility of using coagulant/flocculant polymers for centrifugal filtration of MFT

This section suggests a simple method for pre-screening the polymers and assessment of their effectiveness for centrifugal filtration of MFT. Since the dewatering behaviour of MFT treated with gypsum is fairly known through a number of batch filtering centrifuge tests conducted so far, this treated material (i.e. MFT + gypsum) can be considered as a basis of comparison to predict the effectiveness of other methods of treatment.

To evaluate the anionic Polymer A, laboratory scale bottle centrifuge and filter-bucket centrifuge tests were conducted on the following treated samples of MFT:

1. MFT + 600ppm gypsum;
2. MFT + 0.1% solution (300ppb) of Polymer A; and,
3. Diluted MFT + 0.1% solution (300ppb) of Polymer A.

Figures 5.28 to 5.30 present the photos taken from centrifuge tubes at different stages of test on samples 1 to 3 mentioned above. It can be observed that in the samples treated with gypsum, a distinct interface between the clear water and settled MFT can be observed. Comparison of the Figures 5.29 and 5.30 indicates that when Polymer A is utilized, a more visible interface can be observed between the thin and thick parts of MFT for the diluted MFT rather than non-diluted MFT. Tables 5.10 to 5.12 present the values of solids content for the thin and thick parts of MFT and the percentage of solids captured within the thick part in each test. From comparison of the results presented in Tables 5.11 and 5.12 with the values in Table 5.10 it can be concluded that in a filtering centrifuge, the diluted MFT treated with Polymer A (sample 3 above) will act better than the non-diluted MFT treated with Polymer A (sample 2).

Variations of the solids content for the thick and thin parts of MFT in the above three tests with regard to centrifugation time are presented in Figures 5.31 and 5.32. In Figure 5.31, although the solids content of the cake in sample 2 (non-diluted) is higher than the other two samples, but this treatment is not the desired one. The reason is the high solids content of the thin part for this treatment, which is illustrated in Figure 5.32. Tables 5.13 and 5.14 present the results of lab filtering centrifuge tests on samples 1 and 3 accordingly. It can be observed that for the same duration and RCF, the diluted MFT treated with Polymer A has resulted in a cake with higher solids content in comparison to the MFT treated with gypsum. Also this treatment is more favorable because solids content of the thin part is very low.

To figure out why the diluted MFT treated with Polymer A acts better than the non-diluted MFT, hydrometer tests in the non-dispersed state were conducted on these samples. Figure 5.33 shows the PSD analysis results for these two samples. It can be observed that when MFT is diluted, the polymer agent acts more effectively and larger flocs can be formed. Comparison of Figure 5.33 with Figure 5.25 shows the advantage of the polymeric agents to gypsum: in addition to the clay sized particles, a wider range of particles with larger sizes can be incorporated in formation of the flocs. As a result, a higher hydraulic conductivity can be achieved. From Tables 5.10, 5.12 and Figure 5.31 in can be concluded that use of Polymer A is more cost effective in terms of energy consumption, i.e. a larger percentage of the solid particles can be captured within the cake for the same level of energy. Cost of the required Polymer per unit volume/weight of MFT versus the savings in energy should be studied separately.

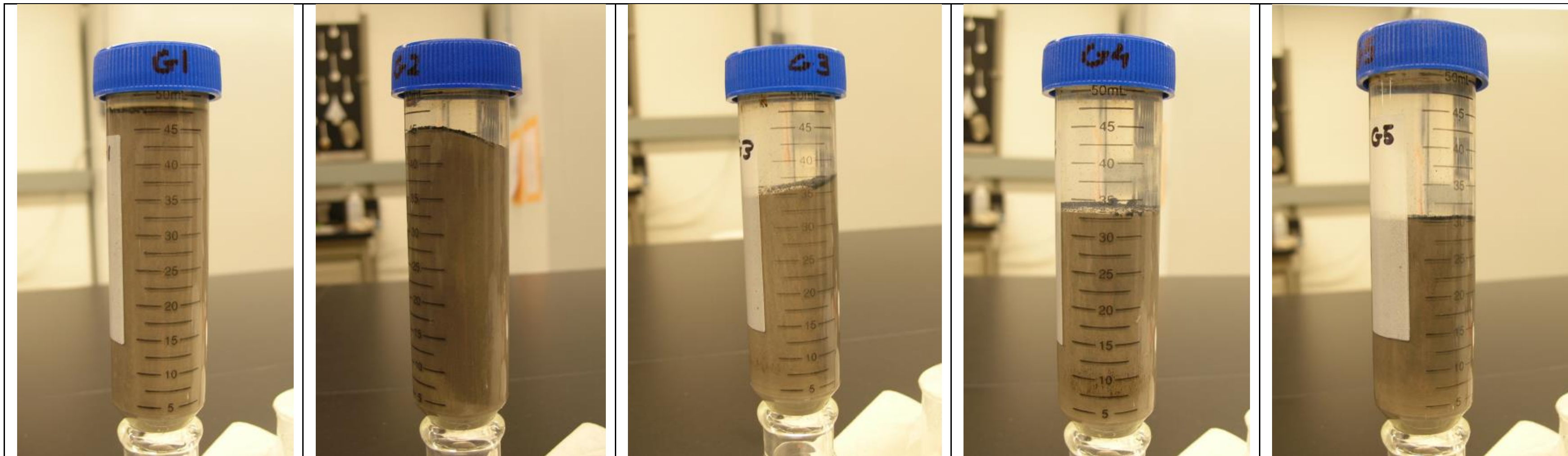

t = 5 min	t = 10 min	t =15 min	t = 20 min	t = 30 min

Figure 5.28 – Bottle Centrifuge tests on MFT (initial SC of 36.7%) treated with 600ppm gypsum at RCF=3700g.

Table 5.10 - Variations of the solids content in the thin part and cake during the bottle centrifuge test on MFT treated with 600ppm gypsum.

Time (min)	Thin Part SC (%)	Thick Part SC (%)	%Solids captured within the thick part
5	0.69%	38.39%	99.92%
10	0.26%	41.58%	99.92%
15	0.13%	47.37%	99.92%
20	0.28%	50.20%	99.79%
30	0.19%	53.24%	99.84%

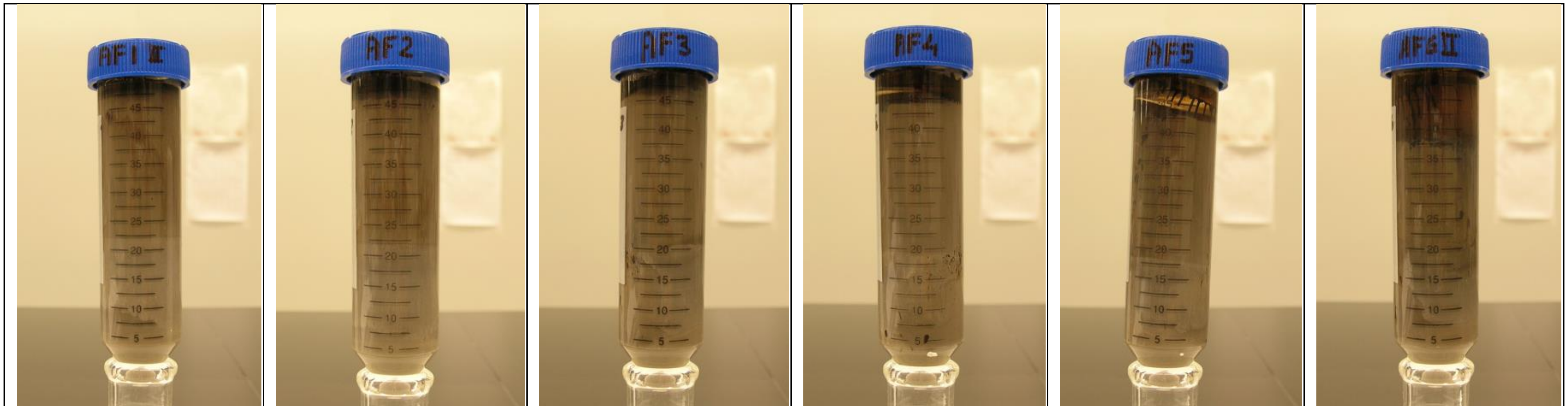

t = 5 min	t = 10 min	t =15 min	t = 20 min	t = 30 min	t = 60 min

Figure 5.29 – Bottle Centrifuge tests on MFT (initial SC of 33.26%) treated with 300 ppb of anionic Polymer A at RCF=3700g.

Table 5.11 - Variations of the solids content in the thin part and cake during the bottle centrifuge test on MFT treated with 300ppb of Polymer A.

Time (min)	Thin Part SC (%)	Thick Part SC (%)	%Solids captured within the thick part
5	13.64%	50.18%	80.99%
10	12.09%	51.52%	83.16%
15	11.35%	53.57%	83.57%
20	10.80%	54.48%	84.22%
30	9.79%	55.87%	85.55%

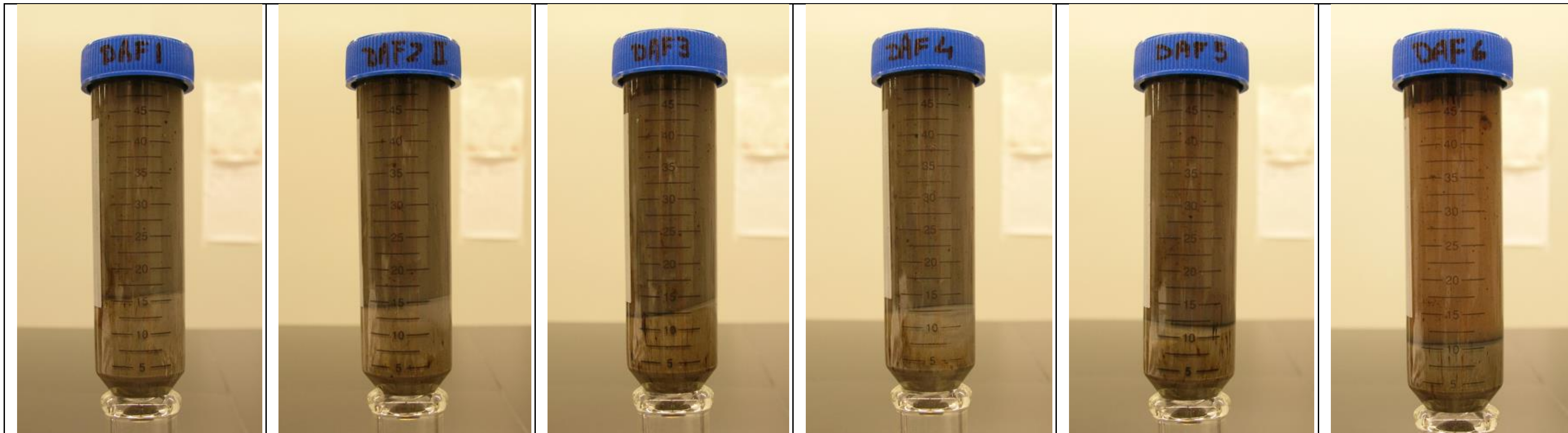

t = 5 min	t = 10 min	t =15 min	t = 20 min	t = 30 min	t = 60 min

Figure 5.30 – Bottle Centrifuge tests on diluted MFT (initial SC of 17.66%) treated with 300 ppb of anionic Polymer A at RCF=3700g.

Table 5.12 - Variations of the solids content in the thin part and cake during the bottle centrifuge test on Diluted MFT treated with 300ppb Polymer A.

Time (min)	Thin Part SC (%)	Thick Part SC (%)	%Solids Captured within Cake
5	1.03%	42.81%	96.42%
10	0.89%	46.69%	96.74%
15	0.76%	49.56%	97.14%
20	0.61%	52.25%	97.65%
30	0.54%	54.35%	97.86%
60	0.43%	58.18%	98.26%

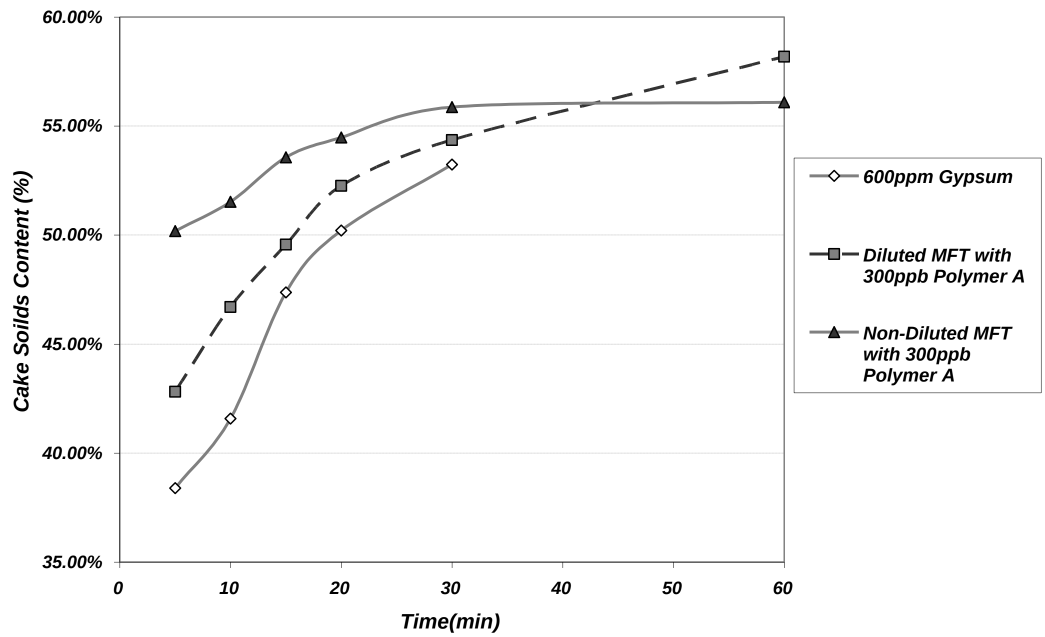

Figure 5.31 - Variations of Solids Content for the thick part of MFT during the centrifuge test

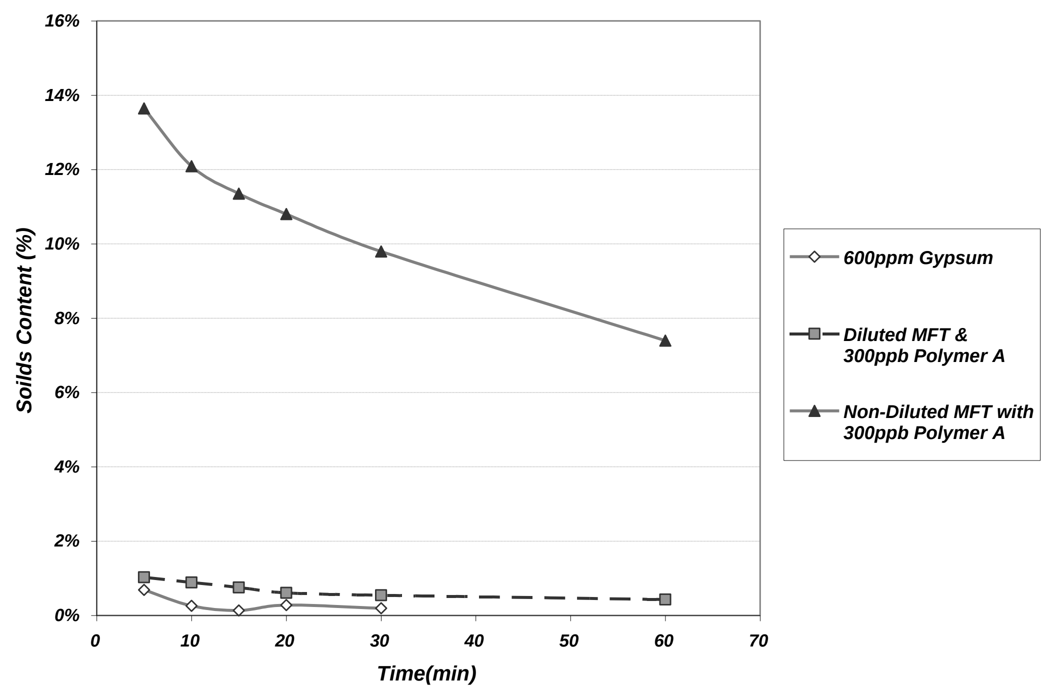

Figure 5.32 - Variations of Solids Content for the thin part of MFT during the centrifuge test

Table 5.13- Results of the lab filtering centrifuge tests on MFT treated with 600ppm gypsum. (Duration: 5min – RCF:3434g – Filter cloth: 0.8μm)

Filtrate	Solids content of the thin part	Solids content of the cake
- Clear	19.77% to 20.78%	40.0% to 40.89%

Table 5.14- Results of the lab filtering centrifuge tests on diluted MFT treated with 300ppb of Polymer A. (Duration: 5min – RCF:3434g – Filter cloth: 0.8μm and 15.0μm)

Filtrate	Solids content of the thin part	Solids content of the cake
- 0.8m Filter cloth: Crystal Clear - 15m Filter cloth: Muddy	0.41% to 0.74%	46.05% to 46.72%

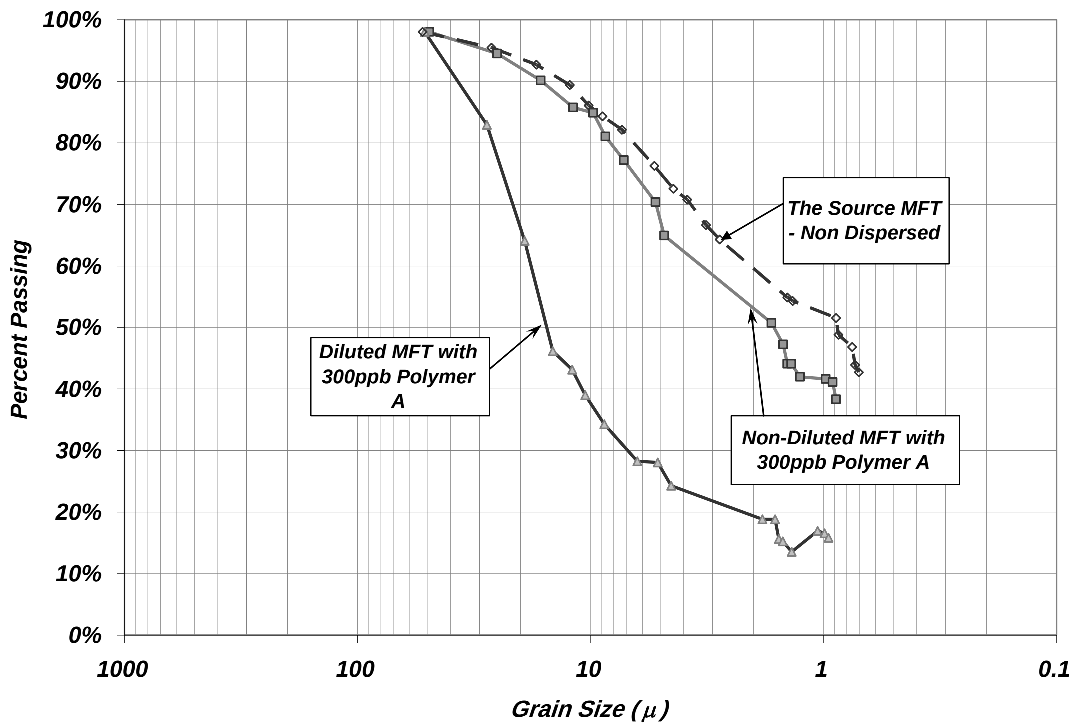

Figure 5.33 - PSD analysis of the regular and diluted MFT treated with 300ppb of Polymer A

5. 7. Suggestion of the proper device for the future studies

As previously explained in Chapter 3, Sambuichi et al. (1987, 1988) utilized a specific experimental setup (Figure 3.22) to analyze all the phases of the centrifugal filtration process. The basket in their device had an ID of 150mm and a height of 83mm and was covered with a transparent plate, so the variations of the slurry interface could be captured with a camera. They used the analysis results to express the theory of batchwise centrifugal filtration.

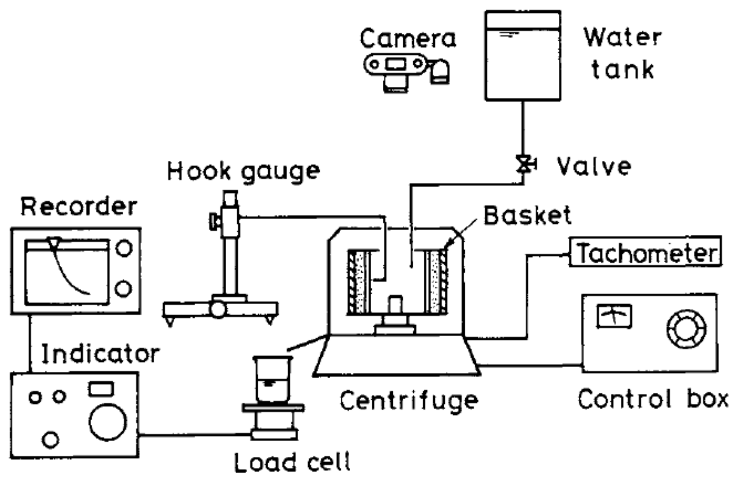

Figure 3.22 (repeated) - Experimental apparatus used by Sambuichi et al. (1987, 1988)

The batch filtering centrifuge utilized in the present research was primarily designed for small scale industrial operations and not specifically for research purposes, therefore its capacity and dimensions (ID of 600mm and height of 400mm) were larger in comparison to the centrifuge used by Sambuichi et al. (1987, 1988). The large capacity of this device was beneficial for production of large volumes of dewatered MFT to be used the next stages of this research.

When the purpose of the study is solely to determine the centrifugal filtration characteristics of a slurry (e.g. MFT), or to choose the proper method/dosage of treatment then utilizing a smaller scale device similar to the one used by the above mentioned researchers should be considered. Considering the large number of tests required, the smaller capacity of the device will reduce the amount of labor work, material and time required for each test. Also, use of the transparent covering and the camera may provide useful data for simulation of the rate of settlement/dewatering which can be used for planning larger scale operations.

5. 8. Summary

In this chapter, design of a filter bucket test setup used for preliminary simulation of the centrifugal filtration tests and evaluation of the filter cloth was presented. The bench top filtering centrifuge tests revealed that during centrifugation, the bitumen present in the MFT remains close to the centre of rotation and has less opportunity to be in touch with the filter cloth. This is a major advantage of the centrifugal filtration compared to the vacuum and pressure filtration methods.

In order to evaluate the centrifugal filtration of MFT in larger scale, also to produce sufficient volumes of dewatered MFT for the next stages of this study, a batch filtering centrifuge was used at the Oil Sands Tailings Research Facility (OSTRF) in Devon, Alberta. A number of filtering centrifuge tests at varying test conditions were conducted on MFT samples obtained from three different tailing ponds. The major factors affecting the dewatering of MFT in a filtering centrifuge can be listed as following:

- Source of MFT (initial PSD and method of extraction);
- Amount of the Gypsum used for treatment;
- Delay time after mixing the gypsum and before pumping the treated MFT into the centrifuge;
- Shearing and breakage of the flocs;
- Duration and speed of centrifugation; and
- Size of the filter cloth opening.

Each of these factors was studied and sample test results were presented.

A prescreening method was suggested for selection of the proper chemical agents to be used as amendments for centrifugal filtration of MFT. Results of bottle centrifuge and filter bucket centrifuge tests were presented for the MFT treated with an anionic polymer.

Results of the tests conducted at the OSTRF show that centrifugal filtration has the potential to be utilized as a method for production of MFT with higher solids content. The filtrate obtained in this method can be reused in the extraction process after a minor treatment, if necessary. The dewatered MFT can be used as a component for making CT/NST with higher solids content. In the next chapter, the flow and robustness of CT/NST made from filtered/centrifuged MFT will be studied.

Chapter 6

Making NST from Filtered/Centrifuged MFT

6.1. Introduction[1]

The CT/NST technology used as a method of tailings management in the oil sands industry has not performed as anticipated. While CT/NST has been expected to be non-segregating when discharged, in practice it has not been particularly robust. Partial segregation and release and re-suspension of the fines has been observed following deposition. To achieve a robust CT/NST, which does not segregate during transportation, at discharge and after deposition, the solids content of this engineered tailings stream must be increased.

The main objective of the present research was to investigate the possibility of producing composite/non-segregating tailings with higher solids content. As stated in Chapter 4, one approach for this purpose would be dewatering the fine tailings prior to mixing it with the cyclone underflow. To investigate this approach, the thick MFT/cake obtained from the filtering centrifuge tests (Chapter 5) was used as a component for making Non-Segregating Tailings (NST). The mixture of sand and pond water (simulating the cyclone underflow) was mixed with the centrifuge cake to produce NST with high solids content. In order to study the flow behavior and robustness of the resultant NST, a flume apparatus was designed and deposition of NST was carried out under laboratory conditions. For each flume test, the flow profile of the deposited material was determined. In addition, several NST samples were collected along the flume to determine the variations of Sand to Fines ratio (SFR) and solids content in the deposit. A strain-controlled viscometer with vane spindles was utilized to measure the yield stress of

[1] Part of this chapter has been previously published: Nik, R. M., Sego. D. C. and Morgenstern, N.R. (2010) "*Flow behavior and robustness of non-segregating tailings made from filtered-centrifuged MFT.*" Proceedings of the Second International Oil Sands Tailings Conference, Edmonton, Alberta, Canada. Dec. 2010., pp. 319 – 329.

NST; and the correlation between the average angle of repose/flow profile and the yield stress was studied.

In the following sections, first the procedure of making NST from filtered/centrifuged MFT and conducting the flume deposition tests will be explained. Then results of representative flume tests will be reviewed. At the end a brief discussion on the possible approaches for utilizing filtered/centrifuged MFT will be provided to guide application of this technology.

6.2. Making Non-Segregating Tailings from concentrated MFT

6.2.1. Test Materials

As explained in Chapter 5 (section 5.4.1), the MFT samples used in the batch filtering centrifuge tests were collected from the tailings ponds of Suncor, Syncrude and Albian Sands operations. Composition of the MFT received from each plant was provided in Table 5.2 of Chapter 5. The diagrams showing particle size distribution of the MFT samples were provided in Figure 5.8.

The sand used for making all of the CT/NST samples was sourced from the beach of Suncor tailings pond. The sand solids content and fines content were about 98.8% and 1.2% accordingly. The fines content was determined by washing the sand over sieve #325.

In Table 5.3 of Chapter 5, solids content of the cakes obtained from 18 representative centrifugal filtration tests were presented. Figure 6.1 shows the position of these cake samples on the Slurry Properties Diagram. Solids content of the cakes varies from 43.1% to 69% and the majority of them have fines content higher than 95%. As can be seen, in four instances the cake samples have higher sand content than the remaining samples. It was found that the feed for these centrifugal filtration tests had been pumped from the lower levels (close to the bottom) of the 250 liter HDPE container used for storage of MFT, where coarse particles had settled during storage.

6.2.2. Procedure for making NST

After conducting each filtering centrifuge test at the OSTRF plant, the cake of MFT collected from the filter cloth was stored inside a pail. To achieve a relatively homogenous cake, the collected material was mixed within the pail for about one minute by means of a dual blade mortar mixer (Figure 5.15). Figure 6.2 illustrates the view of the cake while being collected from the filter cloth and after it has been mixed within the pail. After mixing, the lid was placed over the pail and the test related information (including the source of MFT, test date and identification) was written on the side of the pail. At the end of each test day, the pails containing centrifuged MFT were transferred from the OSTRF plant to the University of Alberta geotechnical laboratories for further experiments.

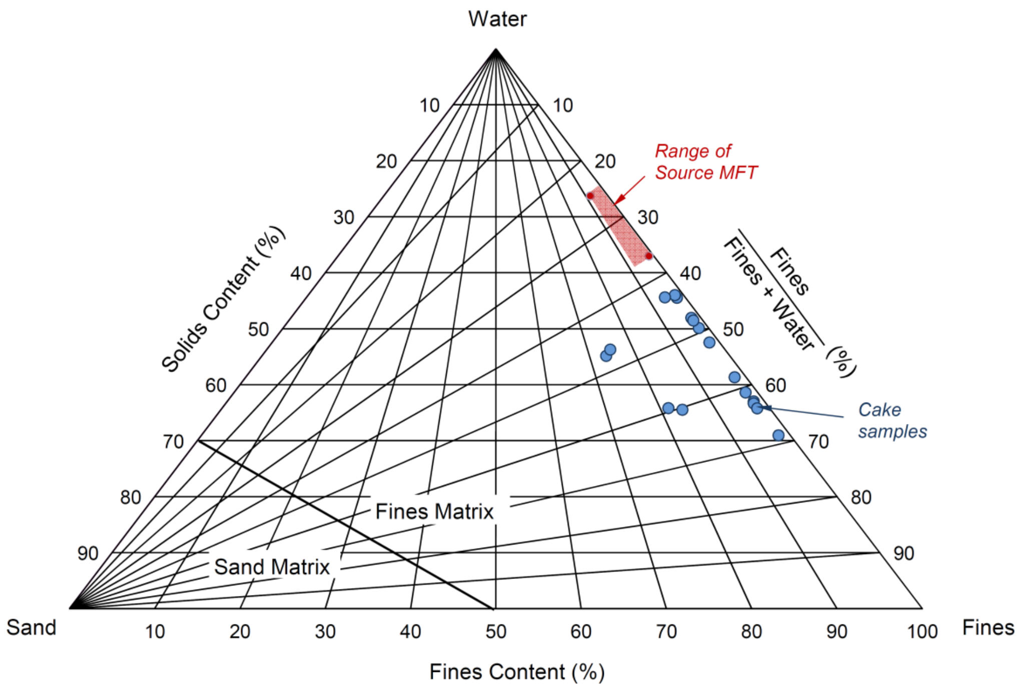

Figure 6.1- Position of the cake samples obtained in the filtering centrifuge tests on the slurry properties diagram.

Figure 6.2. The cake collected from the filter cloth and mixed within the pail.

Prior to making NST in the lab, it was necessary to determine the solids content of the centrifuged MFT, also its SFR (Sand to Fines Ratio). The SFR of the centrifuged MFT can be quite different from the SFR of the source MFT. The reason is that due to the centrifugal force that the material experiences inside the filtering centrifuge, segregation of the fine and coarse fractions occurs. As a consequence, percentage of the coarse particles can increase in the cake in comparison to the source MFT. After determining the solids content and SFR of the centrifuged MFT, the required amount of each component for making NST (i.e. Sand, MFT Cake and Pond Water) was determined. For this purpose the multiphase mass-volume relationships developed by Scott and Boratynec (2003) were used.[2] A group of diagrams showing the parametric solution of these relationships for the specific case of SFR=4 were presented in Figure 4.1.

As mentioned in Chapter 2, in the field production of CT/NST phosphogypsum is added to MFT as a coagulant and the resultant stream is mixed with sand. The sand is sourced from the cyclone underflow and [at ideal/on-spec operation conditions] is expected to have a solids content between 70 to 75%. In this study, the sand used for making NST had a solids content of about 98.8% and was relatively dry. In order to increase water content of the sand similar to its field value, pond water (associated with each source MFT) was added. The concentrated MFT obtained from the filtering centrifuge tests was added to this mixture of sand and pond water to create Non-Segregating Tailings (NST). Because phosphogypsum had already been used for treatment of MFT during the centrifugation stage, no additional gypsum was added to make the NST. Also for the centrifuged MFT's that were produced without addition of gypsum, no further gypsum was added to the NST mixture. The purpose of these specific tests was to investigate the possibility of making NST with no chemical amendments. To ensure obtaining a homogenous CT/NST mixture, a dual blade mortar mixer was utilized to prepare each NST mixture.

For comparison purposes, in addition to the NST samples made from centrifuged MFT, a limited number of CT samples were also produced by mixing regular MFT, gypsum, sand

[2] A handy computer program based on these correlation developed by Marvin Silva (1999) was used for calculation of the NST proportions.

and pond water. The complete list of the NST and CT samples produced is presented in the results section (Table 6.1).

6.3. Characterization Tests

The flow properties and robustness of the NST's produced were studied by using a flume and a strain-controlled viscometer. Detailed procedure of the yield stress measurements by means of a viscometer was previously explained in Chapter 4. In the following section first a brief review of the common types of flume deposition tests will be provided and then the detailed procedure of the flume tests conducted in the present research will be explained.

6.3.1. Common Types of Flume Deposition Tests

Review of the literature indicates two general types of flume deposition tests have been of interest. In the first type, common for hydraulic-fill studies, the "similarity of process" approach proposed by Hooke (1968, cited by Kupper et al., 1992) is used. In this approach direct extrapolation of the results from laboratory to field is not possible, but qualitative conclusions resulted from the experiments are still applicable to the field operations. To conduct the test, a continuous flow of the slurry (solid-liquid mixture) is deposited into the flume for a specific duration of time to determine the equilibrium slope[3] for a particular set of deposition conditions. After the deposition stops and the flume is drained, the beach profile (geometry) and the deposit characteristics along the flume are determined (Kupper et al., 1992). Some examples of such flume deposition tests are the studies by Blight et al. (1985) on a variety of mine tailings, the flume deposition of sand-water mixtures by Kupper (1991) and Kupper et al. (1992) and flume deposition modeling of caustic and non-caustic oil sands tailings by Miller et al. (2009). A flume with adjustable inclination was used by Pirouz et al. (2006) to determine the limiting equilibrium slope of a thickener underflow at Peak Gold Mines in NSW Australia.

To determine the flow characteristics of solid-liquid mixtures with higher concentration (e.g. thickened tailings or paste), another type of flume design and test procedure is

[3] Equilibrium slope is defined as the slope at which sedimentation and erosion are in balance (De Groot et al., 1988; cited by Mihiretu, 2009).

common. In these tests usually a limited volume of tailings is instantly discharged into the flume and then the flow profile and the deposit characteristics along the flume are determined. This type of flume was utilized in the present study; more details are provided in the following section.

6.3.2. Flume Tests in the Present Study

Figure 6.3 illustrates the flume apparatus that was designed to investigate the depositional behaviour of NST under laboratory conditions. Other researchers have used similar flume designs to study the depositional behaviour of tailings (Sofra and Boger, 2001; Kwak et al., 2005; Simms, 2007; Henriquez and Simms, 2009) or flow of other solid-liquid mixtures (Balmforth et al., 2007; Ancey and Cochard, 2009).

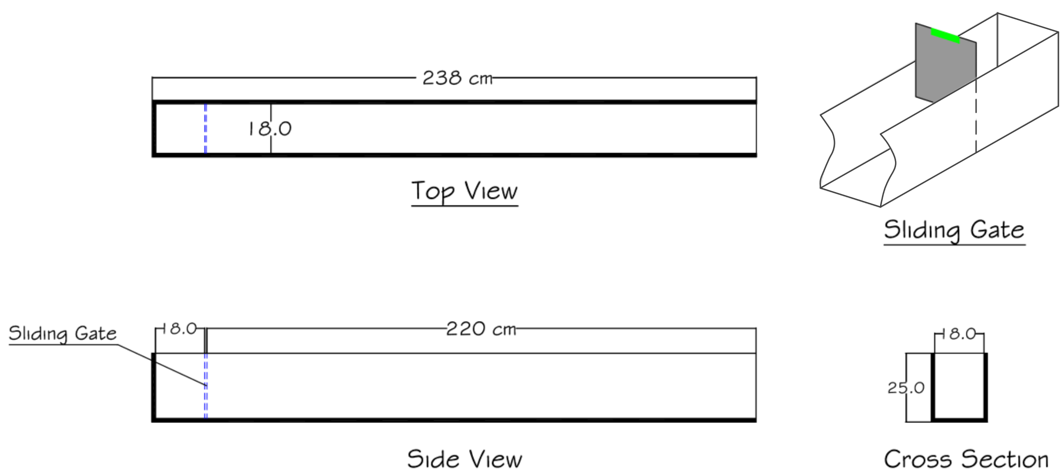

Figure 6.3. Flume apparatus designed for studying flow and robustness of NST samples

The flume was made of ~12mm thick acrylic sheets with high optical quality (Figure 6.4). The total length of the flume was about 240cm with an internal width of 18cm. A sliding gate was devised at the closed end of the flume. When this gate was closed, it created a reservoir with a volume of about 8 liters. The NST sample was poured into this reservoir up to a certain thickness (same volume of material was used for all of the flume tests); then the gate was quickly lifted upwards, letting the NST flow along the flume until it came to rest. As depicted in Figure 6.4, a graph paper covered the back side of the flume, which helped measuring the flow profile and its runout length more precisely. To obtain the flow profile in each flume test, thickness of the deposited NST was measured by means of a ruler at 10cm intervals along the flume centre line and at shorter intervals at the front edge of the flow foot print (Figure 6.5).

All deposition tests were recorded using a digital video camera. The intent was to record duration of the flow for each NST sample. As will be shown in the results section, duration of the flow can be correlated with yield stress of the material.

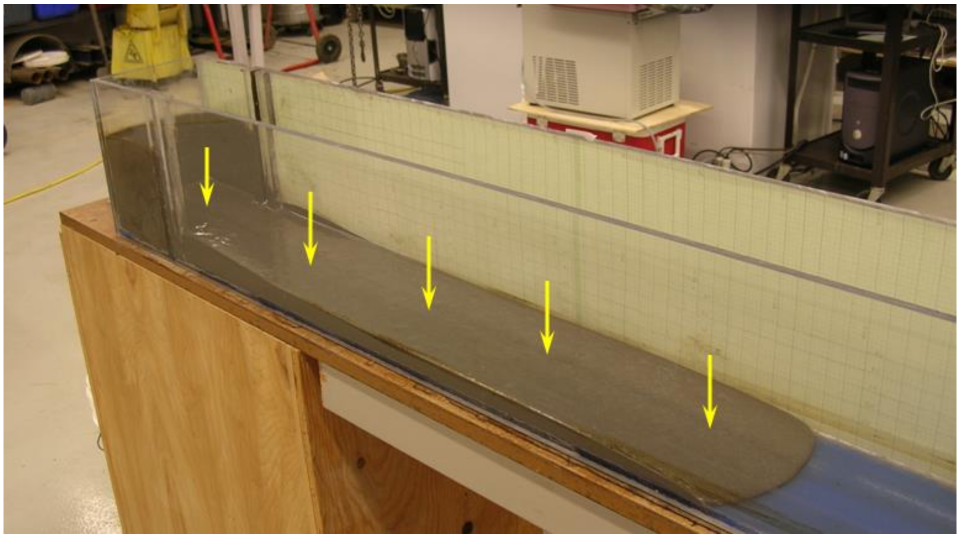

Figure 6.4 – A flume deposition test; arrows along the deposited slurry indicate location of the samples taken for segregation analysis.

Figure 6.5 - Measuring thickness of the deposited NST along the flume centerline to capture the flow profile.

To characterize the NST used for each flume deposition experiment, a 300ml Snapseal® container was filled with a sample of NST and its solids content and SFR were determined. Also a 600ml beaker was filled with a sample of NST and immediately vane shear tests were conducted on it at a strain rate of 0.1 rpm to measure yield stress of the material. A strain controlled viscometer (Brookfiled Digital Viscometer - Model DV-II+) with vane spindles, as previously explained in Chapter 4, was used for this purpose.

To evaluate the level of hydraulic sorting (segregation) along the flume, samples of NST were taken at five or six spots along the centre line of the deposited material (Figure 6.4). Each sample was placed inside a container and later was characterized. Characterization tests comprised of solids content measurement using oven drying and washing over sieve #325 to measure the fines content and the sand to fines ratio.

6.4. Results and Observations

Table 6.1 presents the detailed information for 11 CT/NST samples made from regular MFT and filtered/centrifuged MFT, along with their associated flume and vane test results. These tests were conducted at the University of Alberta geotechnical laboratories. For each CT/NST sample the following information are provided:

- Sample identification, indicating the source of tailings material
- Solids content of the component MFT or Cake
- Amount of gypsum used (either for making CT from MFT, or during centrifugal filtration of MFT to produce cake)
- Solids content and SFR of the resultant CT/NST
- Vane test results:
    - Yield stress (the [initial] peak value observed in the stress history diagram)
    - Maximum elastic yield stress (the stress at the transition between the elastic and viscoelastic regions in the stress history diagram)
- Flume test results:
    - Average slope of the equilibrium profile
    - Duration of the flow (i.e. the time interval between opening the reservoir gate and flow coming to arrest)
    - Robustness Index (explained in Sec. 6.4.1.1)

Table 6.1. List of CT/NST samples and their associated vane and flume test results

Test ID	SC of the MFT/Cake (%wt)	Gypsum (ppm)	SC of the NST (%wt)	SFR	F/(F+W) (%)	Yield Stress (Pa)	Max Elastic Stress (Pa)	Average Slope (%)	Duration of flow (sec)	Robustness Index
Albian NST-1	37.05 (MFT)	600	60.91	4.04	23.62	20.63	16.67	0.57	1.868	287.3
Albian NST-2	64.2 (Cake)	600	73.11	4.05	35.00	53.30	33.63	1.25	1.409	857.4
Albian NST-3	37.05 (MFT)	600	61.66	4.02	24.26	28.34	20.70	0.64	1.813	307.0
Albian NST-4	64.48 (Cake)	600	69.34	4.99	27.41	19.47	13.01	0.63	2.130	476.9
Syncrude NST-1	37.66 (MFT)	600	62.81	4.3	24.17	25.06	17.63	0.44	2.193	391.5
Syncrude NST-2	44.41 (Cake)	300	66.91	4.04	28.63	28.34	19.66	0.63	1.999	604.0
Syncrude NST-3	64.21 (Cake)	No Gypsum	73.72	4.31	34.57	33.73	20.50	0.69	1.733	1095.0
Syncrude NST-4	44.47 (Cake)	600	65.31	4.19	26.62	17.44	11.66	0.53	2.562	284.4
Suncor NST-1	26.29 (MFT)	900	53.14	5.56	14.61	8.10	6.07	0.29	2.560	67.2
Suncor NST-2	54.85 (Cake)	600	66.7	6.1	22.00	16.48	13.20	0.45	2.394	229.1
Suncor NST-3	53.73 (Cake)	600	68.95	4.06	30.50	32.77	20.80	0.80	2.037	481.2

Note: As stated in Chapter 2, by definition the engineered tailings stream produced by addition of sand to coagulated MFT is called CT (Composite Tailings); and addition of sand to treated thickened tailings will result in NST (Non-Segregating Tailings). In the above table, for simplicity, all the samples whether made from regular MFT or from Cake (dewatered MFT) are referred to as NST.

In addition to the flume test results presented in Table 6.1, the equilibrium profiles captured for each individual flume test are illustrated in Figures 6.19 to 6.29. Further discussion on the flow profiles will be provided in section 6.4.5.

Prior to discussing individual flume tests in more detail, the position of all the produced CT/NST samples on the ternary diagram will be reviewed and patterns made on this diagram by the samples collected along the flume will be discussed.

6.4.1. Position of the CT/NST samples on the Slurry Properties Diagram

As previously stated, prior to each flume deposition test a 300 ml container was filled with a sample of CT/NST and later the average solids content and SFR of this sample were determined. Based on these characterization tests, in Figure 6.6 positions of the CT/NST samples presented in Table 6.1 are illustrated on the ternary diagram. In this figure, the source MFT and cake samples are marked as small circles and the CT/NST's produced from them are marked as small triangles. The three example dashed lines with arrows indicate that the CT/NST samples illustrated in a specific color were made from their component MFT/cake shown in the same color.

As can be observed in Figure 6.6, using filtered/centrifuged MFT enabled production of CT/NST samples with solids contents higher than 65%. These CT/NST samples are well below the segregation boundaries discussed in Chapter 2. Producing a concentrated CT/NST by utilizing regular MFT is hardly practicable during field operations, mainly due to variations of the solids content of the feed MFT and cyclone underflow. Dewatering MFT and using it as a component of CT/NST will partially mitigate the effect of cyclone underflow fluctuations and will ensure availability of a relatively uniform fines stream in terms of solids content for CT/NST production.

In Figure 6.7 the position of the CT/NST samples taken along the flume centerline in each deposition test is illustrated. It can be observed that at lower solids concentrations the samples along the flume show a scattered pattern on the ternary diagram, indicating variations of SFR and solids content. As the solids content of the CT/NST sample increases, the data points representing the different samples along the flume get closer to each other and show a more concentrated pattern on the ternary diagram. This indicates that decreasing the water content of CT/NST (or increasing the (F/F+W) ratio) results in a

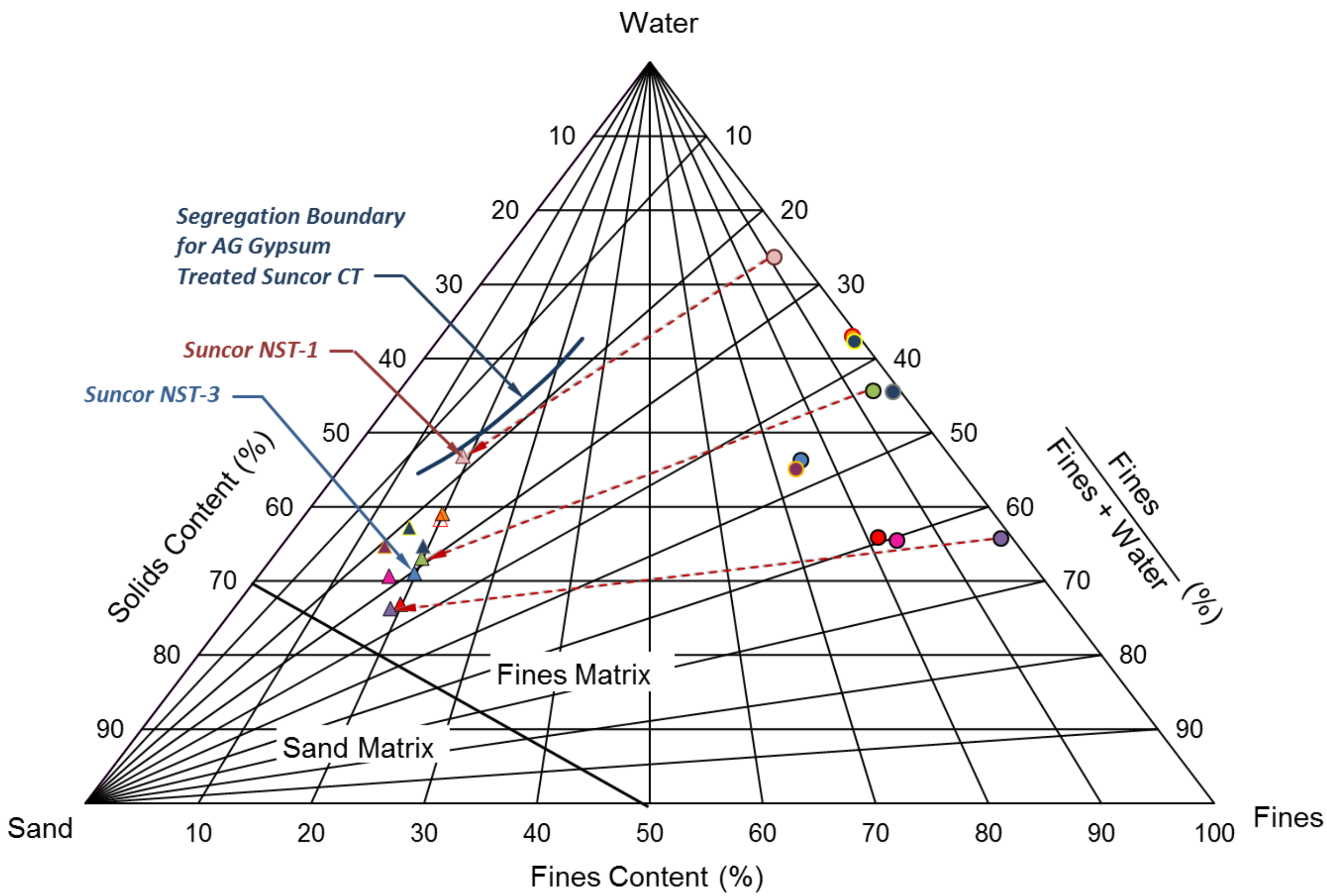

Figure 6.6. Position of CT/NST's made from a variety of MFT/Cake samples on the ternary diagram. The three example dashed lines with arrows indicate that the CT/NST samples illustrated in a specific color were made from their component MFT/Cake shown in the same color.

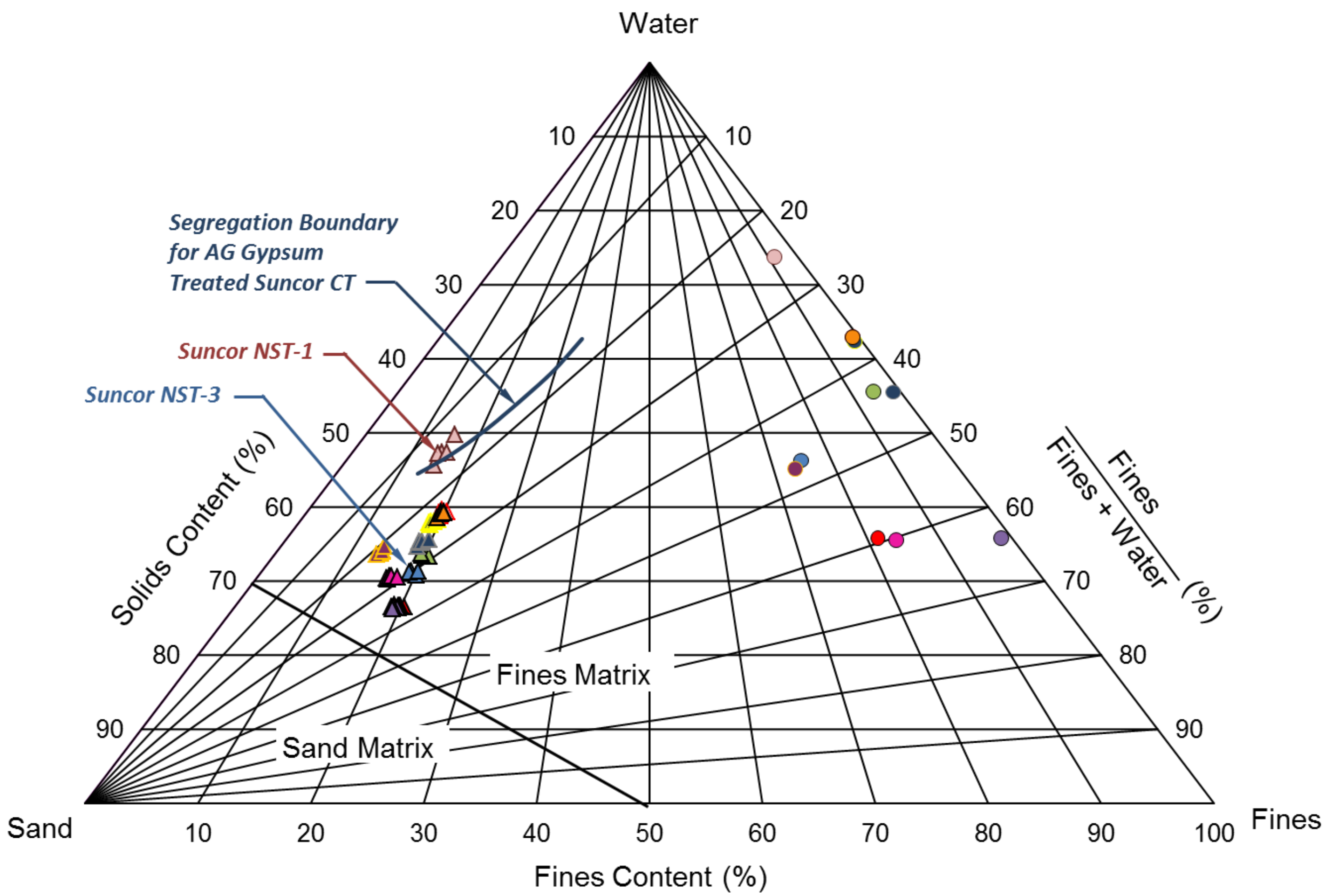

Figure 6.7. Position of the CT/NST samples taken along each flume deposition test on the ternary diagram

more robust tailings stream in which variations of the SFR and solids content along the beach (i.e. due to hydraulic sorting or segregation) is reduced.

One example of a "non-robust" CT is the Suncor NST-1 in Table 6.1, marked in Figure 6.6. Obtaining a CT at this range of solids content is not uncommon during field operations, particularly when the cyclone underflow or the source MFT pumped from the pond have lower solids content than the design requirements. Although this example CT locates below the static segregation boundary of gypsum treated Suncor tailings shown in Figure 2.8 (Chapter 2), but after deposition into the flume the samples collected along the beach show a scattered pattern on the ternary diagram. These samples are marked in Figure 6.7. It should be noted that after deposition into the flume, this sample did not stop flowing before reaching the flume end and part of the material dropped out of the flume. Higher SFR values of Suncor NST-1 samples in Figure 6.7 in comparison to average SFR of the original sample in Figure 6.6 indicate that the coarse fraction settled in the flume and part of the fines are lost due to segregation.

To make a more robust CT/NST, Suncor NST-3 (shown in Table 6.1 and Figure 6.6) was made from cake and mixture of sand and water. It should be noted that dosage of gypsum for Suncor NST-3 was 33% less than Suncor NST-1. In Figure 6.7 position of the samples collected after deposition of Suncor NST-3 into the flume is illustrated. As can be observed, these samples show a more concentrated pattern. Making a CT/NST at this solids content, which keeps a sufficient margin from the segregation boundary, will mitigate the risk of segregation due to cyclone underflow fluctuations or due to shearing caused by high discharge energy conditions.

6.4.1.1. Quantitative Comparison of CT/NST Robustness

Based on the above observations, the statistical measures of dispersion (or "scatteredness") can be used to quantitatively compare the variations of solids content and/or fines content for different flume tests. The author suggests using a combination of both solids and fines content measurements to calculate the "Robustness Index". For *"n"* samples collected at almost equal intervals along a flume (or along a beach, at the same approximate depth), the Robustness Index can be defined as:

$$RI = \left[\sqrt{\left[MD(SC)/\overline{SC}\right]^2 + \left[MD(FC)/\overline{FC}\right]^2}\right] / \left[\left(MD(SC)/\overline{SC}\right).\left(MD(FC)/\overline{FC}\right)\right] \quad (6.1)$$

where *MD (SC)* and *MD (FC)* are the Mean Deviation[4] of the solids content and fines content of the samples taken along the flume:

$$MD(SC) = \frac{1}{n}\sum_{i=1}^{n}\left|SC_i - \overline{SC}\right| \tag{6.2}$$

$$MD(FC) = \frac{1}{n}\sum_{i=1}^{n}\left|FC_i - \overline{FC}\right| \tag{6.3}$$

and $\overline{SC}$ and $\overline{FC}$ are the mean values of the solids content and fines content:

$$\overline{SC} = \sum_{i=1}^{n}\frac{SC_i}{n} \tag{6.4}$$

$$\overline{FC} = \sum_{i=1}^{n}\frac{FC_i}{n}, \tag{6.5}$$

Equation (6.1) results in a nonnegative real number (RI) which has an inverse correlation with perimeter of the scattered zone covered by these *n* samples on the ternary diagram. The larger RI values represent a more robust tailings stream, i.e. the scattered zone will be smaller, indicating less variations of SC and FC along the flume. This index is a useful tool for comparison of robustness of flume tests conducted at different testing conditions. In Table 6.1 the calculated values of RI are presented for the flume tests. Figure 6.8 shows the variations of robustness index with F/(F+W) ratio for all of the flume tests. It can be observed that the robustness index (RI) increases exponentially with the increase of F/(F+W) ratio.

It should be noted that other methods of quantitative evaluation of segregation have been previously suggested by a number of researchers at the University of Alberta. Suthaker (1995) proposed a segregation index for static segregation tests (i.e. column sedimentation tests) based on variations of the solids content along depth of the column. This index was used by Tang (1997) for characterization of segregation behavior of CT. Mihiretu (2009) provided a comprehensive review of different method of measuring segregation and mixing. He suggested the following index for quantitative measurement of segregation in static tests and stated that the suggested method could also be used for dynamic segregation tests (i.e. flume tests) (Mihiretu, 2009):

[4] Mean Deviation or Mean Absolute Deviation is a measure of statistical dispersion and is equal to average of the absolute deviations of a set of data taken from a central (mean) value (Agarwal, 2006).

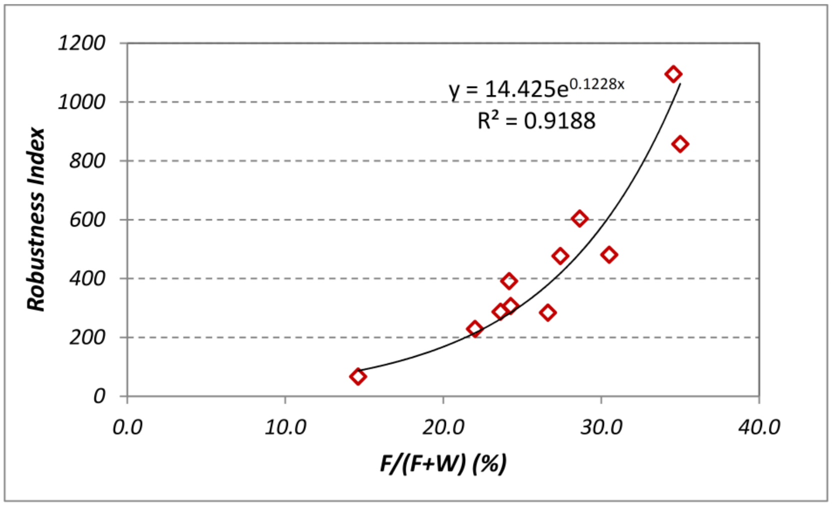

Figure 6.8 – Variations of Robustness Index with F/(F+W) ratio for all of the flume tests.

$$SI = \sqrt{\frac{\left(\sum h_i S_i^2 - \frac{(\sum h_i S_i)^2}{\sum h_i}\right)}{\sum h_i}} \tag{6.6}$$

where SI is the segregation index and S_i is the solids content of the sample section i along the standpipe (or flume) with the height (or length) of h_i.

Donahue et al. (2008) stated that Segregation index for static segregation tests may be computed based on the solids or fines content of each layer. For high SFR values of 5:1 and 6:1, they suggested using solids content; and for lower SFR values of 4:1 or lower they recommended using fines content (Donahue et al., 2008). They defined "fines capture index" equal to "100% minus the segregation index. Their suggested equation for calculation of the segregation index using solids content is as follows (Donahue et al., 2008):

$$SI = \frac{\sum|(s_n - s_{ave}) * (H_n - H_{n+1})|}{s_{ave}} * 100\% \tag{6.7}$$

where s_n is the solids content at slice n along the standpipe, s_{ave} is the average solids content along the total height of the sample, and H_n – H_{n+1} is the normalized height of the slice n in the standpipe.

Sorta and Sego (2010) used Equation (6.7) to find the segregation index in their tests while studying segregation boundary of the oil sands tailings at a range of relative centrifugal accelerations.

In Appendix A, detailed results of the flume deposition tests conducted in the present study are presented. Also the robustness and segregation indices calculated according to equations (6.1), (6.6) and (6.7) are provided. The segregation indices calculated from equation (6.7) were slightly smaller than the values resulted from equation (6.6). Figure 6.9 presents a comparison of the robustness index and segregation index (calculated using equation (6.7)) for the flume tests. It can be observed that the two parameters have an inverse correlation and SI values less than 10% (i.e. non-segregating) are approximately equivalent to RI values higher than 700. From Figure 6.8, this correlates with F/(F+W) ratios of about 32% and higher. It should be noted that Mihiretu (2009), in his segmented vertical standpipe tests, observed that increasing the F/(F+W) ratio to higher than 30% resulted in a non-segregating slurry.

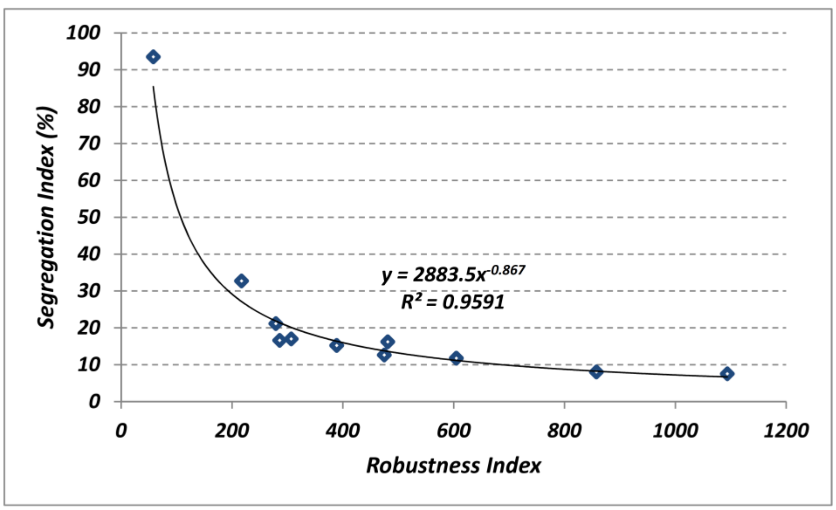

Figure 6.9 -Variations of Robustness Index with Segregation Index [calculated based on Equation (6.7)] for the flume deposition tests.

6.4.2. Comparison of Flume Test Results

The following sub-sections provide a detailed comparison of some of the flume tests summarized in Table 6.1.

6.4.2.1. Albian CT and NST made with 600ppm gypsum

Figure 6.10.a shows two examples of the flume test equilibrium profiles for CT and NST made using Albian Sands MFT and cake accordingly. Table 6.2 provides the related information for each test. As stated in this table, Albian NST-1 (CT) is made by adding 600ppm gypsum to regular MFT at a solids content of 37.05%wt. Solids content of the resultant Albian NST-1 is about 60.91% and the vane shear test has resulted in a yield stress of 20.63 Pa for this material. On the other hand, Albian NST-2 is made from filtered/centrifuged MFT. The amount of gypsum used during production of the MFT cake was 600ppm and the resultant cake has a solids content of 64.2%wt. Solids content of the Albian NST-2 made from this cake is about 73.11%wt. From Figure 6.10.a it can be observed that Albian NST-2 has a significantly steeper angle of repose and a smaller runout length; therefore a smaller land footprint will be required for storage of this material. Figures 6.10.b and 6.10.c illustrate the variations of SFR along the profile of each test. Figure 6.10.b shows a constant decrease in the value of SFR which can be interpreted as hydraulic sorting (segregation) along the flume; i.e. the percentage of coarse particles decreases as the material finds its way towards the end of the flume. The position of Albian NST-2 samples on the ternary diagram shows that there is sufficient margin between these samples and the segregation threshold, so fluctuations of the cyclone underflow can be partially mitigated. The Albian NST-1 sample however, is more susceptible to fluctuations of the feed and segregation.

Table 6.2 – Samples of NST made from Albian Sands MFT/Cake

Test ID	SC of the MFT / Cake (%wt)	Gypsum (ppm)	SC of the NST (%wt)	SFR	Yield Stress (Pa)	Average Slope (%)	Duration of flow (sec)	Robustness Index
Albian NST-1	37.05 (MFT)	600	60.91	4.04	20.63	0.57	1.868	287.3
Albian NST-2	64.2 (Cake)	600	73.11	4.05	53.30	1.25	1.409	857.4

(a)

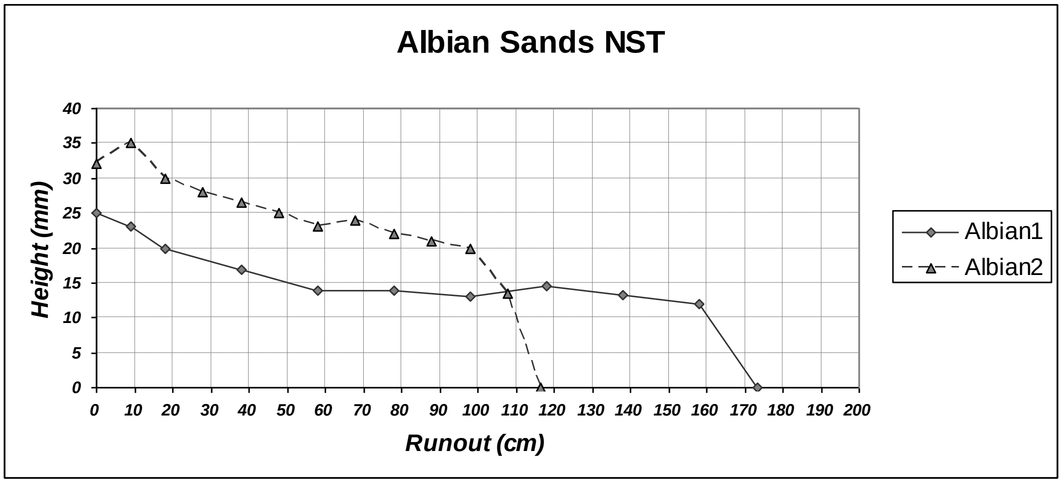

(b)

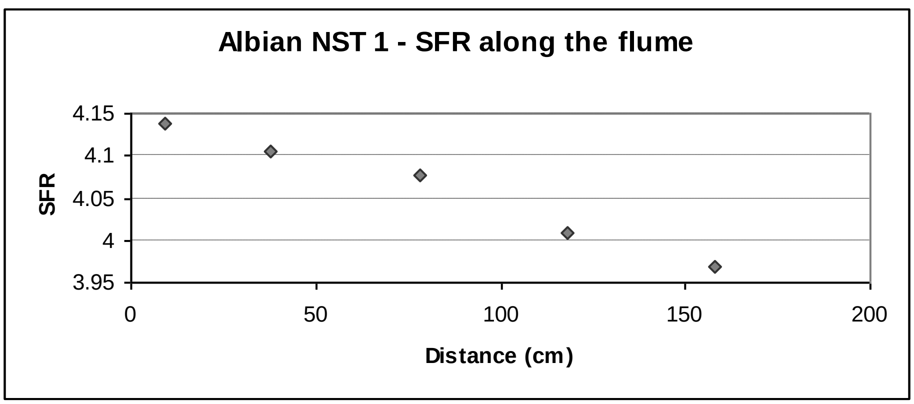

(c)

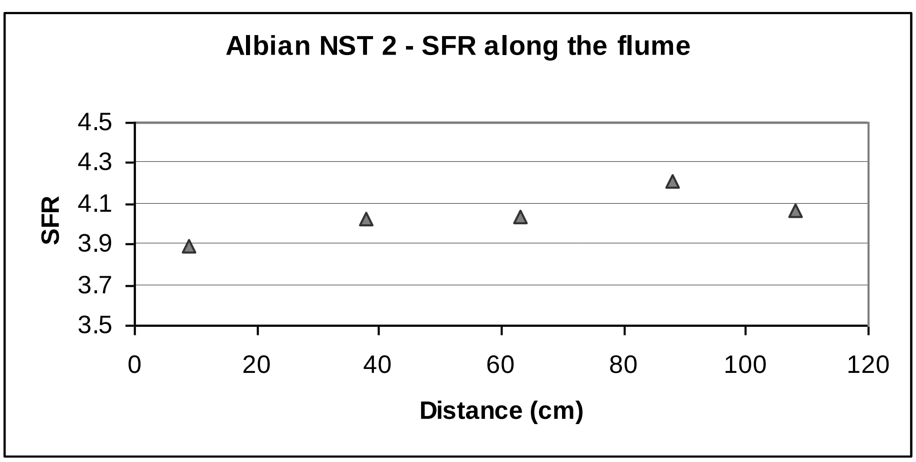

Figure 6.10.(a) Flow profile of the flume deposition tests Albian-NST1 and Albian-NST2 (b) and (c): Variations of SFR along the flume for each test

6.4.2.2. Syncrude CT and NST samples made with varying gypsum contents

Figure 6.11.a illustrates flow profiles of three flume tests conducted on CT and NST's made from Syncrude MFT/Cake. Table 6.3 provides the related information for each test. Syncrude-NST1 (CT) was made by adding 600ppm gypsum to regular MFT at a solids content of 37.66%wt. Solids content of the resultant Syncrude NST-1 was about 62.81% and the vane shear test showed a yield stress of 25.06 Pa. The other two NST samples, Syncrude NST-2 and 3 were made from filtered/centrifuged MFT and have a solids content of 66.91% and 73.72%. The thick MFT used for Syncrude NST-2 had been produced by adding 300ppm gypsum prior to centrifugal filtration, while the MFT paste used for making Syncrude NST-3 had been produced without addition of any gypsum. The flow profiles illustrated in Figure 6.11.a indicate that using concentrated MFT as a component of NST leads to significantly higher angles of deposition. In the meantime, it can be observed that by dewatering MFT the amount of coagulant required to create a more robust NST can be reduced. Figures 6.11.b to 6.11.d show that as the concentration of the tailings stream is increased, variations of the SC along the flume are reduced, in other words a more robust tailings stream is achieved.

Table 6.3 - Samples of NST made from Syncrude MFT/Cake

Test ID	SC of the MFT / Cake (%wt)	Gypsum (ppm)	SC of the NST (%wt)	SFR	Yield Stress (Pa)	Average Slope (%)	Duration of flow (sec)	Robustness Index
Syncrude NST-1	37.66 (MFT)	600	62.81	4.3	25.06	0.44	2.193	391.5
Syncrude NST-2	44.41 (Cake)	300	66.91	4.04	28.34	0.63	1.999	604.0
Syncrude NST-3	64.21 (Cake)	No Gypsum	73.72	4.31	33.73	0.69	1.733	1095.0

It should be noted that although Syncrude NST-3 was created with no chemical additive and achieved a high angle of deposition, this material does not completely satisfy the requirements of a successful tailings management plan. The reason is that due to absence of the chemical additives, segregation of the coarse and fine particles occurs within the filtering centrifuge and the resultant paste (cake) contains only about 30% of the fine particles (see Chapter 5, section 5.5.2.2, Figures 5.21.a and b). On the other hand, Syncrude NST-2 can be regarded as a suitable blend for tailings management purposes. In comparison to the conventional CT/NST mixtures, robustness and angle of deposition of this NST has been improved, also the amount of the coagulant used in this mixture is reduced resulting in a lower amount of the Ca^{2+} ions in the recovered water. Addition of this minimum amount of gypsum to MFT and the delay time applied to the MFT-Gypsum mixture before centrifuging it results in almost 100% capture of the fines within the cake. This issue was discussed in Chapter 5, section 5.5.2.3.

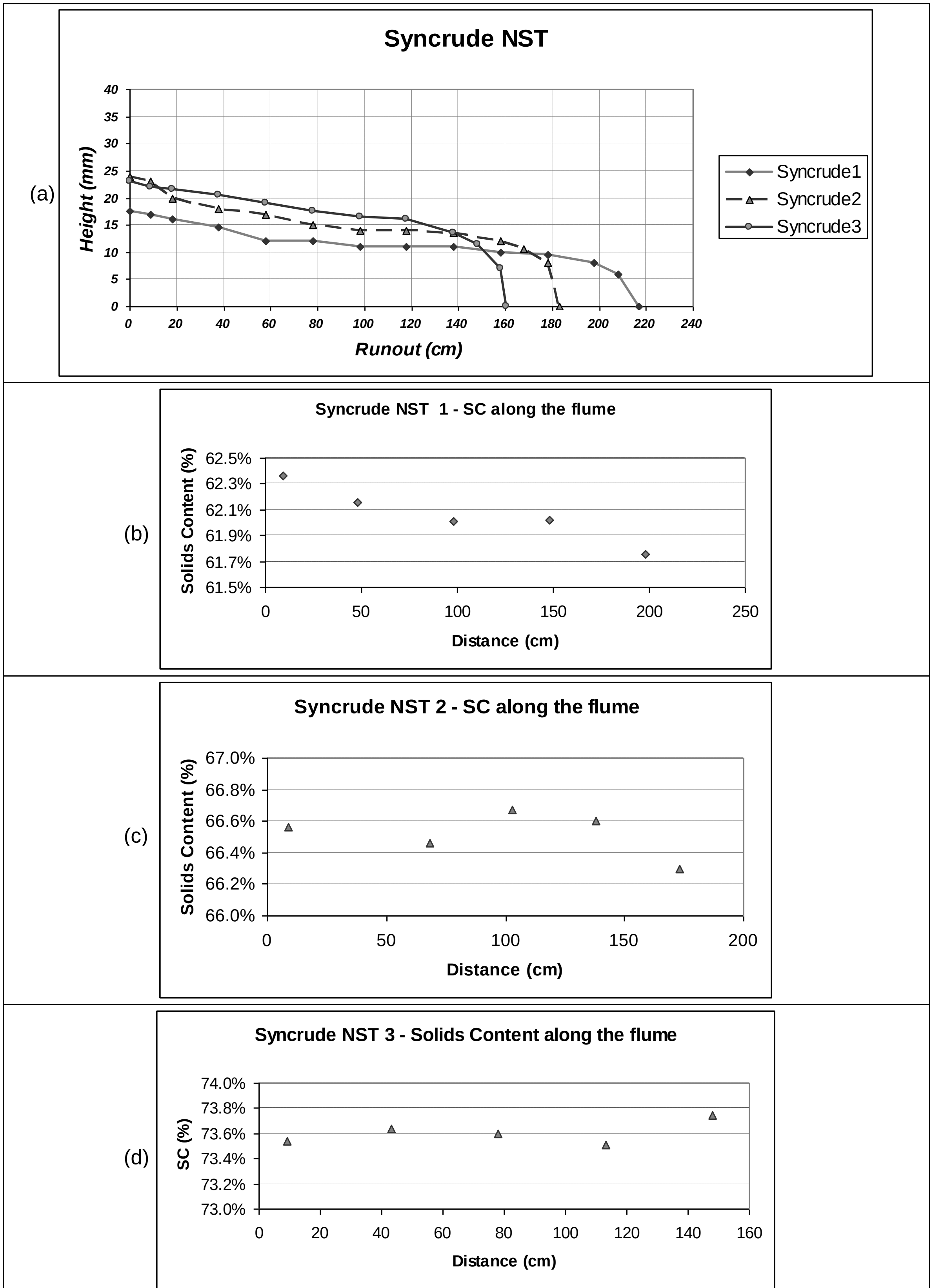

Figure 6.11. (a) Flow profile of the flume deposition tests Syncrude-NST1, NST2 and NST3 (b), (c) and (d): Variations of solids content along the flume for each test

6.4.3. Effect of delay time after addition of gypsum on the yield stress of MFT and CT

In Chapter 5, section 5.5.2.3, it was explained that applying a delay time after addition of gypsum to MFT resulted in a more flocculated structure and capture of almost all the fine particles within the cake during centrifugal filtration. Following this observation, it was deemed important to study if applying some delay time to the mixture of MFT and gypsum can improve the quality of the CT produced.

For this purpose two CT samples with similar characteristics were made (Table 6.4, tests Albian NST-1 and 3). For Albian NST-1, the MFT treated with gypsum was left aside for one hour and then the sand and water were added to it to make CT. For preparation of Albian NST-3, 600ppm gypsum was mixed with MFT and sand and water were added to it instantly. Figure 6.12 shows the flow profiles of the flume test for these two samples. These equilibrium profiles are very similar, as can be expected from the close yield stress values of the two samples (Table 6.4). Apparently, the process of mixing the sand and water with the flocculated MFT results in breakage of the flocs and the delay time applied after treatment of the MFT does not have a significant effect on yield stress of the final product. For Albian NST-3, it appears that the flocculation process continues during the mixing, resulting in a higher yield stress. This phenomenon is discussed further in the following sub-section.

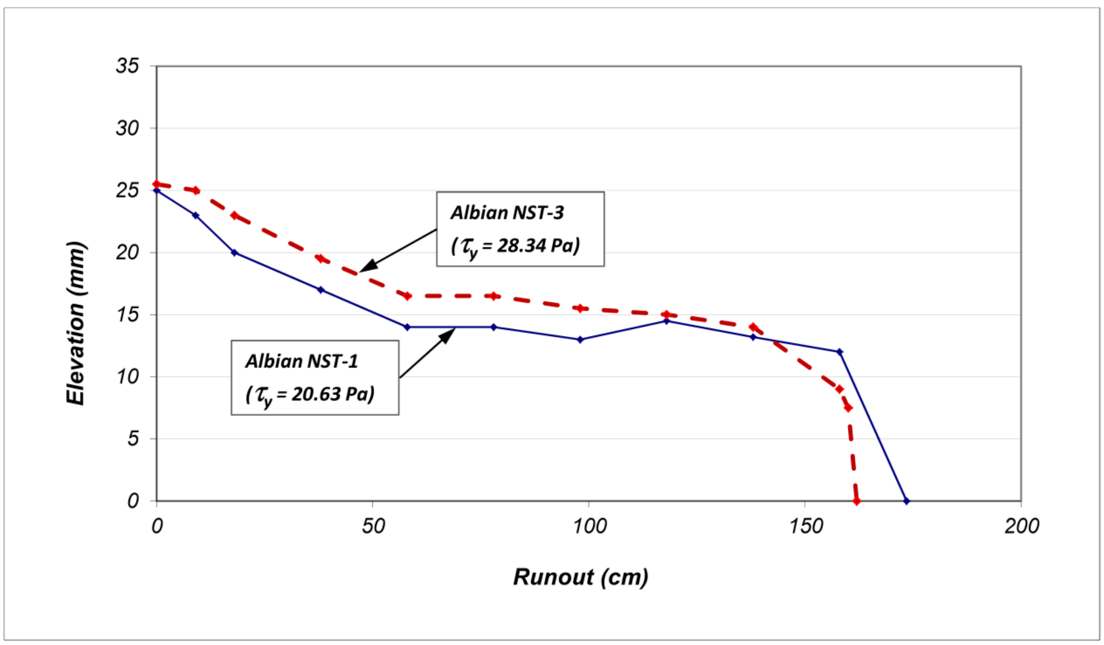

Figure 6.12 – Comparison of the flow profile for Albian NST-1 and Albian NST-3

Table 6.4 - CT samples made from Albian MFT, with and without delay after addition of gypsum

Test ID	SC of the MFT / Cake (%wt)	Gypsum (ppm)	SC of the NST (%wt)	SFR	Yield Stress (Pa)	Average Slope (%)	Duration of flow (sec)	Robustness Index
Albian NST-1	37.05 (MFT)	600	60.91	4.04	20.63	0.57	1.868	287.3
Albian NST-3	37.05 (MFT)	600	61.66	4.02	28.34	0.64	1.813	307.0

6.4.3.1. Effect of delay time on the yield stress of treated MFT

To study the effect of delay time on yield stress of the treated MFT, vane shear tests were conducted on three samples of Albian Sands MFT, each treated with 600ppm gypsum under the following testing conditions:

- Case "A": Treated MFT was instantly tested after addition of gypsum;
- Case "B": Treated MFT was left aside for 1 hour before the vane test, no mixing or shearing was applied prior to the vane shear test; and,
- Case "C": Treated MFT was left aside for 1 hour and was sheared with a mixer blade before conducting the vane test.

All the vane tests were conducted at a strain rate of 0.1 rpm. Figure 6.13 illustrates the variations of vane shear for these three cases for two full rotations of the vane spindles (lasting 20 minutes). For Case "A", it can be seen that the shear strength of the slurry reaches to an initial peak value of ~40 Pa and then gradually increases with time. This indicates gradual solution/diffusion of the gypsum and formation of the flocs. For Case "B", which was tested one hour after the chemical treatment, the peak shear strength is ~106 Pa, almost 2.5 times higher than the initial peak value for Case (A). This indicates that the delay time has let the MFT slurry form a more flocculated structure. Shearing this flocculated structure with a mixer blade in Case "C" resulted in breakage of the flocs and reduction of the peak shear strength to ~60 Pa. Since during the processes of making and transportation of conventional CT/NST, this material is subject to high shear stresses, from the above discussion it can be concluded that applying a delay time after addition of gypsum to MFT will not affect the quality of the final product noticeably. Yet the time interval between adding the gypsum to the mixture and final discharge of the resultant CT/NST must be sufficient to allow desired/designed flocculation of the fines.

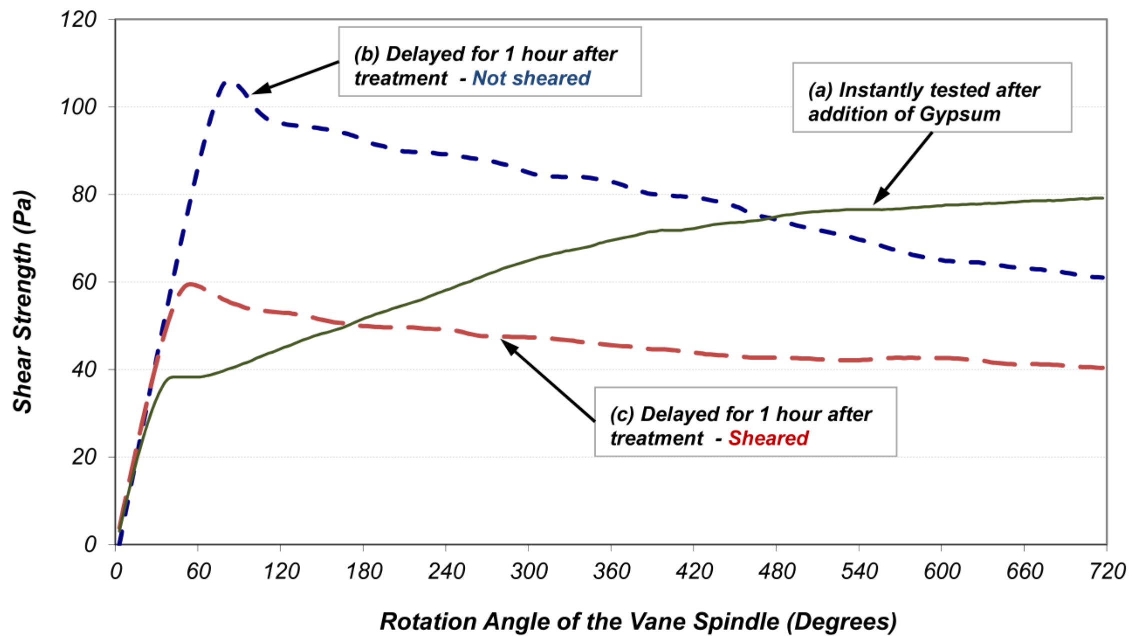

Figure 6.13. Variations of vane shear strength for Albian Sands MFT mixed with 600ppm gypsum:

(a) Treated MFT was instantly tested after addition of gypsum

(b) Treated MFT was left aside for 1 hour before the vane test

(c) **Treated MFT was left aside for 1 hour and was sheared before the vane test**

6.4.4. Correlation between the flow duration and yield stress

As previously stated, all of the flume tests conducted in this study were recorded using a digital video camera. The camera was not a high speed model, so in order to measure the flow duration with the highest possible precision, computer software was used to display the recorded movie at 25% of the original speed. A computer based chronometer was used to calculate the time between lifting the flume gate until the moment the material stopped flowing; this measured time was divided by 4 to obtain the real flow time. Figure 6.14 shows the correlation between the yield stress and flow duration for the samples presented in Table 6.1. Figure 6.15 shows the correlation between maximum elastic stress and flow duration for the same samples. Both diagrams show a linear correlation; however there seems to be a better correlation between the maximum elastic stress of the NST samples and the duration of flow in the flume. This seems reasonable because when the stress in the material reaches values lower than the maximum elastic stress, no further inelastic deformation occurs and the flow should stop.

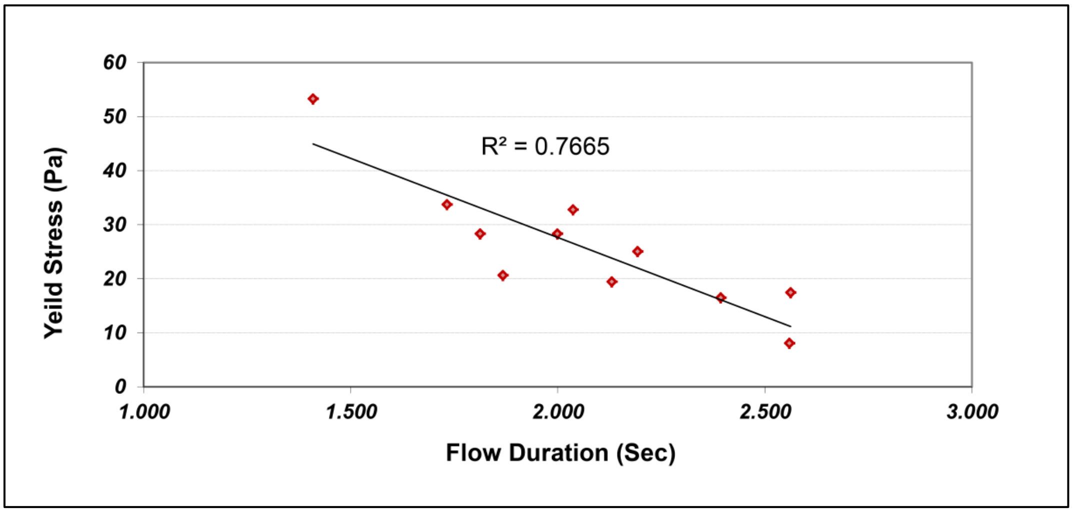

Figure 6.14. Correlation between yield stress and flow duration in flume tests

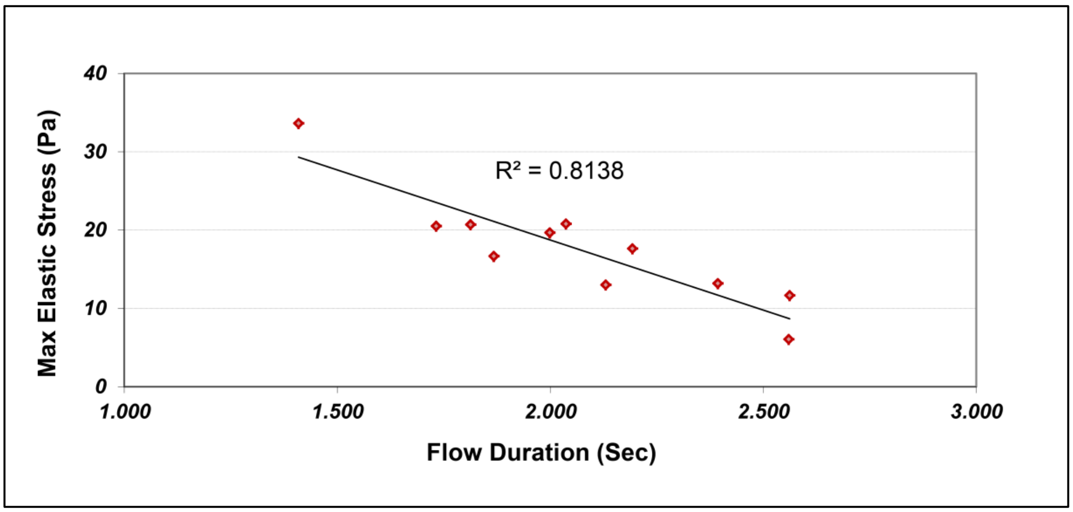

Figure 6.15. Correlation between maximum elastic stress and flow duration in flume tests

In recent years and specifically with the availability of high speed cameras, a number of studies has been conducted to correlate the velocity of the flow front in the flume with the material viscosity parameters (Balmforth et al., 2007; Ancey and Cochard, 2009). Similar studies can be conducted for CT/NST and dewatered MFT to provide a better understanding of their flow characteristics.

6.4.5. Correlation between the average angle of deposition and yield stress

Figure 6.16 shows the average surface slope of the deposited material in the flume tests versus the yield stress (i.e. the peak stress obtained from viscometer measurements). Figure 6.17 illustrates the variations of average surface slope with the maximum elastic stress (see Table 6.1). Both diagrams indicate that angle of repose appears to increase linearly with material strength. A slightly better correlation is obtained when the yield stress is used (Figure 6.16), and a smaller intercept for the trend-line is observed when the maximum elastic stress is used (Figure 6.17). In a series of experiments conducted on Bulyanhulu Gold Mine tailings and Kaolinite paste, Kwak et al. (2005) similarly found a smaller intercept when the maximum elastic strength was used instead of the yield stress. They decided to use the maximum elastic strength arguing that when the yield stress goes to zero the angle of repose should go to zero as well. For characterization purposes in the present research however, the peak yield stress obtained from viscometer measurements will be used. The reason is that determining the peak value in the shear stress-time curve is more practical and straight forward approach than determining the maximum elastic stress. In addition, plotting these two sets of data for the flume tests conducted in this study shows a close linear relationship between these two parameters (Figure 6.18). It should be noted that using the yield stress has also been recommended by Sofra and Boger (2001), Ngyuen and Boger (1985) and Boger et al. (2006).

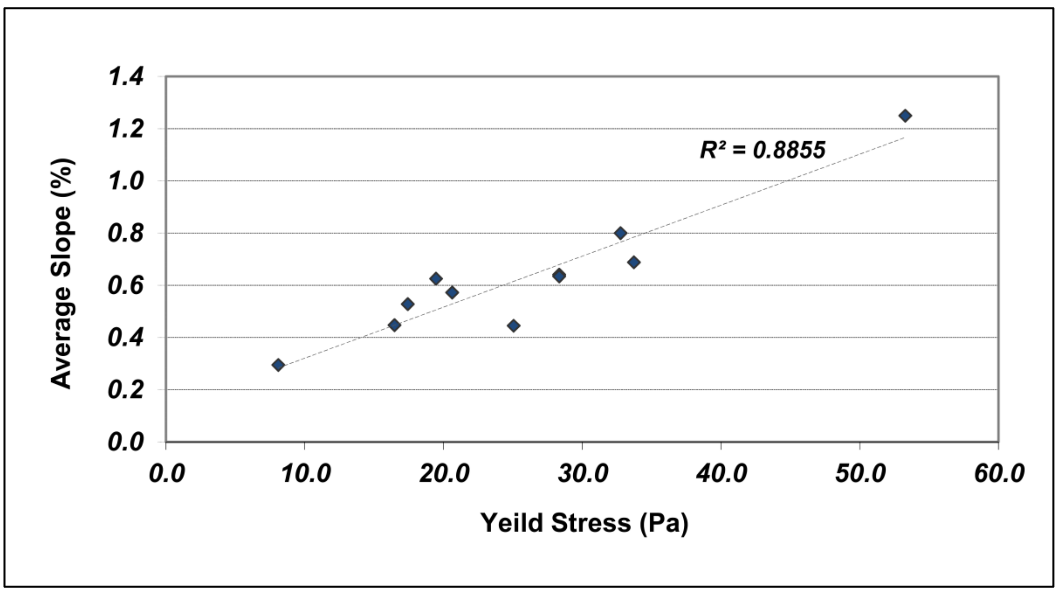

Figure 6.16. Correlation between yield stress and average beach slope of the deposited NST samples

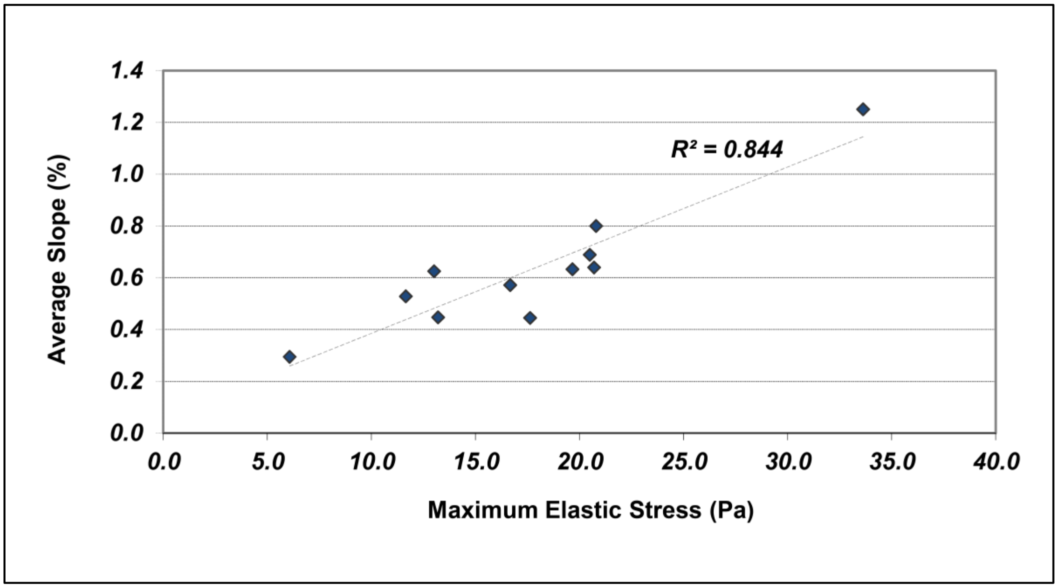

Figure 6.17. Correlation between maximum elastic stress and average beach slope of the deposited NST samples

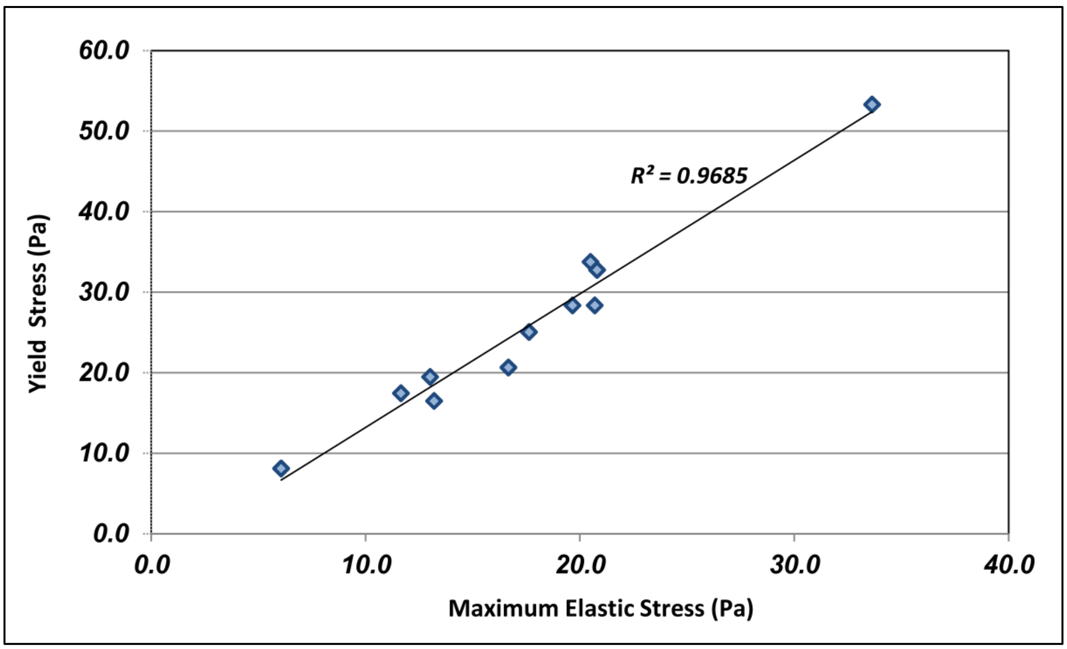

Figure 6.18. Correlation between the yield stress and the maximum elastic stress of the NST samples

6.4.6. Equilibrium profile of individual flume tests

The flow profiles captured for each of the flume deposition tests are illustrated in Figures 6.19 to 6.29 presented at the end of this chapter. In these figures in addition to the actual profile, a predicted equilibrium profile is also presented. These predictions are obtained based on the following equation that gives the steady-state profile of a Bingham fluid discharged on a flat bed (Henriquez and Simms, 2009):

$$h^2 - h_0^2 = \frac{2\tau_y}{\rho g}(x - x_0) \tag{6.9}$$

where h is the height of the free surface or the flow thickness at x and is measured perpendicular to x, h_0 is the height at x_0, τ_y is the yield stress, ρ is the bulk density and g is the acceleration due to gravity.

The above equation is a specific case of a theory presented by Liu and Mei (1989) for slow spreading of a thin sheet of Bingham-plastic fluid on an inclined plane. Equation (6.9) is derived using "Lubrication Theory" (considering the small ratio of flow thickness to its horizontal extent) and by simplifying the continuity and the momentum equations assuming the slow spreading (laminar flow) of a thin layer or film. Details of the derivation of this equation is presented by (Liu and Mei, 1989) and its application has been shown by Simms (2007) and Henriques and Simms (2009).

It should be noted that to apply the above equation, either h_0 (thickness of the deposited layer at the discharge point) or x_0 (run-out length of the deposited material) must be estimated. As can be seen in Figure 6.19 to 6.29, the run-out length x_0 and yield stress τ_y (obtained from viscometer measurements) were used as inputs to the above equation to obtain the predicted profile. Simms (2007) suggested using the flume test as a tool for evaluating yield stress of the tailings slurry, by putting x_0 and h_0 as inputs to the above equation and adjusting τ_y until a profile matching the actual profile is obtained.

From Figures 6.19 to 6.29, it can be seen that except for two cases (Fig. 6.20 and Fig 6.23) the equilibrium profile predicted by Equation (6.9) has a reasonable agreement with the measured flow profile. In the same figures it can be observed that in most cases, specifically at lower yield stress values, the measured flow profile shows a relatively flat slope at the center and steeper slopes at the ends. In the flume tests conducted by Henriques and Simms (2009) the same pattern was observed when the gate and reservoir method was used. These researchers stated that using the gate and reservoir method for deposition purposes involves significant release of potential energy and the inertia generated will be sufficient to violate the assumptions of lubrication theory. For this reason, rather than using a gate, they decided to use a funnel and poured the slurry into the flume through the funnel opening. They obtained a better agreement between the flow profile of the funnel method and the equilibrium profile predicted from lubrication theory (Henriques and Simms, 2009). Figure 6.30 shows a comparison of the profile obtained by reservoir and gate versus the one resulted from funnel tests in their study.

In the present study, the main objective of conducting the flume tests was to determine the hydraulic sorting along the deposited material. For this reason the high discharge energy conditions generated in the gate method could be more representative of the field deposition conditions and the funnel was not utilized.

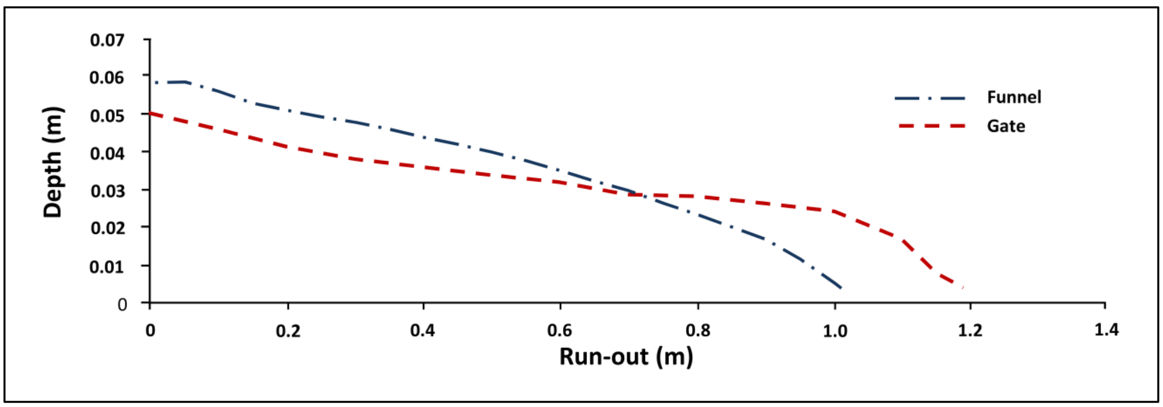

Figure 6.30. Comparison of the flow profile in flume depositions test using funnel vs. gate and reservoir (modified from Henriques and Simms, 2009).

6.4.6.1. Applicability of the small flume tests for prediction of the beach slope

Prediction of the beach slope or deposition profile is necessary for segregating and non-segregating tailings streams. For segregating slurries, the average beach slope determines the location and depth of the pond, and this accordingly affects the position of reclaim barges, decant structures and other pipes/facilities (Kupper, 2012). Similarly for thickened non-segregating tailings, prediction of the deposit profile is required to estimate the storage capacity of a given impoundment/disposal area, also the stack design and geometry (Simms et al., 2011). A review of the different methods of tailings beach slope prediction is provided by Fitton (2007); and for most methods the predicted slope from small scale flume data is not in a reasonable agreement with the measured slopes in the field. Davies et al. (2010) state that the beach slopes considered for design of several paste or thickened tailings stacks have been far steeper than the slopes ultimately achieved in the real operating conditions. The common theme of such designs has been the reliance on small scale flume tests. In these types of experiments the discharge rates are very low and the tailings flow occurs via sheet flow, but in actual operations development of the tailings deposit occurs via sheet flow with significant channelization. The overall slope of the tailings beach is dictated by the slope of these channels (Williams, 1992; Williams and Meynink, 1986 cited by Fitton, 2007; Davies et al., 2010). According to Fourie and Gawu (2010), ignoring the effect of side-wall friction in laboratory flume tests results in predicted slope angles that are significantly steeper than the beach slopes achieved in the field. They presented a model that took into account the effect of side-wall resistance and illustrated that increasing the flume width resulted in a decrease in the slope of the deposited beach. They emphasized that if the tailings are expected to experience a high degree of shearing during transportation to the final disposal area, a similar degree of shearing must be applied to the tailings material prior to conducting yield stress measurements and laboratory flume tests. Fourie and Gawu (2010) also indicated that variations of yield stress (e.g. due to changes in the thickener underflow) and also dynamic flow conditions during deposition play an important role on the equilibrium beach slope; however such factors cannot be simulated in a laboratory flume. From the above discussion, it is advisable to carry out pilot-scale field tests to obtain a more realistic prediction of the beach slope (Fourie et al., 2006).

6.5. Practical Considerations for Using Filtered/Centrifuged MFT

In this section a brief discussion about the design sequence of CT/NST produced from dewatered MFT is provided. When making a decision about tailings management strategies, a question that naturally arises is whether the dewatered MFT should be used as a separate stream or as a component for making CT/NST. The last part of this section reviews the different parameters that must be studied for each of these two tailings management scenarios.

6.5.1. The minimum solids content of dewatered MFT required for production of CT/NST

In order to determine the solids content of the filtered/centrifuged MFT required for making a robust CT/NST, it is necessary to review the design sequence of a tailings disposal system. Figure 6.31 (modified from Boger et al., 2006) illustrates a summary of the stages involved in determining a disposal strategy. As emphasized by Boger et al. (2006), the design sequence

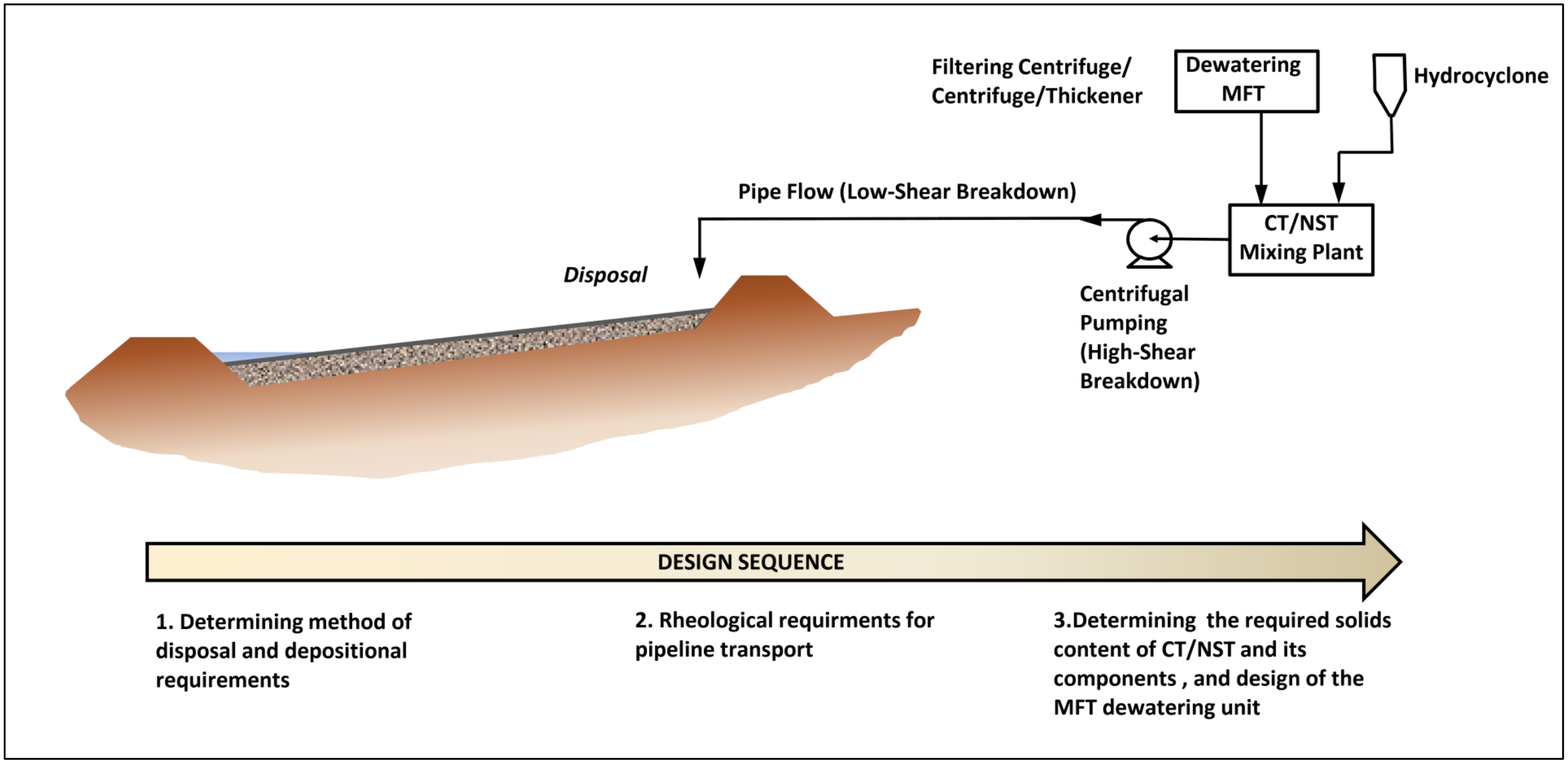

Figure 6.31. Design sequence of a robust CT/NST plant

begins at the disposal point and works backward to the dewatering stage. In the first stage of the design sequence, the disposal method of choice and the required rheological properties to obtain the desired geometry/footprint of the final deposit need to be determined. In the second stage, the pumping and pipeline conditions for optimal transport of the tailings to the disposal site need to be identified. The tailings slurry will experience shear while passing through the centrifugal pump and pipeline and its rheological properties may change. So it is necessary to ensure that the tailings slurry reaching the disposal site still maintains the rheological properties planned for disposal. Once the depositional and pipeline requirements have been identified, it is possible to determine the amount of dewatering (or the material consistency) required in the production/mixing plant (point 3 of the design sequence). An iterative approach must be used to optimize the design of the entire system (Boger et al., 2006).

With regard to a CT/NST disposal system, the major parameters that play a role in each of the above design stages are as following:

Depositional requirements: The CT/NST must have sufficient consistency to prevent segregation of the coarse and fine fractions upon discharge and after deposition (i.e. the yield stress of the carrier fluid (fines + water) must be sufficient to support the sand particles). It is again emphasized that the slurry must have high enough solids content to mitigate the effect of high energy discharge conditions and the possible fluctuations in the feed. In addition, the consistency (yield stress) of this homogenous CT/NST must allow it to flow far enough beyond the discharge point and yet, to form a gentle self-supporting slope. This is necessary to facilitate runoff of the rain and the water released to the surface of the deposit. The results obtained from laboratory flume tests, like the correlation given in Figure 6.16, provide a preliminary assessment of the likely beach slopes. However, as stated in section 6.4.5.1, it is advisable to carry out pilot-scale field tests to determine the yield stress associated with a desired beach slope (Fourie et al., 2006). In the next stage, from the relationship between the solids content and yield stress of the material, the minimum concentration required to obtain this beach slope can be determined. Figure 6.32 shows the variations of yield stress versus solids content for a number of CT/NST samples made in the present study. As the CT/NST concentration is increased, an exponential rise in its yield stress is observed.

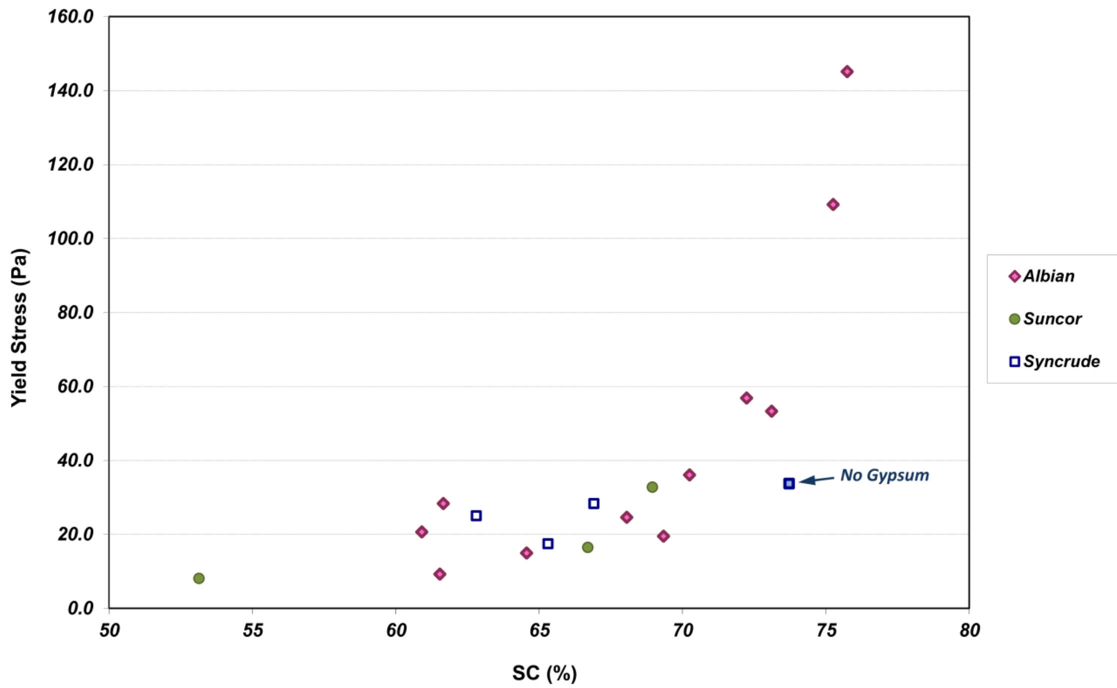

Figure 6.32. Yield Stress vs. Solids Content of the CT/NST samples studied in the present research

Pipeline transportation requirements: Studies by Boger et al. (2006) indicate that there is an optimum slurry concentration at which the pumping energy required for pipeline transport of the slurry is at a minimum. This is the transition point between the turbulent and laminar flows; i.e. at slurry concentrations lower than this optimum value the internal pipeline flow is turbulent and as the concentration is increased, the flow converts to a laminar regime. Figure 6.33 (modified from Boger et al., 2006) shows the predicted pumping energy for an iron ore pipeline where the minimum pumping energy occurs at a solids content of about 65%. According to Boger et al. (2006) this value is close to the optimum consistency used in actual operations and has been determined by trial and error. These researchers state that there is a great reluctance in the mining industry [and similarly, in the oil sands industry] to move into the laminar flow region, and this is due to the fear of sedimentation and blockage of the pipeline. While the prediction shown in Figure 6.33 is quite accurate particularly for relatively uniform fine-particle suspensions, it may not be valid for slurries with a very broad particle size distribution and large particles (Boger at al., 2006).

It is necessary to investigate the concept of optimum solids concentration for pipeline transportation of CT/NST. If such an optimum concentration exists, then it should be determined

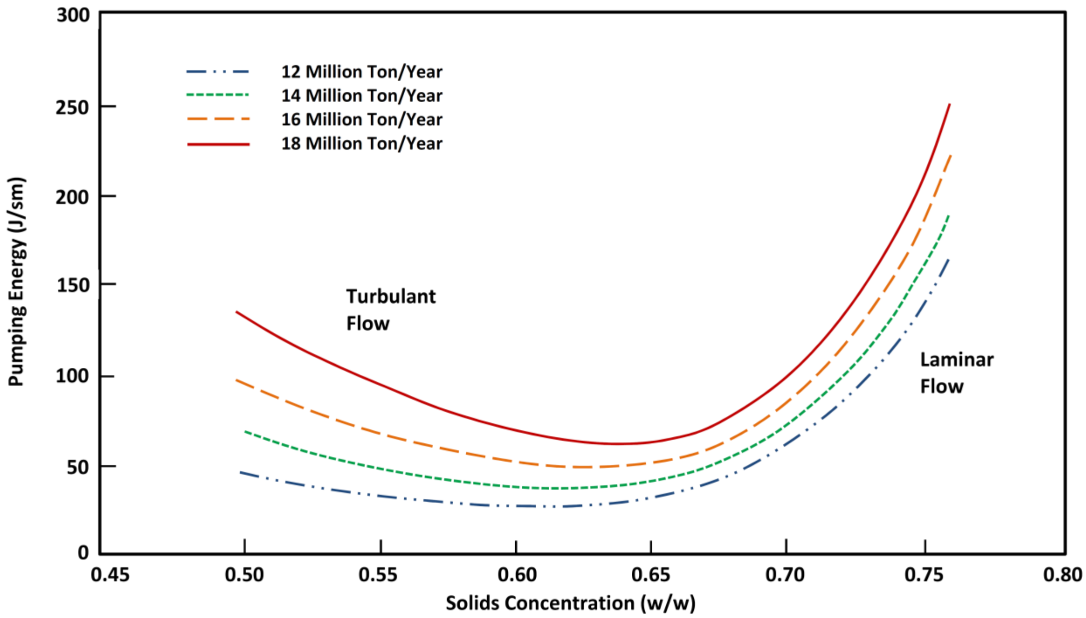

Figure 6.33. The predicted pumping energy as a fraction of solids content for a 50.8 cm (20 inch) diameter pipeline at various capacities. The optimum concentration requiring minimum pumping energy is about 65% (modified form Boger et al., 2006).

if it will satisfy the required disposal requirements; and how practicable it is to produce CT/NST at this solids content.

Dewatering requirements: After determining the minimum solids content of the CT/NST based on the depositional and pipeline requirements, the solids concentration of the dewatered MFT [that is to be used as a component for making CT/NST] can be calculated. Having known the approximate solids content of the coarse fraction (i.e. cyclone underflow), the multi-phase mass volume relationships for tailings (Scott, 2003; Boratynec, 2003) can be used to determine the solids content of the fines fraction. A group of diagrams showing parametric solutions of these relationships were presented in section 4.2 for the specific case of SFR=4. Once the required solids content of the dewatered MFT is determined, the operating conditions of the dewatering unit (e.g. spinning velocity and residence time of the [filtering] centrifuge or proper design of the thickener) can be determined.

6.5.2. Comparison of CT/NST with dewatered (Filtered/Centrifuged) MFT

Figure 6.34 illustrates the variations of yield stress (or maximum shear strength[5]) versus solids content for a number of regular and dewatered MFT samples studied in the present research. As indicated in this diagram, some samples are treated with 600ppm gypsum and the rest have no chemical treatment. The majority of samples are from Albian Sands, and a few samples are from Syncrude and Suncor ponds. The general trend of the data points in this diagram indicates that after reaching a solids content of about 60%, further dewatering of MFT rapidly increases its yield stress. Similar observation was made for CT/NST samples with solids contents higher than 70% (Figure 6.32).

Based on Figures 6.32 and 6.34, a comparison of the general correlation between yield stress and solids content of the CT/NST and dewatered MFT is provided in Figure 6.35. This comparison indicates that the energy required for pumping a unit volume of CT/NST at a solids content of about 70% to 75% would be comparable to the energy required for pumping dewatered MFT at about 55 to 60% solids content. However, mass of the fines present in the unit volume of dewatered MFT at 55 to 60% solids content is about 3 to 4 times the mass of fines present in 70 to 75% CT/NST. Diagrams illustrated in Figure 6.36 provide a comparison of the amount of fines present in MFT and CT/NST at a range of solids content and different sand to fine ratios.

[5] As explained in section 6.4.3.1, when the vane test is conducted on treated MFT samples instantly after addition of gypsum, the shear strength gradually increases during the test and it may not gain its peak value (yield stress) during the two full rotations (720 degrees) of the vane spindle.

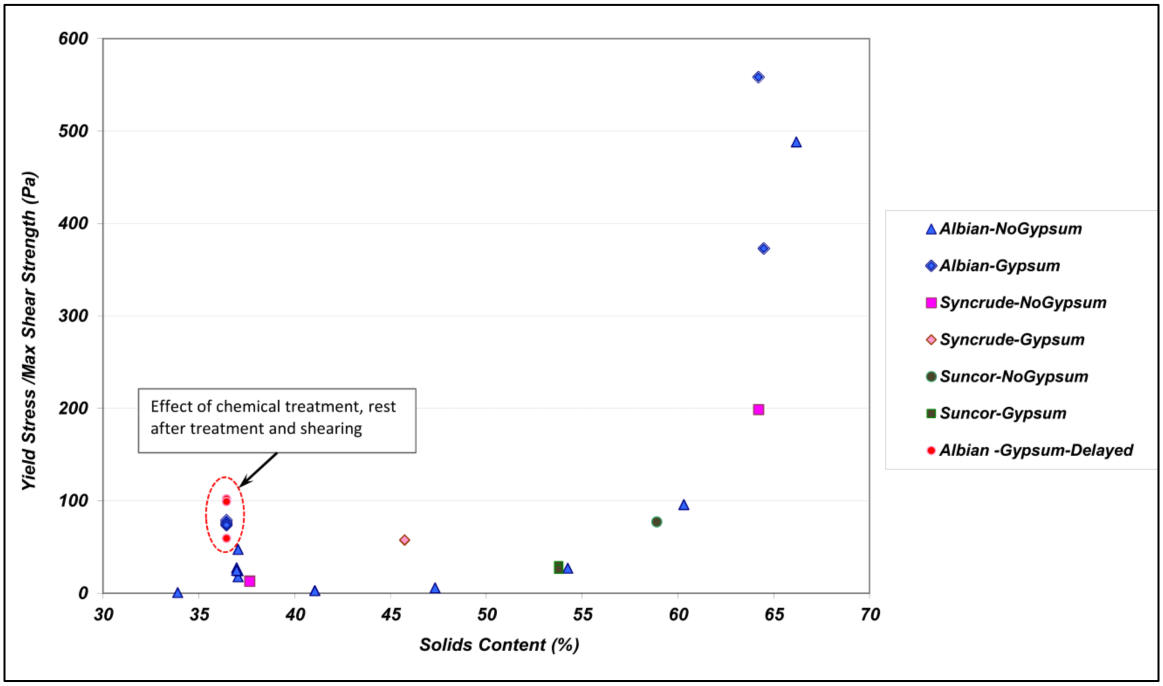

Figure 6.34. The correlation between yield stress/maximum shear strength of the regular and dewatered MFT samples with their Solids Content. The dosage of gypsum used for treated samples was 600ppm.

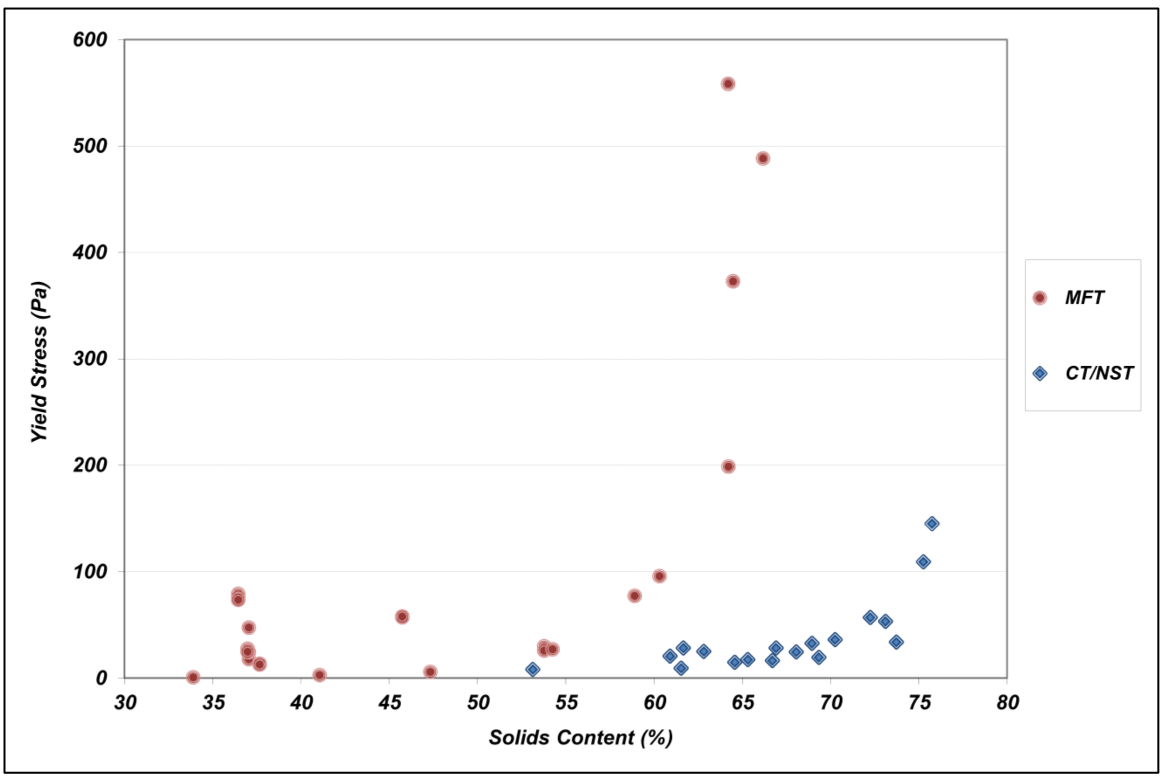

Figure 6.35. Comparison of the yield stress of regular and dewatered MFT with yield stress of CT/NST.

In addition to the pumping energy and efficiency of a deposit in terms of fines captured per its unit volume, there are a number of other parameters that determine whether to use the dewatered MFT as a separate stream for disposal or to mix it with the coarse tailings to make CT/NST; for instance:

- The land available for temporary/final disposal of the tailings (out-of-pit or in-pit);
- Availability of the sand for making CT/NST;
- Availability of the overburden material for co-disposal with dewatered MFT;
- The dewatering/consolidation rate of the concentrated MFT vs. the one for CT/NST;
- The operational time frame allowing optimal use of the evaporation and freeze-thaw effects;
- Optimum lift thicknesses (to result in fast dewatering) versus practically manageable lift thicknesses (i.e. how thin a lift of tailings can be spread is a factor of its yield stress);
- Environmental considerations (greenhouse gas emissions, dust generation, effect of chemicals on water quality, etc.)
- The capital and operational costs of production, transport and discharge of the dewatered MFT or CT/NST to the final disposal area. One important point to note regarding the production costs is that in order to make a robust CT/NST, the MFT need not be dewatered to very high solids contents. [This point was discussed in section 6.4.2.2 and it was shown that dewatering Syncrude MFT to a solids content of about 45% resulted in a robust CT with lower amount of gypsum.] For disposal of centrifuged MFT as a separate tailings deposit however, usually dewatering to higher solids concentrations is required.

In Chapter 2, a number of studies investigating some of the above parameters were reviewed.

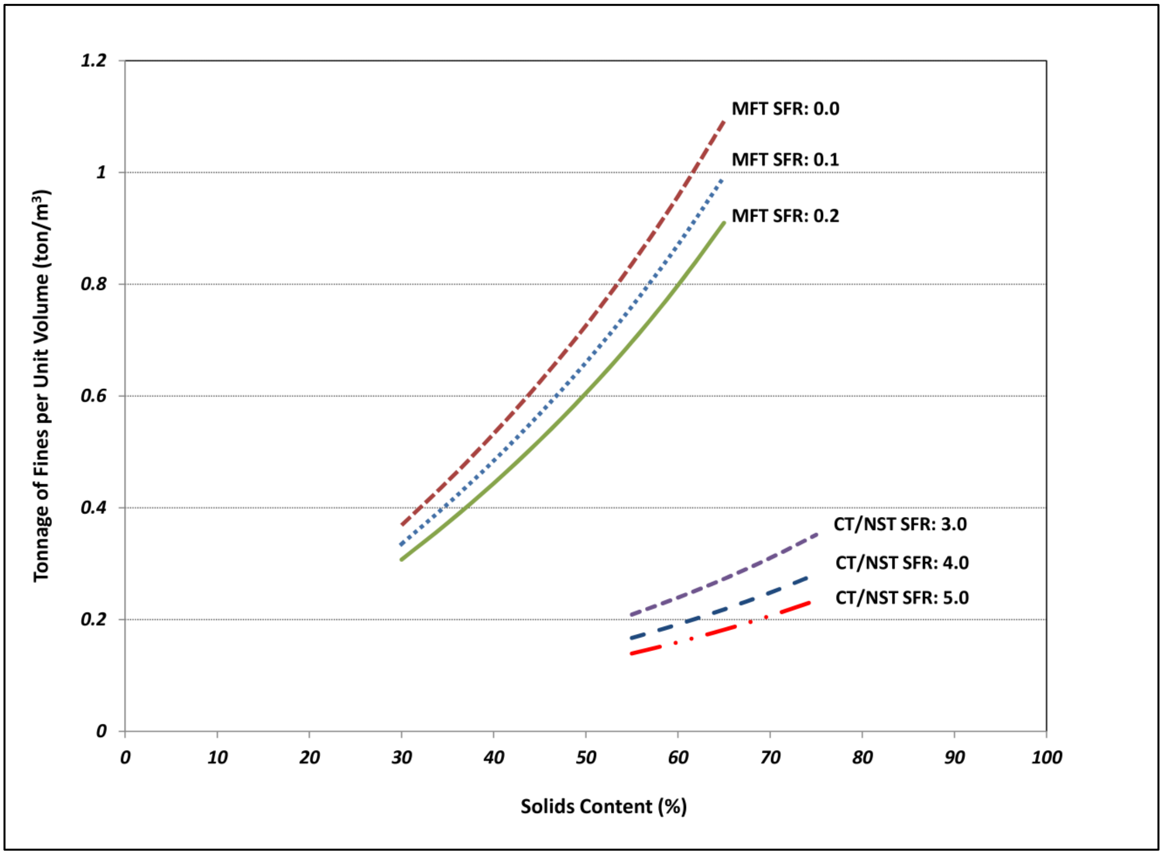

Figure 6.36. The amount of fines present in unit volume of MFT and CT/NST at a range of solids content values and different sand to fines ratios.

6.6. Summary and Conclusions

The cake obtained from several filtering centrifuge tests conducted on MFT was used as a component for making CT/NST. A flume was used to study the flow behaviour of the produced CT/NST samples. For each flume deposition test, the flow profile was recorded and the yield stress of the NST sample was evaluated by means of a strain-controlled viscometer and vane spindles. This yield stress was used to predict the flow profile of each individual flume test using an equation resulted from the lubrication theory and the simplifying assumption of laminar flow. To assess the robustness of each CT/NST deposit, a number of samples were taken along the flume and their solids content and SFR values were measured. Based on the position of these samples on the ternary diagram, a quantitative method for evaluation of the CT/NST robustness was suggested. A reasonable correlation between the calculated Robustness Index and the F/(F+W) ratio of the samples was observed.

Results of the present study indicate that using the filtered/centrifuged MFT as a component for making CT/NST promises a robust tailings stream, which has sufficient distance from the segregation boundary and is less sensitive to the fluctuation of the cyclone underflow. In addition, higher densities of this robust CT/NST results in higher angles of deposition and reduces the land footprint required for depositional purposes. Steeper angles of repose will also contribute for rapid drainage to a collection point for water released to the surface.

Based on the observations made in this research, dewatering of MFT has the potential to be considered as the initial stage of a multistage tailings management plan. Different solid-liquid separation methods (e.g. thickeners, solid bowl centrifuges, filtering centrifuges, etc.) may be used for this purpose. The present study shows that proper treatment of the MFT before introducing it into a filtering centrifuge can result in a cake with suitable consistency in which a high percentage of the fine particles can be captured. In the meantime, the filtrate obtained from a filtering centrifuge can be considered as a source of recycle water to be reused in the extraction process. This study showed that dewatering of MFT reduces the amount of coagulants required for production of CT/NST, thus the water drained either during centrifugation or after deposition of the tailings will have lower level of chemical additives. These findings are all promising steps towards solving the environmental issues associated with production of oil sands fine tailings.

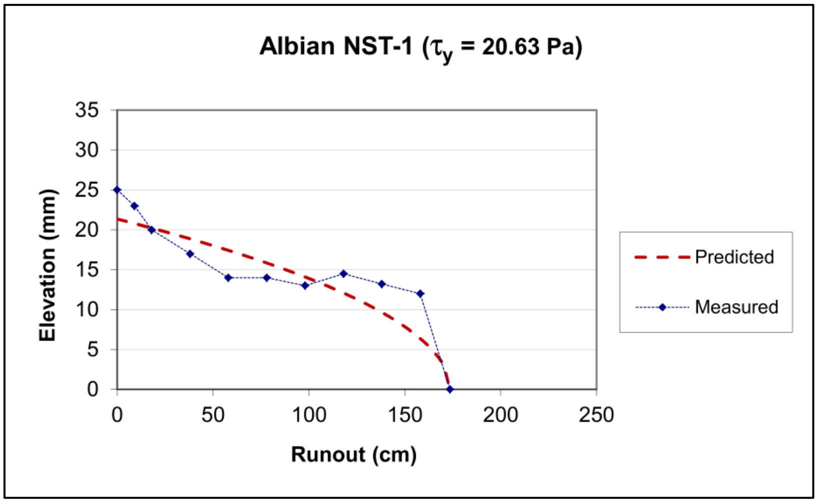

Figure 6.19. Flow profile of Albian NST-1 in the flume deposition test.

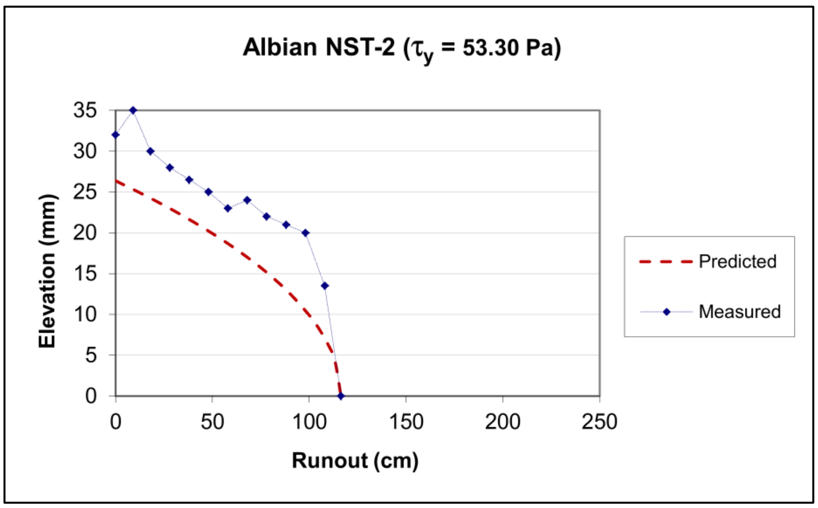

Figure 6.20. Flow profile of Albian NST-2 in the flume deposition test.

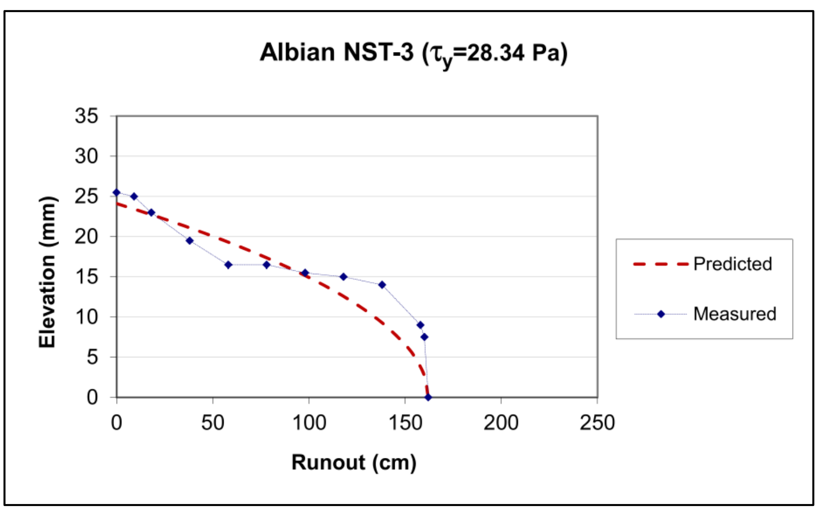

Figure 6.21. Flow profile of Albian NST-3 in the flume deposition test.

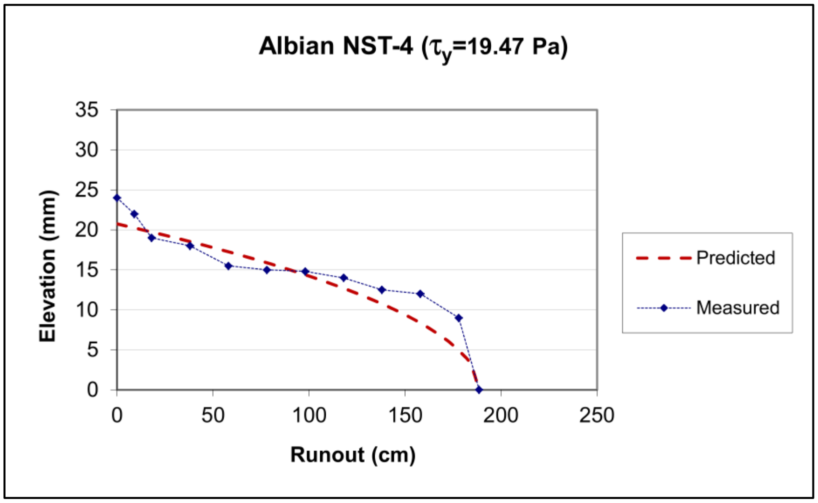

Figure 6.22. Flow profile of Albian NST-4 in the flume deposition test.

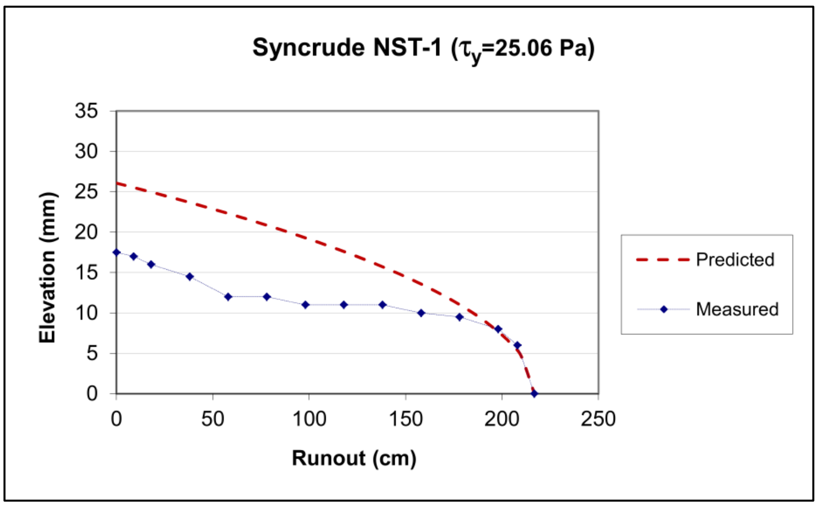

Figure 6.23. Flow profile of Syncrude NST-1 in the flume deposition test.

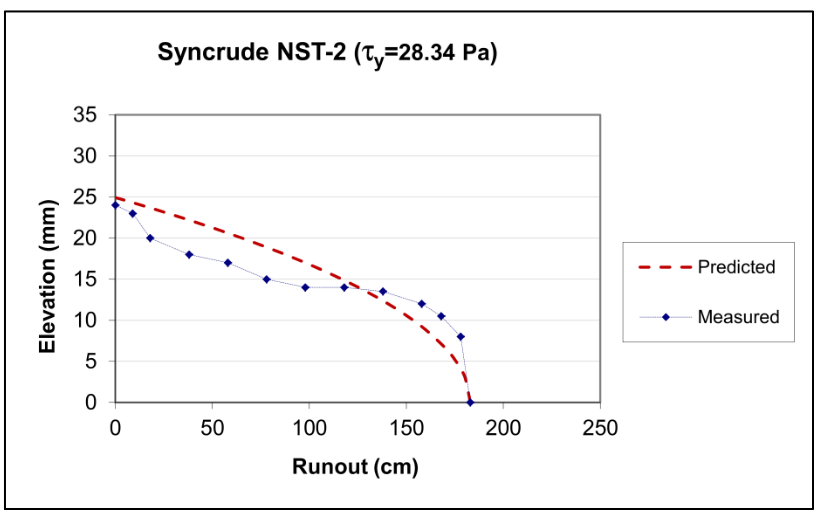

Figure 6.24. Flow profile of Syncrude NST-2 in the flume deposition test.

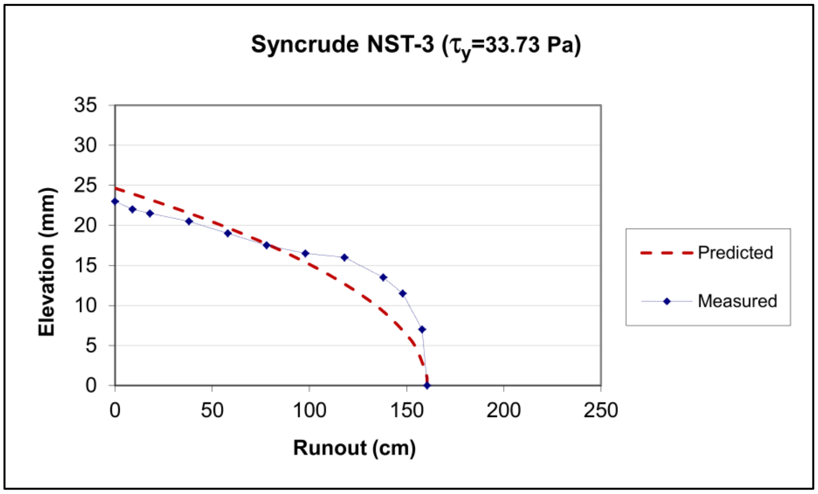

Figure 6.25. Flow profile of Syncrude NST-3 in the flume deposition test.

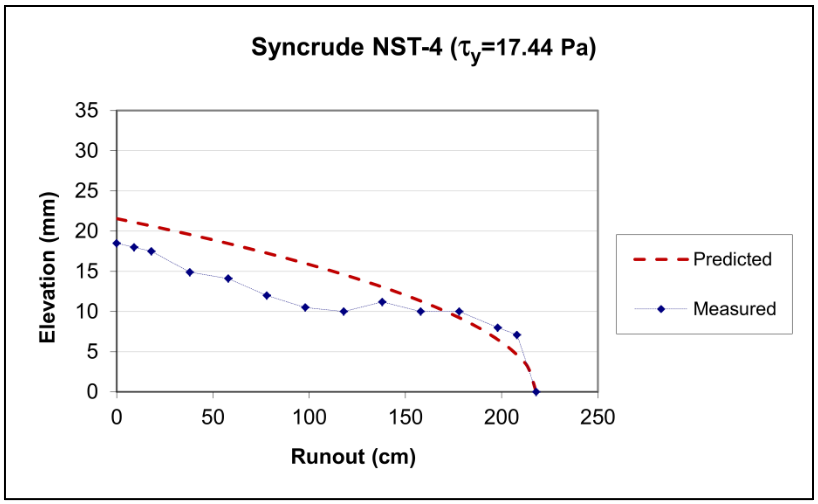

Figure 6.26. Flow profile of Syncrude NST-4 in the flume deposition test.

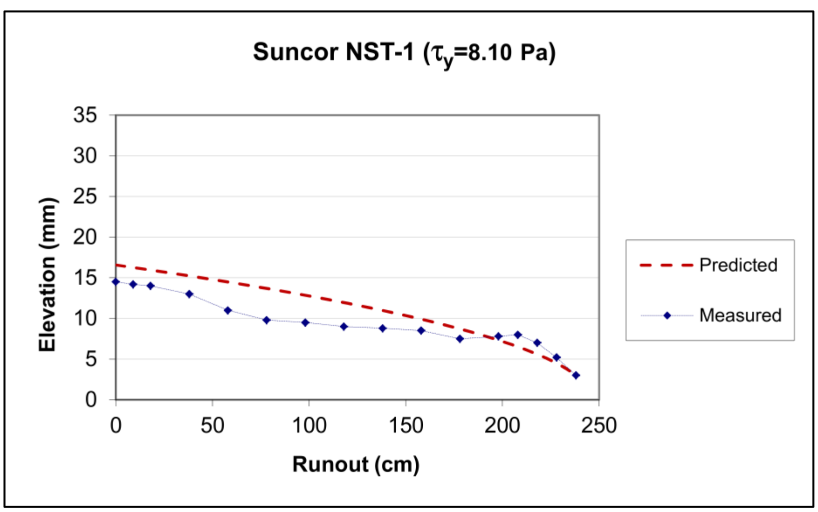

Figure 6.27. Flow profile of Suncor NST-1 in the flume deposition test.

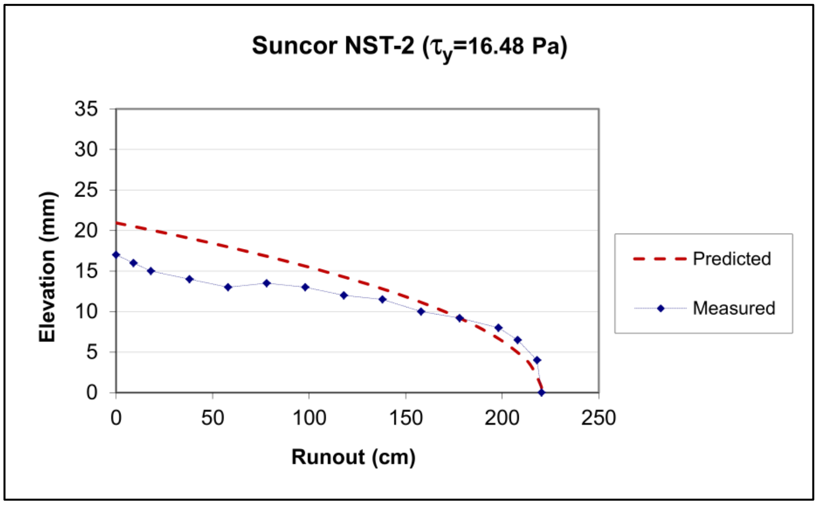

Figure 6.28. Flow profile of Suncor NST-2 in the flume deposition test.

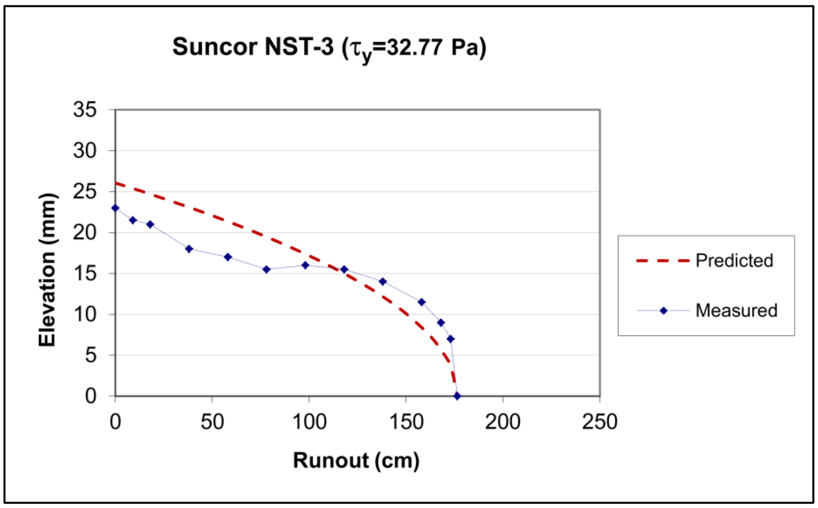

Figure 6.29. Flow profile of Suncor NST-3 in the flume deposition test.

Chapter 7

Summary, Conclusions and Recommendations

7.1. Summary

One of the current technologies used by the oil sands industry to reduce the volume of fluid fine tailings and create a dry landscape is production of CT (Composite/Consolidated Tailings) and NST (Non-Segregating Tailings). CT and NST are engineered tailings streams obtained by recombination of fines (MFT or TT) and coarse tailings (sand) plus a chemical amendment. If produced on-spec, the main advantage of CT/NST would be its improved dewatering behavior and rapid release of relatively clear water during the hindered settling and self-weight consolidation, while a majority of the fine particles are entrapped within the matrix of its coarser fraction (sand).

Production of a robust CT/NST at a commercial scale has been a challenge for the industry and this technology has not performed as anticipated. While CT/NST has been expected to be non-segregating when discharged, partial segregation and release and re-suspension of the fines has been observed following deposition. To achieve a robust CT/NST and reduce its susceptibility to segregation, the yield stress of the carrier fluid (i.e. fines + water) must be enhanced. This can be achieved by increasing the solids content (i.e. decreasing the water content) of CT/NST. The present research reviewed the different methods of solid-liquid separation and experimentally investigated the possible application of some of these methods for improving the quality of CT/NST.

A review of the theory of separation in thickeners, inclined plate settlers, filters, solid bowl centrifuges, filtering centrifuges and hydro-cyclones along with their method of operation was presented. Then two possible approaches for reducing the water content (increasing the solids content) of the CT/NST tailings streams were discussed: mixing the fine and coarse fractions to produce CT/NST and then dewatering the resultant mixture prior to deposition; and, dewatering one or both of the CT/NST components (cyclone underflow and MFT) prior to mixing them together. A family of diagrams explaining the correlation between the solids content of the feed materials (MFT and cyclone underflow) and the resultant CT were presented.

In the preliminary phase of the experimental study, a series of laboratory tests were conducted to explore each of the above approaches:

- Dewatering of CT samples in vessels with inclined walls, also dewatering of thin layers of CT on inclined plates was studied.
- By means of bench-top tube centrifuge tests, a procedure for pre-screening of the chemical additives that are to be used for larger scale centrifugation tests was explained.
- Bench top bottle centrifuge tests were used to dewater MFT and the resultant cake was used as a component for making NST. Using a small flume and standpipe sedimentation tests, flow characteristics and dewatering of some example NST samples made from centrifuged MFT were studied.
- A detailed review of the vane and slump test methods for measurement of the yield stress of tailings slurries was presented. The results of both methods were compared for CT samples prepared at a variety of solids contents.

A major part of the present research was focused on dewatering of MFT and using it as a component for making CT/NST. Review of the literature indicated that solid bowl centrifugation and pressure/vacuum filtration had been previously examined for dewatering of MFT, but it was for the first time in the present research that possibility of using a filtering centrifuge was studied.

A batch filtering centrifuge designed and provided by a private industrial company was utilized for this purpose. The filter cloth provided for this filtering centrifuge had a special coating on one side that facilitated removal of the cake. These centrifugal filtration tests were conducted at the Oil Sands Tailings Research Facility (OSTRF) located in Devon, Alberta. Prior to using the batch filtering centrifuge, a series of bench-top centrifugal filtration tests were conducted at the University of Alberta Geo-Environmental laboratory. A special filter bucket was designed for this purpose and the laboratory scale tests were conducted to study if presence of the unrecovered bitumen/asphaltene in MFT could result in clogging of the filter cloth. The other objectives of these tests were evaluating the filter cloth performance and studying the feasibility of obtaining fine tailings with higher concentration.

The batch filtering centrifuge tests at the OSTRF were conducted at a variety of test conditions on MFT samples provided by Suncor, Syncrude and Albian Sands tailings operations. The main observations and conclusions made during these tests are listed in section 7.2. Results of the filtering centrifuge tests conducted at the OSTRF showed that this method of dewatering has the potential to produce MFT with higher solids content; the dewatered MFT samples had a concentration ranging from 43%wt to 65%wt. Also, the filtrate samples obtained from the tests were fairly clear; with an average concentration less than 1.0%wt (half of the filtrate samples had a concentration less than 0.5%). Therefore the resultant filtrate can be reused in the extraction process after minor treatment, if required.

The dewatered MFT samples obtained from the filtering centrifuge tests were mixed with a mixture of sand and pond water (simulating the cyclone underflow) to produce CT/NST with higher solids content. A flume apparatus was designed to investigate the depositional behaviour of the produced CT/NST samples under laboratory conditions. The flume was made of acrylic sheets with high optical quality, had a total length of 240cm and an internal width of 18cm. For each flume deposition test, the flow profile was recorded and the yield stress of the NST sample was evaluated by means of a strain-controlled viscometer and vane spindles. To assess the robustness of each CT/NST deposit, a number of samples were taken along the flume and their solids content and SFR values were measured. The main findings from the flume deposition tests are listed in section 7.2.

The final part of this study reviewed the different stages involved in determining a disposal strategy (i.e. dewatering, transportation and deposition) and discussed the proper design sequence for achieving a robust CT/NST deposit.

7.2. Observations and Conclusions

The main observations and conclusions made during each phase of this experimental study are listed as following:

Preliminary dewatering experiments:

- CT showed accelerated dewatering in vessels with inclined walls; however, this method of solid-liquid separation may be more practical for slurries with lower solids content (e.g. the cyclone overflow).
- The NST made from MFT cake (produced using a bench top bottle centrifuge) had lower rate of dewatering in comparison to the CT made from regular MFT at the same solids content. Also, when the centrifuged cake was diluted to a 10% solids content suspension, its settling rate was lower than the regular MFT diluted to the same solids content.
- Both the vane and slump test methods resulted in an exponential correlation between the yield stress and solids concentration of the CT samples; however, it was suggested that the vane test method should be used to verify the suitability of the slump tests. A linear correlation between the average slope of the slumped material (i.e. height to spread radius) and the yield stress was observed.
- One important observation made during the laboratory centrifugal filtration tests was that bitumen, due to its lower specific gravity in comparison to the mineral particles, formed an internal layer close to the centre of rotation and had less opportunity to reach the filter medium. Also, since the viscosity of bitumen at lab temperature (20^{o}C) was about one million times higher than the viscosity of water, very little bitumen compared to water could pass through the cake porous medium. This observation revealed an important advantage of the centrifugal filtration over the pressure and vacuum filtration methods.

Batch filtering centrifuge tests conducted at the OSTRF:

- The major factors that affected the dewatering of MFT in the filtering centrifuge were identified as following:
    - Source of MFT (initial PSD and method of extraction): at similar test conditions the MFT received from Albian Sands tailings operations resulted in a higher cake consistency and a larger filtrate volume in comparison to the MFT received from the other operators. Comparison of the PSD of the MFT received from different operators at the non-dispersed (as received) state indicated that the MFT from Albian Sands had a more flocculated structure.
    - Amount of the gypsum used for treatment: In the absence of gypsum, segregation of the MFT occurred in the filtering centrifuge; i.e. the cake

formed over the filter cloth was mainly composed of the coarser fraction of particles and the finer particles were remaining in the form of a suspension. Addition of gypsum reduced the level of segregation and higher dosages of gypsum resulted in cakes with lower solids content in which a higher percentage of the solid particles were captured.

- Delay time after chemical treatment of MFT: It was observed that mixing MFT with gypsum and then leaving the mixture to sit for a while before being introduced into the filtering centrifuge significantly increased percentage of the fines that could be captured within the cake.
- Shearing and breakage of the flocs: To simulate the effect of shear experienced by the material while being transported inside the long pipes and multiple pumping stations [common in the plant operations], the treated MFT was circulated through the centrifugal pump and tubing for a limited time prior to being introduced into the centrifuge. This resulted in breakage of the flocs and significant segregation in the centrifuge, comparable to the results obtained for untreated MFT.
- Duration and speed of centrifugation: In general, increasing the spinning velocity and duration of the centrifugal filtration resulted in higher volume of filtrate and cakes with higher solids content. However, it was observed that increasing the spinning velocity (centrifugal force) higher than a certain limit lead to disintegration of the flocs and segregation of the coarse and fine fractions; as a result a lower percentage of the fines were captured in the cake.
- Size of the filter cloth opening: Increasing the filter cloth aperture resulted in higher volume of filtrate due to lower resistance of the filter cloth against filtration.

Flume deposition tests conducted on CT/NST made from regular/dewatered MFT:

- Using dewatered MFT made it possible to produce more robust CT/NST samples with lower dosage of chemical additives.
- CT/NST samples produced at higher solids content showed steeper angles of repose, and smaller variations of solids content and SFR (i.e. less hydraulic sorting) along the flume.

- Plotting the CT/NST samples taken along the flume tests on the ternary diagram revealed that the samples with lower solids content showed a scattered pattern on this diagram, and the samples with higher solids content showed a more concentrated pattern. Based on this observation, a quantitative method for evaluation of the CT/NST robustness was suggested. A reasonable correlation between the calculated Robustness Index and the F/(F+W) ratio of the samples was observed.
- A linear correlation was observed between the average angle of repose of the deposited CT/NST samples and their measured yield stress.
- Using an equation based on lubrication theory and the simplifying assumption of laminar flow, the measured yield stress of the CT/NST samples was used to predict the flow profile of each individual flume test. A reasonable agreement was observed between the predicted and the measured flow profiles.
- A linear correlation was found between duration of the flow in the flume tests and the maximum elastic stress of the CT/NST samples obtained from viscometer measurements.

Based on the observations made in this research, dewatering of MFT has the potential to be considered as the initial stage of a multistage tailings management plan. Different solid-liquid separation methods (e.g. thickeners, solid bowl centrifuges, filtering centrifuges, etc.) may be used for this purpose. Using such dewatering technologies in a CT/NST production plant would ensure availability of the fine tailings stream at the minimum concentration required for achieving a strong enough carrier fluid. This will promise a robust composite tailings stream, which has sufficient distance from the segregation boundary and is less sensitive to the fluctuations of the cyclone underflow. In addition, higher densities of this robust CT/NST results in steeper angles of deposition and reduces the land footprint required for depositional purposes. Steeper angles of repose will also contribute to rapid drainage to a collection point for water released to the surface.

7.3. Recommendations for future studies

The following is the list of recommended directions for future research:

- Dewatering cyclone underflow: As previously mentioned, fluctuations of the solids content of cyclone underflow is one of the main reasons for production of non-robust

CT/NST streams in the field operations. Further studies are required to find practical methods for controlling the solids content of cyclone underflow and ensuring availability of the coarse sand tailings at a minimum required concentration. The author suggests to:

  - Study possibility of using the cross flow filtration technology (Beier and Sego, 2008; Zhang et al., 2009) discussed in Chapter 2 to dewater the coarse sand tailings from cyclone underflow, prior to mixing it with the dewatered MFT.
  - Study the effectiveness and practicability of using flapper valves and overflow siphons in large scale applications for controlling the cyclone underflow concentration.

- Another possible application of the cross flow filtration that is worth a study would be using this technology to dewater the CT/NST as a mixture while it is being transported to its final disposal location. It is suggested to evaluate effectiveness of this technology for dewatering CT/NST at a range of SFR values and for different conditions of chemical treatment.
- Two-stage centrifugation of MFT: The dosage of chemicals currently used in the oil sands tailings operations is significantly higher than the other mining operations. Based on the observations in the present study, centrifugation of MFT in the absence of chemical additives results in segregation of the material to coarse (silt sized) and fine fractions. Centrifugation of MFT in two stages may possibly reduce the dosage of chemical additives:

  - First stage; centrifugation in the absence of chemicals; to separate the finer fraction (in the form of a suspension) from the silt sized particles (collected as a cake); and,
  - Second stage; centrifuging the fine suspension obtained in the first stage with chemicals (to flocculate the clay sized particles, which are responsible for holding large volumes of water in tailings ponds). The capital and operating costs of the two-stage centrifugation needs to be compared with the possible saving resulted from reduced dosage of chemicals.

- The solids content at which the turbulent flow changes to a laminar flow must be determined for CT/NST at different SFR values. The result of this study will determine the minimum pumping energy required for transporting unit mass of the solid minerals.

- The possible methods for creating a low energy depositional environment to prevent dynamic segregation of the CT/NST needs to be studied. This study will be a specific case of determining the minimum required shear strength of the carrier fluid to prevent segregation at different depositional environments.
- Based on the observations made in the present research, it is suggested to study the effect of delay time after using different chemicals common in the industry on enhancing the dewatering and fines capture in common solid-liquid separation technologies (filtration, centrifugation, etc.).
- Strength of the flocs in the centrifugal field: For oil sands fine tailings treated with different dosages/types of chemicals, what is the maximum safe centrifugal acceleration at which disintegration of the flocs and re-suspension of the fines to the centrate/filtrate does not occur?
- Looking for coagulants/flocculants that can create bonds between the unrecovered bitumen and solid minerals and prevent clogging during filtration.
- One of the challenges in some oil sands operation plants is the limited area available for conventional thickeners. It is suggested that combination of the inclined plate settlers and thickeners be studied for dewatering of the cyclone overflow.
- A type of anionic polymer studied in the present research resulted in better flocculation of the particles when it was combined with diluted MFT. In field operations, using the cyclone overflow as the feed for centrifugation, rather than MFT pumped from the pond, may result in better rate of dewatering at lower dosage of chemicals.
- Figure 7.1 illustrates a comparison of the yield stress-consistency correlations observed for the CT/NST and MFT samples studied in the present research with the correlations provided for other mine tailings by Boger et al. (2006). Reviewing the lessons learned in transportation and deposition of other mine tailings with consistency and yield stress values similar to the ranges observed for MFT and CT/NST can provide useful input for the oil sands tailings operations.

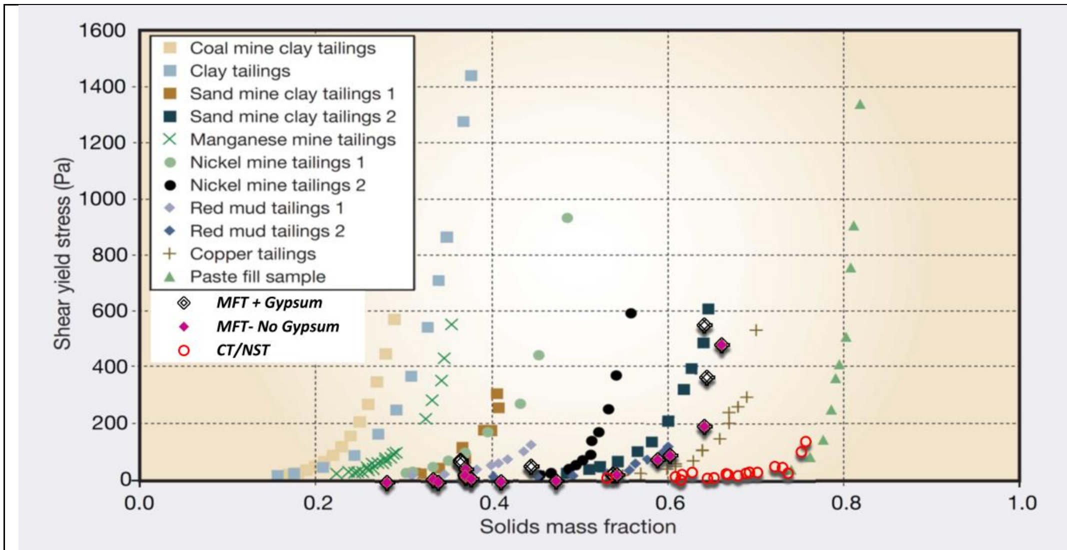

Figure 7.1. Comparison of the yield stress-concentration correlations for MFT and CT/NST samples with the correlations observed for other types of mine tailings (modified from Boger et al., 2006).

List of References

Acrivos, A., and Herbolzheimer, E. 1979. "Enhanced Sedimentation in Settling Tanks with Inclined Walls." J.Fluid Mech., 92(JUN): 435-457.

Adorján, L.A., 1975, "A theory of sediment compression," XI International Mineral Processing Congress, Cagliari, Italy, Paper 11: 1-22.

Adorján, L.A., 1976, "Determination of thickener dimensions from sediment compression and permeability test results," Trans. Inst. Min. Met., Sec C, 85: 157-163.

Agarwal, B. L. 2006. "Basic statistics". New Delhi: New Age Publishers.

Ahmed, I., Labelle, M., Brown, R. and Lahaie, R. 2009. "Paste pumping and deposition field trials and concepts on Syncrude's dewatered MFT (centrifuge cake)". Proceedings of the *Thirteenth International Conference on Tailings and Mine Waste '09, Banff, AB, Canada.* November 1 – 4, 2009: 417-427.

Alam, Saidul. "Dewatering Behavior of Oil Sands Tailings from Different Processes". Thesis (Ph.D.)- University of Alberta, Thesis writing in progress.

Alam, S. 2013. "Personal Communication".

Alberta Environment and Sustainable Resource Development. "Tailings Ponds". Viewed 11 November 2012. http://environment.alberta.ca/apps/osip/

Ancey, C., and Cochard, S. 2009. "The dam-break problem for Herschel-Bulkley viscoplastic fluids down steep flumes". *Journal of Non-Newtonian Fluid Mechanics.* 158 (1-3): 18-35.

Auzerais, F. M., Jackson, R., and Russel, W. B. 1988. "The resolution of shocks and the effects of compressible sediments in transient settling". *Journal of Fluid Mechanics.* 195 (-1).

Azam, S., and Scott, J. D. 2005. "Revisiting the Ternary Diagram for Tailings Characterization and Management". *Geotechnical News -Vancouver*. 23 (4): 43-46.

Baillie, R.A., and E.W. Malmberg. 1969. "Removal of Clay from the Water Streams of the Hot Water Process by Flocculation". *United States Patent 3,487,003*, 1969.

Balmforth, N.J., Craster, R.V., Perona, P., Rust, A.C., and Sassi, R. 2007. "Viscoplastic dam breaks and the Bostwick consistometer". *Journal of Non-Newtonian Fluid Mechanics.* 142 (1-3): 63-78.

Bartholomeeusen, Gert. 2003. “Compound shock waves and creep behaviour in sediment beds”. Thesis (D. Phil.)- University of Oxford, 2003.

Bartholomeeusen, G., Sills, G. C., Znidarcic, D., Van Kesteren, W., Merckelbach, L. M., Pyke, R., Carrier, W. D., et al. 2002. "Sidere: Numerical prediction of large-strain consolidation".*Géotechnique.* 52 (9): 639.

Bedell, D., Slottee, S., Parker, K. and Henderson, L. 2002. “Thickening Process”. Book chapter in “Paste and Thickened Tailings - A Guide”. Australian Centre for Geomechanics, Australia. Jewell et al. (eds): 49-79.

Been, Kenneth. 1980. *Stress strain behaviour of a cohesive soil deposited under water*. Thesis (D. Phil.)--University of Oxford, 1980.

Been, K. and Sills, G. C., 1981. "Self-weight consolidation of soft soils: an experimental and theoretical study". *Géotechnique.* 31 (4): 519-535.

Beier, N., Alostaz, M. and Sego, D. C. 2009. “Natural Dewatering Strategies for Oil Sands Fine Tailings”. Proceedings of the *Thirteenth International Conference on Tailings and Mine Waste ’09, Banff, AB, Canada.* November 1 – 4, 2009: 845-858.

Beier, N. and Sego, D. C. 2008. “Dewatering of Oil Sands Tailings Using Cross Flow Filtration”. Proceedings of the *61st Canadian Geotechnical Conference, Edmonton, AB, Canada.*

Bentz, M., and Stahl, W. 2001. "Investigations on particle destruction in centrifuges for improving product and process quality". *Filtration and Separation.* 38 (6): 42-47.

Blanchard, C., M. Jahoda, and V. Hornof. 2000. "Effects of Mechanical Treatment and Chemical Addition on Air Drying of Oil Sand Fine Tails". *Environmental Technology.* 21 (2): 237-242.

Blight, G. E., Thomson, R. R., and Vorster, K. 1985. "Profiles of hydraulic-fill tailings beaches, and seepage through hydraulically sorted tailings”. *Journal of the South African Institute of Mining and Metallurgy.* 85 (5): 157-161.

Boger, D., Scales, P. and Sofra, F. 2006. “Rheological Concepts”. Book chapter in “Paste and thickened tailings: a guide”. Nedlands, WA: Australian Centre for Geomechanics, The University of Western Australia. Jewell, R. J., and Fourie, A. B. (eds): 25-37.

Boratynec, D. J. 2003. “Fundamentals of rapid dewatering of composite tailings”. Thesis (M. Sc.)- University of Alberta, 2003.

Boratynec, D. J., Chalaturnyk, R. J., and Scott, J. D. 1998. "Experimental and Fundamental Factors Affecting the Water Release Rates of CT." *51st Canadian Geotechnical Conference, Edmonton,* The Canadian Geotechnical Society: 607-614.

Bowels, J. E. 1997. “Foundation Analysis and Design – 5th ed.” Singapore: McGraw-Hill International Editions.

Boycott, A. E. 1920. "Sedimentation of Blood Corpuscles". *Nature.* 104 (2621): 532-532.

Brookfield Engineering Labs. “More Solutions to Sticky Problems”. Manual No. 1056-1014 10M 12/05.

Brookfield Engineering Labs. “Brookfield DV-II+ Programmable Viscometer Operating Instructions”. Manual No. M/97-164-D1000.

Bürger, R., and Concha, F. 1998. "Mathematical model and numerical simulation of the settling of flocculated suspensions". *International Journal of Multiphase Flow*. 24 (6): 1005-1023.

Bürger, R., and Concha, F. 2001. "Settling velocities of particulate systems: 12: Batch centrifugation of flocculated suspensions". *International Journal of Mineral Processing.*63 (3): 115-145.

Bürger, R., Bustos, M.C. and Concha, F. 1999. "Settling velocities of particulate systems: 9. Phenomenological theory of sedimentation processes: numerical simulation of the transient behaviour of flocculated suspensions in an ideal batch or continuous thickener".*International Journal of Mineral Processing.* 55 (4): 267-282.

Bürger R., Ruiz-Baier R., Schneider K., and Torres H. 2012. "A multiresolution method for the simulation of sedimentation in inclined Channels". *International Journal of Numerical Analysis and Modeling.* 9 (3): 479-504.

Buscall, R., and White L. R. 1987. "The consolidation of concentrated suspensions. Part 1.- The theory of sedimentation". *Journal of the Chemical Society, Faraday Transactions 1.* 83 (3): 873-891.

Bustos, M. C. and Concha, F. 1988. "On the construction of global weak solutions in the Kynch theory of sedimentation". *Mathematical Methods in the Applied Sciences.* 10 (3): 245-264.

Bustos, M.C., Concha, F., Bürger, R., and Tory, E.M., 1999, “Sedimentation and Thickening: Phenomenological Foundation and Mathematical Theory”. Kluwer Academic Publishers, Dodrecht, The Netherlands, 304 pp.

Carrier, W. D., Bromwell, L.G, and Somogyi, F. 1983. "Design Capacity of Slurried Mineral Waste Ponds". *Journal of Geotechnical Engineering.* 109 (5): 699-716.

Carrier, W.D., Scott, J.D., Shaw, W.H, and Dusseault, M.B. 1987. “Reclamation of Athabasca Oil Sand Sludge”. *ASCE Specialty Conference on Waste Management*, Ann Arbor, Michigan. Geotechnical Special Publication No. 13, ASCE, New York, NY: 377-391.

Caughill, D. 1992. "Geotechnics of Nonsegregating Oil Sand Tailings". Thesis (M.Sc.)-University of Alberta, 1992.

Caughill, D. L., Morgenstern, N. R., and Scott, J. D. 1993. "Geotechnics of Nonsegregating Oil Sand Tailings." *Canadian Geotechnical Journal.* 30(5): 801-811.

Caughill, D. L., Scott J. D., Liu Y., Burns R., & Shaw W. H., 1994. “1993 Field program on Nonsegregating tailings at Suncor Inc.” Proceedings of the *47th Canadian Geotechnical Conference, September 21-23, Halifax, Canada,* 1994: 524-536.

Chalaturnyk, R. J., Scott, J. D., and Ozum, B. 2002. "Management of Oil Sands Tailings." *PETROLEUM SCIENCE AND TECHNOLOGY*, 20(9-10): 1025-1046.

Christensen, N.C. 1923. “Apparatus for the Settlement of Solid Particles Suspended in Liquids.” *United States Patent 1,458,805. (12 June 1923).*

Chu, A., Paradis, T., Wallwork, V. and Hurdel, J. 2008. “Non Segregating Tailings at the Horizon Oil Sands Project”. Proceedings of the *First International Oil Sands Tailings Conference, Edmonton, AB, Canada.* December 7 – 10, 2008: 3-12.

Coe, H.S., and Clevenger, G.H., 1916, “Methods for determining the capacity of slime settling tanks,” Trans. AIME, 55: 356-385.

Comings, E.W., Pruiss, C.E., and De Bord, C., 1954, “Continuous settling and thickening,” Ind. Eng. Chem. Des. Process. Dev., 46: 1164-1172.

Concha, F. 2009. "Settling Velocities of Particulate Systems". *KONA Powder and Particle Journal.* (27): 18-37.

Concha, F., and Burger, R. 2003. "Thickening in the 20th Century: a historical perspective". *Minerals and Metallurgical Process.* 20: 57-67.

Concha, F. and Bustos, M. C. 1987. "A modification of the Kynch theory of sedimentation". *AIChE Journal.* 33 (2): 312-315.

Concha, F. and Bustos, M. C. 1991. "Settling velocities of particulate systems, 6. Kynch sedimentation processes: batch settling". *International Journal of Mineral Processing.* 32 (3-4): 193-212.

Corti, A. and Falcon, J.A. 1989. "Method and Apparatus for Treatment of Oil Contaminated Sludge". *United States Patent 4,812,225*, 1989.

Crowder, J. J., and Grabinsky, M. W. 2005. "Discussion of "Assessment of the modified slump test as a measure of the yield stress of high-density thickened tailings". *Canadian Geotechnical Journal.* 42 (1): 316-318.

Davies, M., Lupo, J., Martin, T., McRoberts, E., Musse, M. and Ritchie, D. 2010. "Dewatered Tailings Practice". Proceedings of the *Fourteenth International Conference on Tailings and Mine Waste '10 :* 133-142.

Dawson, Richard Frederick. 1994. "Mine waste geotechnics". Thesis (Ph.D.)- University of Alberta, 1994.

Dawson, R. F., D. C. Sego, and G. W. Pollock. 1999. "Freeze-thaw dewatering of oil sands fine tails". *Canadian Geotechnical Journal*. 36: 587-598.

de Groot, M. B.; Heezen, F. T.; Mastbergen, D. R.; Stefess, H. 1988. "Slopes and densities of hydraulically placed sands" In Proc. Conference on *Hydraulic Fill Structures*, Fort Collins, 15–18 April 1988 : 32–51.

Donahue, R., Sego, D., Burk, B., Krahn, A., Kung, J., and Islam, N. 2008. "Impact of ion exchange properties on the sedimentation properties of oil sands mature fine tailings and synthetic clay slurries". Proceedings of the *First International Oil Sands Tailings Conference, Edmonton, AB, Canada.* December 7 – 10, 2008: 55-63.

Dorma, Kevin C. 1998. "Non-diffusive numerical simulations of gravity separation in inclined plate settlers". Thesis (Ph.D.)- University of Alberta, 1998.

Dusseault, M. B., Ash, P.O, and Scott, J.D. 1987. "Use of a Smectitic Clay Shale for Sludge Disposal". Proceedings of the *6th International Conference on Expansive Soils*, New Delhi, India. December 1-4, 1987. Central Board of Irrigation and Power, New Delhi, India.

Dusseault, M. B., and Morgenstern, N.R. 1978a. "Characteristics of natural slopes in the Athabasca Oil Sands". *Canadian Geotechnical Journal.* 15 (2): 202-215.

Dusseault, M. B., and Morgenstern, N.R. 1978b. "Shear strength of Athabasca Oil Sands". *Canadian Geotechnical Journal.* 15 (2): 216-238.

Eckert, W.F., Masliyah, J.H., Gray, M.R. and Fedorak, P.M. 1996. "Prediction of sedimentation and consolidation of fine tails". *AIChE Journal.* 42 (4): 960-972.

ERCB, 2009. Directive 074 "Tailings Performance Criteria and Requirements for Oil Sands Mining Schemes". The Energy Resources Conservation Board of Alberta (ERCB), Calgary, Alberta, Canada.

ERCB (Energy Resources Conservation Board), 2011. "Learn About Energy Regulation: EverFAQs 12 – Oil Sands". Viewed 17 July 2011. http://www.ercb.ca/learn-about-energy/enerfaqs/enerfaqs12

Fitch, E.B. and Stevenson, D.G. 1977. "Gravity separation equipment – Coagulation clarification". Book chapter in "Solid/liquid Separation Equipment Scale-up*"*. Croydon, Eng: Uplands Press. Purchas, D. B. (ed): 81-154.

Fitton, Tim. 2007. "Tailings Beach Slope Prediction*"*. Thesis (Ph.D.)- RMIT University, 2007.

Forsell, B. and Hedström, B. 1975. "Lamella Sedimentation: A Compact Separation Technique". *Journal (Water Pollution Control Federation).* 47 (4): 834-842.

Fourie, A., Davies, P., Fahey, M. and Lowson, R. 2002. "Material Characterisation". Book chapter in "Paste and Thickened Tailings - A Guide". Australian Centre for Geomechanics, Australia. Jewell et al. (eds): 35-47.

Fourie, A. B. and Gawu, S. K. Y. 2010. "The validity of laboratory flume data for predicting beach slopes of thickened tailings deposits." Proceedings of the *13th International Conference on Paste and Thickened Tailings, 3-6 May, Toronto, Canada.* 2010: 241-253.

FTFC. 1995. "Advance in oil sands tailings research". *Fine Tailings Fundamental Consortium (FTFC), Oil Sands and Research Division*, Alberta Department of Energy, Edmonton, Alberta, Canada.

Gale, 1977. "Optimizing the use of pre-treatment chemicals". Book chapter in "Solid/liquid Separation Equipment Scale-up*"*. Croydon, Eng: Uplands Press. Purchas, D. B. (ed): 39-80.

Garrido, P., Bürger, R., and Concha, F. 2000. "Settling velocities of particulate systems:11. Comparison of the phenomenological sedimentation-consolidation model with published experimental results". *International Journal of Mineral Processing*. 60 (3): 213-227.

Gawu, S., and Fourie, A. 2004. "Assessment of the modified slump test as a measure of the yield stress of high-density thickened tailings". *Canadian Geotechnical Journal*. 41: 39-47.

Ghorab, H. Y., Wassef, M. and Fetouh, S. H. 1984. “Factors Affecting the Solubility of Gypsum. Part 1: The Effect of Lime and Temperature in Different Media”. *Journal of Chemical Technology and Biotechnology 34A*: 464-467.

Ghorab, H. Y., and Fetouh, S. H. 1985. “Factors Affecting the Solubility of Gypsum, Part 2: The Effect of Sodium Hydroxide Under Various Conditions”. *Journal of Chemical Technology and Biotechnology 35A:* 36-40.

Gibson, K., 1979. “Large scale tests on sedimenting centrifuges and hydrocyclones for mathematical modeling of efficiency”. In Proc. *Symp. On Solid-Liquid Separation Practice, Yorkshire Branch of the I. Chem. E., Leeds*, 27-29 March: 1-10.

Gibson, R. E., England, G. L. and Hussey, M.J.L. 1967. "The Theory of One-Dimensional Consolidation of Saturated Clays". *Géotechnique.* 17 (3): 261-273.

Gibson, R. E., Schiffman, R.L. and Cargill, K.W. 1981. "The theory of one-dimensional consolidation of saturated clays. II. Finite nonlinear consolidation of thick homogeneous layers". *Canadian Geotechnical Journal.* 18 (2): 280-293.

Gray, D.M. 1970. “Handbook on the Principals of Hydrology”. Canadian National Committee for the International Hydrological Decade, National Research Council of Canada, Ottawa.

Grahame, D. C. 1947. “The electrical double layer and the theory of electrocapillarity.” *Chem. Rev.*, 41: 441- 501.

Gu, G, Z Xu, K Nandakumar, and J.H Masliyah. 2002. "Influence of water-soluble and water-insoluble natural surface active components on the stability of water-in-toluene-diluted bitumen emulsion". *Fuel.* 81 (14): 1859-1869.

Halferdahl, G. 2007. "Personal Communication".

Harvie, D.J.E., Nandakumar, K., and Masliyah, J.H. 2003. “Simulating the sedimentation of a dilute mono-disperse solid-liquid suspension”. In *Seventh U.S. National Congress on Computational Mechanics (USNCCM7)*, Sandia, USA, July 28–30 2003. Presentation.

Hazen, A. 1893. “Selection of sands for a filter”.

Headley, J. V., and D. W. McMartin. 2004. "A Review of the Occurrence and Fate of Naphthenic Acids in Aquatic Environments". *Journal of Environmental Science and Health - Part A: Toxic Hazardous Substances and Environmental Engineering.* 39: 1989-2010.

Henriquez J., and Simms P. 2009. "Dynamic imaging and modelling of multilayer deposition of gold paste tailings". *Minerals Engineering.* 22 (2): 128-139.

Hepp, P.S. and Camp, F.W. 1972. “Treating Hot Water Process Discharge Water by Flocculation and Vacuum Precoat Filtration”. *United States Patent 892,548.*

Herbolzheimer, E., 1983. “The stability of the flow during sedimentation beneath inclined surfaces”. *Physics of Fluid 26* : 2043–2054.

Hill, W., Rothfus, R, and Li, K. 1977. "Boundary-enhanced sedimentation due to settling convection". *International Journal of Multiphase Flow.* 3 (6): 561-583.

Hillel, Daniel. 1980. “*Applications of soil physics”*. New York: Academic Press.

Hogg, R. 2000. "Flocculation and Dewatering". *Int. J. Miner. Process.* 58 (1-4): 223-236.

Hollander, E. 2012. "Personal Communication".

Hooke, R.L. 1967. "Processes on Arid-Region Alluvial Fans". *The Journal of Geology.* 75 (4): 438-460.

Houlihan, R. and Mian, H. 2008. “Oil Sands Tailings: Regulatory Perspective”. Included with Proceedings of the *First International Oil Sands Tailings Conference, Edmonton, AB, Canada.* December 7 – 10, 2008.

Hughes, M. A. 2000. “Coagulation and Flocculation-Part I”. Book chapter in “Solid-Liquid Separation (Fourth Edition)*”.* Butterworth-Heinemann. Svarovsky, L. (ed): 104-129.

Hultsch, G., and Wilkesmann, H. 1977. “Filtering Centrifuges”. Book chapter in “Solid/liquid Separation Equipment Scale-up*”*. Croydon, Eng: Uplands Press. Purchas, D. B. (ed): 493-560.

Hyndman, A. and Sobkowicz, J. 2010. “Oil sands tailings: reclamation goals & the state of technology”. Proceedings of the *63rd Canadian Geotechnical Conference and 6th Canadian Permafrost Conference, 12–16 September, Calgary, Canada*. 2010: 642–655.

Imai, G. 1980. "Settling behavior of clay suspension". *Soils and Foundations.* 20 (2): 61-77.

Imai, G. 1981. "Experimental studies on sedimentation mechanism and sediment formation of clay materials". *Soils and Foundations.* 21 (1): 7-20.

IUPAC. 1997. “Compendium of Chemical Terminology, 2nd ed. (the “Gold Book”)”. Compiled by A. D. McNaught and A. Wilkinson. Blackwell Scientific Publications, Oxford (1997). Retrieved from http://goldbook.iupac.org/C01117.html

Jeeravipoolvarn, S., Scott, J.D., and Chalaturnyk, R.J. 2009. "10 m standpipe tests on oil sands tailings: Longterm experimental results and prediction". *Canadian Geotechnical Journal.* 46 (8): 875-888.

Jeeravipoolvarn, Silawat. 2010. “Geotechnical behavior of in-line thickened oil sands tailings”. Thesis (Ph.D.)- *University of Alberta*. http://hdl.handle.net/10402/era.27629.

Jewell, R. J., Fourie, A. B., and Lord, E. R. 2002. Paste and Thickened Tailings - A Guide. Australian Centre for Geomechanics, Australia.

Jewell, R. J., and A. B. Fourie. 2006. “Paste and thickened tailings: A Guide”. Nedlands, WA: Australian Centre for Geomechanics, The University of Western Australia.

Johnson, R.L., Bork, P., and Layte, P. 1989. “The effect of freezing and thawing on the dewatering of oil sands sludges”. In *A Global Perspective, Proceedings of the International Symposium on Reclamation, Calgary, Alta.*: 687–694.

Johnson, R.L., Bork, P., Allen, E.A.D., James, W.H., and Koverny, L. 1993. “Oil Sands Sludge Dewatering by Freeze-Thaw and Evapotranspiration”. Alberta Conservation and Reclamation Council Report No. RRTAC 93-8, 247p.

Kaminsky, H.A.W., Etsell, T. H., Ivey. D. G. and Omotoso, O. 2008 “Distribution of Minerals in Process Streams after Bitumen Extraction by the Hot Water Extraction Process”. Proceedings of the *First International Oil Sands Tailings Conference, Edmonton, AB, Canada.* December 7 – 10, 2008: 93-101.

Kasperski, K. L. 1992. "A Review of Properties and Treatment of Oil Sands Tailings." *AOSTRA Journal of Research,* 8: 11-53.

Kleine, U., and Stahl, W. 1989. "Model concept of floc disintegration in centrifugal fields". *Chemical Engineering and Technology*, 12(3): 200-204.

Knight, R.B., and Haile, J.P. 1983. “Sub-aerial Tailings Deposition.” Proceedings of the *7th Pan-American Soil Mechanics Conference, Vol.2, Vancouver, Canada*, Canadian Geotechnical Society: 627-639.

Küpper, A.G. 2012. “Hydraulic Fill and Tailings Engineering”. Proceedings of *David C. Sego Symposium, Edmonton, Alberta, April 26-27, 2012* : 147-164.

Küpper, A.A.G., Morgenstern, N. R., and Sego, D.C. 1992. "Laboratory tests to study hydraulic fill". *Canadian Geotechnical Journal.* 29 (3): 405-417.

Kwak, M., James, D. F., and Klein, K. A. 2005. "Flow behaviour of tailings paste for surface disposal." *Int. J. Miner. Process.*, 77(3): 139-153.

Kynch, G. J. 1952. "A theory of sedimentation". *Transactions of the Faraday Society.* 48.

Landman, K. A., and White, L. R. 1994. "Solid/liquid separation of flocculated suspensions". *Advances in Colloid and Interface Science.* 51 (COM): 175.

Laux, H., and Ytrehus, T. 1997. "Computer simulation and experiments on two-phase flow in an inclined sedimentation vessel". *Powder Technology.* 94 (1): 35-49.

Leung, W. F. 1983. "Lamella and tube settlers. 2. Flow stability". *Industrial & Engineering Chemistry Process Design and Development.* 22 (1): 68-73.

Leung, W. F., and Probstein, R. F. 1983. "Lamella and Tube Settlers .1. Model and Operation." *Industrial & Engineering Chemistry Process Design and Development*, 22(1): 58-67.

Li, Hongjun. 2007. “Role of a Temperature-Sensitive Polymer as a Process Aid in Oil Sands Processing and Tailings Treatment”. Thesis (M.Sc.)- University of Alberta, 2007.

Liu, J.K., Lane, S.J., and Cymbalisty, L.M. 1980. “Filtration of Hot Water Extraction Process Whole Tailings”. *United States Patent 4,225,433.*

Liu, K. F., and Mei, C.C. 1989. "Slow spreading of a sheet of Bingham fluid on an inclined plane". *Journal of Fluid Mechanics.* (207): 505-529.

Liu, Y.B., Caughill, D.L., Scott, J.D., and Burns, B. 1994. “Consolidation of Suncor Nonsegregating Tailings.” Proceedings of the *47th Canadian Geotechnical Conference, September 21-23, Halifax, Canada.* 1994: 504-513.

Lord, E.R.F., and Liu, Y. 1998. “Depositional and Geotechnical Characteristics of Paste Produced from Oil Sands Tailings”. Proceedings of the *Fifth International Conference on*

Tailings and Mine Waste '98, Fort Collins, Colorado, USA, 26-28 January 1998: 147-157.

Mackay, J. Ross. 1974. "Reticulate Ice Veins in Permafrost, Northern Canada". *Canadian Geotechnical Journal.* 11 (2): 230-237.

MacKinnon, M.D. 1989. "Development of the Tailings Pond at Syncrude's Oil Sands Plant: 1978-1987". *AOSTRA* J. Res. (5): 109.

MacKinnon, M.D. and Boerger, H. "Assessment of a Wet Landscape Option for Disposal of Fine Tails Sludge from Oil Sands Processing". *The Petroleum Society of CIM and AOSTRA 1991 Technical Confenrence.* Preprints Vol. 3, Banff, Alberta, April 21-24, 1991, p.124-1.

MacKinnon, M.D., J.G. Matthews, W.H. Shaw, and R.G. Cuddy. 2001. "Water Quality Issues Associated With Composite Tailings (CT) Technology for Managing Oil Sands Tailings". *International Journal of Surface Mining, Reclamation and Environment.* 15 (4): 235-256.

Masala, Srboljub. 1998. "Numerical simulation of sedimentation and consolidation of fine tailings". Thesis (M.Sc.)- University of Alberta, 1998.

Matthews, J. G. 2007. "Personal Communication".

Matthews, J. 2008. "Past, Present, and Future Tailings – Tailings Experience at Albian Sands Energy". *First International Oil Sands Tailings Conference, Edmonton, AB, Canada.* December 7 – 10, 2008. Presentation Only.

Matthews, J. G. and Masala, S. 2009. "Tailings Research at Shell's Muskeg River Mine Tailings Testing Facility". Proceedings of the *Thirteenth International Conference on Tailings and Mine Waste '09, Banff, AB, Canada.* November 1 – 4, 2009: 405-416.

Matthews, J.G., W.H. Shaw, M.D. MacKinnon, and R.G. Cuddy. 2002. "Development of Composite Tailings Technology at Syncrude". *International Journal of Surface Mining, Reclamation and Environment.* 16 (1): 24-39.

McRoberts, E. C., and Nixon, J. F. 1976. "A theory of soil sedimentation". *Canadian Geotechnical Journal.* 13 (3): 294-310.

Mehrotra, A.K., and Svrcek, W.Y. 1986. "Viscosity of compressed athabasca bitumen". *The Canadian Journal of Chemical Engineering.* 64 (5): 844-847.

Michaels, A. S., and Bolger, J. C. 1962. "Settling Rates and Sediment Volumes of Flocculated Kaolin Suspensions". *Industrial & Engineering Chemistry Fundamentals.* 1 (1): 24-33.

Mihiretu, Yetimgeta Teklu. 2009. “Fundamentals of segregation”. Thesis (Ph.D.)-*University of Alberta*. http://hdl.handle.net/10048/796.

Mikula, R. J. 2008. "Personal Communication".

Mikula, R.J., Munoz, V.A., Kasperski, K.L., Omotoso O.E. and Sheeran,D. “Commercial Implementation of a Dry Landscape Oil Sands Tailings Reclamation Option: Consolidated Tailings,” *7th UNITAR International Conference on Heavy Oil and Tar Sands, Beijing, China,* 1998.

Mikula, R., V. Munoz, and O. Omotoso. 2009. "Centrifugation Options for Production of Dry Stackable Tailings in Surface- Mined Oil Sands Tailings Management". *Journal of Canadian Petroleum Technology.* 48 (9).

Mikula, R., Omotoso, O. and Kasperski, K.L. 2008. “The Chemistry of Oil Sands Tailings: Production to Treatment”. Proceedings of the *First International Oil Sands Tailings Conference, Edmonton, AB, Canada.* December 7 – 10, 2008: 23-33.

Miller W.G., Scott J.D., and Sego D.C. 2009. "Flume deposition modeling of caustic and noncaustic oil sand tailings". *Canadian Geotechnical Journal.* 46 (6): 679-693.

Miller, W.G., Scott, J.D., and Sego, D.C. 2010. "Influence of extraction process and coagulant addition on thixotropic strength of oil sands fine tailings". *CIM Journal.* 1 (3): 197-205.

Miller, W.G., Scott, J.D., and Sego, D.C.. 2011. "Effect of extraction water chemistry on the self-weight consolidation of oil sands fine tailings". *CIM Journal.* 2 (1): 40-54.

Morgenstern, N., and J. D. Scott. 1995. "Geotechnics of Fine Tailings Management". *Geoenvironment 2000, ASCE,* 2: 1663-1673.

Moussavi Nik, R., Sego. D. C. and Morgenstern, N.R. 2008. “Possibility of Using Centrifugal Filtration for Production of Non-Segregating Tailings”. *Proceedings of the First International Oil Sands Tailings Conference, Edmonton, Alberta, Canada.* Dec. 2008: 200 – 208.

Murata, J. 1984. "Flow and deformation of fresh concrete". *Matériaux Et Constructions.*17 (2): 117-129.

Nakamura, H., Kuroda, K., 1937. "La cause de l'accélération de la vitesse de sédimentation des suspensions dans les r'ecipients inclines". *Keijo Journal of Medicine 8* : 256–296.

NEB (National Energy Board), 2000. "Canada's Oil Sands: A Supply and Market Outlook to 2015 – Energy Market Assessment". Retrieved from http://www.neb-one.gc.ca/clf-nsi/rnrgynfmtn/nrgyrprt/lsnd/lsnd-eng.html

Newson, T. A., and M. Fahey. 2003. "Measurement of Evaporation from Saline Tailings Storages". *Engineering Geology -Amsterdam.* 70 (3-4): 217-233.

Nguyen, Q.D., and Boger, D.V. 1983. "Yield stress measurement for concentrated suspension". *J. Rheology 27 (4)* : 321–349.

Nguyen, Q.D., and Boger, D.V. 1985. "Direct yield stress measurement with the vane method". *J. Rheology 29 (3)* : 335–347.

Nguyen, Q. D., and Boger, D. V. 1992. "Measuring the Flow Properties of Yield Stress Fluids". *Annu. Rev. Fluid Mech.* 24: 47-88

Nik, R. M., Sego. D. C. and Morgenstern, N.R. 2010. "Flow behavior and robustness of non-segregating tailings made from filtered-centrifuged MFT." *Proceedings of the Second International Oil Sands Tailings Conference, Edmonton, Alberta, Canada.* Dec. 2010: 319 – 329.

Omotoso, O. E., and Mikula, R. J. 2004. "High surface areas caused by smectitic interstratification of kaolinite and illite in Athabasca oil sands". *Applied Clay Science.* 25 (1): 37-47.

Oyama, Y., and Sumikawa, S. 1954. "On the Fundamental Study of Centrifugal Filtration". *Chemical Engineering.* 18 (12): 593-600.

Pane, Vincenzo. 1985. "Sedimentation and consolidation of clays". Thesis (Ph. D.)-University of Colorado, 1985.

Pane, V., and Schiffman, R. L. 1985. "A note on sedimentation and consolidation".*Géotechnique.* 35 (1): 69-72.

Parkson Corporation. 2009. "Lamella ® Gravity Settler – Inclined Plate Settler". Retrieved from http://www.edaenv.ca/_mndata/edaltd/uploaded_files/Lamella-Gravity-Settler.pdf

Pashias, N., Boger, D. V., Summers, J., and Glenister, D. J. 1996. "A fifty cent rheometer for yield stress measurement". *JOURNAL OF RHEOLOGY -NEW YORK-*. 40 (6): 1179-1190.

Penman, H. L. 1948. "Natural Evaporation from Open Water, Bare Soil and Grass".*Proceedings of the Royal Society of London. Series A, Mathematical and Physical Sciences.* 193 (1032): 120-145.

Perry, R. H., and Green D. W. 2007. “Perry's chemical engineers' handbook”. New York: McGraw-Hill.

Pirouz B., Kavianpour M.R., and Williams P. 2008. "Sheared and un-sheared segregation and settling behavior of fine sand particles in hyperconcentrated homogeneous sand-water mixture flows". *Journal of Hydraulic Research.* 46 (SUPPL. 1): 105-111.

Ponder, P., 1925. “On sedimentation and rouleaux formation”. *Quarterly Journal of Experimental Physiology* 15: 235.

Probstein, R. F., Yung, D., and Hicks, R. E. 1977. "A Model for Lamella Settlers", In *Theory. Practlce, and Process Principles for Physical Separations*; Engineering Foundation Conference, Asilomar, CA; Engineering Foundation: New York, p 53.

Proskin, Samuel Albert. 1998. “A geotechnical investigation of freeze-thaw dewatering of oil sands fine tailings”. Thesis (Ph.D.)- University of Alberta, 1998.

Purchas, Derek B. 1977. “Solid/liquid Separation Equipment Scale-up”. Croydon, Eng: Uplands Press.

Qiu, Yunxin. 2000. “Optimum deposition for sub-aerial tailings disposal”. Thesis (Ph.D.) - *University of Alberta*, 2000.

Qiu, Y., and Sego, D. C. (1998). "Design of Sub-Aerial Tailings Deposition in Arid Regions." *51st Canadian Geotechnical Conference*, The Canadian Geotechnical Society: 615-622.

Rajani, B., and Morgenstern, N. 1991. "On the yield stress of geotechnical materials from the slump test". *Canadian Geotechnical Journal.* 28 (3): 457-462.

Rattanakawin, Chairoj. 1998. “Aggregate size distributions in flocculation”. Thesis (M.S.)- Pennsylvania State University, 1998.

Rayment, G. E., and D. J. Lyons. 2010. “Soil Chemical Methods – Australasia”. CSIRO Publishing, Collingwood, VIC, Australia.

Records, F.A. 1977. “Sedimenting Centrifuges”. Book chapter in “Solid/liquid Separation Equipment Scale-up*”*. Croydon, Eng: Uplands Press. Purchas, D. B. (ed): 199-240.

Richardson, J. F., Harker, J. H., Backhurst, J. R. and Coulson, J. M. 2002. “Coulson and Richardson's chemical engineering. Vol. 2, Particle technology and separation processes”.Oxford:Butterworth-Heinemann. http://www.knovel.com/knovel2/Toc.jsp?BookID=2997.

Ripperger, S. and Altmann, J. 2002. "Crossflow microfiltration - state of the art". *Separation and Purification Technology*. 26 (1): 19-31.

Robinsky, Eli I. 1999. *Thickened tailings disposal in the mining industry*. Toronto: E.I. Robinsky Associates.

Roussel, N, and P Coussot. 2005. "Fifty-cent rheometer" for yield stress measurements: From slump to spreading flow". *Journal of Rheology*. 49 (3): 705.

Salehi, Mohammadreza. 2010. “Characterization of mature fine tailings in the context of its response to chemical treatment*”*. Edmonton, AB: University of Alberta. http://hdl.handle.net/10048/1378.

Sambuichi, M., Nakakura, H., and Osasa, K. 1988. "Comparison of batchwise centrifugal and constant-pressure filtration". *Journal of Chemical Engineering of Japan*. 21 (4): 418-423.

Sambuichi, M., Nakakura, H., Osasa, K. 1991. "Zone settling of concentrated slurries in a centrifugal field". *Journal of Chemical Engineering of Japan*. 24 (4): 489-494.

Sambuichi, M., Nakakura, H., Osasa, K., and Tiller, F.M. 1987. "Theory of batchwise centrifugal filtration". *AIChE Journal*. 33 (1): 109-120.

Schiffman, R. L., Chen, A.T.F., and Jordan, J. C. 1969. “An analysis of consolidation theories”. Journal of the *Soil Mechanics and Foundation* division, Proceedings of the American Society of Civil Engineers, 95 (SM1): 285-312.

Schiffman, R.L., Pane, V., and Gibson, R.E. 1984. “The theory of one-dimensional consolidation of saturated clays, IV”. An overview of nonlinear finite strain sedimentation and consolidation. In *Sedimentation/Consolidation Models*, ASCE. (Yong, R.N. and Townsend, F.C.): 1-29.

Schiffman, R.L., Vick, S.G. and Gibson, R.E. 1988. “Behavior and properties of hydraulic fills”. In *Hydraulic Fill Structures*, American Society of Civil Engineers, Colorado State University. Van Zyl, D.J. and Vick, S.G. (eds): 166-202.

Scott, J. D. 2003. "Multiphase Mass-Volume Relationships for Tailings." University of Alberta.

Scott, J. D., and Cymerman, G. J. 1984. "Prediction of viable tailings disposal methods." *Symposium on Sedimentation and Consolidation Methods, American Society of Civil Engineers, San Francisco, CA, USA:* 522-544.

Scott, J.D. and Dusseault M.B. 1980. "The Behaviour of Oil Sands Tailings". *Proceedings of the 33rd Canadian Geotechnical Conference, Calgary, AB, Canada*, 25 p.

Scott, J.D., Dusseault, M.B., and Carrier, W.D. 1985. "Behaviour of the clay/bitumen/water sludge system from oil sands extraction plants". *Applied Clay Science.* 1 (1-2): 207-218.

Scott, S.H. 1990. "An Inclined-Plate Technique for Increasing the Settling Rate of Fine-Grained Sediments in Hopper Bins". Army Engineer Waterways Experiment Station, Vicksburg, MS. Retrieved from http://www.dtic.mil/cgi-bin/GetTRDoc?Location=U2&doc=GetTRDoc.pdf&AD=ADA365531

Sego, D. 1992. "Influence of pore fluid chemistry on freeze-thaw behavior of Suncor Oil Sands Fine Tails (Phase I)". Submitted to Reclamation Research Technical Advisory Committee, Alberta Environment, 35p.

Sego, D.C. and Morgenstern, N. R. 2005. "Personal Communication".

Shaqfeh, E. S. G., and Acrivos, A. 1986. "The effects of inertia on the buoyancy-driven convection flow in settling vessels." *Physics of Fluids.* 29 (12): 3935-3948.

Shell Canada Energy. 2012. "Shell Albian Sands – Overview of Tailings and Shell Technologies". Retrieved from http://s07.static-shell.com/content/dam/shell/static/can-en/downloads/aboutshell/our-business/oil-sands/oil-sands-booklet.pdf

Shirato, M., Kato, H., Kobayashi, K., and Sakazahi H.. 1970. "Analysis of settling of thick slurries due to consolidation". *Journal of Chemical Engineering of Japan.* 3 (1): 98-104.

Silva, Marvin Jose. 2003. "Plant dewatering and strengthening of mine waste tailings". Thesis (Ph. D.)- University of Alberta, 1999.

Simms, P. 2007. "On the relation between laboratory flume tests and deposition angles of high density tailings". In: Proceedings of the *Tenth International Seminar on Paste and Thickened Tailings*, Perth, Australia, March 13th–15th: 329–335.

Simms, P., Dunmola, A. and Fisseha, B. 2009. “Generic Productions of Drying Time in Surface Deposited Thickened Tailings in a “Wet” Climate”. Proceedings of the *Thirteenth International Conference on Tailings and Mine Waste ‘09, Banff, AB, Canada.* November 1 – 4, 2009: 749-758.

Simms, P., M. Grabinsky, and G. Zhan. 2007. "Modelling evaporation of paste tailings from the Bulyanhulu mine". *Canadian Geotechnical Journal.* 44 (12): 1417-1432.

Simms, P., Williams, M.P.A., Fitton, T.G., and McPhail, G. 2011. “Beaching angles and evolution of stack geometry for thickened tailings”. Proceeding of the *Paste 2011 Conference*, Perth, Australia. Australian Centre for Geomechanics. 2011: 323-338.

Sobkowicz, J. and Morgenstern, N. R. 2009. “A Geotechnical Perspective on Oil Sands Tailings”. Proceedings of the *Thirteenth International Conference on Tailings and Mine Waste ‘09, Banff, AB, Canada.* November 1 – 4, 2009: xvii-xli.

Sobkowicz, J. and Morgenstern, N. R. 2010. “Reclamation and Closure of an Oil Sands Tailings Facility”. Proceedings of the *Second International Oil Sands Tailings Conference, Edmonton, AB, Canada.* December 5 – 8, 2010: 269-276.

Song, Q., O’Kane, M., Dhadli, N. and Matthews, J. 2011. “Deposition Thickness and Evaporative Drying for Oil Sands Tailings in Northern Alberta”. Proceeding of the *Mine Closure 2011 Conference*, Perth, Australia. Australian Centre for Geomechanics. 2011: 373-382.

Sorta, A. R. and Sego, D.C., 2010. “Segregation Related to Centrifuge Modelling of Oil Sands Tailings”. Proceedings of the *63rd Canadian Geotechnical Conference and 6th Canadian Permafrost Conference, 12–16 September, Calgary, Canada.* 2010: 656–664.

Stern, O. 1924. “Zur Theorie der Elektrolytischen Doppelschicht.” Z. Elektrochem. 30: 508-516.

Stickland, A., Scales, P., and Styles, J. 2005. "Comparison of Geotechnical Engineering Consolidation and Physical Science Filtration Testing Techniques for Soils and Suspensions". *Geotechnical Testing Journal.* 28 (6): 1.

Stocks, P. and Parker, K. 2006. “Reagents” – Chapter 6 of the book “Paste and thickened tailings: A Guide.” Nedlands, WA: Australian Centre for Geomechanics, The University of Western Australia. Jewell, R. J., and Fourie, A. B. (eds): 79-90.

Suncor Energy. 2011. “Suncor 2010 Report on Sustainability”. Viewed 17 July 2011. http://sustainability.suncor.com/2010/en/responsible/2634.aspx?id=3748

Svarovsky, L. 2000. “Solid-Liquid Separation (Fourth Edition)”. Butterworth-Heinemann.

Syncrude Canada Ltd. “Extraction”. Viewed 15 July 2011.
http://www.syncrude.ca/users/folder.asp?FolderID=5730

Syncrude Canada Ltd. “Tailings Management”. Viewed 17 July 2011.
http://www.syncrude.ca/users/folder.asp?FolderID=5913

Talmage, W. P., and E. B. Fitch. 1955. "Determining Thickener Unit Areas". *Industrial & Engineering Chemistry*. 47 (1): 38-41.

Tan, T.S. 1995. “Sedimentation to consolidation: A geotechnical perspective. In Proceedings of Compression and Consolidation of Clayey Soils”, Yoshikuni & Kusakabe (eds). Hiroshima, Japan: 937-948.

Tang, Juliana. 1997. “Fundamental behaviour of composite tailings”. Thesis (M.Sc.)-University of Alberta, 1997.

Theriault, Y., Masliyah, J. H., Fedorak, P. M., Vazquez-Duhalt, R., and Gray, M. R. 1995. "The effect of chemical, physical and enzymatic treatments on the dewatering of tar sands tailings." *Fuel, 74(9)* : 1404-1412.

Tiller, F.M. et al. 1970s to 2000s. "The role of porosity in filtration" paper series.

Tiller, F.M., and Leu, W.F., 1980, “Basic data fitting in filtration,” *J. Chem. Inst. Chem. Engrs*. (11): 61-70.

Tiller, F. M., and Yeh, C. S. 1985. "The role of porosity in filtration. Part X: Deposition of compressible cakes on external radial surfaces". *AIChE Journal*. 31 (8): 1241-1248.

Tiller, F. M., Haynes, S., and Lu, W. 1972. "The role of porosity in filtration VII effect of side-wall friction in compression-permeability cells". *AIChE Journal*. 18 (1): 13-20.

Trawinski, H. 1977. “Hydrocyclones”. Book chapter in “Solid/liquid Separation Equipment Scale-up”. Croydon, Eng: Uplands Press. Purchas, D. B. (ed): 241-288.

Uhlik, P., Hooshiar, A., Kaminsky, H.A.W, Etsell, T. H., Ivey, D.G. and Liu, Q. 2008. “Cation Exchange Capacity of Clay Fractions from Oil Sands Process Streams”. Proceedings of the *First International Oil Sands Tailings Conference, Edmonton, AB, Canada*. December 7 – 10, 2008: 64-72.

Valleroy, V. V., and Maloney, J. O. 1960. "Comparison of the specific resistances of cakes formed in filters and centrifuges". *AIChE Journal.* 6 (3): 382-390.

Van Olphen, H. 1977. "An introduction to clay colloid chemistry: for clay technologists, geologists, and soil scientists." New York: Wiley.

Vinogradov, G. V., and Malkin, A. Ya. 1980. "Rheology of polymers: viscoelasticity and flow of polymers". Berlin: Springer-Verlag.

Vogel, H.-J., H. Hoffmann, A. Leopold, and K. Roth. 2005. "Studies of crack dynamics in clay soil:II. A physically based model for crack formation". *Geoderma.* 125 (3): 213-223.

Wakeman, R. 2007. "The influence of particle properties on filtration". *Separation and Purification Technology.* 58 (2): 234-241.

Wells, P.S., Revington, A. and Omotoso, O. 2011. "Mature Fine Tailings Drying – Technology Update". Proceeding of the *Paste 2011 Conference*, Perth, Australia. Australian Centre for Geomechanics. 2011: 155-166.

Wikipedia. "gtts". Viewed 7 July 2012. http://en.wikipedia.org/wiki/Gtts

Wikipedia. "Phosphogypsum". Viewed 15 July 2011.
http://en.wikipedia.org/wiki/Phosphogypsum

Wikipedia. "Oil Sands". Viewed 27 March 2012. http://en.wikipedia.org/wiki/Oil_sands

Williams, M.P.A., 1992. "Australian Experience with the Central Thickened Discharge Method for Tailings". *Environmental Issues and Waste Management in Energy and Minerals Production*, Singhal et al. (eds).

Williams, M.P.A. and Meynink, W.J.C. 1986. "Tailings beach slopes", paper presented to *Workshop on Mine Tailings Disposal*, The University of Queensland.

Willis, M.S., and Tosun, I. 1980. "A rigorous cake filtration theory". *Chemical Engineering Science.* 35 (12): 2427-2438.

Wills, B. A., and Napier-Munn, T. 2006. "Wills' mineral processing technology an introduction to the practical aspects of ore treatment and mineral recovery". Amsterdam: Butterworth-Heinemann.
http://search.ebscohost.com/login.aspx?direct=true&scope=site&db=nlebk&db=nlabk&AN=196262.

Wilson, G.W., D.G. Fredlund, and S.L. Barbour. 1994. "Coupled Soil-Atmosphere Modelling for Soil Evaporation". *Canadian Geotechnical Journal.* 31 (2): 151-161.

Wilson, G.W., Kabwe, L.K., Donahue, R. and Lahaie, R. 2011. “Field performance of in-line flocculatd fluid fine tailings using thin lifts”. Proceeding of the *Mine Closure 2011 Conference*, Perth, Australia. Australian Centre for Geomechanics. 2011: 473-481.

Wislon, H.W. 1998. “Process for increasing the water solubility of gypsum”. *United States Patent 5,964,940 A.*

WEC (World Energy Council), 2010. “2010 Survey of Energy Resources”. Retrieved from http://www.worldenergy.org/publications/3040.asp

WSE (Water Smart Environmental, Inc.) 1999. “Particle/Liquid Separation Systems”. WSE Publication No. 796. Retrieved from http://www.watersmart.com/media/WP_0796_Design_Manual_And_Tutorial_Particle_Liquid_Separation_Systems.pdf

Xu, Yuming, Tadek Dabros, and Jianmin Kan. 2008. "Filterability of oil sands tailings".*Process Safety and Environmental Protection.* 86 (4): 268-276.

Yan, D, T Parker, and S Ryan. 2003. "Dewatering of fine slurries by the Kalgoorlie Filter Pipe". *Minerals Engineering.* 16 (3): 283-289.

Yao, Y., Van Tol, L., Van Paassen, F., Everts, B. and Mulder, A. 2010. “Experimental Research on Mud Farming of Fine Oil Sands Tailings”. *Proceedings of the Second International Oil Sands Tailings Conference, Edmonton, Alberta, Canada.* Dec. 2010: 59 – 68.

Yoshioka, N., Hotta, Y., Tanaka, S., Naito, S. and Tsugami, S. 1957. "Continuous Thickening of Homogeneous Flocculated Slurries". *Chemical Engineering Japan.* 21 (2): 66-74.

Yuan, S. and Lahaie, R. 2009. “Thickened Tailings (Paste) Technology and its Applicability in Oil Sands Tailings Management”. Proceedings of the *Thirteenth International Conference on Tailings and Mine Waste ’09, Banff, AB, Canada.* November 1 – 4, 2009: 829.

Yuan, X. S., and W. Shaw. 2007. "Novel Processes for Treatment of Syncrude Fine Transition and Marine Ore Tailings". *Canadian Metallurgical Quarterly*. 46 (3): 265-272.

Zhang, C., Alostaz, M., Beier, N and Sego, D. C. 2009. "Cross Flow Filtration of Oil Sands Total Tailings". Proceedings of the *Thirteenth International Conference on Tailings and Mine Waste '09, Banff, AB, Canada.* November 1 – 4, 2009: 799-812.

Appendix A

Analysis of the Samples Taken from Flume Tests

Tables A-1 to A-6 in this appendix present the solids content and fines content of the samples taken along the flume deposition tests discussed in Chapter 6, along with details of the calculation of Robustness Index (RI) and Segregation Index (SI) based on Equations (6.1), (6.6) and (6.7).

Table A-1: Calculation of the Robustness Index for flume tests conducted on Albian Sands tailings

Flume Test	Runout (cm)	Sample #	Distance from start of flume (cm)	SC (%)	FC (%)	ABS[SC-Avg(SC)]	ABS[FC-Avg(FC)]	MD(SC)/(Avg SC)	MD(FC)/(Avg FC)	Robustness Index (RI)
Albian NST-1	173.5	1	9.0	61.4	19.5	0.558	0.37			
		2	20.0	60.7	19.6	0.212	0.24			
		3	60.0	60.9	19.7	0.002	0.13			
		4	100.0	60.7	20.0	0.232	0.12			
		5	140.0	60.8	20.1	0.112	0.30			
			Average	60.9	19.8	0.223	0.23	0.0036661	0.01173	**287.3**
Albian NST-2	116.4	1	9.0	73.5	20.4	0.140	0.60			
		2	20.0	73.3	19.9	0.023	0.07			
		3	45.0	73.4	19.9	0.008	0.05			
		4	70.0	73.2	19.2	0.192	0.64			
		5	90.0	73.4	19.7	0.067	0.08			
			Average	73.4	19.8	0.086	0.29	0.0011701	0.01458	**857.4**
Albian NST-3	162.0	1	9.0	61.22	19.73	0.484	0.10			
		2	25.0	60.76	19.39	0.024	0.44			
		3	70.0	60.69	19.96	0.046	0.13			
		4	105.0	60.41	19.58	0.326	0.24			
		5	140.0	60.60	20.35	0.136	0.52			
			Average	60.74	19.80	0.203	0.29	0.0033456	0.01453	**307.0**
Albian NST-4	188.6	1	9.0	69.78	16.77	0.298	3.05			
		2	20.0	69.55	16.54	0.068	3.29			
		3	70.0	69.30	16.81	0.182	3.02			
		4	120.0	69.32	17.03	0.162	2.79			
		5	160.0	69.46	17.90	0.022	1.93			
			Average	69.48	17.01	0.146	2.82	0.002107	0.16559	**476.9**

Table A-2: Calculation of the Segregation Index for flume tests conducted on Albian Sands tailings

Flume Test	Runout (cm)	Sample #	Distance from start of flume (cm)	SC (%)	FC (%)	Hi	SiHi	Si^2Hi	$Hi(Si\text{-}Savg)^2$	SI (%) (Eq. 6.6)	SI (%) (Eq. 6.7)
Albian NST-1	173.5	1	9.0	61.4	19.5	14.50	890.88	54735.6672	4.514778		
		2	20.0	60.7	19.6	25.50	1547.085	93861.647	1.146072		
		3	60.0	60.9	19.7	40.00	2435.2	148254.976	0.00016		
		4	100.0	60.7	20.0	40.00	2426	147136.9	2.15296		
		5	140.0	60.8	20.1	53.50	3251.195	197575.12	0.671104		
			Average	60.9	19.8	173.50	10550.36	641564.31	8.49	**20.87**	**16.63**
Albian NST-2	116.4	1	9.0	73.5	20.4	14.50	1065.6478	78317.6073	0.285477543		
		2	20.0	73.3	19.9	18.00	1319.9382	96790.9386	0.009307012		
		3	45.0	73.4	19.9	25.00	1834.0045	134542.901	0.001421454		
		4	70.0	73.2	19.2	22.50	1646.1179	120431.302	0.828076597		
		5	90.0	73.4	19.7	36.40	2672.4649	196210.68	0.162067115		
			Average	73.4	19.8	116.40	8538.17	626293.43	1.29	**10.51**	**8.06**
Albian NST-3	162.0	1	9.0	61.22	19.73	17.00	1040.74	63714.1028	3.982352		
		2	25.0	60.76	19.39	30.50	1853.18	112599.217	0.017568		
		3	70.0	60.69	19.96	40.00	2427.6	147331.044	0.08464		
		4	105.0	60.41	19.58	35.00	2114.35	127727.884	3.71966		
		5	140.0	60.60	20.35	39.50	2393.7	145058.22	0.730592		
			Average	60.74	19.80	162.00	9829.57	596430.47	8.53	**22.16**	**17.03**
Albian NST-4	188.6	1	9.0	69.78	16.77	14.50	1011.81	70604.1018	1.287658		
		2	20.0	69.55	16.54	30.50	2121.275	147534.676	0.141032		
		3	70.0	69.30	16.81	50.00	3465	240124.5	1.6562		
		4	120.0	69.32	17.03	45.00	3119.4	216236.808	1.18098		
		5	160.0	69.46	17.90	48.60	3375.756	234480.012	0.0235224		
			Average	69.48	17.01	188.60	13093.24	908980.10	4.29	**13.89**	**12.65**

Table A-3: Calculation of the Robustness Index for flume tests conducted on Syncrude tailings

Flume Test	Runout (cm)	Sample #	Distance from start of flume (cm)	SC (%)	FC (%)	ABS[SC-Avg(SC)]	ABS[FC-Avg(FC)]	MD(SC)/(Avg SC)	MD(FC)/(Avg FC)	Robustness Index (RI)
Syncrude NST-1	216.8	1	9.0	62.4	18.9	0.300	0.90			
		2	30.0	62.2	18.6	0.100	1.26			
		3	80.0	62.0	18.9	0.050	0.97			
		4	130.0	62.0	19.3	0.040	0.52			
		5	180.0	61.8	19.7	0.310	0.08			
			Average	62.1	19.1	0.160	0.75	0.0025782	0.03929	**391.5**
Syncrude NST-2	183	1	9.0	66.6	20.2	0.044	0.41			
		2	50.0	66.5	19.8	0.057	0.06			
		3	85.0	66.7	20.7	0.150	0.87			
		4	120.0	66.6	19.8	0.083	0.01			
		5	155.0	66.3	19.5	0.219	0.28			
			Average	66.5	20.0	0.111	0.33	0.0016626	0.01628	**604.0**
Syncrude NST-3	160.6	1	9.0	73.54	18.94	0.067	0.89			
		2	25.0	73.64	19.76	0.028	0.06			
		3	60.0	73.60	19.68	0.007	0.15			
		4	95.0	73.51	19.22	0.094	0.61			
		5	130.0	73.75	19.21	0.140	0.62			
			Average	73.61	19.36	0.067	0.47	0.000915	0.02405	**1095.0**
Syncrude NST-4	218.0	1	9.0	65.28	18.46	0.506	1.37			
		2	30.0	64.85	18.80	0.076	1.03			
		3	80.0	64.65	18.52	0.124	1.31			
		4	130.0	64.66	18.90	0.114	0.92			
		5	180.0	64.43	19.61	0.344	0.21			
			Average	64.77	18.86	0.233	0.97	0.003594	0.05134	**284.4**

Table A-4: Calculation of the Segregation Index for flume tests conducted on Syncrude tailings

Flume Test	Runout (cm)	Sample #	Distance from start of flume (cm)	SC (%)	FC (%)	Hi	SiHi	Si^2Hi	$Hi(Si-Savg)^2$	SI (%) (Eq. 6.6)	SI (%) (Eq. 6.7)
Syncrude NST-1	216.8	1	9.0	62.4	18.9	19.50	1216.02	75831.0072	1.755		
		2	30.0	62.2	18.6	35.50	2206.68	137167.229	0.355		
		3	80.0	62.0	18.9	50.00	3100.5	192262.005	0.125		
		4	130.0	62.0	19.3	50.00	3101	192324.02	0.08		
		5	180.0	61.8	19.7	61.80	3816.15	235647.263	5.93898		
			Average	62.1	19.1	216.80	13440.35	833231.52	8.25	**18.37**	**15.25**
Syncrude NST-2	183	1	9.0	66.6	20.2	29.50	1963.6228	130705.578	0.057579995		
		2	50.0	66.5	19.8	38.00	2525.556	167853.497	0.124793183		
		3	85.0	66.7	20.7	35.00	2333.4131	155566.191	0.783728533		
		4	120.0	66.6	19.8	35.00	2331.0693	155253.834	0.239232742		
		5	155.0	66.3	19.5	45.50	3016.6553	200004.596	2.185998079		
			Average	66.5	20.0	183.00	12170.32	809383.70	3.39	**13.53**	**11.80**
Syncrude NST-3	160.6	1	9.0	73.54	18.94	17.00	1250.1895	91939.64	0.076154322		
		2	25.0	73.64	19.76	25.50	1877.7157	138267.31	0.020596243		
		3	60.0	73.60	19.68	35.00	2576.0149	189595.787	0.001747899		
		4	95.0	73.51	19.22	35.00	2572.9589	189146.217	0.311760829		
		5	130.0	73.75	19.21	48.10	3547.2522	261600.799	0.942173421		
			Average	73.61	19.36	160.60	11824.13	870549.75	1.35	**9.01**	**7.56**
Syncrude NST-4	218.0	1	9.0	65.28	18.46	19.50	1272.96	83098.8288	4.992702		
		2	30.0	64.85	18.80	35.50	2302.175	149296.049	0.205048		
		3	80.0	64.65	18.52	50.00	3232.5	208981.125	0.7688		
		4	130.0	64.66	18.90	50.00	3233	209045.78	0.6498		
		5	180.0	64.43	19.61	63.00	4059.09	261527.169	7.455168		
			Average	64.77	18.86	218.00	14099.73	911948.95	14.07	**23.51**	**21.16**

Table A-5: Calculation of the Robustness Index for flume tests conducted on Suncor tailings

Flume Test	Runout (cm)	Sample #	Distance from start of flume (cm)	SC (%)	FC (%)	ABS[SC-Avg(SC)]	ABS[FC-Avg(FC)]	MD(SC)/(Avg SC)	MD(FC)/(Avg FC)	Robustness Index (RI)
Suncor NST-1	238	1	9.0	54.4	15.0	1.826	4.85			
		2	30.0	52.7	15.1	0.136	4.72			
		3	80.0	52.8	14.6	0.256	5.27			
		4	130.0	52.6	15.8	0.056	3.98			
		5	200.0	50.3	15.8	2.274	4.06			
			Average	52.6	15.3	0.910	4.58	0.0173079	0.30012	**67.2**
Suncor NST-2	216.8	1	9.0	66.3	14.1	0.360	5.75			
		2	30.0	65.8	14.2	0.110	5.60			
		3	80.0	66.4	13.6	0.400	6.23			
		4	130.0	65.9	13.8	0.010	5.99			
		5	180.0	65.3	14.0	0.640	5.79			
			Average	66.0	14.0	0.304	5.87	0.0046096	0.42071	**229.1**
Suncor NST-3	176.4	1	9.0	68.86	19.30	0.021	0.52			
		2	30.0	68.72	19.29	0.117	0.54			
		3	70.0	69.17	20.12	0.338	0.29			
		4	110.0	68.78	19.09	0.061	0.74			
		5	145.0	68.66	20.20	0.181	0.37			
			Average	68.84	19.60	0.144	0.49	0.0020868	0.02508	**481.2**

Table A-6: Calculation of the Segregation Index for flume tests conducted on Suncor tailings

Flume Test	Runout (cm)	Sample #	Distance from start of flume (cm)	SC (%)	FC (%)	Hi	SiHi	Si^2Hi	$Hi(Si\text{-}Savg)^2$	SI (%) (Eq. 6.6)	SI (%) (Eq. 6.7)
Suncor NST-1	238	1	9.0	54.4	15.0	19.50	1060.41	57665.0958	65.018382		
		2	30.0	52.7	15.1	35.50	1870.495	98556.3816	0.656608		
		3	80.0	52.8	14.6	50.00	2640.5	139444.805	3.2768		
		4	130.0	52.6	15.8	60.00	3156.6	166068.726	0.18816		
		5	200.0	50.3	15.8	73.00	3670.44	184549.723	377.488548		
			Average	52.6	15.3	238.00	12398.45	646284.73	446.63	**129.04***	**93.53**
Suncor NST-2	216.8	1	9.0	66.3	14.1	19.50	1293.045	85741.814	2.5272		
		2	30.0	65.8	14.2	35.50	2337.32	153889.149	0.42955		
		3	80.0	66.4	13.6	50.00	3317.5	220116.125	8		
		4	130.0	65.9	13.8	50.00	3297	217404.18	0.005		
		5	180.0	65.3	14.0	61.80	4036.158	263601.479	25.31328		
			Average	66.0	14.0	216.80	14281.02	940752.75	36.28	**40.15**	**32.74**
Suncor NST-3	176.4	1	9.0	68.86	19.30	19.50	1342.7281	92457.3769	0.008838832		
		2	30.0	68.72	19.29	30.50	2095.9379	144031.328	0.419579893		
		3	70.0	69.17	20.12	40.00	2766.9757	191403.868	4.565177111		
		4	110.0	68.78	19.09	37.50	2579.0953	177379.542	0.138109359		
		5	145.0	68.66	20.20	48.90	3357.25	230493.4	1.604573969		
			Average	68.84	19.60	176.40	12141.99	835765.51	6.74	**19.54**	**16.24**

* This is a fully segregating slurry, however SI>100% cannot phyisically happen.